

### Summary

The drag force is one of the forces acting on immersed particles moving through and with respect to a surrounding fluid, along with gravity and buoyancy. The drag force therefore plays an important role in the calculation of particle motions. Particle velocity is constant when the sum of the forces acting on the particle is zero.

An iterative calculation of the relative velocity of a particle is often indispensable, since the drag coefficient depends on the particle Reynolds number.

# 3 Heat transport

## 3.1 Steady-state heat conduction

The fact that heat can be transported by *conduction* was introduced in § 2.1. Heat conduction refers to the ability of molecules to create a net heat transport without net mass transport. The important equation here is *Fourier's law* which sets out the link between heat flux and the 'driving' temperature gradient

$$\phi_{q,x}'' = -\lambda \frac{dT}{dx} \quad (3.1)$$

According to this law, a gradient in the temperature in the direction of  $x$  causes a heat flux in the direction of  $x$  that always makes the heat flow from a place with a high temperature to one with a low temperature – which is why there is a minus sign on the right-hand side of Equation (3.1). Throughout this chapter, the thermal conductivity coefficient  $\lambda$  will be assumed to be constant (that is, independent of temperature) for the sake of simplicity; the extension to a temperature dependent  $\lambda$  is trivial.

We will first deal with thermal conductivity in steady-state conditions for various elementary 1-D configurations. At the end of this § 3.1, we will introduce numerical techniques in use for more complex, more-dimensional geometries.

### 3.1.1 Heat conduction in Cartesian coordinates

The first situation concerns a flat slab (see Figure 3.1) with thickness  $D$  and made from a solid with thermal conductivity coefficient  $\lambda$ . The left-hand side of the slab is kept at a constant temperature  $T_1$ , and the right-hand side at a constant temperature  $T_2$ . In a steady-state situation, the heat balance for a thin slice somewhere in the slab between  $x_1$  and  $x_2$  is

$$0 = \phi_{q,in} - \phi_{q,out} = \phi_q|_{x_1} - \phi_q|_{x_2} \quad (3.2)$$

In other words

$$\phi_q|_{x_1} = \phi_q|_{x_2} \quad (3.3)$$

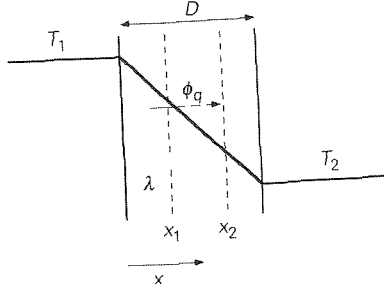


Figure 3.1

Given that this equation applies to any  $x_1$  and  $x_2$  in the slice, the heat flow is independent of  $x$  and is therefore a constant. This also applies to the heat flux, given that surface area  $A$  of the slice through which the heat flow passes, is also independent of  $x$ . From

$$\phi_q'' = -\lambda \frac{dT}{dx} = \text{constant}$$

it follows that

$$\frac{dT}{dx} = -\frac{\phi_q''}{\lambda} = \text{constant} \quad (3.4)$$

Here,  $\phi_q''$  is a constant that has yet to be calculated. Integrating Equation (3.4) produces a (second) integration constant. For this reason, two boundary conditions are needed in order to be able to give a complete description of the heat transport problem. With  $x = 0 \rightarrow T = T_1$  and  $x = D \rightarrow T = T_2$  as the boundary conditions, this gives the following temperature profile across the slab

$$\frac{T_1 - T(x)}{T_1 - T_2} = \frac{x}{D} \quad (3.5)$$

while for the heat flux, the following applies

$$\phi_q'' = \frac{\lambda}{D} (T_1 - T_2) \quad (3.6)$$

Equation (3.5) shows that the temperature profile in the slab is a straight line. Equation (3.5) can also be obtained, incidentally, by drawing up an energy balance for a thin slice between  $x$  and  $x + dx$ . The balance is

$$0 = A \left( -\lambda \frac{dT}{dx} \Big|_x \right) - A \left( -\lambda \frac{dT}{dx} \Big|_{x+dx} \right) \quad (3.7)$$

Equation (3.7) can be simplified with the help of the following rule

$$f(x+dx) = f(x) + \frac{df}{dx} dx \quad (3.8)$$

after which it becomes (after dividing by  $A \lambda$ , assuming that  $\lambda$  does not also depend on place  $x$  via  $T$ )

$$0 = -\frac{dT}{dx} \Big|_x + \left\{ \frac{dT}{dx} \Big|_x + \frac{d}{dx} \left( \frac{dT}{dx} \right) dx \right\} \quad (3.9)$$

This result can be simplified to

$$\frac{d}{dx} \left( \frac{dT}{dx} \right) = \frac{d^2 T}{dx^2} = 0 \quad (3.10)$$

After integrating twice and applying the two boundary conditions, this produces Equation (3.5) again

### Example 3.1. Heat production in a bar

In part  $L \leq x \leq 2L$  of a copper bar with length  $2L$  and cross-sectional area  $A$ , a constant and uniform heat production  $q$  takes place, where  $q$  is expressed in  $\text{W/m}^3$ . The one end of the bar ( $x = 0$ ) is kept at a constant temperature  $T_0$ , while the remainder of the bar (i.e., the whole surface area including the other end  $x = 2L$ ) is perfectly insulated.

The question is to derive the temperature profile in the whole bar in this steady-state situation

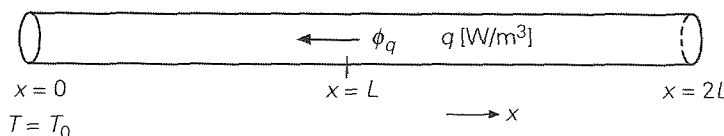


Figure 3.2

A sketch of the problem is represented in Figure 3.2 in which the shading indicates that no heat losses take place at the pertinent surfaces. This keeps the heat transport one-dimensional, while the transport is in the negative  $x$ -direction. As the heat transport is due to conduction with  $dT/dx > 0$ , Fourier's law results in  $\phi_q'' < 0$ . A heat balance for the right-hand part of the bar for this steady-state situation learns that all heat produced in this right part is delivered through the plane at  $x = L$  to the left part.

$$0 = 0 - \phi_q \Big|_{x=L} + qAL \quad (3.11)$$

This means that the size of the heat flux  $\phi_q''$  is equal to  $qL$

$$\phi_q'' \Big|_{x=L} = \lambda \frac{dT}{dx} \Big|_{x=L} = qL \quad (3.12)$$

From the Equation (3.11) and (3.12), however, no conclusions can be drawn as to the temperature profiles in the left part or the right part of the bar. Exactly as with the concentration profile in a plug flow reactor where a species balance had to be drawn up for a thin slice  $dx$  inside the reactor (see § 1.2.2), now a heat balance has to be drawn up for a slice  $dx$  from the bar. In doing this, the part  $0 \leq x \leq L$  in which no heat is produced, and the part  $L \leq x \leq 2L$  with heat production should be distinguished after all, a heat balance over a thin slice  $dx$  in the part  $0 \leq x \leq L$  does not contain a production term, while a heat balance over a slice  $dx$  in the part  $L \leq x \leq 2L$  does.

Drawing up a heat balance for a slice in the left part  $0 \leq x \leq L$  results in the second-order differential Equation (3.10) – the derivation starting at Equation (3.7) perfectly fits this case. The two boundary conditions needed to arrive at the temperature profile in this part of the bar, are  $T = T_0$  op  $x = 0$  (given in the question) and the expression for the temperature gradient at  $x = L$  as given in Equation (3.12). The result for the part  $0 \leq x \leq L$  is

$$T = T_0 + \frac{qL}{\lambda} x \quad (3.13)$$

Drawing up a heat balance for a slice  $dx$  in the part  $L \leq x \leq 2L$  gives

$$0 = -\lambda A \frac{dT}{dx} \Big|_x - \left( -\lambda A \frac{dT}{dx} \Big|_{x+dx} \right) + qAdx \quad (3.14)$$

from which now

$$\frac{d^2T}{dx^2} = -\frac{q}{\lambda} \quad (3.15)$$

follows. Here, too, two boundary conditions are needed as differential Equation (3.15) has to be integrated twice. Perfect insulation implies  $dT/dx = 0$  at  $x = 2L$ , while for the temperature at  $x = L$  an expression can be derived with the help of Equation (3.13). For the temperature profile in the part  $L \leq x \leq 2L$  the following expression is then found:

$$T = T_0 + \frac{2qL}{\lambda} x - \frac{q}{2\lambda} (x^2 + L^2) \quad (3.16)$$

Notice that for solving this problem three different heat balances are needed  $\square$

### 3.1.2 Analogy with Ohm's law

From Equation (3.6), it directly follows that the temperature difference  $\Delta T \equiv T_1 - T_2$  over the slab is simply related to the heat flux as

$$\Delta T = \phi_q'' \frac{D}{\lambda} = \phi_q \frac{D}{\lambda A} \quad (3.17)$$

Equation (3.17) shows that driving force  $\Delta T$  results in a heat flux  $\phi_q''$ . The Equation has a resemblance to *Ohm's law* known from the field of electricity

$$\Delta V = IR = I \frac{\rho L}{A} \quad (3.18)$$

in which  $L$  is the length of the conducting wire,  $A$  the cross-sectional area, and  $\rho$  the specific resistance of the material of which the conducting wire is made

This similarity gives us a slightly different view of thermal conductivity. As Ohm's law says if an electric potential difference (a voltage)  $\Delta V$  is created across a resistance  $R$ , then this driving force  $\Delta V$  results in an electric current  $I$ , which is directly proportional to  $\Delta V$ . The proportionality constant  $R$  describes the resistance of a piece of material to the transport of electricity. With this consideration in mind,  $\Delta T$  can be viewed in Equation (3.17) as the 'driving force' and heat transport  $\phi_q$  as the 'flow'.

This also means that  $D/\lambda A$  in Equation (3.17) can be interpreted as a resistance, but now to the transport of heat. Remember that in Equation (3.17)  $D$  is the path length to be covered for the heat transport, just as  $L$  in Equation (3.18) is the path length that the electric current must cover. The role of the reciprocal thermal conductivity coefficient, that is, of  $1/\lambda$ , is therefore entirely comparable with that of specific resistance  $\rho$ . Note that both  $\lambda$  and  $\rho$  are physical properties of the compound involved. The quantity  $D/\lambda$  is therefore the specific resistance (that is, the resistance per unit of surface area) to heat transport: the greater  $D/\lambda$  is, the smaller is the heat flux  $\phi_q''$  for a given driving force of  $\Delta T$ .

The situation can be slightly complicated by placing two slabs of different thicknesses,  $D_1$  and  $D_2$ , of different materials, with thermal conductivity coefficients  $\lambda_1$  and  $\lambda_2$  against each other. The left-hand side of slab 1 is kept at temperature  $T_1$ , and the right-hand side of slab 2 at  $T_2$  (see Figure 3.3). Here, too, it is possible to

derive the link in a steady-state situation between driving force  $\Delta T$  over the two slabs and the heat flux through the two slabs. This situation presents itself when a layer of insulating material is applied in order to reduce the heat transport from left to right (the heat loss)

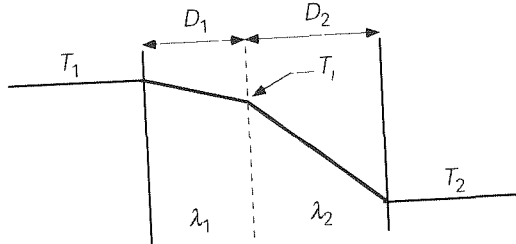


Figure 3.3

If the temperature on the interface between the two slabs is called  $T_1$ , the link between the driving force  $T_1 - T_2$  over slab 1 and the associated flux  $\phi_{q,1}''$  can be written down directly on the basis of Equation (3.17)

$$T_1 - T_2 = \phi_{q,1}'' \frac{D_1}{\lambda_1} \quad (3.19)$$

and, analogously, for the second slab

$$T_1 - T_2 = \phi_{q,2}'' \frac{D_2}{\lambda_2} \quad (3.20)$$

For this case,  $\phi_{q,1}''$  is equal to  $\phi_{q,2}''$ , as can be easily seen from a heat balance for a volume with material 1 on the one side, and material 2 on the other. Adding Equations (3.19) and (3.20) causes the interim unknown temperature  $T_1$  to be omitted.

$$\Delta T = T_1 - T_2 = \phi_q'' \left( \frac{D_1}{\lambda_1} + \frac{D_2}{\lambda_2} \right) = \phi_q \left( \frac{D_1}{\lambda_1 A} + \frac{D_2}{\lambda_2 A} \right) \quad (3.21)$$

The above situation concerning two slabs also has a well-known electric analogue – that is, two electrical resistances in series (see Figure 3.4), to which the following applies

$$\Delta V = I (R_1 + R_2) \quad (3.22)$$

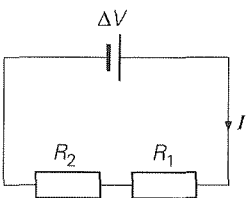


Figure 3.4

Equations (3.21) and (3.22) are entirely analogous in Equation (3.22) too, the individual resistances in a series circuit have to be added up in order to obtain the overall resistance. In which order the resistances are installed, is irrelevant for both the heat transport and the electrical current

### 3.1.3 Heat conduction in cylindrical coordinates

In each of the cases examined up to now, the flux through the material was independent of its position in the material. This is actually the exception, because in reality the flux is usually place-dependent. This can be illustrated on the basis of the link between the driving force and flux in the case of a hollow cylinder. A typical example of such a situation is a pipe through which water flows at a temperature different from that of the medium outside. The result is radial heat transport through the pipe wall due to conduction

Assume that the situation as shown in Figure 3.5 is steady. The inner radius of the hollow cylinder is  $R_1$  and the outer radius is  $R_2$ . The inside surface is kept at temperature  $T_1$ , and the outer surface at  $T_2$ . In order to calculate the (local) heat flux through the cylindrical wall, Fourier's law says the temperature profile in the wall has to be known

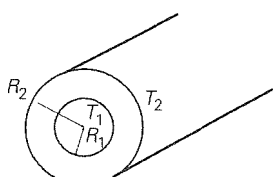


Figure 3.5

To this end, consider a ring (length  $L$ ) in the cylindrical wall with coaxial radii  $r$  and  $r + dr$  (see Figure 3.6). A heat balance for this ring, in steady-state conditions without heat production, is

$$0 = \phi_{q,in} - \phi_{q,out} \quad (3.23)$$

It is still the case that  $\phi_{q,in} = \phi_{q,out} = \text{constant}$ . However, this does not mean that the flux is also constant after all, the geometry is now curved. The radial flux is now shown as follows

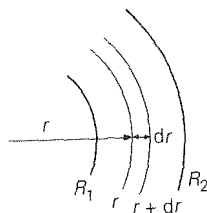


Figure 3.6

$$\phi_q'' = -\lambda \frac{dT}{dr} \quad (3.24)$$

Additionally, in this case, the following applies to the link between flow and flux

$$\phi_q = A \phi_q'' = 2\pi r L \phi_q'' \quad (3.25)$$

Combining Equation (3.23), (3.24), and (3.25) produces the following differential equation

$$-\lambda 2\pi r L \frac{dT}{dr} = C_1 \quad (3.26)$$

The general solution to Equation (3.26) is

$$T(r) = -\frac{C_1}{2\pi\lambda L} \ln r + C_2 \quad (3.27)$$

Constants  $C_1$  and  $C_2$  can be determined with the help of boundary conditions  $r = R_1 \rightarrow T = T_1$  and  $r = R_2 \rightarrow T = T_2$ . This gives the following as the solution to the temperature profile in the cylindrical wall

$$\frac{T - T_2}{T_1 - T_2} = \frac{\ln(r/R_2)}{\ln(R_1/R_2)} \quad (3.28)$$

Now that the temperature profile is known, it is also possible to calculate the flux. Differentiating Equation (3.28) and substituting the temperature gradient into (3.24) – or using Equation (3.26) – produces

$$\phi_q'' = -\lambda \frac{dT}{dr} = -(T_1 - T_2) \frac{\lambda}{\ln(R_1/R_2)} \frac{1}{r} \quad (3.29)$$

Flux  $\phi_q''$  is indeed now dependent on its place in the cylindrical wall as  $r$  increases, so  $\phi_q''$  decreases. Equation (3.29) also provides the link between  $\Delta T (= T_1 - T_2)$  and  $\phi_q$

$$\Delta T = \frac{\ln(R_2/R_1)}{2\pi\lambda L} \phi_q \quad (3.30)$$

Here too, the ‘flow’ is proportional to the ‘driving force’, but in this case the link between geometry and ‘resistance’ is more complicated. When, however,  $R_2$  does not differ too much from  $R_1$ , e.g. when the thickness  $\delta = R_2 - R_1$  of a pipe wall is pretty small with respect to  $R_1$ , owing to a series expansion – for  $\epsilon \ll 1$ , one can write  $\ln(1+\epsilon) \approx \epsilon$  – Equation (3.30) can be rewritten to

$$\Delta T = \frac{\delta}{\lambda} \frac{\phi_q}{2\pi R_1 L} \quad (3.31)$$

in which  $\delta/\lambda$  is recognized as the resistance to heat transport of a flat layer, as in Equation (3.17)

Once again, the same result can be obtained by further working out the steady-state heat balance (3.23). For this, the ‘in’ and ‘out’ flows should be expressed in terms of local temperature gradients

$$0 = -[A]_r \lambda \frac{dT}{dr} \Big|_r - \left( -[A]_{r+dr} \lambda \frac{dT}{dr} \Big|_{r+dr} \right) \quad (3.32)$$

In this equation,  $[A]_r$  is the surface area of the ring with radius  $r$  and  $[A]_{r+dr}$  is the surface area of the ring with radius  $\{r+dr\}$ . Now, the surface area of a ring with radius  $r$  is equal to

$$[A]_r = 2\pi r L \quad (3.33)$$

Equation (3.32) can be simplified with the help of Equation (3.33) by dividing by  $2\pi\lambda L$  and by putting terms  $r$  and  $r+dr$  with the local temperature gradient

$$[A]_{r+dr} \frac{dT}{dr} \Big|_{r+dr} = \left\{ A \frac{dT}{dr} \right\}_{r+dr} = \left\{ 2\pi r L \frac{dT}{dr} \right\}_{r+dr} \quad (3.34)$$

so that

$$0 = -\left\{ r \frac{dT}{dr} \right\}_r - \left\{ -r \frac{dT}{dr} \right\}_{r+dr} \quad (3.35)$$

Here,  $r (dT/dr)$  should be regarded as one function,  $f$ . Equation (3.35) will then contain the difference between  $f(r+dr)$  and  $f(r)$ , which of course is  $(df/dr) dr$ . Entering  $r (dT/dr)$  for  $f$  again produces

$$\frac{d}{dr} \left( r \frac{dT}{dr} \right) = 0 \quad (3.36)$$

Solving Equation (3.36), with the boundary conditions  $r = R_1 \rightarrow T = T_1$  and  $r = R_2 \rightarrow T = T_2$ , produces Equation (3.28) of course

### 3.1.4 Heat conduction in spherical coordinates

A second example of a curved geometry in which the heat transport is independent of place, but the heat flux is not, is that of spherical geometry. Consider a sphere (with radius  $R$ ) that is kept at temperature  $T_1$ . The sphere is surrounded by a stagnant medium. At a long distance from the sphere, the temperature of the medium is  $T_\infty$ . What is the link between driving force and flow in this case, in a steady-state situation?

In order to answer this question, of course, a heat balance will have to be drawn up, this time for a concentric spherical shell with radii of  $r (> R)$  and  $r+dr$ . The heat balance is

$$0 = \phi_{q,\text{in}} - \phi_{q,\text{out}} \quad (3.37)$$

In this case, too, surface area  $A$ , through which the heat is transferred, is a function of  $r$ :  $A = A(r)$ . The link between the local transport rate and the local temperature gradient can therefore be written as follows

$$\phi_q = A(r) \left( -\lambda \frac{dT}{dr} \right) \quad (3.38)$$

Using this in heat balance (3.37) produces

$$0 = -[A]_r \lambda \frac{dT}{dr} \Big|_r - \left( -[A]_{r+dr} \lambda \frac{dT}{dr} \Big|_{r+dr} \right) \quad (3.39)$$

Equation (3.39), analogously to the above, can be written as the following differential equation:

$$0 = \lambda \frac{d}{dr} \left( A(r) \frac{dT}{dr} \right) \quad (3.40)$$

For  $A(r)$ , the following now applies

$$A(r) = 4\pi r^2 \quad (3.41)$$

This means that Equation (3.40) becomes:

$$\frac{d}{dr} \left( r^2 \frac{dT}{dr} \right) = 0 \quad (3.42)$$

The general solution to differential Equation (3.42) is

$$T(r) = -\frac{C_1}{r} + C_2 \quad (3.43)$$

Substituting the boundary conditions  $r = R \rightarrow T = T_1$  and  $r \rightarrow \infty \rightarrow T = T_\infty$  produces

$$T(r) = (T_1 - T_\infty) \frac{R}{r} + T_\infty \quad (3.44)$$

Using this expression for finding the temperature gradient in Equation (3.38) produces a relation between the driving force  $\Delta T (= T_1 - T_\infty)$  and the heat transport  $\phi_q$ , or the heat flux  $\phi_q''$ , at the surface of the sphere (with diameter  $D = 2R$ )

$$\Delta T = \frac{1}{4\pi\lambda R} \phi_q = \frac{D}{2\lambda} \phi_q'' \quad (3.45)$$

#### Example 3.2. Radioactive sphere I

In a sphere, 10 cm in diameter and consisting of uranium oxide, heat production  $q$  (in  $\text{W/m}^3$ ) as a result of the radioactive decay takes place uniformly distributed over the volume. The surface of the sphere is kept at a low and constant temperature  $T_w$ .

Calculate the temperature at the centre of the sphere for  $q = 6 \text{ MW/m}^3$ ,  $T_w = 20^\circ\text{C}$  and  $\lambda = 8 \text{ W/mK}$

The heat production inside the particle, along with the surface temperature being held constant at a low value, results in a radial temperature profile with the maximum temperature at the centre. Such a temperature profile cannot be found by means of a macro balance for the whole sphere, but requires a look inside the sphere. Inside, a spherical shell with thickness  $dr$  has to be selected as a micro control volume for a steady-state heat balance.

$$0 = -4\pi r^2 \lambda \frac{dT}{dr} \Big|_r - \left( -4\pi r^2 \lambda \frac{dT}{dr} \Big|_{r+dr} \right) + q 4\pi r^2 dr \quad (3.46)$$

in which – compared to Equation (3.39) – right away  $4\pi r^2$  has been substituted for  $A(r)$  and the subscripts  $r$  and  $r+dr$  relate to both the area  $4\pi r^2$  and the gradient  $dT/dr$ . The next step is dividing all terms of Equation (3.46) by  $4\pi\lambda dr$  and results in

$$\frac{d}{dr} \left( r^2 \frac{dT}{dr} \right) = -\frac{q}{\lambda} r^2 \quad (3.47)$$

where it is extremely important to keep  $r^2$  between the brackets behind the  $d/dr$  in the left-hand side as when going from position  $r$  to position  $r+dr$  the shell area increases. Integrating Equation (3.47) once results in

$$r^2 \frac{dT}{dr} = -\frac{q}{3\lambda} r^3 + C_1 \quad (348)$$

As at  $r = 0$  the temperature is maximum, i.e.  $dT/dr = 0$ , the integration constant  $C_1$  is concluded to be zero. Then, it follows

$$\frac{dT}{dr} = -\frac{q}{3\lambda} r \quad (349)$$

Integrating once more and using the second boundary condition  $T = T_w$  at  $r = R$  eventually gives

$$T = T_w + \frac{q}{6\lambda} (R^2 - r^2) \quad (350)$$

Substituting the given values for  $q$ ,  $T_w$  and  $\lambda$  results in the answer  $T_0 = 1270^\circ\text{C}$  at  $r = 0$ .  $\square$

### 3.1.5 A numerical treatment for 2-D Cartesian

All the examples that we have looked at so far have been solved entirely analytically. This was possible because the geometries were simple. In many practical cases, finding an analytical solution is difficult, if not impossible. Fortunately, though, many problems can be tackled perfectly well with the help of numerical techniques, and for some steady-state problems, the means are surprisingly easy. Solving problems numerically is now an essential part of modern transport phenomena. Consider, as an illustration (Figure 3.7a), a two-dimensional problem what is the steady-state temperature distribution in a square two sides of which are kept at constant temperature  $T_0 = 0^\circ\text{C}$  and the other two sides at  $T_1 = 50^\circ\text{C}$ ?

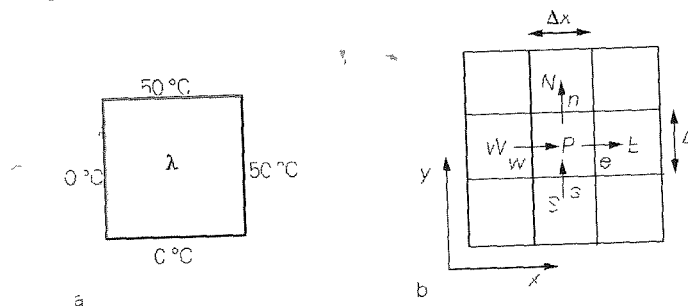


Figure 3.7

The problem can be excellently described in a Cartesian system. First, the square is divided up into  $NM$  small rectangles with sizes  $\Delta x$  and  $\Delta y$ . These small rectangles are shown in Figure 3.7b. The centre rectangle is shown as P, with the four adjacent

rectangles having the four directions of the compass, North, East, South, West, shortened to N, E, S, W. The 'in' and 'out' heat flows have also been drawn for rectangle P.

A steady-state heat balance for the rectangle with centre P is therefore

$$0 = -\lambda \left. \frac{\partial T}{\partial x} \right|_w \Delta y - \left( -\lambda \left. \frac{\partial T}{\partial x} \right|_e \right) \Delta y + \\ + \left( -\lambda \left. \frac{\partial T}{\partial y} \right|_s \right) \Delta x - \left( -\lambda \left. \frac{\partial T}{\partial y} \right|_n \right) \Delta x \quad (351)$$

where the partial derivative symbol  $\partial$  is used. The indices w, e, s, n here refer to the interfaces of the rectangle around P (see Figure 3.7). It is also the case that no heat production occurs in the rectangle around P. Formally, the balance applies only to an infinitesimally small rectangle. As far as realistic dimensions are concerned, this is an approximation. Each of the four gradients in the above equation can be calculated, such as the heat flow through the left-hand side of the rectangle around P

$$\left. \frac{\partial T}{\partial x} \right|_w \approx \frac{T_p - T_w}{\Delta x} \quad (352)$$

If this is done for every term in Equation (351), if  $\Delta x = \Delta y$ , and  $\lambda$  is taken as a constant, then heat balance (351) can be written as

$$0 = T_w + T_e + T_s + T_n - 4T_p \quad (353)$$

In other words, the temperature of P is the mean of its four neighbours. This can be converted very easily into a computer code. Start with an estimate. Let us suppose that the entire square has a uniform temperature of  $T_0$ . Now, for each smaller square, take the mean of its neighbours and regard this temperature as an improved version of the original estimate. Of course, the original estimate changes because temperature  $T_1$  applies on two of the sides. After this first iteration, the new temperature field can be compared with the old one. If the difference between both fields is still too great, we repeat the process until the solution has converged and we have a numerically obtained calculation of the temperature.

In principle, it is possible to arrive at any given point that is near the solution by dividing up the calculation field (the square) into a very large number of elements and by very clearly defining the convergence criterion. Below is a simple algorithm that can be used for the problem described above, with the help of Matlab, for example:

```

% steady state long-term heating, algorithm for Matlab
% square with constant temperature at sides
% bottom and left-hand side 0°C
% top and right-hand side 50°C

clear all,
N=20, %number of internal cells = N*N

Told=zeros(N+2,N+2), %initialise first estimate
%make the temperature field N+2 at N+2 so that we
%can include boundary conditions via so-called virtual
%points These are points situated outside the square
%define the virtual points associated with boundary condition T=50°C
%top side at 50°C
%right-hand side at 50°C

for i=1:N+1
    Told(i+1,N+2)=50,
    Told(N+2,i+1)=50,
end
Tnew=Told, %initialise new field

eps=1, %initialise convergence parameter
epsconv=1e-3, %select the convergence criterion

while eps>epsconv %start iterating until convergence
    for i=2:N+1 %calculate new temperature field in numbers x-direction
        for j=2:N+1
            Tnew(i,j)=1/4*(Told(i-1,j)+Told(i+1,j)+Told(i,j-1)+Told(i,j+1)),
        end
    end
    eps=0, %calculate convergence again
    for i=2:N+1
        for j=2:N+1
            eps=eps+abs(Tnew(i,j)-Told(i,j)),
        end
    end
    Told=Tnew, %replace old field with new one
end

x=linspace(0,1,N+2), %make coordinates
y=x,
contourf(x,y,Tnew,19), %show solution in graph form

```

Advanced methods for finding a solution exist for the above example. Also, the convergence criterion used is just one of the many possibilities. Numerical analysis provides the necessary tools for conducting simulations of this kind in a responsible manner. Knowledge of these is obviously essential for numerical simulations of transport phenomena.

The example illustrates that the balance method can be used to generate the necessary equations fairly simply. The big advantage of using the balance method is that with numerical solving the balances are always complied with at every (local) level. This easily vindicates the basics of transport phenomena. Many books have

been written that deal with numerical techniques in transport phenomena. One of the standard works is Patankar's textbook<sup>10</sup> dating from as far back as 1980, see also Hanjalić *et al*<sup>11</sup>

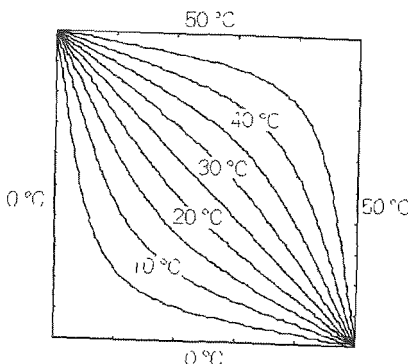


Figure 3.8 Temperature contours of the conducting square in a steady-state situation with two sides at 0 °C and two at 50 °C. Number of cells 50 50

The example of the square can also be relatively easily analytically solved with the help of Fourier analysis. This is because there is still a fair amount of symmetry in the problem. Things look somewhat more tricky if production occurs in the square, but numerically this is not much more difficult. The balance equation will now contain an extra term as a result of this production. Consider the rectangle around P again. The production per unit of surface area is  $q''$ . The heat balance is now

$$0 = -\lambda \left. \frac{\partial T}{\partial x} \right|_w \Delta y - \left( -\lambda \left. \frac{\partial T}{\partial x} \right|_e \right) \Delta y + \\ + \left( -\lambda \left. \frac{\partial T}{\partial y} \right|_s \right) \Delta x - \left( -\lambda \left. \frac{\partial T}{\partial y} \right|_n \right) \Delta x + \iint_{\Delta x, \Delta y} q'' dxdy \quad (3.54)$$

For small  $\Delta x$  and  $\Delta y$ ,  $q''$  can be assumed to be constant over the control volume. The approximate algebraic equation is now (with  $\Delta x = \Delta y$ )

$$0 = \lambda (T_w + T_e + T_s + T_n - 4T_p) + q'' \Delta x \Delta y \quad (3.55)$$

Here, too, the steady-state solution can be found by using a comparative iterative procedure.

By way of example, we assume that a heat source and a heat sink are present in the square. Both sources have the form of a 'delta peak' with strength  $q$  and  $-q$ .

<sup>10</sup> Patankar S V, *Numerical Heat Transfer and Fluid Flow*, Hemisphere Publ Corp, 1980

<sup>11</sup> Hanjalić K, S Kenjereš, M J Tummers and H J J Jonker, *Analysis and Modelling of Physical Transport Phenomena*, VSSD, 2007

respectively. The source is at position  $\{1/4+1/80, 3/4-1/80\}$ , while the sink is at  $\{3/4-1/80, 1/4+1/80\}$  (let the length of the sides of the square be equal to 1)

Once again, the square is divided up into smaller squares, two of which therefore contain an extra source term. None of the others do. Because of the delta peak, the production term in Equation (3.54) is always zero, apart from the two smaller squares that contain the source and the sink. The production term for these is  $+q$  and  $-q$  respectively, regardless of the size of the smaller squares. For the sake of simplicity, the boundary conditions are now  $T = 0^\circ\text{C}$  for each side.

Equation (3.55) can be solved using the same iteration process as for Equation (3.53).

It is a good idea to include a source term for every cell: this is zero in every case apart from the two cells that contain the real source and sink. In terms of the algorithm, the central rule becomes

$$\begin{aligned} T_{\text{new}(i,j)} = & 1/4 * \{T_{\text{old}(i-1,j)} + T_{\text{old}(i+1,j)} + \\ & + T_{\text{old}(i,j-1)} + T_{\text{old}(i,j+1)}\} + 1/4/\lambda * q(i,j) \end{aligned}$$

In Figure 3.9, the numerical solution to this problem is shown for  $40 \times 40$  elements.

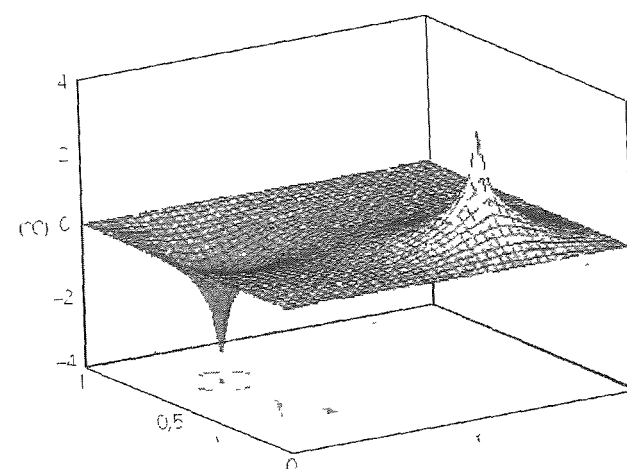


Figure 3.9

The examples discussed here use the simple geometry of a square. However, there is no problem in using the shape of a cooling fan, for example. Numerical techniques are often the only method if the geometry is complex.

### Summary

In the case of steady-state conduction of heat, the link between the driving force  $\Delta T$  and the heat transport is analogous to Ohm's law. The driving temperature difference causes a transport that is directly proportional to this temperature difference. The

proportionality constant can be regarded as resistance to the transport of heat. Both flat and non-flat geometries have been considered, and there is always the same link between driving force and heat transport. However, the heat flux is dependent on place in the case of curved geometries! This can be seen directly from heat balances over thin rings or shells.

We have also touched on numerical methods for solving thermal conductivity questions in multi-dimensional and complex geometries. Discretisation of the differential equation leads to an algebraic equation that links the values of the sought-after variables in nearby points to each other. An iterative solution strategy is needed in order to arrive at the solution.

## 3.2 Heat transfer coefficient and Nusselt number

### 3.2.1 Newton's Law of Cooling

The concept of a driving force that results in a flow that is proportional to the driving force has proved to be of great value in complex situations (unsteady and steady) as well. For engineers, the idea plays an important role in the complex situations they encounter in practice. Heat flow and driving force are generally linked to each other by *Newton's Law of Cooling* (which also describes heating up). The law states

$$\phi_q = h A \Delta T \quad (3.56)$$

Flow and driving force are therefore linked the other way around with regard to Ohm's law. Instead of working in terms of resistance, a measure for heat transport, or heat transfer, is used here. In Equation (3.56),  $A$  is the surface area through which the heat flow passes, and coefficient  $h$  is called the *heat transfer coefficient* (the unit of which is  $\text{W m}^{-2}\text{K}^{-1}$ ). It is therefore  $1/h$  itself that can be interpreted as heat resistance. Surface area  $A$  is included explicitly in Equation (3.56), because it is obvious that the heat flow increases (more or less) proportionally to the surface area across which the driving force is located.

The results of § 3.1 can now be summarised in terms of an  $h$ -value for every situation (*check this!*)

Table 3.1

heat transfer coefficient	flat slab	cylindrical wall (related to outer surface)	sphere
$h$	$\frac{\lambda}{D}$	$\frac{2\lambda}{D_2 \ln(D_2/D_1)}$	$\frac{2\lambda}{D}$

### 3.2.2 The Nusselt number

As mentioned previously, it is often a good idea to use such links in a non-dimensional form. In the case of heat conduction, too, a non-dimensional form of  $h$  is defined. This number is known as the *Nusselt number*, or  $\text{Nu}$  for short. The Nusselt number is defined as

$$\begin{aligned} \text{Nu} &= \frac{\text{heat resistance if 1-D steady-state conduction}}{\text{actual resistance (at prevailing conditions)}} = \\ &= \frac{D/\lambda}{1/h} = \frac{hD}{\lambda} \end{aligned} \quad (3.57)$$

This makes it possible, for example, to indicate quickly and easily the situation of steady-state heat conduction through a thin solid slice with thickness  $D$ , for example, as  $\text{Nu} = 1$ , or that from the surface of a sphere to 'infinity', see Equation (3.45), as  $\text{Nu} = 2$ . Thanks to the definitions of the heat transfer coefficient, in (3.56), and the Nusselt number, in Equation (3.57), it is possible to understand directly from  $\text{Nu} = 2$ , for example, that it concerns heat conduction from a spherical surface in steady-state for conditions (and not time-dependent conditions or convective heat transport, for example)

### 3.2.3 Overall heat transfer coefficient

Many cases of heat flow involve two heat resistances in series. The conduction of heat through two thin slices has already been covered in § 3.1, for example. The result of the analysis was

$$\phi_q'' = \left( \frac{D_1}{\lambda_1} + \frac{D_2}{\lambda_2} \right)^{-1} \Delta T = \left( \frac{1}{h_1} + \frac{1}{h_2} \right)^{-1} \Delta T \quad (3.58)$$

The items in brackets can also be replaced by one 'heat exchange coefficient'. This contains both heat transfer coefficients,  $h_1$  and  $h_2$ . This coefficient is therefore also known as the *overall heat transfer coefficient* and is denoted as  $U$ . From Equation (3.58) it therefore follows that

$$\frac{1}{U} = \frac{1}{h_1} + \frac{1}{h_2} \quad (3.59)$$

Equation (3.59) appears to have general validity and is easy to derive. To that end, look at the heat flow in Figure 3.10, which goes into medium 2 from medium 1. Give the temperature of interface  $T_i$ . The following then applies to the heat flux from medium 1 to the interface

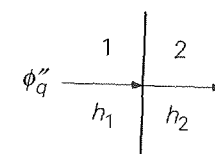


Figure 3.10

$$\phi_q'' = h_1 (T_i - T_1) \quad (3.60)$$

This flux also runs into medium 2 from the interface, as an interface cannot absorb or produce heat. The expression for the flux in medium 2 is

$$\phi_q'' = h_2 (T_i - T_2) \quad (3.61)$$

Eliminating the temperature from the interface provides the sought-after link

$$\phi_q'' = \left( \frac{1}{h_1} + \frac{1}{h_2} \right)^{-1} \Delta T \quad (3.62)$$

This result can be interpreted analogously to Ohm's law: the overall resistance ( $1/U$ ) is the sum of the two secondary resistances,  $1/h_1$  and  $1/h_2$ .

It is common practice among engineers to ignore the smallest of the two resistances to heat transfer when the ratio of the two resistances is beyond a certain value. Which critical value is used, determines of course how accurate the estimate may be upon ignoring the smallest resistance. A typical example of such a situation is heat transfer from a solid object to its ambient medium (or the other way around). The ratio of the object's internal resistance to heat transfer – in the case of a flat plate  $D/\lambda_i$ , of course – to the external resistance  $1/h_e$  is often represented by the *Biot-number*, denoted as  $\text{Bi}_i$ .

$$\text{Bi}_i = \frac{D/\lambda_i}{1/h_e} = \frac{h_e D}{\lambda_i} \quad (3.63)$$

The Biot-number should not be confused with the *Nusselt-number*:  $\text{Bi}_i$  compares for an object the internal and external resistances to heat transfer, while  $\text{Nu}$  compares the resistance to heat transfer (external or internal) under the actual conditions with that in the case of 1-D steady-state heat transport across a flat slab ( $\text{Nu}=1$ ).

#### Example 3.3. Radioactive sphere II

In a sphere, 10 cm in diameter and consisting of uranium oxide, heat production  $q$  (in  $\text{W/m}^3$ ) as a result of the radioactive decay takes place uniformly distributed

over the volume. The sphere is now in a medium that in the bulk, i.e. far away from the sphere, has a constant, lower temperature  $T_\infty$ .

Derive an expression for the temperature at the centre of the sphere that comprises  $T_\infty$ .

Inside the sphere there are no changes with respect to Example 3.2. Inside,

(3.64)

$$\frac{dT}{dr} = -\frac{q}{3\lambda_i} r$$

therefore still applies – see Equation (3.49). Unlike in Example 3.2, now the temperature at  $r = R$  is determined by the heat loss to the environment. In any steady state, the heat flux from the sphere's interior towards the sphere's surface equals the heat flux from the surface into the ambient medium.

$$-\lambda_i \frac{dT}{dr} \Big|_{r=R} = \frac{qr}{3} \Big|_{r=R} = \frac{qR}{3} = h_e (T_{r=R} - T_\infty) \quad (3.65)$$

Then it follows that

(3.66)

$$T_{r=R} = T_\infty + \frac{qR}{3h_e}$$

[Note that the latter result can also be obtained with the help of an overall heat balance over the sphere that expresses that under steady-state conditions the heat production inside the sphere equals the heat transfer to the ambient medium.]

Integrating Equation (3.64) with boundary condition (3.66) at  $r = R$  gives for the temperature  $T_0$  at the heart of the sphere

$$T_0 = T_\infty + \frac{qR}{3h_e} + \frac{qR^2}{6\lambda_i} = T_\infty + \frac{qR}{3} \left( \frac{1}{h_e} + \frac{R}{2\lambda_i} \right) \quad (3.67)$$

This equation illustrates that  $T_0$  depends on both the internal and the external heat transport. When the internal resistance to heat transport may be ignored with respect to the external resistance, then Equation (3.67) simplifies to Equation (3.66)

(3.68)

$$T_0 \approx T_{r=R} = T_\infty + \frac{qR}{3h_e}$$

while for negligible external resistance an expression for  $T_0$  is obtained that agrees with Equation (3.50). Table 3.1 shows that, if the external medium is stagnant and external heat transfer therefore is by conduction only, then  $h_e =$

$2\lambda_e/D$  applies to the Equations (3.65) – (3.68). It is crucial to make a marked distinction between internal and external resistance, and between internal and external physical properties indeed.  $\square$

## Summary

Analogous to Ohm's law, the link between the temperature difference and the resulting heat flow is shown by Newton's Law of Cooling: transfer rate  $\phi_q$  (in W) is linked to driving force  $\Delta T$  via the heat transfer coefficient  $h$ :

$$\phi_q = h A \Delta T$$

The heat transfer coefficient (= reciprocal resistance) has different values for different situations. The non-dimensional form of  $h$  is the Nusselt number,  $Nu$ . For heat transfer through conduction round a sphere,  $Nu = 2$  applies.

More complex situations (when an object exchanges heat with the ambient medium for instance) can be described more usefully with an overall heat transfer coefficient  $U$ , which is composed from the individual heat transfer coefficients according to  $1/U = 1/h_1 + 1/h_2$ . This relation expresses that the total resistance to heat transfer is the sum of two partial resistances in series, on the analogy of Ohm's law. Whenever one of these two resistances is much smaller than the other, the smallest is often ignored.

## 3.3 Unsteady-state heat conduction

### 3.3.1 Penetration theory: conceptual

In the Sections above, we have looked at heat conduction in steady-state situations. It is now time to consider the more difficult case of unsteady-state (that is, time-dependent, or transient) heat conduction: the temperature in the material or in the fluid-at-rest at a given location is now a function of time, while in general the temperature will vary from one place to another as well. We will first look in detail at the simplest geometry, the 'semi-infinite slab'.

To that end, consider a very large piece of material that takes up half of space, namely that part where  $x \geq 0$ . Initially, the temperature of the whole block is  $T_0$ . At time  $t = 0$ , the temperature of the left-hand side surface ( $x = 0$ ) is suddenly raised to  $T_1$ , where it remains. In many practical situations, it is then important to know how the heat penetrates the material. Or put another way, what is the temperature profile in the material at any given time?

After all the previous examples, it will be obvious that in order to answer these questions, it will be necessary to draw up an unsteady-state heat balance for a

random volume in the material. Given that the material in the directions of  $y$  and  $z$  stretches out into infinity, and that one uniform temperature is being imposed on the entire left-hand side, this is a one-dimensional problem, changes will therefore only be possible in direction  $x$ . A heat balance (= thermal energy balance) for a slice between  $x$  and  $x + dx$  (see Figure 3.11) is therefore sufficient.

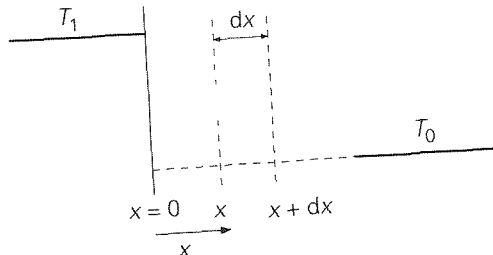


Figure 3.11

The volume for this area is  $V = L W dx$  ( $L$  is the dimension in the direction of  $y$ ,  $W$  in the direction of  $z$ ). The unsteady-state thermal energy balance is now

$$\frac{\partial U}{\partial t} = \frac{\partial(\rho V c_p T)}{\partial t} = LW dx \rho c_p \frac{\partial T}{\partial t} = \phi_{q,in} - \phi_{q,out} \quad (3.69)$$

where the size of the control volume is constant, the fluid is Newtonian, the specific heat  $c_p$  is taken constant, and further the assumption of either constant pressure or constant density has been used (see Bird *et al.*<sup>12</sup>)

The link between the heat flow and the temperature gradient is also shown by Fourier's law in the unsteady-state situation, namely

$$\phi_{q,in} = -LW \lambda \left. \frac{\partial T}{\partial x} \right|_x \quad (3.70)$$

A similar equation applies to the outgoing flow as well, of course. The thermal energy balance can therefore be written as follows

$$\frac{\partial T}{\partial t} = \frac{\lambda}{\rho c_p} \left[ \left. \frac{\partial T}{\partial x} \right|_{x+dx} - \left. \frac{\partial T}{\partial x} \right|_x \right] = \frac{\lambda}{\rho c_p} \frac{\partial^2 T}{\partial x^2} \quad (3.71)$$

As already seen in Chapter 2, the factor  $\lambda/(\rho c_p)$  is usually abbreviated to the symbol  $a$ , the *thermal diffusivity*. This means Equation (3.71) is

$$\frac{\partial T}{\partial t} = a \frac{\partial^2 T}{\partial x^2} \quad (3.72)$$

Differential Equation (3.72) still requires appropriate boundary and initial conditions in order for it to describe the problem in full. These boundary conditions are:

$$\begin{aligned} T(x=0) &= T_1 & \text{for } t \geq 0 \\ T(t=0) &= T_0 & \text{for } x \geq 0 \\ T(x \rightarrow \infty) &= T_0 & \text{for } x \rightarrow \infty \text{ for each } t \end{aligned} \quad (3.73)$$

The first boundary condition means that exactly so much heat can be supplied from the domain  $x < 0$  that at  $x = 0$  the temperature can be kept at  $T_1$ , in other words, the resistance to heat transport lies entirely in domain  $x > 0$  where the molecules account for the heat transport. The last boundary condition means that 'far away' temperature is not (yet) affected by the change to the temperature on the left. This will be dealt with in greater detail later.

### 3.3.2 Temperature profile and penetration depth

With the help of dimensional analysis, it is easy to gain an understanding of which combinations of variables ultimately determine the problem of differential Equation (3.72). For this, the change in temperature from the initial temperature  $T_0$  can be examined (note like in many heat transport cases, the interest is in the temperature difference!). Owing to the above heat balance the relevant parameters are already known.  $T - T_0$  is dependent on  $T_1 - T_0$ ,  $a$ ,  $t$  and  $x$ , therefore

$$T - T_0 = k (T_1 - T_0)^\alpha a^\beta t^\gamma x^\delta \quad (3.74)$$

Solving the resulting set of equations for  $\alpha$ ,  $\beta$ ,  $\gamma$  and  $\delta$  produces  $\alpha = 1$ ,  $\beta = -\delta/2$  and  $\gamma = -\delta/2$  for  $\delta$ , which is yet to be determined (see Chapter 2). From the dimensional analysis, it therefore follows that this problem is determined by two non-dimensional groups, namely

$$\frac{T - T_0}{T_1 - T_0} = F \left( \frac{x}{\sqrt{at}} \right) \quad (3.75)$$

As already discussed in Chapter 2, the form of function  $F$  cannot be determined through dimensional analysis. For that, the exact solution to the problem must be found. Apart from the exact solution, experience shows that in order to find a particular difference in temperature  $T - T_0$  at a certain position  $x$ , more time has to elapse the greater  $x$  is. This experience-based fact can also be inferred from the result of the dimensional analysis. Imagine a particular value for  $T - T_0$ , the value of  $F$  is then established. Suppose that this is measured at time  $t_1$  at place  $x_1$ , then it is logical

<sup>12</sup> Bird R B, W E Stewart and E N Lightfoot, *Transport Phenomena*, Wiley, 2<sup>nd</sup> Ed., 2002, p 337

that this value for  $T - T_0$  at position  $x_2$  ( $> x_1$ ) will be measured later, specifically at time  $t_2$  that complies with

$$\frac{x_2}{\sqrt{at_2}} = \frac{x_1}{\sqrt{at_1}} \rightarrow t_2 = \frac{x_2^2}{x_1^2} t_1 \quad (376)$$

It is only then that the same value for  $F$  is found again. Conversely, if the temperature is measured at fixed position  $x$ , it will appear that the rise in temperature will proceed increasingly slowly at that point.

As already mentioned, the exact temperature profile follows from the solution to differential Equation (372) with boundary conditions (373). Written in two non-dimensional groups, the solution is

$$\frac{T - T_0}{T_1 - T_0} = 1 - \frac{2}{\sqrt{\pi}} \int_0^{\frac{x}{\sqrt{at}}} \exp(-s^2) ds \quad (377)$$

The integral on the right-hand side cannot be solved analytically and is known as error function. This *error function* is tabulated in various handbooks and available in many computer programs such as Excel, Matlab or Maple. The temperature profile according to Equation (377) for a number of different points in time is shown in Figure 3.12.

With the help of temperature profile (377), it is now possible to calculate the heat flux through interface  $x = 0$ , thanks to Fourier's law. This, in other words, is the heat flux that penetrates the material. The result is

$$\phi_q''|_{x=0} = -\lambda \left. \frac{\partial T}{\partial x} \right|_{x=0} = \lambda \frac{T_1 - T_0}{\sqrt{\pi at}} \quad (378)$$

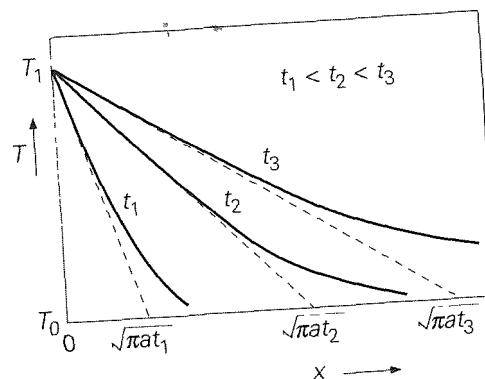


Figure 3.12

The flux decreases over time, as may be expected from the profiles in Figure 3.11 – this shows the gradient in the temperature at  $x = 0$  becoming smaller and smaller over time, so that the flux across the interface decreases. Equation (378) further expresses that the driving force for the heat transport is constant, *viz.*  $T_1 - T_0$  in agreement with the constant boundary conditions at  $x = 0$  and at  $x \rightarrow \infty$ .

Equation (378) is very important and, luckily, easy to remember: the flux at  $x = 0$  can be calculated by dividing the constant driving force  $\Delta T = T_1 - T_0$  by the length scale  $\sqrt{\pi at}$  and then by multiplying by  $\lambda$ . It was already clear that  $\sqrt{\pi at}$  had the dimension of a length scale in Equations (375) and (376). Analogous to Equation (3.17), the combination  $\sqrt{\pi at}/\lambda$  stands for the resistance to heat transport that increases over time because the thickness  $\sqrt{\pi at}$  to which  $\Delta T$  relates, increases.

Length  $\sqrt{\pi at}$  is called the *penetration depth* because this is a typical length over which the temperature of the material noticeably changes within time interval  $t$ . This measure of length therefore expresses how far the heat has penetrated the material. There are two reasons for this choice of dimension: first, the tangent line to the temperature profile at  $x = 0$  at point of time  $t$  cuts through the  $x$ -axis precisely at  $\sqrt{\pi at}$ ; second, the increase in temperature at that position is less than some 20% of the overall driving force.

The penetration depth is a useful quantity for quickly estimating how far the heat has penetrated a material, but it is clear from Figure 3.8 that at each moment the temperature is already rising even where  $x$ -values are greater than the penetration depth. The nature of the temperature profile does not allow an exact measure for the penetration of heat, however. Because of the aforementioned considerations, the heat transport model dealt with above is referred to as the *penetration theory*.

### 3.3.3 Applying penetration theory

An important question that remains is this – when can the penetration theory be applied in practical situations? Answer: in every case that involves unsteady-state heat conduction in a material, the initial temperature of which is uniform, and the temperature of one side of which is suddenly raised and kept at the new temperature. Also, the ‘rear’ of the material may not have undergone any notable change of temperature. After all, one of the boundary conditions is  $T = T_0$  for  $x \rightarrow \infty$  for every  $t$ . This latter condition for the penetration theory imposes a limitation on the duration of validity of the penetration theory. After some time, the temperature of the rear will also have noticeably changed. This can be roughly estimated with the help of the penetration depth.

Suppose that the dimension of the body (towards  $x$ ) is  $D$ , then the penetration theory will be valid as long as the penetration depth is clearly less than  $D$ . To be sure that the temperature at the rear still is the original one (see Figure 3.12), the restriction  $\sqrt{\pi at} < 0.6 D$  is used for security's sake, which translates into

$$\frac{at}{D^2} < 0.1 \quad (3.79)$$

The non-dimensional group  $at/D^2$  has its own name and is known as the Fourier number, or  $Fo$

$$Fo = \frac{at}{D^2} \quad (3.80)$$

$Fo$  is therefore the square of the ratio of two length scales.  $Fo$  compares the distance over which the temperature noticeably changes as a result of conduction with the actual size of the body. This number can also be interpreted in another way.  $Fo$  is also the ratio of two times, namely the actual process time  $t$  in relation to the time needed to noticeably change the temperature of the rear side of the material ( $= D^2/a$ )

Note that the mathematics as discussed above relates to a flat geometry and does not apply directly to curved geometries such as a sphere. Nevertheless, this theory can then still be used as long as the penetration depth is so small that the curvature is not felt. For instance, heat penetrating into a sphere with radius  $R$  will first only be noticed in a very thin shell of thickness  $\delta$ , providing that  $\delta \ll R$ . Penetration theory may safely be applied.

#### Example 3.4. A copper slab

A flat copper slab ( $a = 1.17 \cdot 10^{-4} \text{ m}^2/\text{s}$ ) forms the top of a square channel through which water is flowing (see Figure 3.13). The thickness of the slab,  $D$ , is 3 mm. The water and the slab are both at a temperature of  $20^\circ\text{C}$ . Suddenly, water at  $40^\circ\text{C}$  flows through the channel. (Note that such an abrupt change is not easy to achieve in practice, also, it is assumed that the resistance to the heating up is located in the slab.)

Give an estimate of the time that elapses before the temperature of the top side of the slab noticeably changes.

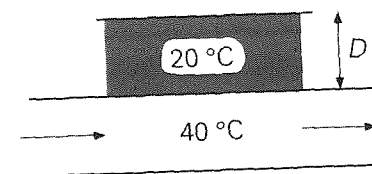


Figure 3.13

The solution to this transient problem can be found by using the error function. If we could apply a quantitative criterion for the qualitative 'noticeable' change of temperature, we could decide that the temperature had changed noticeably if such a change were 5% of the overall difference in temperature. In this case, it is  $1^\circ\text{C}$ . With the help of Equation (3.77), it therefore follows that

$$\operatorname{erf}\left(\frac{D}{2\sqrt{at}}\right) = 1 - \frac{T-T_0}{T_1-T_0} = 0.95 \quad (3.81)$$

Consulting an error function table produces

$$\frac{D}{2\sqrt{at}} = 1.386 \rightarrow t = 0.01 \text{ s}$$

If this time could be estimated by equating the penetration depth to the thickness, then the time could be found from  $D = \sqrt{\pi at}$  and the result would be 0.025 s. The latter value – of course larger than the result found on the basis of the exact solution with the error function (see Figure 3.12) – illustrates once again the somewhat arbitrary nature of the definition of penetration depth.  $\square$

#### Example 3.5. Bitumen on oak

A very large flat sheet of oak ( $\lambda = 0.19 \text{ W/mK}$ ,  $\rho = 800 \text{ kg/m}^3$ ,  $c_p = 2.4 \cdot 10^3 \text{ J/kgK}$ ) has a thickness  $D$  of 1 cm and a uniform initial temperature  $T_w = 20^\circ\text{C}$ .

At  $t = 0$ , a layer of bitumen ( $\lambda = 0.74 \text{ W/mK}$ ,  $\rho = 1300 \text{ kg/m}^3$ ,  $c_p = 920 \text{ J/kgK}$ ) of the same thickness  $D$  is laid onto the wood (see Figure 3.14). This layer has a uniform initial temperature of  $T_b = 50^\circ\text{C}$ .

What, after 5 seconds,

- is the penetration depth in both materials?
- is the temperature of the interface?
- is the heat flux through the interface?
- are the values of the temperature gradients on both sides of the interface between the wood and the bitumen?

It can be assumed that no heat exchange occurs with the surroundings.

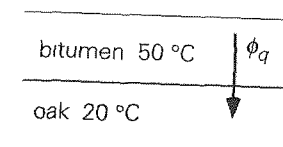


Figure 3.14

It is clear that this is an unsteady-state problem. In order to be able to answer the questions with the help of the penetration theory, it is first necessary to investigate whether the penetration depths are clearly smaller than the thickness of the wood and the bitumen. This effectively amounts to asking question a)

- a) with subscript  $b$  for bitumen and  $w$  for oak, it follows for both penetration depths that

$$\sqrt{\pi a_w t} = 125 \text{ mm}, \sqrt{\pi a_b t} = 31 \text{ mm} \quad (3.82)$$

Given that both penetration depths are clearly less than 0.6 times the thicknesses of the wood and the bitumen layer, the penetration theory may indeed be used for the rest of this problem.

- b) To answer questions b and c, it is first a good idea to establish the terms for the heat flux through the interface. Call the temperature of the interface  $T_i$ . At a random point of time, the heat flux from the bitumen to the interface will be given by (providing that the penetration theory may be used)

$$\phi_q'' = \frac{\lambda_b}{\sqrt{\pi a_b t}} (T_b - T_i) \quad (3.83)$$

Similarly, the flux from the interface into the oak is shown by

$$\phi_q'' = \frac{\lambda_h}{\sqrt{\pi a_h t}} (T_i - T_h) \quad (3.84)$$

Deducting both flux equations (remember that both fluxes are equal) gives.

$$T_i = \frac{\frac{\lambda_b}{\sqrt{a_b}} T_b + \frac{\lambda_h}{\sqrt{a_h}} T_h}{\frac{\lambda_b}{\sqrt{a_b}} + \frac{\lambda_h}{\sqrt{a_h}}} = 311 \text{ K} = 38^\circ\text{C} \quad (3.85)$$

This result illustrates that the interface temperature is not time-dependent and adjusts itself instantaneously at  $t = 0$ .

- c) The fluxes on both sides of the interface are calculated using Equations (3.83) and (3.85), and are therefore, where  $t = 5 \text{ s}$

$$\phi_q'' = 2.7 \text{ kW m}^{-2} \quad (3.86)$$

Both fluxes are therefore time-dependent, but always equal to each other.

- d) The temperature gradients can be calculated from

$$\left. \frac{\partial T}{\partial x} \right|_{\text{interface}} = -\frac{1}{\lambda} \phi_q'' = -\frac{\Delta T}{\sqrt{\pi a t}} \quad (3.87)$$

After 5 seconds, Equation (3.87) produces, for the bitumen

$$\left. \frac{\partial T}{\partial x} \right|_{\text{interface}} = -\frac{(T_b - T_i)}{\sqrt{\pi a_b t}} = -3.9 \cdot 10^3 \text{ K m}^{-1} \quad (3.88)$$

and for oak

$$\left. \frac{\partial T}{\partial x} \right|_{\text{interface}} = -\frac{(T_i - T_h)}{\sqrt{\pi a_h t}} = -14.4 \cdot 10^3 \text{ K m}^{-1} \quad (3.89)$$

This situation, which has now been calculated in full, is illustrated in Figure 3.15. The typical error function profiles (of Figure 3.12) that meet at the constant interface temperature  $T_i$  can clearly be seen on both sides of the interface. Of note also is that the penetration depths and the temperature gradients (both time-dependent) are different on the two sides, which is the result of the different properties of the two materials.

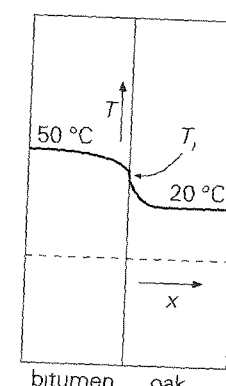


Figure 3.15

### 3.3.4 Heat transfer coefficient for short times

The result of the penetration theory – see Equation (3.78) – can also be written in the form of Newton's Law of Cooling

$$\phi_q'' = h \Delta T = \frac{\lambda}{\sqrt{\pi a t}} \Delta T = \sqrt{\frac{\lambda \rho c_p}{\pi t}} \Delta T \quad (3.90)$$

In other words (note that Equation (3 90) includes the flux)

$$h = \sqrt{\frac{\lambda \rho c_p}{\pi t}} \quad (3 91)$$

In this case, therefore,  $h$  is a function of time! Note that again  $h$  is the reciprocal of the resistance to heat transfer already discussed in the context of Equation (3 78). The related equation for the Nusselt number is now

$$\text{Nu} = \frac{hD}{\lambda} = \sqrt{\frac{\lambda \rho c_p}{\pi t}} \frac{D}{\lambda} = \frac{1}{\sqrt{\pi}} \sqrt{\frac{D^2}{at}} \quad (3 92)$$

or

$$\text{Nu} = 0.564 \text{ Fo}^{-1/2} \text{ providing that } \text{Fo} < 0.1 \quad (3 93)$$

Many cases involve a penetration process that in total takes  $t_e$  seconds (starting from  $t = 0$ , the start of the penetration), it is then often a good idea to calculate the mean heat flow for this process. As the driving force  $\Delta T$  is constant, this amounts to averaging  $h(t)$  over interval  $(0, t_e)$ . In that case, the following applies to the mean flux:

$$\bar{\phi}_q = \frac{1}{t_e} \int_0^{t_e} h(t) A \Delta T dt = \frac{1}{t_e} \int_0^{t_e} h(t) dt A \Delta T = \bar{h} A \Delta T \quad (3 94)$$

With the help of Equation (3 91), it then follows for the mean heat transfer coefficient  $\bar{h}$  that

$$\bar{h} = \frac{1}{t_e} \int_0^{t_e} \sqrt{\frac{\lambda \rho c_p}{\pi t}} dt = 2 \sqrt{\frac{\lambda \rho c_p}{\pi t_e}} = 2 h(t_e) \quad (3 95)$$

As given in Equation (3 95), the time-average  $h$ -value for the interval  $(0, t_e)$  is equal to twice the  $h$ -value at point of time  $t_e$ .

### Example 3.6. A copper slab II

How much heat was supplied to the copper slab in Example 3.4 per unit of surface area during the first 4 ms and how large was the temperature rise after these 4 ms?

The physical properties of copper you may need:  $\lambda = 403 \text{ W/mK}$ ,  $\rho = 8960 \text{ kg/m}^3$ ,  $c_p = 386 \text{ J/kgK}$

The penetration depth at  $t_e = 4 \text{ ms}$  is  $\sqrt{\pi at_e} = 1.21 \text{ mm}$ , so clearly less than  $0.6 D$ . The penetration theory may therefore be used during the entire period of 4 ms. Now that Equation (3 87) is available for  $\bar{h}$ , the question can be easily answered: the total amount of heat (per unit of surface area)  $Q''$  that goes into the slab

follows from integrating the heat flux during the 4 ms

$$Q'' = \int_0^{t_e} \bar{\phi}_q'' dt = \bar{h} t_e \Delta T = 2h(t_e) t_e \Delta T = 5.33 \cdot 10^4 \text{ J m}^{-2} \quad (3 96)$$

This may seem like a very large amount of heat, but the mean rise in temperature  $\Delta T = Q'' / (\rho c_p D)$  of the copper slab in those 4 ms is just  $5.1^\circ\text{C}$

□

### Summary

The partial differential equation for  $T(x,t)$ , which describes the unsteady-state penetration of heat through conduction in a flat slab, has been derived with the help of a micro balance. Both the theory and a few applications of the penetration theory have been looked at, in relation to short periods of time.

The penetration theory, and its associated profiles and formulas, can be used effectively if:

- only conduction is involved;
- if the geometry is flat,
- the temperature of the body is initially uniform, while at  $t = 0$  one side suddenly ‘acquires’ a different fixed temperature;
- if the penetration depth is  $\sqrt{\pi at} < 0.6 D$  – or  $\text{Fo} = (at/D^2) < 0.1$ .

In curved geometries (with radius  $R$ ) penetration theory is applicable as long as  $\sqrt{\pi at} \ll R$

Under these conditions, the temperature profile is written in terms of the error function. You have to be able to sketch the typical temperature profiles that are associated with this and those that illustrate the course of the heat penetration. For the time-dependent heat flux that penetrates the material, the following applies:

$$\bar{\phi}_q'' = h \Delta T = \frac{\lambda}{\sqrt{\pi at}} \Delta T = \sqrt{\frac{\lambda \rho c_p}{\pi t}} \Delta T$$

From this, it follows

$$h = h(t) = \frac{\lambda}{\sqrt{\pi at}} = \sqrt{\frac{\lambda \rho c_p}{\pi t}} \text{ and } \bar{h} = 2 h(t_e)$$

For short periods of time, therefore,  $\Delta T = \text{constant}$ , but  $h = h(t)$ . The latter can also be expressed in terms of non-dimensional numbers.  $\text{Nu} = 0.564 \text{ Fo}^{-1/2}$  (providing that  $\text{Fo} < 0.1$  for a unilaterally heated or cooled slab).

### 3.3.5 Long-term heating

When examining the penetration theory, it was stated expressly that the rear side of the slab should not initially be affected by the penetration of the heat. This requirement is reformulated as follows: at unilateral heating, the penetration depth must be clearly less than the thickness  $D$  of the slab, in other words, if  $Fo < 0.1$ . What course of action should now be taken if this is not (or no longer) the case? The problem can, of course(!), in that case still be described and solved with the help of partial differential Equation (3.72), for which three boundary conditions are still required. However, because the boundary condition at the rear side is now different, the mathematics become complex. Fortunately, though, it appears that in a certain category of problems the situation can be simplified after some time. This is the case with bodies heated from both sides (double-sided) or all round (in the case of a sphere or a cylinder). Here, too, the standard example is a flat geometry, see Figure 3.16.

Figure 3.16 shows a slab of finite thickness  $D$ . Before  $t = 0$ , the whole slab was at temperature  $T_0$ . At  $t = 0$ , the temperature of both surfaces is suddenly raised to, and kept at, temperature  $T_1$ . Now, though, heat is penetrating the material from both sides. The resistance to the heat transport is located entirely in the slab: heat exists in abundance outside it. Clearly (see Figure 3.16), the penetration theory is applicable for short periods of time (for  $t < t_1$  when  $\sqrt{\pi a t_1} < 0.6R$ , i.e., with  $R = D/2$ , when  $\sqrt{\pi a t_1} < 0.3D$  or  $Fo < 0.03$ ).

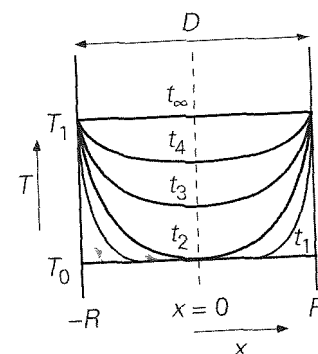


Figure 3.16

However, at a certain moment,  $t = t_2$ , the temperature will start to rise in the middle of the material as well and the penetration theory will no longer be valid: the temperature  $T_0$  disappears, so that the third boundary condition of Equation (3.73) no longer applies either. After some time, for example after  $t = t_3$  (that is, when  $Fo > 0.03$ ), the situation simplifies itself again: it seems that the successive temperature profiles have become spatially similar. For  $t > t_3$ , separation of variables leads to a solution of the form

$$\frac{T - T_0}{T_1 - T_0} = 1 - A(t) f\left(\frac{x}{R}\right) \quad (3.97)$$

The associated boundary conditions are

$$\begin{aligned} T(t=0) &= T_0 && \text{for } |x| \leq R \\ T(x=R) &= T_1 && \text{for } t > 0 \\ \frac{\partial T}{\partial x} &= 0 && \text{for } x=0 \text{ and } t > 0 \end{aligned} \quad (3.98)$$

Substituting Equation (3.97) in the partial differential Equation (3.72), with regard for the boundary conditions (3.98), leads to an exact solution (first found by Fourier) that consists of a series of terms that all have the form of Equation (3.97). Function  $A$  is always an exponential function of time with a negative argument in which  $k^2$  occurs, while  $\cos(k\pi x/D)$  is found for the  $f$  function with just the odd  $k$ -values. The first term in this series gives a sufficiently accurate result for the double-sided heated slab (provided  $Fo > 0.03$ ) in Figure 3.16

$$\frac{T - T_0}{T_1 - T_0} = 1 - \frac{4}{\pi} \exp\left(-\pi^2 \frac{at}{D^2}\right) \cos\left(\pi \frac{x}{D}\right) \quad (3.99)$$

Because the temperature in the slab is now changing *everywhere*, the term *long-term heating* is used.

Now that the temperature profile is known, it is possible to again look at the link between driving force and flux, according to the tested formula of Newton's Law of Cooling, from which an expression for the heat transfer coefficient  $h$  can be expected. Because the temperature is now no longer constant anywhere in the body, it is first necessary to select a temperature in the body on the basis of which the driving force  $\Delta T$  can be established. In practice, there are two choices that are important here: the temperature ( $T_c$ ) of the centre of the body and the mean temperature ( $\langle T \rangle$ ) of the body. Both options are discussed here.

In terms of the *mean temperature*  $\langle T \rangle$ , Newton's Law of Cooling states

$$\phi_q'' = h(T_1 - \langle T \rangle) \quad (3.100)$$

The mean temperature  $\langle T \rangle$  follows by averaging Equation (3.99) and is

$$\langle T \rangle = T_1 - \frac{8}{\pi^2} (T_1 - T_0) \exp\left(-\pi^2 \frac{at}{D^2}\right) \quad (3.101)$$

We then determine  $\phi_q''$  at position  $x = -R$  with the help of temperature profile (3.99), remember that Fourier's law still applies to conduction, even in unsteady-state conditions

$$\phi_q'' = -\lambda \left. \frac{\partial T}{\partial x} \right|_{x=-R} = \frac{2\lambda}{R} (T_1 - T_0) \exp \left( -\pi^2 \frac{at}{D^2} \right) \quad (3.102)$$

Combining Equations (3.100), (3.101), and (3.102) produces (still on the basis of  $\langle T \rangle'$ )

$$h = \frac{2\lambda/R}{8/\pi^2} = \frac{\pi^2 \lambda}{4 R} \quad (3.103)$$

$$\text{or } \text{Nu} = \frac{h 2R}{\lambda} = \frac{\pi^2}{2} = 4.93 \quad (3.104)$$

All in all, this is a very simple and compact result for the condition  $Fo > 0.03$  for double-sided heating or cooling – due to the fact that the temperature profiles are similar in shape

Similarly, in the case of long times ( $Fo > 0.03$ ), the following apply:

$$\begin{aligned} \text{for a long cylinder} \quad \text{Nu} &= 5.8 \\ \text{for a sphere} \quad \text{Nu} &= 6.6 \end{aligned} \quad (3.105)$$

The second way of defining the driving force for the heating up is based on the *temperature of the centre* of the body. The analogy to Equation (3.100) is then

$$\phi_q'' = h(T_1 - T_c) \quad (3.106)$$

Note this concerns the same heat flux, but the driving force has been selected differently, which means there is also a different  $h$ . By eliminating  $T_1 - T_c$  with the help of Equation (3.99), and by comparing the resulting expression for  $\phi_q''$  with Equation (3.102), it is now found that  $\text{Nu} = \pi$ . Here, too,  $h$  is a constant for the longer times, while the driving force for the heat transport, namely  $\Delta T = T_1 - T_c$ , is a function of time. However, the value of  $h$  when  $T_c$  is used differs from the  $h$ -value when  $\langle T \rangle'$  is used.

### Summary

When both sides of a slab are heated up (or cooled down), the temperature profiles become spatially similar at successive points in time, after some initial time has passed ( $Fo > 0.03$ ). The solution to  $T(x, t)$  for this situation has been presented. As this long-term heating continues, the heat flow through the surface can be described

using a constant heat transfer coefficient, while the driving force is actually a function of time. The driving force that is used is either the difference between the surface temperature and the mean temperature, or the difference in temperature between the surface and the centre

The difference between penetration theory and the long-term heating concept can be summarised for a double-sided heated (or cooled) object as follows:

penetration theory	$Fo < 0.03$	$h = h(t)$	$\Delta T = \text{constant}$
long-term heating	$Fo > 0.03$	$h = \text{constant}$	$\Delta T = \Delta T(t)$

For long periods of time, and based on  $\langle T \rangle'$ , the following constant Nusselt numbers should be used:

sphere	6.6
cylinder	5.8
flat slab	4.93

### 3.3.6 The overall heating up of an object

In the foregoing Sections, we have looked at unsteady-state heating through conduction during short and long periods of time separately. For the intermediate range of  $Fo$  values – around 0.1 for unilateral, or around 0.03 for double-sided heating or cooling – the differential equation can also be solved, but this will not be dealt with here.

The exact solutions for the total heating process for a number of finite-size objects are shown in graphic form in Figures 3.17 and 3.18 for the driving force based on  $\langle T \rangle'$  and  $T_c$  respectively. In both graphs, a non-dimensional difference in temperature is shown on the vertical axis, while the Fourier number  $Fo$  (the non-dimensional time) is on the horizontal axis. Notice that the gradients of corresponding lines are the same for longer periods of time and that all straight lines (for  $Fo > 0.03$ ) do not go through point (0,1) on extrapolation.

Finally, it should be mentioned that Figures 3.17 and 3.18 are very practical for, say,  $Fo > 0.03$ , but that for smaller  $Fo$ -values, reading the plot may lead to rather inaccurate results and it is better to use penetration theory anyhow.

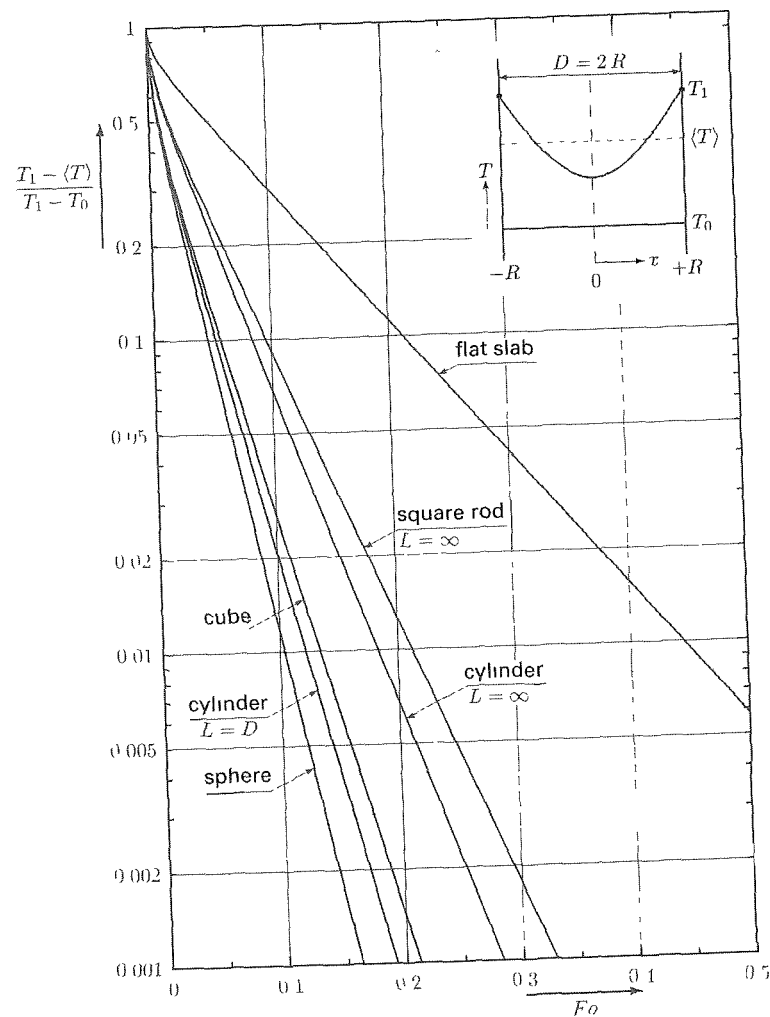


Figure 3.17

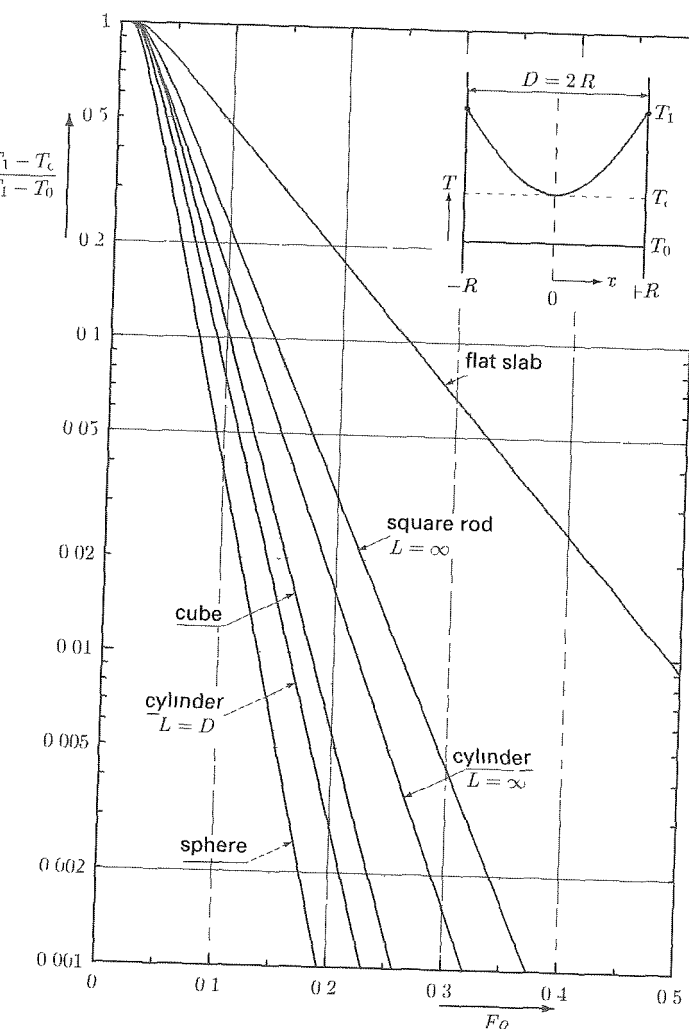


Figure 3.18

**Example 3.7. A glass sphere**

A solid glass sphere ( $a_{\text{glass}} = 4 \cdot 10^{-7} \text{ m}^2/\text{s}$ ) with a diameter of 2 dm has a temperature of 20 °C. Suddenly, the temperature of the surface is increased by 10 °C.

How long does it take until the mean temperature of the sphere has risen by 9 °C?

From the values it follows that

$$\frac{T_1 - \langle T \rangle}{T_1 - T_0} = 0.1$$

Taking this value in Figure 3.17 on the curve for the sphere produces  $Fo = 0.045$

This means that it takes  $4090 \text{ s} \approx 1.1 \text{ hours}$  before  $\langle T \rangle = T_0 + 9 \text{ }^{\circ}\text{C}$

□

### Example 3.8. The glass sphere II

For the same glass sphere of Example 3.7, how long does it take until the temperature at the centre of the sphere has risen by  $9 \text{ }^{\circ}\text{C}$  and calculate the mean temperature of the sphere at that moment in time

First, when the temperature of the centre of the glass sphere has risen by  $9 \text{ }^{\circ}\text{C}$ , the non-dimensional temperature difference

$$\frac{T_1 - T_c}{T_1 - T_0} = 0.1$$

Then it follows from Figure 3.18 that  $Fo = 0.075$ . It therefore takes  $6820 \text{ s} \approx 1.89 \text{ hours}$  before the centre of the sphere has risen by  $9 \text{ }^{\circ}\text{C}$ . As expected, this is markedly longer than in the  $\langle T \rangle$ -example the temperature of the centre is, after all, always the furthest removed from the temperature at the edge,  $T_1$ .

It is now easy to calculate what the mean temperature is if  $T_c = 9 \text{ }^{\circ}\text{C} + T_0$ . Look now at  $Fo = 0.075$  in Figure 3.17. This gives

$$\frac{T_1 - \langle T \rangle}{T_1 - T_0} = 0.03 \rightarrow \langle T \rangle = T_1 - 0.03 (T_1 - T_0) = 29.7 \text{ }^{\circ}\text{C}$$

□

Now that it has been established that for longer periods of time, the internal heat transfer coefficient  $h$  is constant, unsteady-state heating up and cooling down-related problems that only concern the mean temperature of a body can be solved relatively straightforwardly, based on a heat balance for the body in question. Because  $h$  is assumed to be constant (and this is incorrect at the start of the heating up or cooling down process), the solution and outcomes are only approximations.

This method will be illustrated for a sphere that is initially at a uniform temperature of  $T_0$ . At  $t = 0$ , the surface of the sphere is changed to temperature  $T_1$ . The heat balance for the sphere (based on  $\langle T \rangle$ ) is

$$\frac{d(\rho V c_p \langle T \rangle)}{dt} = A h (T_1 - \langle T \rangle) \quad (3.107)$$

from which for constant physical properties

$$\frac{d\langle T \rangle}{dt} = \frac{6h}{\rho c_p D} (T_1 - \langle T \rangle) \quad (3.108)$$

The general solution to this differential equation is, if  $h$  is constant

$$\langle T \rangle - T_1 = K \exp \left( -\frac{6h}{\rho c_p D} t \right) \quad (3.109)$$

Here,  $K$  is an integration constant that has to be determined from the boundary condition. This causes a problem, however. At  $t = 0$ , the temperature in the sphere was  $T_0$ , but  $T_0$  cannot be used as a boundary condition, given that when determining solution (3.109) to the differential Equation (3.108), it was assumed that  $h$  was a constant. This is only the case for the longer periods of time, for shorter periods,  $h = h(t)$ ! This can also be clearly seen in Figures 3.17 and 3.18: for short times, that is for a small  $Fo$ , the lines are curved. As the vertical axis in the figure is logarithmic, this illustrates that the solution to the unsteady-state heat conduction problem for short periods of time does not indeed correspond to the form of Equation (3.109). The line in the figures is straight and the temperature is an e-power only for the longer periods of time, as expressed by Equation (3.109).

Nonetheless, boundary condition  $t = 0 \rightarrow \langle T \rangle = T_0$  is used. In principle, this is incorrect. Whether the error that this leads to is acceptable is difficult to say, generally speaking – this has to be assessed in each individual case.

### Example 3.9. The glass sphere III

For the glass sphere in Examples 3.7 and 3.8, use differential Equation (3.108) and the assumption that  $h$  is constant in order to estimate how long it takes before the mean temperature has risen by  $9 \text{ }^{\circ}\text{C}$ .

From the exact solution obtained with the help of Figure 3.18, it is already known (see Example 3.7) that  $\langle T \rangle = T_0 + 9 \text{ }^{\circ}\text{C}$  after  $t = 4090 \text{ s}$ . Solving Equation (3.108) with  $h = \text{constant}$  for every  $t$  and with boundary condition  $\langle T \rangle = T_0$  produces

$$\frac{T_1 - \langle T \rangle}{T_1 - T_0} = \exp \left( -\frac{6h}{\rho c_p D} t \right) \quad (3.110)$$

With the help of non-dimensional numbers, Equation (3.110) is written as

$$\frac{T_1 - \langle T \rangle}{T_1 - T_0} = \exp \left( -\frac{6 \text{Nu} (\lambda/D)}{\rho c_p D} t \right) = \exp (-6 \text{Nu} Fo) \quad (3.111)$$

In the case of long-term heating of a sphere,  $\text{Nu} = 6.6$ . With the help of the values for  $a$ ,  $D$  and  $\text{Nu}$ , it now follows that  $\langle T \rangle = T_0 + 9 \text{ }^{\circ}\text{C}$  after  $t = 5290 \text{ s}$ . This

approach results in a clearly longer time than that found in Example 3.7 with the help of Figure 3.18

□

Finally, we will demonstrate through an example how a long-term heating problem with one insulated wall can quickly be solved with the help of Figures 3.17 and 3.18

#### Example 3.10. A drum cooler

A drum cooler (diameter  $D = 1 \text{ m}$ ) has a surface temperature of  $20^\circ\text{C}$  and rotates at a rate of one revolution per minute. A bituminous product at a temperature of  $80^\circ\text{C}$  (bitumen just about flows at this temperature) is applied to the drum cooler, before being scraped off again after one quarter of a revolution. It is required that then the mean temperature of the cooled bitumen is no higher than  $25^\circ\text{C}$ . Heat exchanged between the bitumen and the surrounding air is negligible. For the bitumen it is given that  $c_p = 920 \text{ J/kgK}$ ,  $\rho = 10^3 \text{ kg/m}^3$  and  $\lambda = 0.17 \text{ W/mK}$ . The question to be answered is this: how thick may the layer of bitumen be in order for the requirement regarding the mean temperature at the point at which it is scraped off to be met?

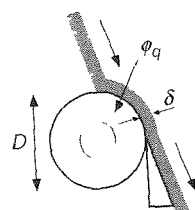


Figure 3.19

First of all, it should be realized that bitumen at the conditions of interest ('just about flowing') more or less behaves as a solid material moving in plug flow with the drum. When moving with a small volume element in the bitumen layer, one would notice how temperature decreases in time. This also implies that the heat to be removed via the drum can only be transported towards the drum by conduction.

It may further be assumed that the thickness of the layer of bitumen is much less than the radius of the drum cooler and this implies that the curvature of the bitumen layer may be ignored. The problem can therefore be regarded as the cooling off of a flat plate. Figure 3.19 shows the typical dimensions and flows.

Finally, it may safely be assumed that there is no heat exchange between the bitumen and the air – in reality it is not absolutely zero, but very small in comparison with the heat flow on the side of the drum cooler. But then, owing to Fourier's law, the temperature gradient on the surface of the bitumen is also zero (more or less).

$$\phi_q'' = -\lambda \frac{dT}{dx} = 0 \rightarrow \frac{dT}{dx} = 0 \quad (3.112)$$

If the layer of bitumen is now reflected in this interface and this mirror image is 'attached' to the actual layers, then the situation arises that was dealt with in the case of long-term heating of a thin layer (from both sides). Consequently, Figures 3.17 and 3.18 can be used *providing* that  $2\delta$  is used as the thickness of the layer. It was required that the cooled bitumen was no higher than  $25^\circ\text{C}$ . Of course, the highest temperature is found on the airside of the bitumen. This is therefore the centre of the layer including its mirror image. Using Figure 3.18 then produces the following

$$\frac{T_1 - T_c}{T_1 - T_0} = \frac{20 - 25}{20 - 80} = 0.083 \rightarrow \text{Fo} = 0.275 \quad (3.113)$$

or  $at/(2\delta)^2 = 0.275$ . The time can be inferred from the fact that the bitumen spends one quarter of a revolution on the drum cooler, so  $t = 15 \text{ s}$ . From this, it follows that the maximum layer thickness is  $\delta_{\max} = 1.6 \text{ mm}$

□

#### Summary

When solving unsteady-state long-term heat conduction problems, it is possible to use two graphs in which the non-dimensional driving force has been plotted versus the Fourier number. These graphs represent the exact solution.

In addition, the technique of a heat balance with a constant heat transfer coefficient can be used for the heating up or cooling down of a body, for an approximate solution.

#### 3.3.7 Internal and external heat transport

It was assumed throughout the previous Sections that the surface temperature of the object was changed to a fixed level at a given point in time ( $t = 0$ ). In practice, however, it will *not* usually be the surface temperature that is changed to a constant level. In most cases, the object will suddenly enter an environment in which the temperature is different to that of the object. Heat has to be transported from the bulk of the environment to the surface of the object (or indeed vice versa) before the heat can flow into (or out of) the object. This will involve not just an internal heat resistance ( $1/h_i$ ) in the object, but also an external heat resistance ( $1/h_e$ ) in the surrounding medium.

Analogous to the topic covered in § 3.2.3, this produces an overall heat resistance ( $1/U$ ), in accordance with

$$\frac{1}{U} = \frac{1}{h_i} + \frac{1}{h_e} = \frac{1}{\text{Nu}_i \lambda_i} + \frac{1}{\text{Nu}_e \lambda_e} \quad (3.114)$$

Equation (3.114) builds upon Equation (3.59). An important difference is that now we have to do with a transient situation which should be reflected by the value of  $\text{Nu}_i$ . With a view to situations (to be dealt with later on) that the medium around the object is not stagnant, also the external resistance has been expressed in terms of an external Nusselt number  $\text{Nu}_e$ , in the case of a stagnant external medium around a spherical object, usually  $\text{Nu}_e = 2$  (see § 3.2.2) is used for the sake of simplicity. Here, too, a clear distinction has to be made between internal and external resistance to heat transport, between internal and external Nusselt numbers, and between the thermal conductivity coefficients of the internal and external media.

Again, in case one of the two partial resistances to heat transport is much smaller than the other, it is not unusual to ignore the smallest resistance of the two (either the internal or the external). Note that in the very beginning of the heating or cooling process the value of the internal heat transfer coefficient is very high for a short while see Equation (3.91). As a matter of fact, the external resistance to heat transport has been ignored in the earlier treatment of transient heat conduction. In the example below, both resistances will be taken into account – resulting in a slower heating of the object than in the earlier examples.

#### Example 3.11. The glass sphere IV

The initial temperature of the sphere we ‘used’ before was  $20^\circ\text{C}$ . Now, the ambient temperature suddenly rises by  $10^\circ\text{C}$ . The heat transfer coefficient for heat transport from the bulk of the surroundings to the sphere is  $h_e = 10 \text{ W/m}^2\text{K}$ . How long does it now take for the mean temperature of the sphere to rise by  $9^\circ\text{C}$ ?

Figure 3.17 cannot be used for finding the solution, as there is also an external heat resistance. However, a heat balance can still be drawn up, entirely analogous to that of Equation (3.108). Here, boundary condition  $\langle T \rangle = T_0$  at  $t = 0$  is applied, which means we again act as if the overall heat transfer coefficient  $U$  is constant throughout the heating up period. The same function will then be found for the mean temperature as that in (3.110).

$$\frac{T_1 - \langle T \rangle}{T_1 - T_0} = \exp\left(-\frac{6U}{\rho c_p D} t\right) \quad (3.115)$$

The only thing to have changed is that  $h$  has been replaced by  $U$ . Again, however, this is *not* an exact solution (because  $U$  is not constant from the beginning). The overall heat transfer coefficient  $U$  follows from

$$\frac{1}{U} = \frac{1}{h_e} + \frac{1}{h_i} = \frac{1}{h_e} + \frac{1}{\text{Nu}_i \lambda_i} \quad (3.116)$$

Unlike in the previous examples (where just the value of  $\alpha_{\text{glass}}$  was needed), we now require  $\lambda_{\text{glass}} = 0.8 \text{ W/mK}$ . This produces  $U = 7.3 \text{ W/m}^2\text{K}$ , which means the time needed is  $t = 1.9 \cdot 10^4 \text{ s} \approx 5.3 \text{ hours}$ . As expected, this is longer than in the case without external heat resistance.  $\square$

#### Summary

Also in unsteady-state heat conduction problems, the internal heat transport resistance should be clearly distinguished from the external one. The overall heat transfer coefficient  $U$  follows from

$$\frac{1}{U} = \frac{1}{h_i} + \frac{1}{h_e}$$

This relation expresses that the total resistance is the sum of two partial resistances, the internal and the external. As a result, there are also two Nusselt numbers,  $\text{Nu}_i$  and  $\text{Nu}_e$ , each defined with the thermal conductivity coefficient of the medium involved. Whenever one of the two partial resistances is (much) smaller than the other one, the smallest may be ignored.

#### 3.3.8 Numerical approach

The unsteady-state penetration theory can also be tackled numerically. The equation

$$\rho c_p \frac{\partial T}{\partial t} = \lambda \frac{\partial^2 T}{\partial x^2} \quad (3.117)$$

$$\text{with } T(t=0) = T_1, \quad T(0, x) = T_0, \quad T(t, x \rightarrow \infty) = T_0$$

is different in terms of structure to that for steady-state heat conduction. By again looking at the derivative of the equation in § 3.3.1, it is easy to derive the discrete variable of the above differential equation here. The semi-infinite slab is divided into strips of finite thickness  $\Delta x$ . Consider a random strip, P, and name its neighbours West (W) and East (E). The heat balance drawn up for strip P for a time step  $\Delta t$  is

$$\begin{aligned} \rho c_p \frac{T_P(t+\Delta t, x) A \Delta x - T_P(t, x) A \Delta x}{\Delta t} &= \\ &= -\lambda \frac{T_P - T_W}{\Delta x} A - \left( -\lambda \frac{T_E - T_P}{\Delta x} A \right) \end{aligned} \quad (3.118)$$

The time is now also discretised the temperature distribution is only calculated on the multiples of  $\Delta t$  ( $t_i = i \Delta t$ , where  $i = 1, 2, 3, \dots$ ) It is therefore sufficient to indicate the time using an index  $i$  This means the above equation can be written as follows

$$T_P^{i+1} = T_P^i + \frac{a \Delta t}{\Delta x^2} (T_W^i + T_E^i - 2T_P^i) \quad (3.119)$$

where  $a = \frac{\lambda}{\rho c_p}$  as before

In Equation (3.119), we can put the terms together, using  $T_P^i$

$$T_P^{i+1} = \left(1 - \frac{2a \Delta t}{\Delta x^2}\right) T_P^i + \frac{a \Delta t}{\Delta x^2} (T_W^i + T_E^i) \quad (3.120)$$

The superscript refers to the point in time, and the subscript to the position Solving the above equation is easy for each new time step, the only thing that is needed is information from the previous time step However, choices still have to be made for  $\Delta x$  and  $\Delta t$ , and they cannot be made entirely independently of each other It is easy to understand that for  $\frac{a \Delta t}{\Delta x^2} > \frac{1}{2}$ , a negative (that is, unstable) link arises between  $T_P^{i+1}$  and  $T_P^i$

In Figure 3.20, a number of examples are given of the numerical solution to the penetration theory problem This is done for a slab of copper ( $a = 1.17 \cdot 10^{-4} \text{ m}^2/\text{s}$ ), with thickness  $D = 1 \text{ m}$  At  $t = 0$ , the temperature on one side is raised by  $10^\circ\text{C}$  For the numerical simulations, the domain of the calculation must be finite, of course: the other side is subject to the boundary condition that the copper there is insulated The penetration theory can be used if  $\sqrt{\pi a t} < 0.6 D$  This corresponds to  $t < 980 \text{ s}$

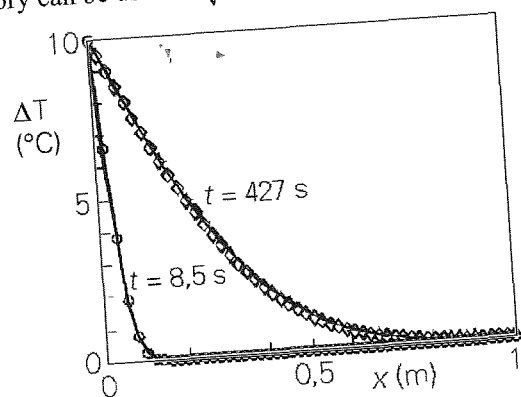


Figure 3.20

Figure 3.20 shows numerical solutions for two points of time  $t = 8.5 \text{ s}$  and  $427 \text{ s}$ , respectively (where  $\Delta x = 0.02 \text{ m}$  and  $\Delta t = 0.85 \text{ s}$ ) It also shows the analytical solutions as solid lines for these two moments in time It is clear that the numerical solutions closely correspond to the analytical ones

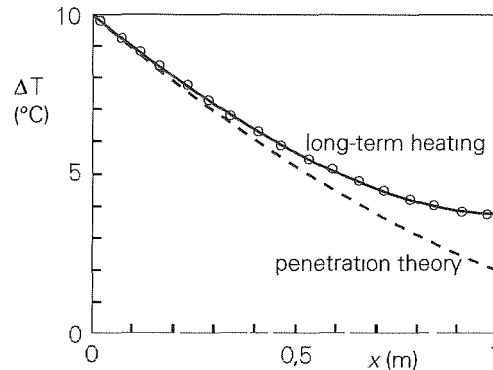


Figure 3.21

The numerical methods can of course be used effectively in the case of long-term heating The temperature distribution of the copper strip for  $t = 2654 \text{ s}$  is shown in Figure 3.21 The numerical solution is denoted by the symbols, while the solid line is the analytical long-term solution to Equation (3.99) There is a good agreement between numerical and analytical solutions The broken line is the solution according to penetration theory which, it is clear, is no longer valid here

### Summary

The coverage of numerical methods has been extended to time-dependent problems The discretisation according to time has been explained and illustrated The choice of the time step is linked to the size of  $\Delta x$

## 3.4 The general micro balance for heat transport

In general, pure heat conduction will not be the only factor at play A liquid or a gas can of course also transport heat convectively Moreover, heat does not always have to be transported in one direction This Section will therefore look at how situations are described in which both convection and conduction play a role Just as with simple one-dimensional heat conduction cases, the starting point is a micro balance for an elementary volume somewhere in the domain under consideration In order for the micro balance to be valid as generally as possible, as few assumptions as possible

will be made. For the sake of simplicity, however, a Cartesian coordinate system will be used.

Consider in the three-dimensional domain a fluid that is flowing, the temperature of which varies from one place to another. Take any block from somewhere in the flow between  $x$  and  $x + dx$ ,  $y$  and  $y + dy$ , and  $z$  and  $z + dz$  in the fluid. This is the control volume, the size of which is  $dxdydz$ . The situation is illustrated in Figure 3.22.

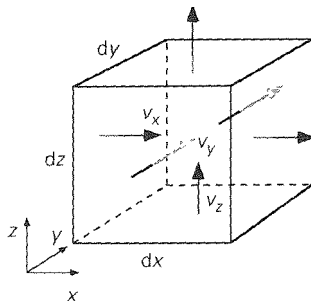


Figure 3.22

A heat balance can now be drawn up for this control volume. The various terms of a heat balance of this kind will now be discussed: the heat accumulation term that is always on the left-hand side of a balance, the heat transport terms ‘in’ and ‘out’ on the six surfaces of the control volume, and the heat production. A distinction must be made between convection and conduction when using the heat transport terms. Because, in principle, each variable depends on time and place, all derivatives may be partial derivatives, denoted by the partial-derivative symbol  $\partial$ .

#### Accumulation

The unsteady-state term is

$$\frac{\partial U}{\partial t} = \frac{\partial}{\partial t} (\rho u dxdydz) = \rho c_p \frac{\partial T}{\partial t} dxdydz \quad (3.121)$$

where the size of the control volume ( $= dxdydz$ ) is constant, the fluid is Newtonian, the specific heat  $c_p$  is taken constant, and further the assumption of either constant pressure or constant density has been used (see Bird *et al*<sup>13</sup>).

#### Convective transport

Flow rate  $v_x(x,y,z) dydz$  with an internal energy concentration of  $\rho c_p T(x,y,z)$  in J/m<sup>3</sup> enters a volume through the surface on the left-hand side. Therefore, entering this side convectively is

$$[v_x \rho c_p T]_{x,y,z} dydz \quad (3.122)$$

<sup>13</sup> Bird R B, W E Stewart and E N Lightfoot, *Transport Phenomena*, Wiley, 2<sup>nd</sup> Ed., 2002, p. 337

However, thermal energy flows *out* convectively through the right-hand side of the volume. The magnitude of this flow is, of course

$$[v_x \rho c_p T]_{x+dx,y,z} dydz \quad (3.123)$$

Together, these two flows make a net contribution to convective transport in the direction of  $x$  (the  $y$  and  $z$  subscripts can be left out; they have them in common anyway)

$$\begin{aligned} & [v_x \rho c_p T]_x dydz - [v_x \rho c_p T]_{x+dx} dydz = \\ & = - \frac{\partial}{\partial x} (v_x \rho c_p T) dxdydz \end{aligned} \quad (3.124)$$

Entirely analogously, the convective flows through the front and rear sides produce, net

$$\begin{aligned} & [v_y \rho c_p T]_y dx dz - [v_y \rho c_p T]_{y+dy} dx dz = \\ & = - \frac{\partial}{\partial y} (v_y \rho c_p T) dx dy dz \end{aligned} \quad (3.125)$$

and through the bottom and top sides

$$\begin{aligned} & [v_z \rho c_p T]_z dx dy - [v_z \rho c_p T]_{z+dz} dx dy = \\ & = - \frac{\partial}{\partial z} (v_z \rho c_p T) dx dy dz \end{aligned} \quad (3.126)$$

#### Molecular transport

The molecular heat flow (conduction) can be described using Fourier’s law. The following comes in through the left-hand side of the control volume, via conduction

$$-\lambda \left[ \frac{\partial T}{\partial x} \right]_{x,y,z} dy dz \quad (3.127)$$

The following leaves through the right-hand side, again via conduction

$$-\lambda \left[ \frac{\partial T}{\partial x} \right]_{x+dx,y,z} dy dz \quad (3.128)$$

Merging these two flows in the direction of  $x$  produces

$$-\lambda \left[ \frac{\partial T}{\partial x} \right]_{x,y,z} dy dz - \left\{ -\lambda \left[ \frac{\partial T}{\partial x} \right]_{x+dx,y,z} \right\} dy dz =$$

$$= \frac{\partial}{\partial x} \left[ \lambda \frac{\partial T}{\partial x} \right] dx dy dz \quad (3.129)$$

The front and rear sides contribute to the net flow in the direction of  $y$  in the same way:

$$\begin{aligned} -\lambda \left[ \frac{\partial T}{\partial y} \right]_{x,y,z} dx dz - \left\{ -\lambda \left[ \frac{\partial T}{\partial y} \right]_{x,y+dy,z} \right\} dx dz = \\ = \frac{\partial}{\partial y} \left[ \lambda \frac{\partial T}{\partial y} \right] dx dy dz \end{aligned} \quad (3.130)$$

while in the direction of  $z$ , the net contribution is equal to

$$\begin{aligned} -\lambda \left[ \frac{\partial T}{\partial z} \right]_{x,y,z} dx dy - \left\{ -\lambda \left[ \frac{\partial T}{\partial z} \right]_{x,y,z+dz} \right\} dx dy = \\ = \frac{\partial}{\partial z} \left[ \lambda \frac{\partial T}{\partial z} \right] dx dy dz \end{aligned} \quad (3.131)$$

#### Production

Finally, it is still possible for heat to be produced in the control volume. It is usual to indicate the production per unit of volume using the letter  $q$  (just as the transformation per unit of volume is usually used with chemical reactions). In the control volume, therefore,

(3.132)

$$q dx dy dz$$

In general, heat production is a function of position and time, therefore of  $\{t,x,y,z\}$

#### The general micro balance for heat transport

Combining the accumulation term, all the net flows (six in all), and the production term now gives us the heat balance for the control volume

$$\begin{aligned} \frac{\partial(\rho c_p T)}{\partial t} dx dy dz = \\ -\frac{\partial}{\partial x} (v_x \rho c_p T) dx dy dz - \frac{\partial}{\partial y} (v_y \rho c_p T) dx dy dz - \frac{\partial}{\partial z} (v_z \rho c_p T) dx dy dz + \\ + \frac{\partial}{\partial x} \left[ \lambda \frac{\partial T}{\partial x} \right] dx dy dz + \frac{\partial}{\partial y} \left[ \lambda \frac{\partial T}{\partial y} \right] dx dy dz + \frac{\partial}{\partial z} \left[ \lambda \frac{\partial T}{\partial z} \right] dx dy dz + \\ + q dx dy dz \end{aligned} \quad (3.133)$$

The method used here for drawing up the general micro balance is known as the *cubic volume element method*.

Equation (3.133) can be simplified by dividing by  $dx dy dz$  and is usually written in a slightly different form, namely by transferring the convective terms to the left-hand side

$$\begin{aligned} \frac{\partial(\rho c_p T)}{\partial t} + \frac{\partial}{\partial x} (v_x \rho c_p T) + \frac{\partial}{\partial y} (v_y \rho c_p T) + \frac{\partial}{\partial z} (v_z \rho c_p T) = \\ = \frac{\partial}{\partial x} \left[ \lambda \frac{\partial T}{\partial x} \right] + \frac{\partial}{\partial y} \left[ \lambda \frac{\partial T}{\partial y} \right] + \frac{\partial}{\partial z} \left[ \lambda \frac{\partial T}{\partial z} \right] + q \end{aligned} \quad (3.134)$$

If the differences in temperature are now not so great, it is possible to work with a constant  $\lambda$  and to allow Equation (3.134) to be simplified to

$$\begin{aligned} \frac{\partial(\rho c_p T)}{\partial t} + \frac{\partial}{\partial x} (v_x \rho c_p T) + \frac{\partial}{\partial y} (v_y \rho c_p T) + \frac{\partial}{\partial z} (v_z \rho c_p T) = \\ = \lambda \left[ \frac{\partial^2 T}{\partial x^2} + \frac{\partial^2 T}{\partial y^2} + \frac{\partial^2 T}{\partial z^2} \right] + q \end{aligned} \quad (3.135)$$

Equation (3.134) is the general form of heat transport in a fluid if the fluid conforms to Fourier's law. Remember that it is not just the temperature  $T$  that is unknown in this Equation, the same applies to the entire velocity field  $\{v_x, v_y, v_z\}$ , and it too therefore has to be solved! In Chapter 5, we will derive what the general balance for velocity (= momentum concentration) looks like. It will also deal with how the balance for the density of the liquid generally looks. All these balances have to be solved at the same time in order that the three-dimensional temperature profile in the fluid can be determined. Numerical solving techniques are available for this purpose. Remember that for solving differential equations, initial and boundary conditions are always required.

In practical situations that many engineers have to deal with, the problems are mostly too complex to be calculated with these general micro balances. In addition, it is by no means always necessary for the whole temperature profile or the whole velocity field to be solved exactly or numerically. Reasonably accurate models and calculations will suffice. For that reason, a more phenomenological approach will be adopted in the Sections that follow, firmly aimed at thinking in terms of driving force (cause) and its associated flow (consequence). Transfer coefficients and non-dimensional numbers play an important role here.

In everyday practice, the use of numbers and correlations between them is still the most suitable method. This does not mean, however, that such correlations are not theoretically substantiated, and it does not mean either that the use of numerical solutions to the general micro balances will not become increasingly important in industrial practice in the future!

### Summary

The generally valid micro balance for heat transport is derived with the help of the cubic volume element method. In this analysis, account has been taken of the possibility of transporting heat both by convection and conduction. This micro balance contains not only the temperature field, but also the velocity field and the density field as unknown functions, and therefore cannot be solved without additional equations. However, the balance does contain every case of heat conduction in a fluid that complies with Fourier's law.

## 3.5 Heat transfer coefficient with convection

### 3.5.1 General observations

After the introduction of the generally valid micro balance for heat transport in the previous Section, the rest of this chapter will look at more specific heat transfer situations. First, the focus will be directed at the phenomenon of heat transport from a solid wall to a flowing medium (or in the reverse direction). This is a very common situation in the real world.

An example that comes to mind is that of an exothermic reaction in an ideally stirred tank. The heat that is released will, in many cases, have to be removed. This can be done by hanging a cooling spiral in the container, for example, through which cold water flows. In order to properly dimension and operate equipment of this nature, it is necessary to know how much heat the cooling water will remove under the different range of conditions that could occur. The transfer of heat from the contents of the tank to the wall of the spiral, for example, will certainly depend on the flow conditions in the tank. Similarly, the transfer of heat from the wall of the spiral to the cooling water will depend on the flow conditions in the cooling spiral.

It is therefore important to analyse in greater detail what heat transport from a solid wall to a medium flowing along it depends on. To that end, let us reduce this (and similar) situations to the case of a warm wall along which a cold liquid flows by. Two mechanisms are involved, which occur simultaneously. This is illustrated in Figure 3.23 in this case.

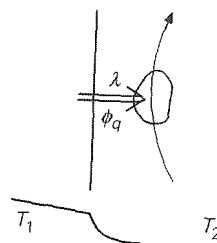


Figure 3.23

Firstly, *heat conduction* perpendicular to the wall is needed in order for the heat from the solid wall to get transferred to the initial layers of liquid. After all, the layer of liquid immediately next to the wall is motionless in relation to the wall, as a matter of fact, there is also no flow normal to the wall. This means that no heat transport through convection can occur here. Once the heat has penetrated the initial layers, through conduction, the second mechanism becomes operational. Now, the heat no longer needs to be transported via conduction only, but the liquid packages in the vicinity of the wall (which are warmer than the bulk of the liquid) are carried past the wall by the much more powerful *convective transport* and, in the case of turbulent flow as a result of the occurrence of eddies, at right-angles to the wall, this means that the heat that was 'conducted' into the liquid will be also be carried off. This in turn means that the driving force for the heat conduction into the initial layers continues to exist.

Newton's phenomenological law of cooling is used to describe this complex heat transfer process:

$$\phi_q = h A \Delta T \quad (3.136)$$

It is therefore important to find  $h$  and/or Nusselt values for the various situations and geometries. Because account now has to be taken of the flow of the liquid (or the gas), the situation becomes much more complex than if only conduction were to play a role. An exact solution using analysis is therefore only achievable in a small number of cases. However, it is possible to derive approximate solutions via the so-called 'boundary layer theory', which are also supported by experiments, but for this it is necessary to consider the energy balance and the momentum and mass balances for the flowing liquids. Here, only the phenomenological approach in terms of  $h$  and  $Nu$  will be pursued.

First, using dimensional analysis, an examination will be made of which non-dimensional groups can play a part. It will be clear from the start that the Reynolds number will occur, as well as  $Nu$ , given that flow is involved. The analysis starts with an inventory of the variables on which the heat transfer coefficient  $h$  may depend. In general,  $h$  depends on

$\lambda$	there is conduction from the wall into the liquid (see Figure 3.18),
$D, \rho, \langle v \rangle$	this can be used to determine the mass flow rate of liquid that flows past a wall or object,
$x$	distance $x$ from the start of the tube or from the point at which heat transfer occurs potentially of importance in the case of flow in a pipe if the conditions in the vicinity of the pipe wall are still changing,
$c_p$	co-determines how much heat the liquid can absorb and carry off (or give up),
$\mu, \mu_w$	the viscosity of the bulk of the fluid and the viscosity on the wall respectively after all, the viscosity is a measure of the mobility of a fluid and co-determines the distance from the wall at which convection starts to predominate over conduction, in addition, the viscosity is needed to describe the flow, such as with Re, but with a (large) difference in temperature between the bulk of the liquid and the liquid at the wall, $\mu$ and $\mu_w$ can differ somewhat,
$\Delta T$	the driving force behind the heat flow from the wall to the bulk can sometimes actually affect the value of $h$ itself, namely by introducing extra flow through changes in density,
$\beta$	the thermal expansion coefficient $\beta = -(1/\rho)(dp/dT)$ in combination with a difference in temperature $\Delta T$ , a difference in density may occur in a fluid, thereby inducing flow, thanks to gravity $g$ (known as free convection),
$g$	the gravitational acceleration, only relevant in the case of free convection

In other words

$$h = f(\lambda, D, \rho, \langle v \rangle, x, c_p, \mu, \mu_w, \Delta T, \beta, g) \quad (3.137)$$

All these variables should be included in a dimensional analysis twelve variables with four basic units According to the Buckingham II theorem, therefore, eight non-dimensional groups play a role Performing the dimensional analysis, perhaps after some rearranging, results in the following groups:

$$\text{Nu} = f(\text{Re}, \text{Pr}, \text{Br}, \beta\Delta T, \text{Gz}, \text{Gr}, \text{Vi}) \quad (3.138)$$

where Nu stands for the Nusselt number, Re for the Reynolds number, Pr for the Prandtl number, Br for the Brinkman number, Gz for the Graetz number, Gr for the Grashof number, and Vi for the 'viscosity group' The various numbers are given below, with their physical meanings

$$\text{Nu} = \frac{hD}{\lambda} = \frac{\text{actual heat transfer}}{\text{heat transfer caused only by conduction}}$$

$$\text{Re} = \frac{\rho \langle v \rangle D}{\mu} = \frac{v \rho v}{\mu v / D} = \frac{\text{inertia}}{\text{friction}} \quad (\text{see } \S 2.2.2)$$

$$\text{Pr} = \frac{c_p \mu}{\lambda} = \frac{v}{a} = \frac{\text{velocity of molecular momentum transfer}}{\text{velocity of molecular heat transfer}}$$

(see § 2.2.1)

$$\text{Br} = \frac{\mu \langle v \rangle^2}{\lambda \Delta T} = \frac{\mu \langle v \rangle^2 D}{\frac{\lambda}{D} \Delta T} = \frac{\text{heat production through dissipation}}{\text{heat transport through conduction}}$$

$$\beta \Delta T = \frac{\Delta \rho}{\rho} = \text{relative density difference as a result of } \Delta T$$

$$\text{Gz} = \frac{ax}{\langle v \rangle D^2} = \frac{\text{heat transfer through conduction}}{\text{heat transfer through convection}}$$

(also a kind of Fourier number)

$$\text{Gr} = \frac{\beta \Delta T g x^3}{\nu^2} = \frac{\Delta \rho g x}{\rho \langle v \rangle^2} \left( \frac{\rho \langle v \rangle D}{\mu} \right)^2 \left( \frac{x}{D} \right)^2 = \frac{\text{buoyancy}}{\text{friction}}$$

$$\text{Vi} = \frac{\mu}{\mu_w} = \text{measure for viscosity differences as a result of } \Delta T$$

As can be seen, all the numbers stand for ratios of driving forces, transport velocities, or transport quantities It is also evident that some of the widely used numbers are actually composed of several others, in many cases, this is a question of preferences that have evolved over time Not all these numbers play a role all the time The Grashof number, for example (a kind of Reynolds number for free convection) plays no part in conditions that are fully dominated by forced convection Forced and free convection are discussed separately below, for that reason The Brinkman number will not feature in the remainder of this book it is relevant primarily in the case of flows of highly viscous polymers in which a large amount of frictional heat develops

### Summary

Two mechanisms play a role in the case of heat transfer from a solid wall to a flowing medium: conduction from heat at right-angles to the wall through the initial layers of the liquid, which are located immediately next to the wall, and convective transport of heat parallel to the wall through the flowing liquid (or gas). Dimensional analysis can be used to determine which non-dimensional numbers can determine heat transfer. Problems of this kind are generally governed by eight numbers, but in practice it is rarely the case that all eight are needed at the same time.

### 3.5.2 Heat transfer in the case of forced convection

#### Heat transfer in the case of forced pipe flow

In the case of heat transfer from or to a fluid that is *forced* to flow through a tube, under the influence of a difference in pressure, for example, no more than five of the aforementioned eight numbers play a role, namely

$$\text{Nu} = f(\text{Re}, \text{Pr}, \text{Gz}, V_1) \quad (3.139)$$

One role of the Reynolds number is certainly clear here: it very much matters for the heat transfer whether the flow through the tube is laminar or turbulent. With turbulent flow, the eddies also transport the heat across the main direction of flow, while with laminar flow, only conduction is responsible for transport in that direction. These two types of flow therefore have to be treated separately.

Below, Nu relations will be presented for a variety of situations. The first remark to be made is that this selection is not exhaustive: just typical cases have been identified. After all, the bottomline is about how such relations are used in heat balances for solving heat transfer problems. Further, these correlations are often empirically determined – see also the discussion after Equation (2.53) – although in a number of cases the exponents of the non-dimensional numbers are also found with the help of analytical derivations or models (which are beyond the scope of this introductory textbook).

#### Laminar pipe flow

As said, in laminar pipe flows radial heat transport only takes place through conduction within and between the layers ('*laminae*') that are typical of laminar flow; the radial velocity profile then affects the speed at which these *laminae* slide over each other and in this way also affects the conductive radial heat transport. As a result, laminar flows exhibit radial temperature profiles. In many cases, however, one is not really interested in these radial temperature profiles; rather, information about the average temperature as a function of the downstream coordinate  $x$  may be sufficient. Conceptually, this average temperature  $\langle T(x) \rangle$  could be obtained by

collecting at any position  $x$  the flow of liquid in a cup and mixing the collected liquid, and may therefore be denoted as the *mixing cup temperature*.

If a fluid flows into a tube at a particular flow rate, then the velocity profile at the tube entrance depends strongly on the situation prior to this – that is, upstream from the entrance. The velocity profile then has to adapt to the circumstances of the tubular flow (as described by the Reynolds number, for example). The boundary condition for the pipe wall is especially important here. This entry section, in which the velocity profile is still adapting, will be disregarded below with the view of the heat transfer.

Starting at a position  $x = 0$  downstream of which the velocity profile is no longer changing, follow a fluid element that is flowing close to the wall and which is exchanging heat with it. It is important to distinguish two situations here:

- a) initially, the following applies

$$\text{Nu} = 1.08 \text{ Gz}^{-1/3} \quad \text{as long as } \text{Gz} < 0.05 \quad (3.140)$$

Nusselt is only a function of the Graetz number  $\text{Gz}$  (which contains  $x$ ). On closer consideration this is not very surprising, as the Graetz number is actually a Fourier number. It should be remembered that  $x/\langle v \rangle$  is an estimate of the average time that a liquid package needs to get from the aforementioned point  $x = 0$  to position  $x$  in the tube. Replacing  $x/\langle v \rangle$  by  $t$  in the Graetz number does indeed produce  $\text{Fo}$ . This means that  $x/\langle v \rangle$  is a measure of the time during which such a package is exposed to these new conditions.

In fact, this is a case reminiscent of penetration theory for short periods of time: the heat penetrates the fluid element from the tube wall and the fluid at the wall therefore increases or decreases in temperature, while the bulk of the liquid notices nothing of this. As a result, the radial temperature profile keeps changing all the time (in the way that it always does in the case of the penetration theory for short periods of time). Note that, as expressed by the negative exponent of  $\text{Gz}$ , the heat transfer and therefore also Nu decrease with  $x$  – quite comparable with Equation (3.93).

Equation (3.140) can be defined via integration in relation to  $x$  according to the mean Nusselt number for distance  $L$  (measured from  $x = 0$ ). The result is

$$\langle \text{Nu} \rangle = 1.62 \left( \frac{aL}{\langle v \rangle D^2} \right)^{-1/3} \quad \text{providing that } \frac{aL}{\langle v \rangle D^2} < 0.05 \quad (3.141)$$

This latter equation can also be written as

$$\langle \text{Nu} \rangle = 1.62 \text{ Re}^{1/3} \text{ Pr}^{1/3} \left( \frac{L}{D} \right)^{-1/3} \text{ providing that } \frac{aL}{\langle v \rangle D^2} < 0.05 \quad (3.142)$$

- b) At a greater distance from  $x = 0$ , there will again be kind of long-term heating where the form of the radial temperature profile no longer changes (as is the case with long-term heating of a solid body – see Figure 3.16), and where  $h$  and also  $\text{Nu}$  become constant as well (meaning they are no longer a function of time  $x/\langle v \rangle$ ) This expectation is correct the following applies

$$\text{Nu} = 3.66 \text{ providing that } Gz > 0.1 \quad (3.143)$$

Obviously, the Graetz number has assumed the role of the Fourier number in determining the question of when  $\text{Nu}$  is constant. The domain  $x < 0.05 (\langle v \rangle D^2/a)$  is called the thermal entry section, if  $x > 0.1 (\langle v \rangle D^2/a)$ , then it is customary to speak of thermally developed

#### Turbulent pipe flow

As already mentioned, in the case of turbulent tubular flow, heat transfer to the bulk of the liquid is much more effective due to the presence of eddies. However, the eddies can never penetrate as far as just next to the wall of the tube they succumb to the viscosity. This means that, next to the wall, there will always be a thin and largely laminar flowing interface layer without eddies, a ‘film’. The thickness of the film depends very much on the turbulence intensity of the fluid. Given that the turbulent eddies outside this film transport momentum much more effectively than the molecules in the film, the velocity gradient is often thought to be concentrated in the film. For the same reason, the resistance to heat transport is often ascribed to such a film.

The temperature profile shown in Figure 3.23 corresponds to this picture at the wall, the temperature gradient is very steep, and more or less zero in the bulk of the fluid. In fact, the profile looks similar to that of unsteady-state heat conduction (for short periods of time – see Figure 3.12), the convection prevents the penetration depth from being able to increase over time. There is competition between the supply and removal of heat, with the turbulent flow being responsible for the latter. This competition determines the thickness of the film.

Working with an interface or film in which the whole gradient is thought to be concentrated (and outside of which the transport is provided entirely by eddies) is a much-used method and is known as *film theory*. When using the film theory it is assumed that the profile in the film is always a straight line (even if the whole situation is unsteady this assumes that the film is always able to adapt to changes very quickly). This image of a film along the wall is used both for momentum management and for heat transport. Strictly speaking, the *hydraulic film thickness*  $\delta_h$

for momentum transport and *thermal film thickness*  $\delta_q$  for heat transport do not have to be equal in practice, the two film thicknesses appear to be in a ratio of  $\text{Pr}^{1/3}$ , providing that  $\text{Pr} \geq 1$ . Both film thicknesses are illustrated in Figure 3.24. Of course, that  $\text{Pr}$  appears here should not be surprising the thickness  $\delta_h$  can be expected to depend on  $v$ , while  $a$  will determine thickness  $\delta_q$  to a significant degree.

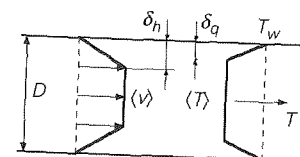


Figure 3.24

This way, and with a view to modelling heat transfer at a wall where a turbulent flow exists parallel to the wall, the entire temperature profile is schematised the bulk of the liquid is at a uniform temperature (as a result of the activity of the eddies), while the progress of the temperature from the bulk value to the wall value is a straight line. The heat flux can then be modelled as

$$\phi_q'' = \lambda \frac{T_w - \langle T \rangle}{\delta_q} \quad (3.144)$$

The resistance to heat transport is therefore entirely in the film, this is expressed in the statement

$$h = \frac{\lambda}{\delta_q} \quad (3.145)$$

for the heat transfer coefficient. (Incidentally, Equation (3.144) is very similar to Equation (3.78) and Equation (3.145) ties in excellently with the  $h$  values in Table 3.1. In fact, the problem has now shifted to finding the correct expression for  $\delta_q$ , which ensures that Equation (3.144) does indeed represent the heat flux correctly. Remember that the above is a schematised version of reality the temperature and velocity profiles are not really flat and neither  $\delta_q$  nor  $\delta_h$  is clearly defined, moreover, thicknesses  $\delta_q$  and  $\delta_h$  depend on the degree of turbulence in the bulk of the flow (in other words, on the Reynolds number).

There are several ways of expressing the Nusselt number for heat transfer calculations involving turbulent flow through pipes, one of the most commonly used is

$$\text{Nu} = 0.027 \text{ Re}^{0.8} \text{ Pr}^{1/3}$$

$$\text{providing that } \text{Re} > 10^4 \text{ and } \text{Pr} \geq 0.7 \quad (3.146)$$

in which the factor  $\text{Pr}^{1/3}$  stands for the film thickness ratio  $\delta_q/\delta_h$ . Turbulent tubular flows also involve an entry section  $L_i$ , which is shorter than the case of a laminar flow. As a result, the heat transfer coefficient in this entry section is higher; the value averaged over  $L_i$  is found by multiplying with the factor  $\{1 + (D/L_i)^{0.7}\}$ .

### Example 3.12. Heating up water flowing through a tube

A flow of water of 1 kg/s flows through a tube (length  $L = 5$  m, diameter  $D = 2$  cm). The liquid enters the tube at a temperature of  $20^\circ\text{C}$ , while the temperature of the tube wall is  $40^\circ\text{C}$ . The situation is steady.

What is the mean temperature of the liquid as it flows out?

It is first of all necessary to determine whether the flow is laminar or turbulent, for which the velocity must first be calculated. This follows from  $\phi_m = \frac{\pi}{4} D^2 \rho \langle v \rangle$ , so that  $\langle v \rangle = 3.2$  m/s. This means the Reynolds number is  $\text{Re} = 64 \cdot 10^4$ , so the flow is clearly turbulent. The question about the average water temperature (as function of  $x$ ) is a quite natural one after the above explanation about the film model and the bulk mixing for the case of turbulent flow. The Prandtl number for water (for example, at  $30^\circ\text{C}$ ) is  $\text{Pr} = 5.45$ . This means that Nu relation (3.146) can be used:

In order to now determine the temperature at the exit, it is necessary to answer the question of how much heat is absorbed by the water as it flows through the tube. Given that the water heats up, the driving force  $\Delta T$  is place-dependent, so the temperature profile has to be calculated. This can be done on the basis of a heat balance for a small slice of the tube between  $x$  and  $x + dx$  (see Figure 3.25).

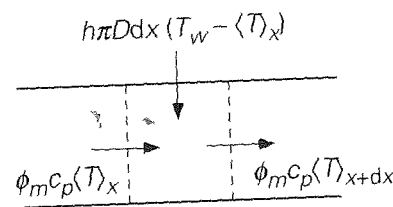


Figure 3.25

The (steady-state) heat balance for this slice is

$$0 = \frac{\pi}{4} D^2 \rho \langle v \rangle c_p \langle T \rangle|_x - \frac{\pi}{4} D^2 \rho \langle v \rangle c_p \langle T \rangle|_{x+dx} + h \pi D dx (T_w - \langle T \rangle) \quad (3.147)$$

The associated boundary condition runs as  $x = 0 \rightarrow \langle T \rangle = T_0 = 20^\circ\text{C}$ . For the temperature profile, this gives

$$\ln \frac{T_w - \langle T \rangle}{T_w - T_0} = \frac{4h}{\rho \langle v \rangle c_p D} \quad (3.148)$$

The heat transfer coefficient  $h$  can be calculated from Equation (3.146)

$$h = \text{Nu} \frac{\lambda}{D} = 0.027 \frac{\lambda}{D} \text{Re}^{0.8} \text{Pr}^{1/3} = 1.0 \cdot 10^4 \text{ W/m}^2 \text{K} \quad (3.149)$$

This means that the mean temperature at the end of the tube is  $29.5^\circ\text{C}$ . In making this calculation, it should be noted that, strictly speaking,  $h$  is not constant because  $T$  changes along the tube,  $\text{Pr}$  is not constant, so  $h$  is not either, and in fact this dependence on  $x$  should be taken into account in the integration as well. However, this is very much a secondary effect that can generally be ignored (it should be verified numerically). The same remark applies to  $\rho$  and  $c_p$ , which generally are (weak) functions of temperature.  $\square$

### Heat transfer in the case of forced flow around objects

#### Flat plate

As discussed previously during the introduction of the concept of *friction drag* (see Figure 2.15 in § 2.3.1), a laminar hydrodynamic boundary layer of increasing thickness  $\delta_h(x)$  builds up along a flat plate located in a liquid parallel to the flow in the direction of  $x$ . In this interface, the velocity decreases from the undisturbed velocity  $v$  just at the edge  $y = \delta_h(x)$  of the interface to zero (motionless liquid) just by the wall ( $y = 0$ ). Analogous to the description of turbulent tubular flows, in the case of heat transfer to/from the wall there is here too a thermal boundary layer of thickness  $\delta_q(x)$ , which again is not necessarily as thick as the hydrodynamic boundary layer. As a result, the local heat transfer resistance will depend very much on the local thickness  $\delta_q(x)$ . Calculations using the laminar boundary layer theory (substantiated by experiments) produce the following for the local value of the Nusselt number

$$\text{Nu}_x = \frac{hx}{\lambda} = 0.332 \left( \frac{\rho vx}{\mu} \right)^{1/2} \left( \frac{v}{a} \right)^{1/3} = 0.332 \text{Re}_x^{1/2} \text{Pr}^{1/3}$$

providing that  $\text{Re}_x < 3 \cdot 10^5$  (3.150)

Notice that both  $\text{Nu}$  and  $\text{Re}$  are defined here with the help of distance  $x$  from the point under examination, to the start of the slice. The background to this is that there is no other length scale available and that the thickness of the interface  $\delta_q$  (which can therefore be regarded as a direct measure of the heat transfer resistance) happens to be a function of  $x$ . The restriction  $\text{Re} < 3 \cdot 10^5$  is necessary because with greater  $\text{Re}$  values, the interface will become turbulent.

**Sphere**

The interface that builds up in the case of a flow around a sphere and the wake that forms behind the sphere were discussed when determining the resistance coefficient for such circumstances. The so-called ‘dead water’ that is located here makes only a limited contribution to the heat transfer. It is ‘refreshed’ far less frequently than the water that flows alongside the sphere at the front. A commonly-used Nu relation for convective heat transfer to spheres is

$$\text{Nu} = 2.0 + 0.66 \text{Re}^{1/2} \text{Pr}^{1/3} \quad (3.151)$$

providing that  $10 < \text{Re} < 10^4$  and  $\text{Pr} \geq 0.7$

In the first term on the right-hand side, it is possible to see the contribution of pure conduction to the heat transfer (see § 3.2.2). The second term on the right is the increase in the heat transfer as a result of the flow around the sphere (convection).

*Cylinder long and across the direction of flow*

A similar thing applies to a long cylinder across the main direction of flow.

$$\text{Nu} = 0.57 \text{Re}^{1/2} \text{Pr}^{1/3} \quad (3.152)$$

providing that  $10 < \text{Re} < 10^4$  and  $\text{Pr} \geq 0.7$

**Example 3.13. Cooling of falling grains**

Round copper grains of diameter  $D = 3$  mm,  $\rho = 9 \cdot 10^3$  kg/m<sup>3</sup> and  $c_p = 386$  J/kgK have to be cooled from 80 °C to a mean temperature of 35 °C. This is done by dropping the grains into water, the temperature of which is 30 °C. The falling velocity  $v$  is 0.88 m/s. The resistance to heat transport is entirely in the water. It can be assumed that the water does not heat up to any notable degree. How high must the column be through which the grains fall?

In order to be able to calculate the rate of cooling, it is necessary to draw up a heat balance for a whole grain. As it is accepted that the heat resistance is entirely in the water, it can be assumed that a grain is practically at uniform temperature  $T$  (metal is an excellent conductor of heat). The balance is ( $T_w$  is the temperature of the water)

$$\frac{d\left(\frac{\pi}{6} D^3 \rho c_p T\right)}{dt} = -h \pi D^2 (T - T_w) \quad (3.153)$$

The boundary condition associated with this is  $t = 0 \rightarrow T = T_0 = 80$  °C. This means that the solution is (providing that  $h$  is constant over time)

$$\ln \frac{T - T_w}{T_0 - T_w} = -\frac{6h}{\rho c_p D} t = -\frac{6hv}{\rho c_p D} \quad (3.154)$$

Here, with the second equality of Equation (3.154), the time has been replaced by the route covered divided by the velocity of a grain.

Heat transfer coefficient  $h$  now follows from a Nu relation for the flow around an immersed sphere. Based on the substance constants of water, it follows that  $\text{Re} = 2650$  and  $\text{Pr} = 5.45$ . This means that the use of Nu relation (3.151) is permitted, which produces  $\text{Nu} = 61.8$  and therefore  $h = \text{Nu} \lambda_w / D = 1.24 \cdot 10^4$  W/m<sup>2</sup>K (where  $\lambda_w = 0.60$  W/mK). Entering the values into Equation (3.154) tells us that the column must be at least 28 cm in length. □

**Heat transfer with differences in viscosity**

In the general discussion on the heat transfer and on the Nu dependency of the other non-dimensional groups in Equation (3.138), the *viscosity group*  $V_1$  was also mentioned. With this number, it is possible to account for the creation of a temperature gradient perpendicular to the wall as a result of the heat transfer, which in turn creates a viscosity gradient. In the case of turbulent tubular flow and flow around bodies, we therefore include  $V_1^{0.14}$  on the right-hand side of the Nu statements. This means that Equation (3.146) now becomes

$$\text{Nu} = 0.027 \text{Re}^{0.8} \text{Pr}^{1/3} V_1^{0.14} \quad (3.155)$$

This correction by  $V_1$  is known as the *Sieder & Tate correction*.

**3.5.3 Heat transfer in the case of free convection**

In § 3.5.1, it was derived through dimensional analysis that Nu generally depends on seven other non-dimensional groups, one of which was the Grashof number  $Gr$ , which is not needed when describing forced convection. After all, the Grashof number takes into account the fact that a difference in density in the fluid can arise as a result of local heating or cooling. Under the influence of gravity, this difference in density can lead to flow, known as *free convection*. This free convection is only relevant if a considerable forced flow was not already present as a result of differences in pressure.

One of the best-known examples of free convection is that of rising air along and above heating radiators. The warm radiator gives off its heat to the layer of air adjacent to it (via conduction). This heated air expands slightly, of course, which means it has a lower density than the air in the rest of the room. The warm air will rise and the area it ‘vacates’ will be taken over by cooler air, which itself will in turn be heated. The heat transport is of course much more effective through this free convection than when the same amount of heat has to be transported through conduction alone. Notice that  $Gr$  can also be defined with the help of the difference in density instead of the difference in temperature, after all,

$$\beta \Delta T = \beta(T_w - T_\infty) = \frac{\rho_\infty - \rho_w}{\langle \rho \rangle} \quad (3.156)$$

In the above statement,  $\langle \rho \rangle$  is calculated when  $\langle T \rangle = \frac{1}{2}(T_w + T_\infty)$ , that is, in average conditions. In that case,  $Gr$  is

$$Gr = \frac{\beta \Delta T g x^3}{v^2} = \frac{x^3 g \Delta \rho}{v^2 \langle \rho \rangle} \quad (3.157)$$

The length scale (referred to here as  $x$ ) to be used in this Grashof number depends on the geometry under consideration.

There are three situations at which we will look in more detail free convection along a vertical plate, free convection above a horizontal plate, and free convection between two large horizontal plates.

#### Vertical plate

Consider a vertical plate with a (fixed, uniform) temperature  $T_w$  which is higher than temperature  $T_\infty$  of the air far away from the plate. The air a long distance away from the plate (in the bulk) is motionless. The situation is illustrated in Figure 3.26.

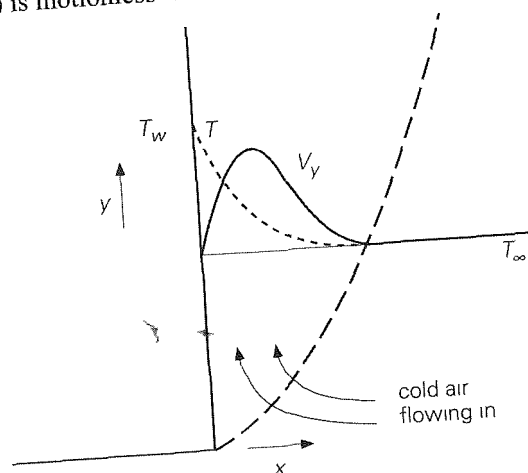


Figure 3.26

At first, the layer of air directly adjacent to the plate will be heated up and will therefore expand. This air will therefore rise and be replaced by colder air. This means that a velocity profile will develop along the plate, in the same way that it does in the case of forced flow along a plate, for example (see Figure 2.15). At the same time, a temperature profile will also be created. Both are illustrated in Figure

3.26. Here, too, the velocity boundary layer and the temperature boundary layer do not have to be of the same thickness (see the discussion in § 3.5.2).

Because the velocity profile and the temperature profile develop alongside the slice, the heat transfer coefficient  $h$  is a function of  $y$  and therefore varies from one place to another. The greater the  $y$  coordinate, the thicker the boundary layer becomes and the smaller the local  $h$  is there.

For a vertical plate of height  $L$ , it appears that the mean heat transport coefficient  $\langle h \rangle$  can be written as

$$\frac{\langle h \rangle L}{\lambda} = f \left( \frac{L^3 g}{\alpha v} \beta |T_w - T_\infty| \right) \quad (3.158)$$

With the help of the non-dimensional groups covered earlier, this can be written as

$$\langle Nu \rangle = f(Gr Pr) \quad (3.159)$$

In order to be able to specify the form of function  $f$ , it is again necessary to make a distinction between *laminar* and *turbulent* conditions. Unlike the situation involving forced convection, the flow in the case of free convection cannot be characterised using a Reynolds number. The reason for this is that with free convection, no characteristic velocity is known in advance. Here, it is the case that the difference between laminar and turbulent can be made on the basis of the product of  $Gr Pr$ .

Recent research has produced the following statements for  $\langle Nu \rangle$  (which are somewhat different to those from the Transport Phenomena Data Companion).

#### Laminar

$$\langle Nu \rangle = 0.52 (Gr Pr)^{1/4} \quad \text{providing that } 10^4 < Gr Pr < 10^8 \quad (3.160)$$

#### Turbulent

$$\langle Nu \rangle = 0.12 (Gr Pr)^{1/3} \quad \text{providing that } Gr Pr > 10^8 \quad (3.161)$$

It should be noted here that under laminar flow conditions  $\langle h \rangle$  is a function of height  $L$  (as a result of the development of the laminar boundary layer along the plate), while in turbulent flows  $\langle h \rangle$  does not depend on height  $L$  (because the heat transfer is then governed by the turbulent eddies, the magnitude of which has nothing to do with  $L$ ).

#### A horizontal tube

Laminar free convection from/around a horizontal cylindrical tube may be described in a good approximation with the help of Equation (3.160) in which the tube diameter is now selected as the height  $L$ .

### One horizontal plate

Free convection can also occur either below or above a horizontal plate as a result of heat transfer (above an electric hob, for example, or a fire). This free convection cannot develop here into a developing boundary layer, but will instead lead to 'bursts' that free themselves from the plate and rise or fall, as the case may be. The resulting turbulent eddies assist considerably in the removal of the heat. It cannot be assumed from this scenario that  $\langle h \rangle$  depends on the dimension  $L$  of the plate. Consequently, it follows that

$$\langle \text{Nu} \rangle = 0.17 (\text{Gr Pr})^{1/3} \quad \text{providing that } \text{Gr Pr} > 10^8 \quad (3.162)$$

### Two horizontal plates

Consider now the heat transport through a fluid that is located between two very large horizontal plates, one above the other. The distance between the plates is  $D$ . If the temperature of the upper plate is greater than that of the lower one, a stable situation will generally be created (water at approximately  $T = 4^\circ\text{C}$  is an exception to this). No free convection will occur and heat transport will take place as a result of conduction. However, if the upper plate is the colder of the two and the lower plate the warmer, then free convection may occur between them. Here, too, there is a distinction between the various flow regimes based on  $\text{Gr Pr}$ . The length scale that has to be used in  $\text{Gr}$  is plate spacing  $D$ .

#### Hardly any free convection

If  $\text{Gr Pr} < 1800$ , the flow will be so slight that the heat transport is caused almost entirely through conduction.

$$\langle \text{Nu} \rangle = 1 \quad \text{providing that } \text{Gr Pr} < 1800 \quad (3.163)$$

#### Laminar

$$\langle \text{Nu} \rangle = 0.15 (\text{Gr Pr})^{1/4} \quad \text{providing that } 10^4 < \text{Gr Pr} < 10^7 \quad (3.164)$$

In this case, a remarkable phenomenon occurs: the flow takes place in a pattern of small cells, which together fill up the whole area between the plates. The height of the cells is equal to the distance between the plates, while the horizontal dimensions are approximately the same as this. This pattern is known by the name of *Bénard cells* and is illustrated in Figure 3.27.

#### Turbulent

$$\langle \text{Nu} \rangle = 0.17 (\text{Gr Pr})^{1/3} \quad \text{providing that } \text{Gr Pr} > 10^7 \quad (3.165)$$

The neat, steady-state structure of the *Bénard cells* has now disappeared of course: the turbulent eddies thoroughly even out the differences in velocity and temperature, but turn the flow structures transient and complicated.

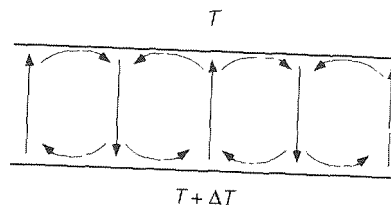


Figure 3.27

#### Example 3.14. Heat transport between two horizontal plates

Consider two large, horizontal plates, one above the other, and separated by distance  $D$ , of 4 cm. The space between them is filled with air (pressure is 1 bar). Consider the two following situations

- the upper plate has a temperature of  $40^\circ\text{C}$ , that of the lower is  $20^\circ\text{C}$ ,
- the lower plate has a temperature of  $40^\circ\text{C}$ , that of the upper is  $20^\circ\text{C}$

The question now is to determine the heat flux for both steady-state situations.

#### Solution to situation a

No free convection is involved here: the warmest layer with the least density is at the top. Therefore, the heat transport is determined by conduction in the air, and  $\text{Nu} = 1$ . The heat flux now follows from

$$\phi_q'' = h \Delta T = \frac{\text{Nu} \lambda}{D} \Delta T = \frac{1.0026}{0.04} 20 = 13 \text{ W/m}^2 \quad (3.166)$$

#### Solution to situation b

Free convection may well be involved here. In order to assess the conditions, it is first necessary to calculate  $\text{Gr Pr}$ . The expansion coefficient  $\beta$  can be estimated with the help of the ideal gas law

$$\beta = \frac{1}{V} \left( \frac{\partial V}{\partial T} \right)_p = \frac{1}{V} \frac{nR}{p} = \frac{1}{T} \quad (3.167)$$

This means that, for  $\text{Gr Pr}$

$$\text{Gr Pr} = \frac{D^3 g}{\nu^2} \frac{\Delta T}{\langle T \rangle} \frac{\nu}{a} = 1.2 \cdot 10^5 \quad (3.168)$$

and therefore laminar free convection is involved. For  $\text{Nu}$ , it now follows that

$$\langle \text{Nu} \rangle = 0.15 (\text{Gr Pr})^{1/4} = 2.79 \quad (3.169)$$

which means the heat flux is greater than is the case with a, namely

$$\phi_q'' = h \Delta T = \frac{\text{Nu} \lambda}{D} \Delta T = 36 \text{ W/m}^2 \quad (3.170)$$

□

### Summary

If flow occurs as a result of differences in density caused by differences in temperature in a fluid, this is known as free convection. This type of flow results in a greater heat transport than in the case of conduction alone. There is a distinction between laminar and turbulent free convection. In the case of free convection, the regimes are classified with the help of  $\text{Gr Pr}$  instead of with a Reynolds number. In every regime, the Nusselt number is a simple function of  $\text{Gr Pr}$ . This applies to a number of elementary geometries.

#### 3.5.4 The numerical approach of convective heat transport

A numerical approach to heat transport to and from the wall of a tube through which a laminar flow of liquid is passing, is more complicated than the earlier examples in § 3.1.5 and § 3.3.8 that involved only conduction as a transport mechanism. Now, we must also consider convective transport. The heat transport is still described by the heat balance. Because the medium is now flowing, we also need to know about the field of flow. For laminar flow (of a Newtonian liquid) in a straight, cylindrical-shaped tube, we know the exact solution to the velocity field (see Chapter 5). The velocity of a liquid element in the tube is parallel to the tube's axis and depends only on its radial position in the tube:

$$\frac{v_z(r)}{\langle v \rangle} = 2 \left( 1 - \left[ \frac{r}{R} \right]^2 \right) \quad (3.171)$$

where  $\langle v \rangle$  denotes the mean velocity of the liquid,  $R$  is the radius of the tube,  $r$  the radial coordinate, and  $z$  the axial coordinate.

In the numerical analysis of heat transport, we use the symmetry in the problem. The elementary volumes into which we divide up the domain are now ring-shaped, with radii between  $\{r, r + \Delta r\}$  and a position between  $\{z, z + \Delta z\}$ . For a steady-state situation, we can again consider a random element and its immediate neighbours; see Figure 3.28.

Here, the direction of flow of the liquid is 'west-east', while 'south-north' is the direction from the pipe centre-line to the pipe wall. We should now consider that both the west and east faces of cell P have a cell face area of  $A_w = A_e = 2\pi r_p \Delta z$ , while the north (outer) cell face area has a magnitude of  $A_n = 2\pi (r_p + \Delta r/2) \Delta z$ , and the south (inner) cell face area is  $A_s = 2\pi (r_p - \Delta r/2) \Delta z$ .

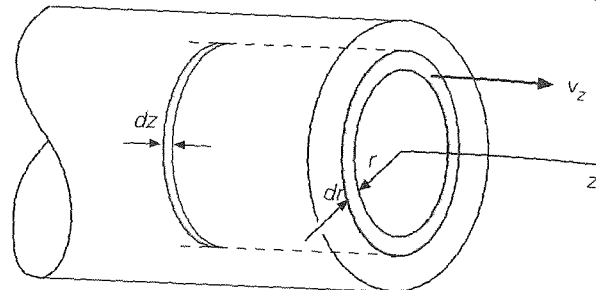


Figure 3.28

A steady-state heat balance for 'ring' P is now

$$0 = A_w \left( v_w T_w - a \left. \frac{dT}{dz} \right|_w \right) - A_e \left( v_e T_e - a \left. \frac{dT}{dz} \right|_e \right) + A_s \left( -a \left. \frac{dT}{dr} \right|_s \right) - A_n \left( -a \left. \frac{dT}{dr} \right|_n \right) \quad (3.172)$$

Note that the indices  $w, e, s, n$  show that the quantities at the interfaces of 'cell' P must be calculated (in other words, it is not the velocity in cell W but at the boundary of cells W and P that matters). This equation can be solved in the same way as with the steady-state heat conduction. Because both convection and conduction are now at play, the accuracy of the 'discretisation scheme' that we use is much more important. An initial, naive attempt could perhaps involve discretising the temperature gradient in a normal way, for example

$$\left. \frac{dT}{dz} \right|_w \approx \frac{T_P - T_W}{\Delta z} \quad (3.173)$$

For the convective term, we take the upstream values. That, after all, is what is flowing into the cell, therefore (note the difference in the subscripts between upper case and lower case letters)

$$v_w T_w \approx v_W T_W \quad \text{and} \quad v_e T_e \approx v_P T_P \quad (3.174)$$

This method of discretisation is known as 'upwind'. It does indeed seem to be a logical choice, although it is not without its problems. The accuracy of this method of discretisation is not very great; the scheme introduces a degree of numerical diffusion. This means that the diffusion coefficient becomes artificially greater. In this case, this is rather annoying because the problem depends on the relationship between convective and diffusive transport. By using the upwind scheme, we are causing huge disruption to this relationship.

Fortunately, there are discretisation schemes that are far less affected by this problem. To describe these in detail here would be to go beyond the remit of this book. Figure 3.29 shows the progress of the local Nusselt number as a function of the (equally local) Graetz number, as follows from a numerical simulation. It demonstrates that the numerical solution first follows Equation (3.140) and then switches smoothly to the constant Nu value of 3.66 as given by Equation (3.143).

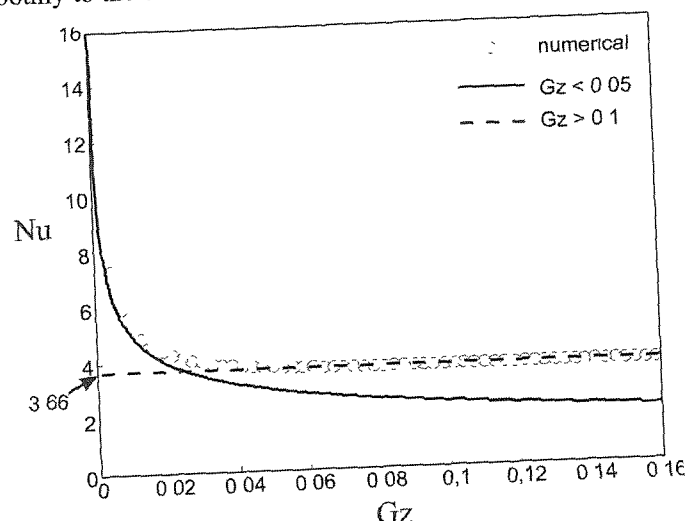


Figure 3.29

### Summary

For forced tubular flow, a distinction has to be made between laminar and turbulent flow. In the case of laminar flow, Nu is a function of the Graetz number and therefore of the place in the tube, while in the case of the turbulent flow, Nu is a function of the Reynolds number and is constant along the tube. For convective heat transfer to and from bodies, Nu statements have been discussed that are analogous to those for forced turbulent tubular flows. Finally, reference has been made to the Sieder-Tate correction for important gradients in the viscosity.

Assuming that the field of flow is known, the numerical treatment of heat transport is extended to include the convective terms in the heat balance for an elementary volume. At the edges, a choice has to be made during discretisation of the values of the local velocity and the temperature. The upwind scheme has been introduced for that purpose, however, this can cause numerical diffusion.

## 3.6 Heat exchangers

### 3.6.1 Introduction

This chapter does not deal with any new correlations for heat transfer coefficients or Nusselt numbers, but it does examine devices that have been expressly designed for effectively realising heat transfer, that is, heat exchangers. Heat exchangers are found in the processing industry in very many shapes and sizes. An exhaustive examination of how they work and how they are constructed goes beyond the remit of a book on transport phenomena such as this one. Instead, we will restrict ourselves to some general comments and a few illustrations regarding how heat exchangers work.

Previous coverage of heat transfer has shown every time that heat flow  $\phi_q$  (the purpose of a heat exchanger) is directly proportional to surface area  $A$  that is exchanging heat. For this reason, the heat exchanging surface in most heat exchangers is made as large as possible. It should be borne in mind that this surface becomes smaller in relative terms, the larger the device becomes, because the surface area per unit of volume is proportional to  $L^2/L^3$ , that is, to  $L^{-1}$ .

It is also important with heat exchangers to let the heat transfer coefficients be as great as possible. High velocities are advantageous for convective heat transfer (but also cost energy!), which is why devices with stirrers and circulation systems with pumps are used extensively. In general, free convection cannot be expected to be very useful. It is also important, generally speaking, to use favourable construction materials with a high heat conduction coefficient for the heat exchanging surface. Contamination of the surface by the liquids involved in the process must be prevented as much as possible, or periodically removed. Sometimes (in the case of non-mixable phases) it is possible to completely avoid having a partition between the process flows.

Any list of examples of heat exchangers should at least include the following (list is not exhaustive):

- ‘Shell and tube heat exchangers’: two process flows exchange heat, where one flow usually flows through a large number of parallel pipes, while the other passes over the outside of the pipes when going through the heat exchanger. This can be either concurrently or countercurrently. Baffle plates are often used to make sure the fluid on the outside of the pipes flows more or less in a zigzag pattern through the heat exchanger (dead corners should be avoided). The other flow that runs through the pipes is often passed through the heat exchanger in several tube passes.

- Stirred containers in which (reaction) heat is developed that has to be removed are fitted for that purpose either with a water jacket or a spiral through which a coolant is circulated by means of a pump
- Scrapped heat exchangers in order to frequently remove the layers of crystals that grow on the heat exchanging surface, crystallisers are often fitted with fast-moving rotors with one or more scrapers. This scraping is not only needed for preventing the device from being covered with crystals, but in many cases, crystallisation occurs on an externally cooled wall (because of the removal of crystallisation heat). This wall has to be scraped in order not to undermine the cooling process
- Stoves process liquids are often heated up by conducting them through tube bundles (spirals, hairpins) placed in stoves (above the hearth and/or in the chimney). Steam is generally produced in this way as well
- Chemical reactors are sometimes cooled by allowing one of the components of the reaction mix (often the solvent) to evaporate and then to condense again externally – an effective method of using a phase transition for removing heat – after all, the heat of evaporation is often large (in comparison with an achievable  $c_p\Delta T$  effect). Variants of this are the use of boiling liquid in a water jacket and the cooling of a nuclear reactor with water/steam. The temperature in a reactor is always more or less constant in such cases: greater production of heat can be dealt with through greater evaporation and more intensive recirculation

### 3.6.2 Heat transfer without phase transition

The example we will take of the use of the calculation of a heat flow from one flowing medium to another is that of an elementary heat exchanger. For the sake of simplicity, this consists of a straight tube through which liquid A flows, which has to be cooled down. This cooling is achieved by fitting a second tube concentrically around the first one, through which a colder liquid, B, flows. As a result of the difference in temperature between the two liquids, a heat flow from liquid A to liquid B will be created.

In principle, there are two versions: the A and B flows run parallel (concurrent flow), or they run in opposite directions (countercurrent flow). We will examine only the concurrent flow here. This situation is illustrated in Figure 3.30, and is steady.

An important practical question is this: how large is heat flow  $\phi_q$ , which is transferred through the tube wall from flow A to flow B?

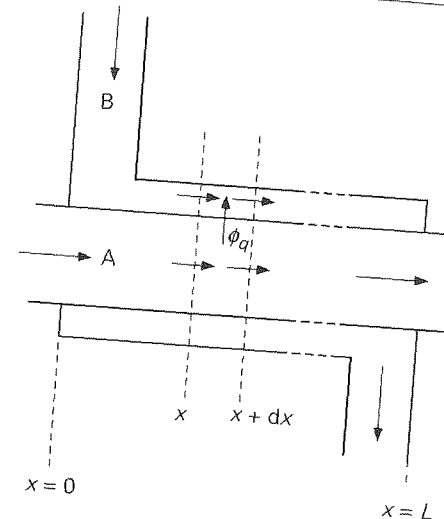


Figure 3.30

The heat transfer between the two liquids depends on the exchanging area  $A$  between the two liquids streams and the overall heat transfer coefficient  $U$ . The reciprocal of the latter quantity stands for the total resistance to heat transfer which in this case comprises three partial resistances: one in liquid A (denoted by  $1/h_i$ ), one in liquid B (denoted by  $1/h_e$ ), and one of the wall keeping the two liquids apart (denoted by  $d/\lambda_w$ , where  $d$  stands for the thickness of the tube wall and  $\lambda_w$  for the thermal conductivity coefficient of the wall material).

$$\frac{1}{U} = \frac{1}{h_i} + \frac{d}{\lambda_w} + \frac{1}{h_e} \quad (3.175)$$

The two heat transfer coefficients  $h_i$  and  $h_e$  depend on the type of flow (laminar, turbulent) and should each be calculated from an appropriate Nu-Re correlation. For the sake of simplicity, it is assumed that  $U$  is constant (so independent of position  $x$ ) and also that the tube through which A flows is constant in diameter.

The transfer of heat depends on the difference in temperature of liquids A and B. But because heat is transferred all the time as the liquids flow through the tube (see also Example 3.12), this  $\Delta T$  is a function of position along the heat exchanger. It is therefore necessary to draw up a micro balance for a slice of the heat exchanger between  $x$  and  $x + dx$ . This can be done twice – once for the liquid A inside the innermost tube and once for liquid B in the outer tube.

liquid A:

$$0 = \phi_m^A c_p^A (T^A|_x - T^A|_{x+dx}) - U \pi D dx (T^A|_x - T^B|_x) \quad (3.176)$$

liquid B

$$0 = \phi_m^B c_p^B (T^B|_x - T^B|_{x+dx}) + U \pi D dx (T^A|_x - T^B|_x) \quad (3.177)$$

Both balances can be simplified to

$$\frac{dT^A}{dx} = - \frac{U \pi D}{\phi_m^A c_p^A} (T^A - T^B) \quad (3.178)$$

$$\frac{dT^B}{dx} = + \frac{U \pi D}{\phi_m^B c_p^B} (T^A - T^B) \quad (3.179)$$

Equations (3.178) and (3.179) form a coupled system. Deducting Equation (3.179) from Equation (3.178) produces an equation in  $(T^A - T^B)$  which is easy to solve

$$\frac{d}{dx} (T^A - T^B) = - U \pi D \left\{ \frac{1}{\phi_m^A c_p^A} + \frac{1}{\phi_m^B c_p^B} \right\} (T^A - T^B) \quad (3.180)$$

This differential equation, with the addition of the boundary condition,

$$x=0 \rightarrow (T^A - T^B) = T_0^A - T_0^B \quad (3.181)$$

has the following solution for the difference in temperature as a function of  $x$

$$\ln \frac{T^A - T^B}{T_0^A - T_0^B} = - U \pi D \left\{ \frac{1}{\phi_m^A c_p^A} + \frac{1}{\phi_m^B c_p^B} \right\} x \quad (3.182)$$

The solution to  $x=L$  is therefore now known as well. However, this does not include heat flow  $\phi_q$ ! This can be brought in by eliminating the term between brackets with the help of the two macro balances. This takes place as follows

The balance for the entire innermost tube

$$0 = \phi_m^A c_p^A T_0^A - \phi_m^A c_p^A T_L^A - \phi_q \quad (3.183)$$

The balance for the entire outer tube

$$0 = \phi_m^B c_p^B T_0^B - \phi_m^B c_p^B T_L^B + \phi_q \quad (3.184)$$

Combining the last two equations produces

$$\frac{1}{\phi_m^A c_p^A} + \frac{1}{\phi_m^B c_p^B} = \frac{1}{\phi_q} \left\{ (T_0^A - T_0^B) - (T_L^A - T_L^B) \right\} \quad (3.185)$$

This means that the heat flow can be expressed in the differences in temperature between the two liquids where the heat exchanger starts and ends

$$\phi_q = U A \frac{(T_0^A - T_0^B) - (T_L^A - T_L^B)}{\ln(T_0^A - T_0^B) - \ln(T_L^A - T_L^B)} \quad (3.186)$$

The two mass flow rates and the specific heats no longer feature in this statement. Equation (3.186) is usually written in a much more compact form. Two abbreviations are introduced to that end, namely

$$\Delta T = T^A - T^B \quad (3.187)$$

and

$$(\Delta T)_{\ln} = \frac{\Delta T_L - \Delta T_0}{\ln \frac{\Delta T_L}{\Delta T_0}} \quad (3.188)$$

Definition (3.187) is known as the *logarithmic mean temperature difference*. This means that result (3.185) of the whole calculation can be written in the form of Newton's Law of Cooling

$$\phi_q = U A (\Delta T)_{\ln} \quad (3.189)$$

If the heat exchanger were to be operated countercurrently, a similar analysis would obtain exactly the same result. However, it should not be concluded from this that it does not matter whether the heat exchanger is operated concurrently or countercurrently. The values of the exit temperatures in the case of countercurrent flows will actually differ from those in the case of concurrent flows. With the former, the change in temperature along the heat exchanger also depends on what is known as the *heat extraction coefficient*  $E_q = \phi_m^A c_p^A / \phi_m^B c_p^B$ . This is all illustrated in Figure 3.31.

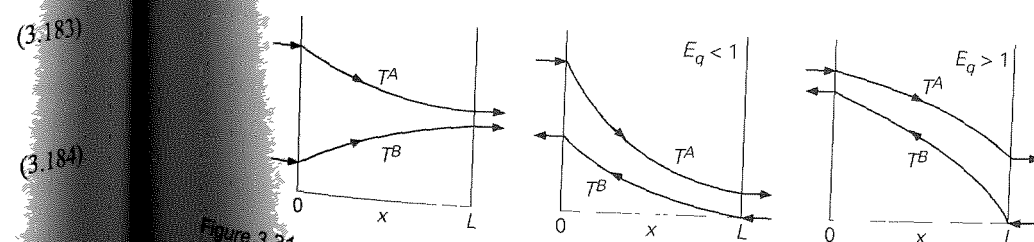


Figure 3.31

### Summary

In this Section, we have looked at a highly simplified heat exchanger. An important parameter in such a heat exchanger is the overall heat transfer coefficient that comprises three contributions:

$$\frac{1}{U} = \frac{1}{h_i} + \frac{d}{\lambda_w} + \frac{1}{h_e}$$

Apart from the elementary geometry, an important simplification is that this  $U$  does not depend on its position in the heat exchanger. This allows the micro balances of the heat exchanger to be solved. However, the  $\Delta T$  between the two liquids is a function of place.

With the help of two macro balances, the heat flow has been brought into the expression for the temperature difference. The result is a relation for the heat flow that is given solely in terms of the liquid temperatures at both ends of the heat exchanger. The two mass flow rates and the specific heats no longer feature in this relation. Using the term 'logarithmic mean temperature difference' enables us to express the heat flow in the form of Newton's Law of Cooling. Concurrent and countercurrent are two modes of operation of a heat exchanger. The temperature profiles along a heat exchanger depend on the mode of operation and on the heat extraction coefficient.

### 3.6.3 Heat transfer with phase transition

It was explained in the introduction to § 3.6 how the heat effect of a phase transition can be used effectively for removing heat and of course for supplying it. Another factor is that the phase formed during the phase transition is generally of a different density to the original phase. This difference in density can, depending on the geometrical situation, lead to a difference in speed and therefore to more rapid removal of heat. This means that vapour that has formed from liquid in a vertical evaporation pipe is able to rise more quickly in the form of vapour bubbles, and therefore bring about extra mixing and extra heat transfer in the liquid phase. Conversely, in the case of a condenser pipe, condensed liquid can flow away more quickly under the influence of gravity. These are in fact examples of free convection as a result of a difference in density.

Below are two examples: one demonstrates how condensation heat features in a concrete heat transfer problem, and the other deals with how condensation influences the heat transfer coefficient on the steam side.

### Example 3.15. A steam condenser

In a condenser, steam condenses on the outside wall of a bundle of parallel pipes. The total surface area of the outside of the pipes,  $A$ , is  $5 \text{ m}^2$ . In continuous, steady-state conditions, 1200 kg of steam condenses every hour (denoted by  $\phi_{m,st}$ ). The pressure in the condenser is 1 bar. A flow rate of  $\phi_{m,w}$  of 14000 kg of cooling water per hour passes through the pipes. The temperature  $T_i$  of the cooling water that is added to the condenser is  $15^\circ\text{C}$ . The condensation heat  $\Delta h_v$  of steam is 2685 kJ/kg. The condenser is well insulated; there is no heat exchanged with the local environment.

What is the overall heat transfer coefficient  $U$  between the cooling water and the steam?

Because of the condensation heat that is released, the temperature of the cooling water moving downstream rises. As a result, the driving force for heat transport along the pipes is not constant. It is therefore obvious that the logarithmic mean temperature difference  $(\Delta T)_{ln}$  should be used so that the overall heat transfer coefficient  $U$  can be calculated from

$$U = \frac{\phi_q}{A(\Delta T)_{ln}} \quad (3.190)$$

In order to be able to work with this statement, both the temperature  $T_e$  of the cooling water at the exit of the pipes and the overall level of transferred heat flow  $\phi_q$  must first be calculated. Both these quantities follow from a heat balance for the whole condenser.

$$\phi_{m,w} c_{p,w} (T_e - T_i) = \phi_q = \phi_{m,st} \Delta h_v \quad (3.191)$$

From this, it first follows that  $\phi_q = 3222 \text{ MJ/h}$  and that  $T_e = 69.8^\circ\text{C}$ . This makes it possible to calculate that  $(\Delta T)_{ln} = 53.0^\circ\text{C}$  and finally that  $U = 3384 \text{ W/m}^2\text{K}$ .

### Example 3.16. Film condensation

Consider condensation of a pure vapour on a vertical plane of height  $L$  and width  $b$  (see Figure 3.32). The plane is entirely covered by a film which, under the influence of gravity, neatly flows laminarly downwards. The liquid has density  $\rho$ , heat of evaporation  $\Delta h_v$  (in J/kg), and heat conduction coefficient  $\lambda$ . For the sake of simplicity, it can be assumed that the wall temperature  $T_w$  and temperature  $T$  of the condensing vapour are both constant.

Derive how the mean heat transfer coefficient depends on height  $L$ .

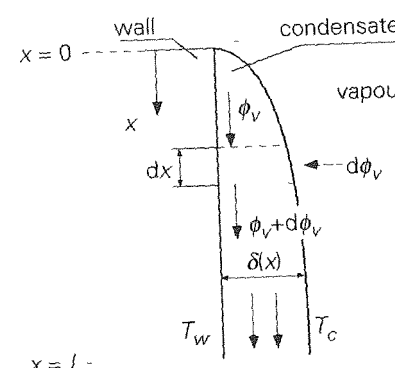


Figure 3.32

Because condensation occurs over the entire height  $L$ , film thickness  $\delta$  and liquid flow rate  $\phi_v$  increase in the direction of  $x$ . Condensation takes place on the vapour side of the film, the removal of the heat of evaporation through the film to the wall depends on the local thickness  $\delta(x)$ . This heat removal is shown locally by

$$\frac{\lambda}{\delta} (T - T_w) b \, dx \quad (3.192)$$

where  $\delta = \delta(x)$ . For the local condensation velocity (that is, the local increase in liquid flow rate), the following local heat balance applies

$$\Delta h_v \rho d\phi_v = \lambda(T - T_w) \frac{b}{\delta} dx \quad (3.193)$$

with  $\delta = \delta(x)$ , still. Further elaboration of Equation (3.193) requires familiarity with the link between  $\phi_v$  and  $\delta$  (which will be dealt with in Chapter 5). Ultimately, the mean heat transfer coefficient  $\langle h \rangle$  for height  $L$  is found thus

$$\langle h \rangle = 0.94 \left[ \frac{\Delta h_v \rho^2 \lambda_{fg}^3 g}{L \mu (T - T_w)} \right]^{1/4} \quad (3.194)$$

It can be seen that  $\langle h \rangle$  is inversely proportional to  $L^{1/4}$ . For this reason, condensers are often horizontal in shape, increasing the capacity by enlarging width  $b$ .

### Summary

Using changes in enthalpy during phase transitions is a widely used and effective means of heat transport. It is sometimes possible to calculate the relevant heat transfer coefficients through modelling.

## 3.7 Heat transport through radiation

We have previously looked in detail at heat transport maintained by molecules, or by collective behaviour (convection) or by individual behaviour (conduction). However, there is another important form of heat transport that is caused by (electromagnetic) radiation – by photons, in other words. In fact, it is more accurate to refer to energy transport, although in many practical applications the radiation will only manifest itself when it is absorbed and converted into heat.

It should also be mentioned that this type of energy transport occurs independently of and parallel to transport caused by conduction and convection. It can therefore be described as a parallel circuit of resistances to heat transport. Analogous to the electric analogue, this results in the following total resistance

$$\frac{1}{R_{\text{tot}}} = \frac{1}{R_1} + \frac{1}{R_2} \quad (3.195)$$

In the event that, in addition to thermal radiation, convection plays a role but conduction can be ignored, the following applies

$$U = h_{\text{radiation}} + h_{\text{convection}} \quad (3.196)$$

The heat transfer coefficient  $h_{\text{radiation}}$ , or the contribution of radiation to the heat balance of a particular control volume, is the subject of § 3.7. Describing heat transfer by radiation in precise terms is a complex matter, one reason being the complex way in which the heat radiation that is emitted and absorbed by objects depends on the material properties of those objects, the angle at which the radiation is emitted, and the wavelength of the radiation. Below is an initial simple introduction to heat transfer by radiation, which can be used for approximate technical calculations.

### 3.7.1 Emission

All objects emit electromagnetic radiation continuously. For a ‘completely black’ body, or object, it can be derived in theory that the radiation emitted is proportional to the absolute temperature (in K) of (the surface of) the object to the power of four:

$$\phi_{\text{black}}'' = \sigma T^4 \quad (3.197)$$

This is the *Stefan-Boltzmann Law*. The proportionality constant  $\sigma$  is called the *Stefan-Boltzmann constant* and has a value of  $5.67 \cdot 10^{-8} \text{ W/m}^2 \text{K}^4$ . Nusselt’s notation<sup>14</sup> is very useful for making calculations.

<sup>14</sup> Nusselt W., *Technische Thermodynamik II*, Ed. Walter de Gruyter, Berlin, 1951

$$\phi''_{\text{black}} = \sigma' \left( \frac{T}{100} \right)^4 \quad (3.198)$$

with  $T$  still in K and  $\sigma' = 5.67 \text{ W/m}^2\text{K}^4$ . [The derivative of this law belongs in the field of statistic mechanics and tells us that  $\sigma$  is exactly equal to  $\pi^2 k_B^4 / 60 \hbar^3 c^2$  where  $k_B$  is the Boltzmann constant,  $\hbar$  the Planck constant, and  $c$  the velocity of light. The Stefan-Boltzmann Law follows from Planck's Law, which gives the energy flux that is emitted in the field of wavelength between  $\lambda$  and  $\lambda + d\lambda$  by an object of surface temperature  $T$ .] However, there is hardly any object that is completely black. This problem is resolved through the addition of the *emission coefficient*  $e$ , which has a value between 0 and 1. Generally speaking, an object emits radiation as follows

$$\phi''_q = e \sigma T^4 \quad (3.199)$$

If  $e = 1$ , then the object is a completely *black radiator*. In the case of the other extreme,  $e = 0$ , the object in question emits no radiation. If  $0 < e < 1$  and with the emission coefficient being independent of the wavelength of the emitted radiation, then this is referred to as a *grey body* (or object). An example of this is given in Figure 3.33, which shows the spectrum of a completely black object ( $e = 1$ ) and a grey object ( $e = 1/3$  in this example).

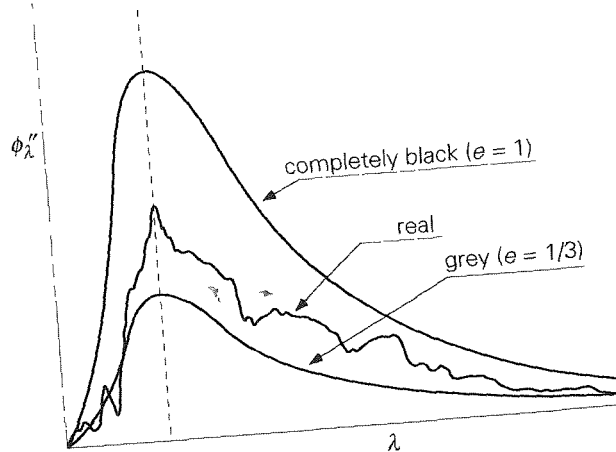


Figure 3.33

For a black or grey object, wavelength  $\lambda_{\max}$ , where the maximum occurs in the spectrum, depends solely on the surface temperature of the object:

$$\lambda_{\max} T = 2.898 \cdot 10^{-3} \text{ m K}$$

This is called *Wien's displacement law*. The sun, with a surface temperature  $T_s$  of some 5800 K, emits most of its energy in the visible light spectrum at wavelengths of 400–800 nm, while most of the energy emitted by warm objects on earth is in the range of infrared, at wavelengths of 2–10  $\mu\text{m}$ .

The actual spectrum emitted or absorbed by a body is much more complex than Planck's Law might lead us to expect see Figure 3.33 again. In fact, it is necessary to work with a wavelength-dependent emission coefficient  $e_\lambda$ . In the real technological world, however, it is possible to obtain a good first-order approximation of heat radiation by using the grey-body approach with Equation (3.199), where  $0 < e < 1$ . A few typical values of the emission coefficients of some materials for infrared thermal radiation are given in Table 3.2.

Table 3.2 Typical values of emission coefficients for thermal radiation

Polished metal and metal foil	0.01 - 0.13	Human skin	0.88 - 0.97
Clean metal	0.1 - 0.3	Surface water	0.88 - 0.97
Oxidised metal	0.25 - 0.7	Paint (white and black!)	0.90 - 0.95
Ceramic materials	0.4 - 0.8	Stone, concrete, asphalt	0.90 - 0.95
Sandy soil	0.7 - 0.8	Snow	0.95
Glass	0.8 - 0.95		

### 3.7.2 Reflection, transmission, absorption

When radiation falls on an object, it may be absorbed, reflected, or transmitted. In principle, each of these processes depends in turn on the wavelength of the incoming light, but here too, the grey approach is often used, in which none of these processes depends on the wavelength.

The proportion of the incoming radiation that is absorbed is represented by the *absorption coefficient*  $a$ . According to Kirchhoff's Law (which is not being proved here), for a grey body  $a = e$  always holds true. A completely black object absorbs all incoming radiation, for this,  $a = e = 1$ .

The proportion of the incoming radiation that is transmitted is represented by the *transmission coefficient*  $t$ . Radiation that is not absorbed or transmitted by a body is reflected. This proportion is represented by the *reflection coefficient*  $r$ . Obviously,

$$a + t + r = 1 \quad (3.201)$$

An object (or a medium) is completely transparent if  $t = 1$ , and completely *opaque* if  $t = 0$ . In the case of a transparent material (such as glass, water, or air), the transmission coefficient depends on the thickness of the material. For a flat layer of thickness  $L$  of such a material, Beer's Law applies

$$t = \exp(-\alpha L) \quad (3.202)$$

where  $\alpha$  is the *absorptivity* (unit  $\text{m}^{-1}$ ) If  $L \gg 1/\alpha$ , then the layer is ‘optically thick’, and  $t \approx 0$ . If  $L \ll 1/\alpha$ , the layer is ‘optically thin’, and  $t \approx 1$ . Here, too, there is often a strong dependency on the wavelength.

Window glass, for example, has an absorptivity of  $\alpha = 30 \text{ m}^{-1}$  for visible light and  $\alpha = 10^6 \text{ m}^{-1}$  for infrared radiation. This means that window glass 5 mm thick is optically thin for visible light and almost opaque for infrared radiation (verify this!) Something similar applies to the atmosphere for solar radiation, the atmosphere has a transmission coefficient of  $t_{\text{atm}}$  that is roughly equal to 1, while for infrared radiation (emitted by the earth) we can regard the atmosphere as a grey body with an emission coefficient of  $e_{\text{atm}}$  and an absorption coefficient of  $a_{\text{atm}}$  that both equal 0.8.

### Example 3.17. The temperature of the earth

The earth receives radiation energy from the sun, part of which is reflected by the surface of the earth. This reflection coefficient, often referred to as the *albedo* of the earth, has a value of around  $r = 0.3$ . The earth itself also emits radiation. The earth-sun system is steady. The maximum in the solar spectrum occurs at  $\lambda_{\text{max}} = 500 \text{ nm}$ .

Consider the sun and the earth as completely black bodies. According to this data, what is the steady-state temperature  $T$  of the earth surface? It can be assumed that the earth surface is at a uniform temperature. Convective heat transport may be neglected.

Data: the radius of the sun  $R_s = 6.92 \cdot 10^8 \text{ m}$   
the radius of the earth  $R = 6.37 \cdot 10^6 \text{ m}$   
the distance between the earth and the sun  $s = 1.49 \cdot 10^{11} \text{ m}$

### Solution I

The surface temperature of the earth under steady-state conditions follows from a heat balance for the earth that equates the incoming and outgoing heat flows to each other. In order to determine how great the incoming energy flow to earth is, it is first necessary to establish how much energy the sun radiates and then the proportion of that radiation that reaches the earth. With the help of Wien’s displacement law, it follows for the surface temperature  $T_s$  of the sun that

$$T_s = \frac{2.898 \cdot 10^{-3}}{\lambda_{\text{max}}} = 5800 \text{ K} \quad (3.203)$$

The sun therefore emits an energy flow  $\phi_s$  of magnitude

$$\phi_s = 4\pi R_s^2 \sigma T_s^4 = 3.86 \cdot 10^{26} \text{ W} \quad (3.204)$$

Of this, only a small fraction reaches the earth, because solar radiation is emitted in every direction. At a distance  $s$  from the sun, all the emitted radiation is spread

over a sphere whose surface measures  $4\pi s^2$ , of which the earth takes up a surface area of  $\pi R^2$ . Of the radiation that reaches the earth’s atmosphere, fraction  $r$  is reflected by the atmosphere, while the remainder is absorbed by the earth. The amount of solar radiation absorbed by the surface of the earth is therefore

$$\phi_{\text{in}} = (1-r) \frac{\pi R^2}{4\pi s^2} 4\pi R_s^2 \sigma T_s^4 \quad (3.205)$$

The amount of radiation emitted by the surface of the earth is equal to

$$\phi_{\text{out}} = 4\pi R^2 \sigma T^4 \quad (3.206)$$

From this, from the steady-state heat balance for the earth,  $0 = \phi_{\text{in}} - \phi_{\text{out}}$ , it follows that

$$T = \left( (1-r) \frac{R_s^2}{4s^2} \right)^{1/4} T_s = 256 \text{ K} = -17^\circ\text{C} \quad (3.207)$$

It should be noted first of all that this expression does not include the radius of the earth! Also, this outcome is clearly incorrect – in reality, ‘the’ temperature of the surface of the earth is around  $15^\circ\text{C}$ ! The error we have made is not to have taken account of the so-called greenhouse effect of the atmosphere.

### Solution 2

For solar radiation, the atmosphere has a transmission coefficient  $t_{\text{atm}}$  of around 1, but a fraction  $a_{\text{atm}}$  of around 0.8 of the infrared radiation emitted by the earth is absorbed by the atmosphere and then emitted in two directions – to the surface of the earth and into space.

A steady-state heat balance for the surface of the earth then gives

$$0 = (1-r) \frac{\pi R^2}{4\pi s^2} 4\pi R_s^2 \sigma T_s^4 + 4\pi R^2 \sigma e_{\text{atm}} T_{\text{atm}}^4 - 4\pi R^2 \sigma T^4 \quad (3.208)$$

With  $e_{\text{atm}} = a_{\text{atm}}$ , this balance can then be rewritten as

$$T^4 - a_{\text{atm}} T_{\text{atm}}^4 = (1-r) \frac{R_s^2}{4s^2} T_s^4 \quad (3.209)$$

In the meantime, another unknown, *viz*  $T_{\text{atm}}$ , has been introduced and this asks for another (balance) equation. A steady-state energy balance for the atmosphere gives

$$0 = a_{\text{atm}} 4\pi R^2 \sigma T^4 - 2 \cdot 4\pi R^2 e_{\text{atm}} \sigma T_{\text{atm}}^4 \quad (3.210)$$

from which it follows that

$$T_{\text{atm}} = \left(\frac{1}{2}\right)^{1/4} T \quad (3.211)$$

Substituting Equation (3.211) in Equation (3.209) results in

$$T = \left( \frac{(1-r) \frac{R_s^2}{4s^2}}{1 - \frac{1}{2} a_{\text{atm}}} \right)^{1/4} \quad T_s = 290.5 \text{ K} = 17.3^\circ\text{C} \quad (3.212)$$

This outcome is much more in keeping with reality

□

### Summary

As well as by molecules (convectively or through conduction), heat can be transported by radiation (photons). For a completely 'black' body, the flux of the radiation that is emitted can be described using Stefan-Boltzmann's Law. It is also the case that a completely black body absorbs all incoming radiation.

In practice, no completely black radiators exist, and emission and absorption coefficients are used. In general, absorption and emission coefficients are numerically equal. As a rule,

$$\phi_{q,\text{rad}}'' = e \sigma T^4$$

is used and we refer to a grey body when  $0 < e < 1$  and when also the emission coefficient does not depend on the wavelength of the emitted radiation.

Whether a medium is opaque or transparent, and whether this medium can be regarded as a grey body, depends on the wavelength-dependent absorptivity of the material.

### 3.7.3 Heat transfer through radiation

Because every object emits heat radiation continuously, the heat transfer between two objects, 1 and 2, is the net result of the heat radiation  $\phi_{1 \rightarrow 2}$  from object 1 to object 2, and the heat radiation  $\phi_{2 \rightarrow 1}$  from object 2 to 1. If both objects are black radiators, then all the radiation from object 1 that falls on object 2 will be absorbed by object 2, and vice versa. This gives

$$\phi_{\text{net},1 \rightarrow 2} = \phi_{1 \rightarrow 2} - \phi_{2 \rightarrow 1} \quad (3.213)$$

Usually, just a fraction of the radiation emitted by object 1 will fall on object 2, and vice versa. These fractions are denoted by *visibility factors*  $F_{1 \rightarrow 2}$  and  $F_{2 \rightarrow 1}$ . For black bodies, this then leads to

$$\phi_{\text{net},1 \rightarrow 2} = F_{1 \rightarrow 2} A_1 \sigma T_1^4 - F_{2 \rightarrow 1} A_2 \sigma T_2^4 \quad (3.214)$$

Visibility factors  $F_{1 \rightarrow 2}$  and  $F_{2 \rightarrow 1}$  are determined solely by the geometry of the two objects and their position in relation to each other. If the two objects have the same temperature, in other words if  $T_1 = T_2$ , then of course they do not exchange any net radiation, and it follows from Equation (3.214) that

$$\frac{F_{1 \rightarrow 2}}{F_{2 \rightarrow 1}} = \frac{A_2}{A_1} \quad (3.215)$$

This is known as the *reciprocity relation* for the visibility factors. Although this relation has been derived here for the case of two black radiators at the same temperature, it is generally valid, as visibility factors depend only on the geometry of the objects.

For two parallel disks of equal size with a radius of  $R$  and separated by distance  $b$ , where  $b \ll R$ , the visibility factors are  $F_{1 \rightarrow 2} = F_{2 \rightarrow 1} = 1$ . For two concentric spheres or two infinitely long concentric cylinders of radii  $R_1$  and  $R_2$ , where  $R_1 < R_2$ , the visibility factors are  $F_{1 \rightarrow 2} = 1$  (because all the radiation emitted by object 1 reaches object 2) and, due to Equation (3.215),  $F_{2 \rightarrow 1} = R_1^2 / R_2^2$  (because part of the radiation emitted by object 2 lands elsewhere on object 2).

### Example 3.18. Radiant heat losses from an oven

A spherical-shaped oven (diameter  $D = 0.5 \text{ m}$ ) with an exterior wall temperature  $T_1 = 700^\circ\text{C}$  is located in a factory. All the other objects in the factory, as well as the floors, ceilings, and walls, have a temperature  $T_a = 20^\circ\text{C}$ . The oven and all the other objects, floors, ceilings, and walls may be regarded as black radiators. Calculate the net loss of heat from the oven through radiation.

By interpreting the factory as a concentric sphere around the oven, with a diameter of  $D_2 > D$ , then it follows from Equation (3.214), with  $F_{1 \rightarrow 2} = 1$  and  $F_{2 \rightarrow 1} \rightarrow 0$ , that the net heat flux from oven to environment  $\phi_{\text{net}} = A_1 \sigma (T_1^4 - T_a^4)$ .

[The same result is also found by treating the remaining objects as separate black radiators.] The numerical answer that was asked for then is 3.3 kW

□

For two non-transparent ( $t = 0$ ) grey radiators, it is more difficult to calculate the net heat transport from object 1 to object 2 than is the case with two black radiators, because some of the radiation emitted by object 1 is reflected by object 2 back to object 1. For both objects ( $i = 1, 2$ ) non-transparent and grey, obviously

$\alpha_i = e_i = 1 - r_i$ . If there is no radiant heat transfer to other objects, it can be derived for two grey radiators with emissivities  $e_1$  and  $e_2$ , surfaces  $A_1$  and  $A_2$ , and mutual visibility factors  $F_{1 \rightarrow 2}$  and  $F_{2 \rightarrow 1}$ , that

$$\phi_{\text{net},1 \rightarrow 2} = A_1 e_{\text{eff}} \sigma (T_1^4 - T_2^4) \quad (3.216)$$

where

$$e_{\text{eff}} = \left( \frac{1-e_1}{e_1} + \frac{A_1}{A_2} \frac{1-e_2}{e_2} + \frac{1}{F_{1 \rightarrow 2}} \right)^{-1} \quad (3.217)$$

stands for the *effective emission coefficient* or *effective emissivity*.

For engineers, three frequently useful applications of Equation (3.217) are

- Radiant heat transfer between two infinitely large, parallel grey plates with emission coefficients of  $e_1$  and  $e_2$  when  $F_{1 \rightarrow 2} = 1$  (in other words, all the radiation from plate 1 falls on plate 2) and  $A_1/A_2 = 1$ , Equation (3.217) results in

$$e_{\text{eff}} = \frac{e_1 e_2}{e_1 + e_2 - e_1 e_2} \quad (3.218)$$

- Radiant heat transfer between two concentric, grey spheres (or infinitely long cylinders) with emission coefficients of  $e_1$  and  $e_2$  and with diameters of  $D_1$  and  $D_2$  when  $F_{1 \rightarrow 2} = 1$  (all the radiation from the inner sphere or cylinder 1 falls on the outer sphere or cylinder 2), Equation (3.217) now gives

$$e_{\text{eff}} = \left( \frac{1}{e_1} + \frac{D_1^2}{D_2^2} \frac{1-e_2}{e_2} \right)^{-1} \quad (3.219)$$

- Radiant heat transfer between a convex grey object and its grey environment. If we regard a convex grey object 1 as enclosed by a grey environment 2, where  $A_2 \gg A_1$  and where  $F_{1 \rightarrow 2} = 1$  (because all the radiation from the object falls on the environment), then Equation (3.219) is simplified to  $e_{\text{eff}} = e_1$ . Where  $e_{\text{eff}} = e_1 = 1$  (that is, for a black radiator in a 'large' environment), Equation (3.216) is reduced to the equation used in Example 3.14.

This model is also excellently suited for calculating the net radiation losses from an object to the atmosphere, the emissivity of the atmosphere does not therefore play a role here.

### Summary

Visibility factors play a major role in the case of heat transfer through radiation between two black or grey objects, they are determined solely by the geometry of the two objects and their position in relation to each other.

Where every grey object emits, reflects and absorbs, the interest always is in the net heat transport

$$\phi_{\text{net},1 \rightarrow 2} = A_1 e_{\text{eff}} \sigma (T_1^4 - T_2^4)$$

where the effective emission coefficient, or effective emissivity, stands for

$$e_{\text{eff}} = \left( \frac{1-e_1}{e_1} + \frac{A_1}{A_2} \frac{1-e_2}{e_2} + \frac{1}{F_{1 \rightarrow 2}} \right)^{-1}$$

and is a function of the emission coefficients of both objects, of their surfaces, and of visibility factor  $F_{1 \rightarrow 2}$ . This relation can be simplified for some typical situations. If a 'small' object is enclosed by a 'large' environment, the emissivity of the environment plays no role.

### 3.7.4 Radiant heat transfer coefficient

It is often a good idea to write a heat flux through radiation in terms of a heat transfer coefficient and a driving force  $\Delta T$ . This radiant heat transfer coefficient is denoted by  $h_r$  and can be obtained on the basis of Equation (3.216). To this end,  $T_1^4 - T_2^4$  is rewritten by linearising  $T^4$

$$T_1^4, T_2^4 + 4\bar{T}^3 (T_1 - T_2) \quad (3.220)$$

since  $dT^4/dT = 4T^3$  and using  $\bar{T} = \frac{1}{2}(T_1 + T_2)$ . In an alternative derivation  $T_1^4 - T_2^4$  is decomposed into factors

$$\begin{aligned} T_1^4 - T_2^4 &= (T_1^2 + T_2^2)(T_1^2 - T_2^2) = \\ &= \{(T_1 + T_2)^2 - 2T_1 T_2\} (T_1 + T_2)(T_1 - T_2) \end{aligned} \quad (3.221)$$

Using  $\bar{T} = \frac{1}{2}(T_1 + T_2)$  and  $T_1 T_2 \approx \bar{T}^2$ , Equation (3.220) is also obtained.

Combining Equation (3.220) with Equation (3.216) results in an expression similar to Newton's Law of Cooling (§ 3.2.1)

$$\phi_{\text{net},1 \rightarrow 2} = h_r A_1 (T_1 - T_2) \quad (3.222)$$

in which

$$h_r \approx 4 e_{\text{eff}} \sigma \bar{T}^3 \quad (3.223)$$

It is clear that the coefficient  $h_r$  not only depends on radiation constant  $\sigma$ , but also on emission coefficients  $e_1$  and  $e_2$  (and therefore on the materials of which both objects are made or with which they are coated) and on temperatures  $T_1$  and  $T_2$ .

Verify that the above calculation in terms of  $\bar{T}$  for  $T_1 = 300$  K and  $T_2 = 400$  K leads to an error of just 2%, and that for  $T_1 = 300$  K and  $T_2 = 1000$  K, the error amounts to around 20%. Also verify that, for average temperatures in the vicinity of room temperature,  $h_r$  is of the order of 1-10 W/m<sup>2</sup>K, and therefore cannot be neglected in comparison with free convection, for example. With higher temperatures,  $h_r$  increases considerably, and therefore so does the contribution of radiation to the overall heat transport.

#### Example 3.19. A thermometer in a cold room

In the middle of a room in which the temperature of the air is  $T_a$ , hangs a thermometer. If the walls have uniform, lower temperature  $T_w$ , what temperature  $T_1$  does the thermometer show?

Carry out the calculation for  $\bar{T} = 300$  K, for  $T_1 - T_w = 10$  K, and on the basis of an emission coefficient of  $e = 0.05$  for the thermometer. Consider the situation as steady.

The idea is that the thermometer shows the air temperature  $T_a$ . The problem here is that the thermometer 'sees' the colder walls. This means that radiation will cause heat to 'flow away' from the thermometer to the wall and the temperature  $T_1$  of the thermometer will be lower than  $T_a$ . As a result of the difference in temperature ( $T_a - T_1$ ), heat will then be transferred from the air to the thermometer. This transport will be maintained by free convection (why?). In a steady-state situation, the heat discharge through radiation will form an equilibrium with the heat supplied through free convection.

$$e\sigma(T_1^4 - T_w^4) = h(T_a - T_1) \quad (3.224)$$

from which it follows, approximately, that

$$T_a - T_1 = \frac{4e\sigma}{h} \bar{T}^3 (T_1 - T_w) \quad (3.225)$$

If a normal value of 6 W/m<sup>2</sup>K is taken for heat transfer coefficient  $h$  for free convection, it follows that  $T_a - T_1 \approx 0.5$  K.

#### Example 3.20. Solar radiation onto a flat roof

The sun shines onto a horizontal flat roof, there is no wind. Heat flux  $\phi_s''$  through the solar radiation to the roof is 300 W/m<sup>2</sup>. All the radiation is absorbed by the roof, while heat loss on the underside of the roof is negligible due to good insulation there. Calculate, for a steady-state situation, the surface temperature  $T_w$  of the roof if the ambient temperature  $T_a$  is 20 °C.

As a result of the heat radiation from the sun, the temperature of the roof rises. When there is no wind, two heat transport mechanisms are possible, apart from heat conduction: free convection is caused because the roof heats up the air immediately above it, and the consequent lower air density induces free convection. The warm roof will of course start to radiate, but the heat radiation depends on the still unknown roof temperature, but can be calculated with the help of Equation (3.216) in which  $e_{\text{eff}} = e_1 = a_1 = 1$ .

$$\phi_{\text{net},1 \rightarrow 2}'' = \sigma(T_w^4 - T_a^4) \quad (3.226)$$

The heat transfer coefficient  $h$  for the heat discharge through free convection follows from Equation (3.162). If, for the sake of simplicity, air can be regarded as an ideal gas, so that

$$\frac{\Delta\rho}{\rho_w} = \frac{T_w - T_a}{T_a} \quad (3.227)$$

(where  $\rho_w$  represents the density of air at  $T = T_w$ ), then it follows that

$$\phi_{\text{free convection}}'' = 0.17\lambda \left( \frac{g}{\nu a T_a} \right)^{1/3} (T_w - T_a)^{4/3} \quad (3.228)$$

In steady-state conditions, the fluxes (3.216) and (3.228) then reach equilibrium with the solar influx  $\phi_s''$ .

$$\phi_s'' = \sigma(T_w^4 - T_a^4) + 0.17\lambda \left( \frac{g}{\nu a T_a} \right)^{1/3} (T_w - T_a)^{4/3} \quad (3.229)$$

From this,  $T_w$  should be calculated iteratively or estimated with the help of an equation like (3.223) for example. The roof temperature that was asked for is around 44°C. Neglecting the contribution of radiation to the heat discharge would have led to a roof temperature of around 63°C. The contribution by radiation to free convection would have been of the same order of magnitude.

**Summary**

It is possible to use with a heat transfer coefficient in the case of heat transfer through radiation. In general, this  $h_r$  depends on emission coefficients, temperatures, and surfaces and the radiating bodies:

$$h_r \approx 4 e_{\text{eff}} \sigma \bar{T}^3$$

where  $e_{\text{eff}}$  represents the effective emission coefficient or effective emissivity.

Heat transfer through radiation and heat transfer through free convection frequently occur simultaneously, and with ambient temperatures are often of the same order of magnitude. As temperatures rise, the importance of radiation increases.

# 4 Mass transport

## 4.1 Analogy between mass transport and heat transport

It emerged in Chapter 1 that convective transport of heat and convective transport of mass occur and can be described analogously. And indeed, the expressions for convective transport of heat and species look the same.

$$\phi_q = \phi_V \rho c_p T \quad (4.1)$$

$$\phi_m = \phi_V c \quad (4.2)$$

Both equations take the form of volumetric flow rate times the relevant concentration. The fluxes are given by the product of velocity and the relevant concentration.

Chapter 2 looked in detail at *molecular transport*. During their temperature movements, molecules transport their own mass and their own critical energy. In a phenomenological approach, the resulting diffusive net fluxes of mass and heat are described in the same manner: the mass and heat fluxes are proportional to the gradients in the mass or species concentration and thermal energy concentration respectively. The proportionality constant (or respectively, the diffusion coefficient  $ID$  and the thermal diffusivity coefficient  $\alpha$ ) both have the same dimension, that is  $\text{m}^2/\text{s}$ . Both coefficients are physical properties that reflect the mobility of the individual molecules and their capacity to pass on thermal energy. The phenomenological expressions for the fluxes (i.e., the flow rates per unit of cross-sectional area) are as follows:

$$\phi_q'' = -\lambda \frac{dT}{dx} = -\alpha \frac{d(\rho c_p T)}{dx} \quad \text{Fourier's law} \quad (4.3)$$

$$\phi_m'' = -ID \frac{dc}{dx} \quad \text{Fick's law} \quad (4.4)$$

As noted in Chapter 2, the second version of Fourier's law is only correct if the product of  $\rho c_p$  is constant; however, writing it in this way shows more clearly the

similarity with Fick's law for species transport and explicitly links the transport of 'something' to the concentration gradient in that same 'something'

With Fick's law, it should be restated here that it is of only limited validity. Fick describes mass transport resulting from differences in concentration (and disregards other driving forces for mass transport), it applies to diluted systems, is limited to binary systems and gives a moderate or poor description of the diffusion of complex (that is, non-spherical and polar) molecules<sup>15</sup>. The analogy with heat transport therefore does not hold under every condition. This should be carefully borne in mind at all times!

The species concentration and the species flow in Fick's law can be expressed in two different ways on the basis of mass (that is, in kg/m<sup>3</sup> and kg/m<sup>2</sup>s) and in terms of moles (that is, in kmol/m<sup>3</sup> and kmol/m<sup>2</sup>s). The latter is often the more obvious one to use in the case of chemical reactions. With Fick's law, the diffusion coefficient is defined in such a way that the net molecular transport of two species A and B through a surface in space is zero. A distinction should be made here according to whether 'kg' or 'kmol' is the basis.

a) *the net mass flow (in kg) is zero*

in this 'barycentric' approach, the following applies in every plane in the domain

$$\phi''_{m,A,x} + \phi''_{m,B,x} = 0 \quad (4.5)$$

where – with mass concentrations  $c_i$  in kg/m<sup>3</sup> – the following applies

$$\phi''_{m,A,x} = -ID_{AB} \frac{dc_A}{dx} \quad (4.6)$$

and

$$\phi''_{m,B,x} = -ID_{BA} \frac{dc_B}{dx} \quad (4.7)$$

while

$$c_A + c_B = c = \text{constant} \quad (4.8)$$

so that

$$ID_{AB} = ID_{BA} \quad (4.9)$$

<sup>15</sup> It falls outside the scope of this introduction on transport phenomena to deal with the generally applicable Stefan-Maxwell equations for mass transport. Readers are advised to consult J.A. Wesselingh & R. Krishna, 'Mass Transfer in Multicomponent Mixtures', VSSD, Delft 2000, for example.

The definitions have been set in such a way that the diffusion coefficients of A in B and of B in A have the same numerical value. These definitions are generally used with diffusion in solids and liquids because when concentrations of A in B, for example, are not too high, the density can be assumed to be constant.

b) *the net mole flow is zero.*

the same equations as above apply here as well, but now with the concentrations  $c_i$  in kmol/m<sup>3</sup> and with the fluxes  $\phi''_{\text{mol}}$  in kmol/m<sup>2</sup>s. It is also true here that the diffusion coefficients of A in B and of B in A have the same numerical value. This choice is very suitable for describing diffusion in gases, as Equation (4.8) certainly applies to ideal gases when pressure and temperature are constant.

In the rest of this chapter, we will work both in terms of kg and in terms of 'moles', depending on the issue of interest. In the case of species balances with chemical reactions, working in terms of moles is the preferred approach.

Thanks to the above analogies between heat and species transport, it will be possible to convert much of what was discussed and derived in Chapter 3 from heat transport to species transport terms without much difficulty. The technique of drawing up balances, which usually involves the terms that feature in Equations (4.1) to (4.4), and deriving and solving differential equations from them with due regard to the boundary conditions, works in exactly the same way with questions relating to mass transport and heat transport.

However, there are two important differences:

- a) depending on the boundary conditions, the diffusion of mass of species A leaves species B various options for movement or transport which, in turn, influence the transport from species A, and
- b) if two media are in thermal equilibrium, then the temperature of the two is identical, however, if two different media (or phases) that contain dissolved A are in equilibrium with each other, then in general the concentrations of A in both media (or phases) will be *different*!

Before dealing with these exceptional situations in depth in § 4.3 and § 4.6, we will first look in § 4.2 in more detail at the analogies in the ways of describing molecular transport. In § 4.2 and § 4.3 processes with a diffusive character will be examined, while convective mass transport in different conditions will be covered in § 4.5, based on the analogy with convective heat transport. Mass transport in the most general sense will feature in § 4.4. Finally, § 4.6 will discuss mass transport from one phase to another phase, while § 4.7 will deal with the simultaneous occurrence of heat and mass transfer.

### Summary

This Section has referred to how mass transport is, in principle, entirely analogous to heat transport. It has pointed out limits of the validity of Fick's law in particular, and therefore of the analogy. In addition, two types of situation have been highlighted that merit separate attention, as the analogy does not hold for them. One can work in terms of kg's as well of 'moles'.

## 4.2 Mutual diffusion based on the analogy with heat transport

This Section will deal with binary systems (that is, systems with just two species, such as substance (or species) A in a pure solvent B) which involve only pure diffusion and in which no convective transport occurs. If the two types of molecule, A and B, exchange places, net, then Fick's law applies. This means there is *mutual diffusion*. In this case, diffusion is entirely analogous to conduction. We will again deal with the three basic geometries.

### 4.2.1 Steady-state diffusion in Cartesian coordinates

Consider two parallel plates (distance between the two is  $D$ ) between which two gaseous (or two liquid) substances A and B are located (see Figure 4.1). Suppose that there is a difference in concentration  $\Delta c_A$  between the plates. Macroscopically, the situation is unchangeable over time (steady state). The overall concentration  $c$  is constant (that is, not a function of  $x$ ):  $c = c_A + c_B = \text{constant}$ . This means therefore that a difference in concentration for substance B of  $\Delta c_B = -\Delta c_A$  exists between the slices. The result of this is that there are two equally sized but opposing fluxes,  $\phi_A''$  and  $\phi_B''$ . This is easy to understand: draw up a mass balance for substance A for a thin slice between  $x$  and  $x + dx$  (see Figure 4.1):

$$0 = -ID \frac{dc_A}{dx} \Big|_x - \left( -ID \frac{dc_A}{dx} \Big|_{x+dx} \right) \quad (4.10)$$

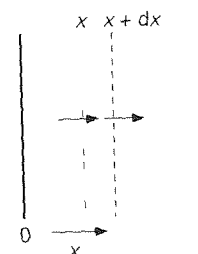


Figure 4.1

Solving Equation (4.10) with boundary conditions  $x = 0 \rightarrow c_A = c_{A,0}$  and  $x = D \rightarrow c_A = c_{A,D}$  produces

$$c_A(x) = c_{A,0} + (c_{A,D} - c_{A,0}) \frac{x}{D} \quad (4.11)$$

Equation (4.11) is entirely equivalent to Equation (3.5) for heat transport. Now, too, the link between the driving force  $\Delta c_A$  and the mass flux can be determined.

$$\Delta c_A = \phi_{m,A}'' \frac{D}{ID} \quad (4.12)$$

This is again completely analogous to Ohm's law: the driving force  $\Delta c_A$  and the mass flux are linearly linked by a resistance. Compare Equation (4.12) with Equation (3.17).

Precisely this logic can be used for the transport of substance B. The result is

$$\Delta c_B = \phi_{m,B}'' \frac{D}{ID} \quad (4.13)$$

Because  $\Delta c_A = -\Delta c_B$ , it follows directly from Equations (4.12) and (4.13) that both mass fluxes are indeed the same size but in opposing directions. The resistance to transport is of the same magnitude for both substances.

### 4.2.2 Steady-state diffusion in cylindrical coordinates

The mutual diffusion of two substances A and B between two concentric cylinders in a steady-state situation is shown in Figure 4.2. The overall concentration  $c = c_A + c_B$  is again constant, that is, it is not a function of place. The concentrations on both cylinder surfaces have a fixed value:  $r = R_1 \rightarrow c_A = c_{A1}, c_B = c_{B1}$  and  $r = R_2 \rightarrow c_A = c_{A2}, c_B = c_{B2}$ . Completely analogous to the cylinder geometry in the case of heat transport, it is possible to determine the concentration profile of, say, substance A from a mass balance for substance A for a volume between the cylinders of between  $r$  and  $r + dr$  (and the same length  $L$  as both cylinders). This balance is as follows (remember that there is only transport from A as a result of mutual diffusion):

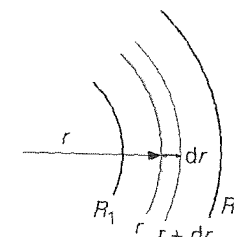


Figure 4.2

$$0 = 2\pi L \left( -IDr \frac{dc_A}{dr} \right)_r - 2\pi L \left( -IDr \frac{dc_A}{dr} \right)_{r+dr} \quad (4.14)$$

After simplification, Equation (4.14) produces a second-order differential equation

$$\frac{d}{dr} \left( r \frac{dc}{dr} \right) = 0 \quad (4.15)$$

Equation (4.15) is entirely analogous to Equation (3.36), integrating once shows that  $r dc/dr$  is constant, after which the solution proceeds further, as presented after Equation (3.26). For the link between the driving force  $\Delta c_A$  and mass flow  $\phi_{m,A}$ , the following expression results

$$\Delta c_A = \frac{\ln(R_2/R_1)}{2\pi IDL} \phi_{m,A} \quad (4.16)$$

entirely analogous to Equation (3.30). Here, too, the distance  $R_2 - R_1$  (to which the difference in concentration relates) does not appear as such, although it implicitly does in  $\ln(R_2/R_1) = \ln R_2 - \ln R_1$ ! This is therefore a result of the cylinder geometry

#### Example 4.1. Transport of oxygen in human tissue

In a study on oxygen transport in human tissue, Nobel Prize laureat August Krogh (Danmark, 1874–1949) considered a cylindrical vein surrounded by an annular ring of tissue. The metabolism through which in the tissue oxygen is converted into carbon dioxide, was modelled by a zeroth order reaction with reaction rate  $k_r$  (in mol/m<sup>3</sup>s). Transport in the tissue takes place through diffusion with diffusion coefficient  $ID$ .

On the inner side of the tissue ring, adjacent to the vein, at  $r = R_1$ , an oxygen concentration  $c = c_0$  was assumed, while on the outer side, at  $r = R_2$  (with  $R_2 > R_1$ ), no oxygen transport was supposed, i.e.  $dc/dr = 0$ . In Krogh's study, a steady-state case was considered.

Derive, on the basis of a proper mass balance, expressions for the radial concentration profile in the tissue as well as for the transport rate per unit of length at which oxygen is transferred from the vein into the tissue.

Actually, the mass balance (in terms of mol/s) looked after is an extension of Equation (4.14) because of the chemical reaction, a consumption term should be added to the balance equation, namely  $-k_r 2\pi r L dr$ . Dividing all terms of the equation through  $2\pi r L / ID dr$  results in the second-order differential equation

$$\frac{d}{dr} \left( r \frac{dc}{dr} \right) = \frac{k_r}{ID} r \quad (4.17)$$

Integrating twice gives

$$c = A \ln r + \frac{k_r}{4ID} r^2 + B \quad (4.18)$$

With the help of the two boundary conditions provided, the radial concentration profile in the tissue becomes

$$(c - c_0) \frac{2ID}{k_r R^2} = \ln \left( \frac{r}{R_1} \right) - \frac{r^2 - R_1^2}{2R_2^2} \quad (4.19)$$

and the oxygen supply rate (per unit of length of the vein) from vein into tissue

$$\frac{\phi_m}{L} = -ID \frac{dc}{dr} \Big|_{r=R_1} 2\pi R_1 = \pi k_r (R_2^2 - R_1^2) \quad (4.20)$$

The latter result could also have been found from a steady-state overall mass balance for an annular ring of tissue: supply rate = consumption rate in the metabolism.  $\square$

#### 4.2.3 Steady-state diffusion in spherical coordinates

Consider finally two concentric spheres with radii of  $R_1$  and  $R_2$  ( $R_2 > R_1$ ). In the space between them are two substances, A and B, which are mutually diffusing. The situation is steady. The fixed boundary conditions

$$r = R_1 \rightarrow c_A = c_{A1}, c_B = c_{B1} \quad \text{and} \quad r = R_2 \rightarrow c_A = c_{A2}, c_B = c_{B2}$$

apply at the edges. The link between the driving force and mass flow can of course be found by solving the concentration profile. The result of this calculation is

$$\Delta c_A = c_{A1} - c_{A2} = \frac{1}{4\pi ID} \left( \frac{1}{R_1} - \frac{1}{R_2} \right) \phi_{m,A} \quad (4.21)$$

For  $R_2 \rightarrow \infty$ , this results in an expression that is again entirely analogous to Equation (3.45) for heat conduction from the surface of a sphere into an infinite motionless medium.

The above observations on mutual diffusion in a binary mixture also apply if diffusion occurs by just one substance through a motionless medium (which is actually mutual diffusion of that one substance and 'empty places'). This occurs in the case of diffusion of a gas through a solid, for example.

#### Example 4.2. Gas diffusion through a solid wall

Pure helium (gas) is contained in a glass sphere (internal diameter  $D_1 = 20$  cm, external diameter  $D_2 = 21$  cm). The sphere is surrounded by air, in which the concentration of helium is negligible. Helium can diffuse through the glass, while

the air is not able to do so (helium molecules are much smaller than 'air' molecules) This, then, is a case of diffusion by one substance (helium) through a motionless medium (glass)

The diffusion coefficient  $ID$  of helium through glass amounts to  $0.2 \cdot 10^{-11} \text{ m}^2/\text{s}$ . The solubility  $c^*$  of helium in glass ( $\text{in kg/m}^3$ ) is just 0.84% of the density (also in  $\text{kg/m}^3$ ) of the helium gas the glass is (long-term) exposed to. The temperature of the sphere and air is  $20^\circ\text{C}$

If the pressure in the sphere is 2 bar, how great is the flow of mass through the glass?

Given that the diffusion coefficient is very small, the flow and therefore the decrease in helium mass in the sphere will be very small. This means that the transport of the helium through the glass can be assumed to be quasi-steady: the change in the boundary condition on the inside of the glass is so slight that the effect of the change on the transport can be disregarded.

The first step, then, is to draw up a mass balance for a concentric shell in the glass between  $r$  and  $r + dr$ , in the same way as in § 3.1.4 for heat conduction in a spherical geometry. The solution to the resulting differential equation – which has the same form as Equation (3.42) – produces the profile of the concentration of the helium in the glass. From this it follows, via Equation (4.21), for the mass flow of helium, that

$$\phi_{m,\text{He}} = \frac{4\pi ID}{\frac{1}{R_1} - \frac{1}{R_2}} (c^* - 0) \quad (4.22)$$

where  $c^*$  represents the helium concentration in the glass at the inside wall of the sphere, and the helium concentration in the glass on the outer wall is taken to be equal to 0. Equation (4.22), after all, is the result of a mass balance for a shell in the glass and so therefore the helium concentrations at the inside and outside edges in the glass must also be filled in.

Of course, even at the inside edge, the helium concentration in the glass is – and this includes equilibrium situations – much smaller than the helium concentration in the gas phase inside the glass sphere. It is given that the solubility  $c^*$  of helium in glass depends on the helium density (or concentration)  $c$  in the adjacent gas; here, it is sufficiently accurate to assume that helium behaves like an ideal gas:

$$c_{\text{He}} = \frac{M_p}{RT} = 0.33 \text{ kg/m}^3 \quad (4.23)$$

where  $M$  stands for the molar mass of helium. Filling in the various numerical values in Equation (4.22) produces  $\phi_{m,\text{He}} = 1.5 \cdot 10^{-13} \text{ kg/s}$ .

### Example 4.3. A spherical fungus flake

An aerated bioreactor is used to grow fungus flakes which for convenience sake may be conceived as spheres. For its growth, such a fungus needs oxygen which is consumed according to a zeroth-order reaction. As this growth takes place uniformly distributed across the flake, oxygen has to diffuse into the flake. The need of oxygen therefore increases as the flake grows. As soon as oxygen can no longer penetrate to the core of the flake, anaerobic (oxygen-less) reactions start producing toxic substances. The growth process has therefore to be interrupted before the core of the flake becomes poor in oxygen.

Consider now a quasi-steady state of a flake with radius  $R$  while ignoring the growth for the time being. Derive from an oxygen balance for such a flake the differential equation for the oxygen concentration  $c$ . Solve this differential equation, specify the boundary condition(s) used, find the concentration profile in the flake, and calculate the maximum flake diameter when using the following data:

diffusion coefficient of oxygen in a flake  $ID = 5 \cdot 10^{-9} \text{ m}^2/\text{s}$ , reaction constant for oxygen consumption  $k_r = 3.6 \cdot 10^{-4} \text{ mol/m}^3\text{s}$ , oxygen concentration  $c_0$  at the flake surface inside the flake  $c^* = 0.3 \text{ mol/m}^3$

Again, this problem has to be solved by drawing up a mass balance for oxygen over a spherical shell inside a flake between  $r$  and  $r + dr$ , in the same way as in the preceding Example. The difference is that the balance now also comprises a negative production term owing to the zeroth-order chemical reaction. The balance for the steady-state condition suggested runs as

$$0 = \left( -4\pi r^2 ID \frac{dc}{dr} \right)_{r} - \left( -4\pi r^2 ID \frac{dc}{dr} \right)_{r+dr} - k_r 4\pi r^2 dr \quad (4.24)$$

Combining the two diffusion terms in the right-hand side and dividing all terms by  $4\pi dr$  gives

$$0 = ID \frac{d}{dr} \left( r^2 \frac{dc}{dr} \right) - k_r r^2 \quad (4.25)$$

Integrating once results in

$$r^2 \frac{dc}{dr} = \frac{k_r}{ID} \frac{1}{3} r^3 + \alpha \quad (4.26)$$

The boundary condition  $r = 0 \rightarrow dc/dr = 0$  makes  $\alpha = 0$  and therefore

$$\frac{dc}{dr} = \frac{k_i}{3ID} r \quad (4.27)$$

Integrating once more with the second boundary condition  $r = R \rightarrow c = c^*$  leads to the concentration profile

$$c = c^* - \frac{k_i}{3ID} (R^2 - r^2) \quad (4.28)$$

The condition that  $c = 0$  at  $r = 0$  has to be avoided, results in the conclusion that the maximum flake radius  $R_{\max}$  is given by

$$R_{\max}^2 = \frac{6IDc^*}{k_i} \quad (4.29)$$

Substituting the numerical data provided leads to a maximum flake diameter  $D_{\max}$  of 1 cm

□

### Summary

The Section above has looked at steady-state mutual diffusion in binary systems, analogous to heat transport. The link between driving force  $\Delta c_A$  and mass flow  $\phi_{m,A}$  can be written analogously to Ohm's law. Driving force and mass flow are directly proportional, the proportionality constant can be taken as resistance, in this case to mass transport. Expressions have been found for flat and non-flat geometries – with the help of micro balances for thin slices, rings and shells – which are entirely similar to those for heat transport.

#### 4.2.4 Mass transfer coefficient and Sherwood number

It was stated in the previous Section that the mass flow and the driving force are proportionate to each other. This finding can be used for linking driving force and mass flow to each other according to the recipe of Newton's Law of Cooling. For mass transport, the following applies

$$\phi_{m,A} = kA\Delta c_A \quad (4.30)$$

where the constant  $k$  is called the *mass transfer coefficient* (SI-unit m/s). Entirely analogous with heat transport,  $1/k$  is now interpreted as the resistance to mass transport. The results from the previous Section can now be shown in terms of a  $k$  value for every situation

mass transfer coefficient	between two flat plates	for annular space between two cylinders (related to outer surface)	for sphere in an infinite medium
$k$	$\frac{ID}{D}$	$\frac{2ID}{D_2 \ln D_2/D_1}$	$\frac{2ID}{D}$

These relations too can now be put into a non-dimensional form. The non-dimensional number that goes with mass transfer is the *Sherwood number*, abbreviated to  $Sh$  and defined as

$$Sh = \frac{\text{resistance to mass transfer due to diffusion}}{\text{actual resistance to mass transfer}} = \frac{D/ID}{1/k} = \frac{kD}{ID} \quad (4.31)$$

For mutual diffusion from a spherical surface in an infinite medium,  $Sh = 2$ , just as  $Nu = 2$  applies to the cooling down of a sphere through conduction in an infinite medium

The term *overall mass transfer coefficient* cannot yet be dealt with analogously to the term overall heat transfer coefficient. Because this involves diffusion across the interface of two different media in which even in a state of equilibrium the concentrations will not generally be equal, discussion of the topic will have to wait until § 4.6

### Summary

There is also a kind of 'cooling law' in the event that mass transport is determined by driving force (a difference in concentration in this case), the surface through which the mass flow goes, and the mass transfer coefficient  $k$ :

$$\phi_{m,A} = kA\Delta c_A$$

This mass transfer coefficient  $k$  is a key variable in a new non-dimensional number – the Sherwood number  $Sh = kD/ID$ . Specific expressions for the Sherwood number apply to the various basic geometries in the way that they do for the Nusselt number in relation to conductive heat transport.

#### 4.2.5 Unsteady-state diffusion: penetration theory

As with unsteady-state heat conduction, we will only deal with flat basic geometry below. Consider a medium (see Figure 4.3) that is bordered on one side, at  $x = 0$ , by a flat wall, while on the other it stretches out into 'infinity'. The dimensions  $W$  and  $L$  in the two remaining directions are also very large. The medium consists of a species A and a species B. The situation is in equilibrium, which means that the concentrations of both species,  $c_{A0}$  and  $c_{B0}$  respectively, are constant

At a certain point in time,  $t = 0$ , the concentration of species A at position  $x = 0$  is suddenly raised,  $\Delta c_A$ , while at the same time the concentration of species B at  $x = 0$  is reduced by  $\Delta c_B = -\Delta c_A$  [this way, requirement (4.10) is met  $c_A + c_B = c$ ] These new boundary conditions then remain in place. What will happen?

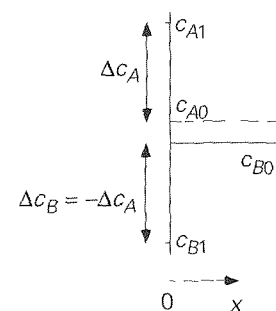


Figure 4.3

These new concentrations will start to penetrate the medium, analogous to the penetration of heat (see Figure 3.11 and § 3.3.1), where it is again assumed that mutual diffusion will be involved [Notice that the boundary conditions have been chosen with this in mind] Below, however, only species A will be considered.

In order to be able to determine how the concentration of, say, species A progresses, it is necessary to draw up a mass balance for species A for a slice of the medium between  $x$  and  $x + dx$ . This balance is as follows

$$\frac{\partial(WLdx c_A)}{\partial t} = WL \left\{ -ID \frac{\partial c_A}{\partial x} \Big|_x \right\} - WL \cdot \left\{ -ID \frac{\partial c_A}{\partial x} \Big|_{x+dx} \right\} \quad (4.32)$$

Equation (4.32) can be simplified to

$$\frac{\partial c_A}{\partial t} = ID \frac{\partial^2 c_A}{\partial x^2} \quad (4.33)$$

This result corresponds completely with Equation (3.72), in relation to heat transport. Because the boundary conditions are also the same, the whole solution is the same all the results in § 3.3.1 can be replicated unconditionally. The solution to Equation (4.33) is therefore once again the *error function*. This means that here too we are working with the *penetration theory*.

The *penetration depth* is now defined as  $x = \sqrt{\pi IDt}$ . This penetration depth has the same meaning as it does with heat transport: the mass flux that flows through the interface ( $x = 0$ ) into the medium, is given by

$$\begin{aligned} \phi''_{m,A} &= -ID \frac{\partial c_A}{\partial x} \Big|_{x=0} = ID \frac{c_{A1} - c_{A0}}{\sqrt{\pi IDt}} = \\ &= \sqrt{\frac{ID}{\pi t}} (c_{A1} - c_{A0}) = k (c_{A1} - c_{A0}) \end{aligned} \quad (4.34)$$

This means that Equation (4.34) is entirely analogous to Equation (3.78). Here, too, the driving force  $\Delta c_A = c_{A1} - c_{A0}$  is a constant, while the mass transfer coefficient  $k$  is a function of the time

Of course, the validity of the penetration theory is again limited to a flat geometry and to short periods of time. Whether the time interval in question is indeed sufficiently short to be able to apply the penetration theory can be estimated by comparing the penetration depth with the scale of length  $D$  (the thickness of the layer into which the heat penetrates from one side), or with the help of the Fourier number. The following must apply

$$\sqrt{\pi IDt} < 0.6D, \text{ or } Fo = \frac{IDt}{D^2} < 0.1 \quad (4.35)$$

This condition is completely identical to Condition (3.79) for applying short-term penetration theory in the case of transient conduction. The Fourier number is, apart from non-dimensional constants, also now the square of the ratio of two scales of length (or the ratio of two scales of time) see the discussion after Equation (3.80).

For the mass transfer coefficient  $k$ , it is found that, similar to Equation (3.91),

$$k(t) = \sqrt{\frac{ID}{\pi t}} \quad (4.36)$$

From this follows the mean mass flux through plane  $x = 0$  that enters the medium for  $t_e$  seconds (starting from  $t = 0$ ), the mean transfer coefficient for this interval, and the Sherwood relation that goes with  $k(t)$

$$\overline{\phi''_{m,A}} = \frac{1}{t_e} \int_0^{t_e} k(t) \Delta c_A dt = 2 \sqrt{\frac{ID}{\pi t_e}} \Delta c_A \quad (4.37)$$

$$\bar{k} = 2 \sqrt{\frac{ID}{\pi t_e}} = 2 k(t_e) \quad (4.38)$$

$$Sh = \frac{kD}{ID} = 0.564 Fo^{-1/2} \quad (4.39)$$

**Example 4.4. A contaminated landfill I**

Ten years ago, contaminated soil was deposited at a landfill in location L. During this period, the substance has slowly penetrated the clean soil underneath (caused by the rainwater seeping down, for example). This process can be described in terms of a diffusion or dispersion process with an effective diffusion coefficient  $ID = 2 \cdot 10^{-10} \text{ m}^2/\text{s}$ . It can be assumed that the concentration of the contamination on the surface of the clean soil has a constant value of  $c^* = 2 \text{ kg/m}^3$ . To decide on the thickness of the soil that has to be dug up, and on what to do with it once it has been dug up, first a number of questions have to be answered:

- How deeply has this substance diffused into the soil over the ten-year period?
- How much of the substance has ended up in the underlying soil?

Question (a) is answered by calculating the penetration depth

$$x_e = \sqrt{\pi ID t_e} = 45 \text{ cm} \quad (4.40)$$

As it can be assumed that the clear layer of soil is much thicker than 45 cm, the penetration theory may be applied here. The penetration depth gives immediately a reasonable estimate of how far the contamination has penetrated.

The answer to question (b) is determined first by calculating the mean mass flow rate through the interface of the clean and contaminated soil

$$\overline{\phi_m''} = \bar{k} (c^* - 0) = 2 \sqrt{\frac{ID}{\pi t_e}} c^* \quad (4.41)$$

From this, it is easy to determine the mass that has penetrated the soil per unit of surface area during the ten years

$$M'' = \overline{\phi_m''} t_e = \frac{2}{\pi} \sqrt{\pi ID t_e} c^* = 0,57 \text{ kg/m}^2 \quad (4.42)$$

□

**4.2.6 Unsteady-state long-term diffusion**

Unsteady-state long-term diffusion, too, is entirely analogous to unsteady-state long-term heat conduction (§ 3.3.5 and § 3.3.6). This is nicely illustrated by the Fourier number for heat transport it has been defined as  $Fo = a t / D^2$  while for mass transport  $Fo = ID t / D^2$  is used. Just like with long-term conduction, we speak of long-term diffusion

- when  $Fo > 0,03$  in cases the diffusion is double-sided (from or towards the two planes of a stagnant or solid slab of material) or from or towards the surface of a solid or stagnant cylindrical or spherical body

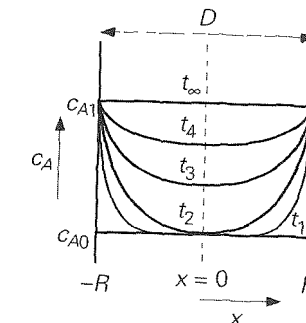


Figure 4.4

For long-term two-sided diffusion, the concentration profiles (see Figure 4.4) still have to obey the unsteady-state diffusion equation

$$\frac{\partial c_A}{\partial t} = ID \frac{\partial^2 c_A}{\partial x^2} \quad (4.43)$$

but again – see also the conditions of Equation (3.98) – with the following initial and boundary conditions

$$\begin{aligned} c_A(t=0) &= c_{A0} && \text{for } |x| \leq R \\ c_A(x=R) &= c_{A1} && \text{for } t > 0 \\ \frac{\partial c_A}{\partial x} &= 0 && \text{for } x=0 \text{ and } t > 0 \end{aligned} \quad (4.44)$$

Here, too, it is the case that for sufficiently long times ( $Fo > 0,03$ ), the profiles become spatially similar (providing that the boundary conditions remain the same the whole time, of course). The results in § 3.3.5 and § 3.3.6 can be translated directly and Figures 3.17 and 3.18 can be used again, providing that  $T$  is replaced by  $c_A$  (and therefore also  $\langle T \rangle$  and  $T_c$  by  $\langle c_A \rangle$  and  $c_{Ac}$  respectively) and, as remarked before,  $Fo$  is defined using  $ID$  instead of  $a^2$ .

For the slab, the cylinder and the sphere, the same values for the Sherwood number apply as in the case of heat transport for the Nusselt number. Remember that it involves mass transport into a body where the resistance to the mass transport is located inside the body itself (the boundary conditions apply and are constant over time!).

So for long periods of time

slab	$Sh = 4.93$
cylinder	$Sh = 5.8$
sphere	$Sh = 6.6$

The findings for the penetration theory and long-term diffusion can be summarised as

$$\begin{array}{lll} \text{penetration theory} & Fo < 0.03 & k = k(t) \quad \Delta c_A = \text{constant} \\ \text{long-term diffusion} & Fo > 0.03 & k = \text{constant} \quad \Delta c_A = \Delta c_A(t) \end{array}$$

In fact, this summary is identical to the one at the end of § 3.3.5

#### Example 4.5. A contaminated landfill II

Consider now what happens with the landfill in location L (see Example 4.4) if no action is taken. The thickness of the layer of clean undersoil is 1 m. Below this is a layer of clay, which is (practically) impermeable as far as the contamination is concerned. The concentration of the contaminated soil right on the surface of the clean soil was  $c^* = 2 \text{ kg/m}^3$ , and the diffusion coefficient  $D = 2 \cdot 10^{-10} \text{ m}^2/\text{s}$ . How long does it take before the mean concentration of the contamination amounts to  $1 \text{ kg/m}^3$  in this 1 m layer of soil?

This problem can be solved most quickly with the help of Figure 3.16. It is first necessary to determine the parameter along the vertical axis, from the following

$$\frac{c_1 - \langle c \rangle}{c_1 - c_0} = \frac{2 - 1}{2 - 0} = 0.5 \quad (4.45)$$

Verifying this with Figure 3.16 produces  $Fo = 0.05$ . From this it follows that (remember that for  $D$  it is not the thickness of the layer that should be taken, but twice the thickness see also Example 3.10)

$$t = 10 \cdot 10^9 \text{ s} \approx 32 \text{ years}$$

□

#### Summary

The analysis of unsteady-state mutual diffusion runs entirely analogously to that of unsteady-state heat conduction. Here, too, a distinction is made between the penetration theory (during short periods of time) and long-term diffusion. Again, the following summary applies to diffusion from or towards the two planes of a flat layer and to the cases of a cylinder and a sphere:

penetration theory	$Fo < 0.03$	$k = k(t)$	$\Delta c_A = \text{constant}$
long-term diffusion	$Fo > 0.03$	$k = \text{constant}$	$\Delta c_A = \Delta c_A(t)$

The same theory and principles apply here as in the case of heat transport. Even the diagrams 3.16 and 3.17 can be used again. The Fourier number is defined differently (with the help of the diffusion coefficient) and the place of the Nusselt number is taken by the Sherwood number to which in any case the same numerical values apply for the various basic geometries (slab, cylinder, sphere).

### 4.3 Diffusion and drift flux

So far, we have very deliberately only discussed situations in which the transport of mass has been described using Fick's law: mutual diffusion and diffusion of just one species in a solid. With mutual diffusion, it is on average the case that the molecules of the two substances only exchange position within an enclosed space. In that case, in gases for example, there is no change in the overall concentration of the molecules (regardless of what kind they are) at a given location.

In general, diffusion problems will be more complex. It is very simple to generate another form of diffusion phenomena in a mixture of substances A and B: there is a net transport of substance A, while substance B is not transported, net. An example of this is the *Winkelman experiment* (see Figure 4.5): in a test tube there is a layer of volatile<sup>16</sup> substance A. This substance evaporates constantly and diffuses to the edge of the test tube. Pure air is blown over the edge so that the concentration of substance A at the edge of the tube is (essentially) zero.

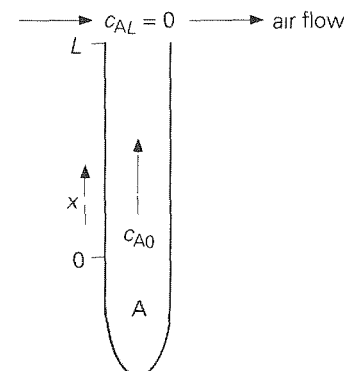


Figure 4.5

At first sight, it appears that this could be described using Fick's law. After all, there is a driving difference in concentration: the concentration of substance A just above the surface of the liquid minus the concentration at the edge of the tube. As a result of this, substance will diffuse to the exit of the test tube.

<sup>16</sup> Example 2.2 looked at the case of a substance of a very slight level of volatility.

This, however, is not the full story. This can be understood by looking at the 'air' molecules. The concentration of the air molecules (shown as B) is not constant in the tube either at the edge of the tube, the concentration  $c_B$  is equal to that of the outside air ( $c_{BL} = p/RT$ , in mol/m<sup>3</sup>), while the air concentration at the surface of the liquid is much lower. The total concentration  $c = c_A + c_B$  is constant because the pressure in the tube is the same throughout – If this were not the case, a large convective mass flow would occur immediately, because a difference in pressure (apart from just a hydrostatic pressure difference) always causes flow – This means that the concentration of the air just above the liquid surface is equal to  $c_{B0} = c - c_{A0} = (p - p_{A0})/RT$  (where  $p_A$  is the vapour pressure of substance A, which for the sake of convenience is regarded as an ideal gas). Nonetheless, in the steady-state situation<sup>17</sup> there is no net transport of air into the test tube from top to bottom. After all, where would this air go?

The diffusion flow of the air, which is a result of the difference in concentration, is apparently compensated by a convective flow: the total concentration  $c$  is not exactly constant, but is slightly higher at the liquid surface than at the edge of the tube. However, this difference is so slight that the drop in pressure over the tube ( $p_0 > p_L$ ) is so small that there is only a very slight convective flow, exactly enough to ensure that the net flow of the air molecules is zero!

This convective flow, caused by a very small difference in pressure, makes no distinction between substance A or B. Both are transported there is therefore also a convective flow of substance A. This convective flow is called the *drift transport* (shown as  $\phi$  in mol/s). The net mass fluxes for substances A and B in the test tube (with the concentrations in mol/m<sup>3</sup>) are now

$$\phi_A'' = -ID \frac{dc_A}{dx} + \phi'' \frac{c_A}{c} \quad (4.46)$$

$$\phi_B'' = -ID \frac{dc_B}{dx} + \phi'' \frac{c_B}{c} \quad (4.47)$$

Equations (4.46) and (4.47) are still very general. In each of the two equations, the first term on the right-hand side represents the diffusion flux (according to Fick's law), while the second term shows that *drift flux* carries both species.

Because the total concentration is (almost) constant  $c = c_A + c_B$ , for the concentration gradients,  $dc_B/dx = -dc_A/dx$ . Adding up Equations (4.46) and (4.47) now produces

$$\phi'' = \phi_A'' + \phi_B'' \quad (4.48)$$

In the Winkelmann experiment,  $\phi_B'' = 0$ . It now follows therefore that  $\phi'' = \phi_A''$  (see above). Entering this into Equation (4.46) results in

$$\phi_A'' = -ID \frac{c}{c - c_A} \frac{dc_A}{dx} \quad (4.49)$$

Equation (4.49) is known as *Stefan's law* and describes what is known as *unilateral diffusion*.

If a mole balance for species A is now drawn up for a thin slice between  $x$  and  $x + dx$  from the tube, then the following will be found (the situation is still quasi steady)

$$0 = \phi_A''|_x - \phi_A''|_{x+dx} \quad (4.50)$$

Combining Equations (4.49) and (4.50) produces

$$\frac{c}{c - c_A} \frac{dc_A}{dx} = \text{constant} \quad (4.51)$$

With  $c = \text{constant}$ , the solution to this differential equation, with the two boundary conditions  $x = 0 \rightarrow c_A = c_{A0}$  and  $x = L \rightarrow c_A = c_{AL}$ , is

$$\frac{c - c_A(x)}{c - c_{A0}} = \left( \frac{c - c_{AL}}{c - c_{A0}} \right)^{x/L} \quad (4.52)$$

Now that the concentration profile is known, the flux of substance A can be calculated using Stefan's law, Equation (4.49).

$$\phi_A'' = \frac{IDc}{L} \ln \left( \frac{c - c_{AL}}{c - c_{A0}} \right) \quad (4.53)$$

An analysis based solely on Fick's law produces the following erroneous result

$$\phi_A'' = -ID \frac{c_{AL} - c_{A0}}{L} \quad (4.54)$$

The last two equations differ by one factor that is known as *Stefan's correction factor*.

$$f_D = \frac{c}{c_{A0} - c_{AL}} \ln \left( \frac{c - c_{AL}}{c - c_{A0}} \right) \quad (4.55)$$

<sup>17</sup> In fact, the evaporation of the liquid in this test tube is of course an unsteady-state process. However, the height of the liquid (actually a boundary condition for the transport through the gas phase) changes so slowly (given the difference in density between the liquid and gas phase) that the situation can be regarded as quasi-steady for the transport through the gas phase.

A correction factor of this kind also occurs with unilateral diffusion from the surface of a sphere, for example, into ‘infinity’, such as in the case of an *evaporating droplet* or a *dissolving particle*. This correction factor is also at play of course in processes in the opposite direction, such as condensation or crystallisation. For Sherwood, this gives  $Sh = 2f_D$  (instead of  $Sh = 2$ )

For  $c_{AL}$  and  $c_{A0}$  small in relation to  $c$ , Stefan’s correction factor  $f_D$  can incidentally be written as

$$f_D = 1 + \frac{1}{2} \frac{c_{A0} + c_{AL}}{c} \quad (4.56)$$

and it is therefore possible, if  $c_{A0} + c_{AL} \ll c$ , to assume that mutual diffusion will occur. This tallies with the limit situation that for  $c_A \ll c$ , Stefan’s law, Equation (4.49), transfers to Fick’s law (see Example 2.2).

Both the basic Equations (4.46) and (4.47) are of general validity for binary diffusion (that is, without externally imposed flow) and therefore also cover mutual diffusion. In that case, the drift transport is equal to zero and Stefan’s law transfers to Fick’s law.

Remember that the above theory is formulated in mole flows and mole balances. This can also be done in mass flows and mass balances, but the way they are described is a little more complicated.

Other forms of mutual and unilateral diffusion are described by Equations (4.46) and (4.47). see the example below

#### Example 4.6. Nickel carbonyl

Consider a process in which carbon monoxide reacts with nickel (present in the form of a thin slice) to form gaseous nickel carbonyl



The reaction (see Figure 4.6) occurs on the surface of the solid nickel, which is located in an atmosphere that initially consists entirely of CO. Because of the reaction, a layer is created in the vicinity of the nickel surface where there is less CO present and more nickel carbonyl. The reaction velocity is determined by the flux of CO molecules through this interface (thickness  $\delta$ ) to the nickel surface. [Referring to the film theory discussed in § 3.5.2 may be useful.]

All the CO molecules that reach the nickel surface react instantaneously, so that the CO concentration there is zero. At the same time, the nickel carbonyl diffuses away from the surface to the bulk of the gas phase, where the nickel carbonyl concentration can be assumed to be zero. Consider this process in the steady-state situation.

The question is how large is the CO flux through the interface?

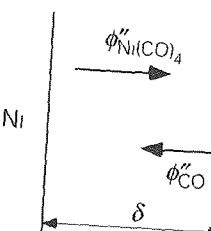


Figure 4.6

This is an example of a diffusion process that involves a drift flux. The drift flux is the sum of the nickel carbonyl flux and the CO flux and can be derived from the reaction equation. After all, four CO molecules have to be supplied for every nickel carbonyl molecule that is formed.

$$\phi''_{\text{Ni}(\text{CO})_4} = -\frac{1}{4} \phi''_{\text{CO}} \quad (4.58)$$

The minus sign shows that both fluxes (in mol/s) are in opposing directions.

In this situation, the total concentration  $c$  can be taken to be practically constant:  $c = c_1 + c_2 = \text{constant}$  (where  $c_1 = \text{concentration CO}$  and  $c_2 = \text{concentration Ni}(\text{CO})_4$ , both in mol/m³). This means therefore that the gradients are equal in size but have opposing signs:  $dc_1/dx = -dc_2/dx$ . This means Equations (4.46) and (4.47) become

$$\phi''_{\text{CO}} = -ID \frac{dc_1}{dx} + \frac{c_2}{c} (\phi''_{\text{CO}} + \phi''_{\text{Ni}(\text{CO})_4}) \quad (4.59)$$

$$\phi''_{\text{Ni}(\text{CO})_4} = -ID \frac{dc_2}{dx} + \frac{c_1}{c} (\phi''_{\text{CO}} + \phi''_{\text{Ni}(\text{CO})_4}) \quad (4.60)$$

In both equations the drift flux is written as the sum of both net fluxes, as derived in Equation (4.48).

If the nickel carbonyl flux is now eliminated from Equation (4.59) with the help of Equation (4.58), the following applies:

$$\phi''_{\text{CO}} = -ID \frac{4c}{4c - 3c_1} \frac{dc_1}{dx} \quad (4.61)$$

A CO mole balance for a slice between  $x$  and  $x + dx$  in the interface shows that the CO flux is constant, that is, that it is not dependent on  $x$ . The CO concentration profile can be determined from Equation (4.61), with boundary conditions  $x = 0 \rightarrow c_1 = 0$  and  $x = \delta \rightarrow c_1 = c$ .

$$c_1(x) = \frac{4}{3} c \left\{ 1 - \left( \frac{1}{4} \right)^{x/\delta} \right\} \quad (462)$$

From this, the CO flux can be calculated via Equation (461)

$$\phi_{CO}'' = -\left(\frac{4}{3} \ln 4\right) \frac{IDc}{\delta} \quad (463)$$

This example does not therefore involve mutual diffusion, but it does not involve unilateral diffusion either. It involves two species that do not diffuse into each other one-to-one, but in a ratio that is imposed by the chemical reaction. It is therefore the chemical reaction that determines the strength of and the expression for the drift flux.  $\square$

### Summary

It is often the case that net transport involves one species passing through a medium (unilateral diffusion) or of multiple species diffusing in each other in a ratio other than one-to-one. It is only in the case of two species completely exchanging with each other (mutual diffusion) that the analogy with molecular heat transport (conduction) is a perfect one. The Winkelmann experiment with an evaporating substance shows simply that account has to be taken of the so-called drift flux,  $\phi''$ . In the case of unilateral diffusion, this has the effect that flows can arise as a result of differences in pressure, leading to the occurrence of convective transport. The general expression for mole fluxes in a binary system is:

$$\phi_A'' = -ID \frac{dc_A}{dx} + \phi'' \frac{c_A}{c}$$

$$\phi_B'' = -ID \frac{dc_B}{dx} + \phi'' \frac{c_B}{c}$$

where

$$\phi'' = \phi_A'' + \phi_B''$$

In the special case of unilateral diffusion (that is, where the flow from one of the two species equals zero), the transport of the diffusing species can be described with the help of Stefan's law. Sometimes it is a phase change process, sometimes a chemical reaction that imposes the drift flux towards or from a boundary plane. Fick's law will suffice with low concentrations.

## 4.4 The general micro balance for mass transport

This chapter on mass transport has so far looked only at diffusion (molecular transport), and then only in one direction resulting from a concentration gradient in that direction. In general – both in industrial applications (in processing machines) and in other cases (in the home, in the environment) – time-dependent, three-dimensional concentration distributions will be at play: the concentration is a function of all three space coordinates and of time. As well as diffusion resulting from concentration gradients, the convective transport of species is also generally involved, as a result of flow (generally a three-dimensional velocity field).

This general description is nothing more than that given under heat transport (§ 3.4). This situation is therefore described entirely analogously with the help of a general micro balance, the derivative of which is made on the basis of a small control volume,  $dxdydz$ , as shown in Figure 3.21 (*cubic volume element method*).

This derivation involves the basic form of a balance, and it should cover both the convective transport and the diffusion on the six planes. Each convective transport term takes the form  $v c$ . This means that a flow

$$[v_x c]_{x,y,z} dydz \quad (464)$$

passes into the cube through the left-hand side, and

$$[v_x c]_{x+\Delta x,y,z} dydz \quad (465)$$

leaves again through the right-hand side. This makes the net contribution by the transport in the direction of  $x$

$$-\frac{\partial}{\partial x} (v_x c) dx dy dz \quad (466)$$

Similar expressions apply to the net transport in the two other directions. If the diffusion obeys Fick's law, then

$$-ID \left[ \frac{\partial c}{\partial x} \right]_{x,y,z} dy dz \quad (467)$$

will enter the cube on the left-hand side, because of diffusion, and

$$-ID \left[ \frac{\partial c}{\partial x} \right]_{x+\Delta x,y,z} dy dz \quad (468)$$

will leave the cube on the right-hand side, because of diffusion Net, these two terms give

$$\frac{\partial}{\partial x} \left[ ID \frac{\partial c}{\partial x} \right] dx dy dz \quad (4.69)$$

Similar expressions apply to the other surfaces of the cube Finally, the accumulation term takes the form

$$\frac{\partial c}{\partial t} dx dy dz \quad (4.70)$$

and the production term is

$$r dx dy dz \quad (4.71)$$

where  $r$  represents the reaction rate (in mol/m<sup>3</sup>s)

The general micro balance is then created through the merging of the three net contributions of convective transport, of the three net diffusion terms (now with constant  $ID$ ), of the accumulation term and of the production term, and by dividing all three by  $dx dy dz$

$$\begin{aligned} \frac{\partial c}{\partial t} = & - \frac{\partial}{\partial x} (v_x c) - \frac{\partial}{\partial y} (v_y c) - \frac{\partial}{\partial z} (v_z c) + \\ & + ID \left\{ \frac{\partial^2 c}{\partial x^2} + \frac{\partial^2 c}{\partial y^2} + \frac{\partial^2 c}{\partial z^2} \right\} + r \end{aligned} \quad (4.72)$$

This equation is entirely analogous to Equation (3.135) for heat transport Solving the concentration field also requires solving the velocity field, but this will not be dealt with until Chapter 5

However, for many applications, no knowledge of the whole velocity and concentration fields are needed, all that is required are mass transfer models in which mass transfer coefficients for mass transport at the boundary or boundaries of the field of flow play a major part The rest of this chapter is therefore devoted completely to this phenomenological approach

### Summary

The generally valid micro balance for mass transport has been derived with the help of the cubic volume element method This analyse has again taken account of both convective and molecular mass transport It has been assumed that Fick's law applies.

However, the micro balance can only be used to calculate the concentration distribution if the velocity field is known

## 4.5 Mass transfer coefficients during convection

### 4.5.1 General observations

As with heat transport in § 3.5, convective mass transport can be conveniently described using the analogue of Newton's Law of Cooling as a starting point

$$\phi_m = k A \Delta c \quad (4.73)$$

This equation certainly applies in a single phase, but with a suitable choice of driving force can also be used for mass transfer across phase interfaces, providing the term *overall mass transfer coefficient* is used (see § 4.6 for more details)

The transfer coefficient  $k$  is generally dependent on  $\rho$ ,  $\langle v \rangle$ ,  $ID$ ,  $\mu$ ,  $D$ , etc

$$k = k(\rho, \langle v \rangle, ID, \mu, D, \dots) \quad (4.74)$$

Here, too, a far-reaching analogy with convective transport can be expected The same considerations as those discussed in § 3.5 also apply to the choice of independent variables that could influence the mass transfer coefficient – except that now, quantities that are typical of those involved in heat transport must be converted into those that are typically associated with mass transport, such as  $a \rightarrow ID$  With the help of dimensional analysis, Equation (4.74) can then be reduced to

$$Sh = Sh(Re, Sc, \dots) \quad (4.75)$$

The Schmidt number  $Sc$ , defined as  $v/ID$ , replaces the Prandtl number and is related to the ratio of the hydrodynamic boundary layer thickness and the mass transfer boundary layer thickness See also the discussion about the role of boundary layers in convective heat transport after Figure 3.24 The Reynolds number now also shows the ratio of convective to molecular transport of momentum in the flow

Expressions for the Sherwood number analogous to those for the Sherwood number for heat transport exist for various situations These are discussed in more detail below

### 4.5.2 Mass transfer in the case of forced convection

Entirely analogously with convective heat transport, the following correlations apply to various flow configurations

*Laminar pipe flow*

Providing the velocity profile of the flow is fully developed, the following applies to mass transfer from a given point,  $x = 0$

$$Sh = 1.08 \left( \frac{IDx}{\langle v \rangle D^2} \right)^{-1/3} \quad \text{if} \quad \frac{IDx}{\langle v \rangle D^2} < 0.05 \quad (4.76)$$

$$\langle Sh \rangle = 1.62 \left( \frac{IDL}{\langle v \rangle D^2} \right)^{-1/3} \quad \text{if} \quad \frac{IDL}{\langle v \rangle D^2} < 0.05 \quad (4.77)$$

$$Sh = 3.66 \quad \text{if} \quad \frac{IDx}{\langle v \rangle D^2} > 0.1 \quad (4.78)$$

The same considerations apply to these expressions as those mentioned under heat transport (see § 3.5.2)

*Turbulent pipe flow*

*Film theory* (see also § 3.5.2, Figure 3.24) can also be used here in order to model the mass transfer, leading to  $k = ID/\delta$ , the following correlation can be used for calculation purposes

$$Sh = 0.027 Re^{0.8} Sc^{0.33} \quad \text{providing that } Re > 10^4 \text{ and } Sc \geq 0.7 \quad (4.79)$$

*Forced flow around a sphere*

The following correlation applies here

$$Sh = 2.0 + 0.66 Re^{0.50} Sc^{0.33}$$

providing that  $10 < Re < 10^4$  and  $Sc \geq 0.7$  (4.80)

where it is assumed that no drift flux occurs (see § 4.3)

**Example 4.7. A wetted-wall column**

Air containing a low concentration  $c_0$  of  $\text{SO}_2$  has to be stripped of this  $\text{SO}_2$ . This is done in a *wetted-wall column* in which the air is flowing upward at a flow rate  $\phi_V$  while an alkaline solution flows downward as a thin liquid film on the inside of the column – reason why this piece of equipment is also denoted as a *film contactor*. The thickness of this liquid film is very small with respect to the column diameter  $D$ .

In this countercurrently operated process, the  $\text{SO}_2$  has first to be transported from the bulk of the air flow to the interface with the liquid film, this gas phase transport is facilitated by operating in the turbulent regime such that the bulk of the gas flow is radially well mixed rendering the concentration  $c$  a function of  $x$

only, with the mass transfer resistance being concentrated in a thin air film adjacent to the liquid film. At the air-liquid interface, the  $\text{SO}_2$  is transferred to the liquid where it reacts immediately with the alkaline to sulphite resulting in a zero  $\text{SO}_2$  concentration at the film interface ( $c_i = 0$ )

The question is to derive the expression describing how during a steady-state operation of the process the  $\text{SO}_2$  concentration  $c$  in the air decreases as a function of  $x$ , which is the upward (downstream) coordinate. It is also asked how the total amount  $M$  of  $\text{SO}_2$  transferred per unit of time depends on column height  $L$ .

The question with respect to the  $\text{SO}_2$  concentration profile  $c(x)$  asks for drawing up a species ( $\text{SO}_2$ ) mass balance over a thin slice of thickness  $dx$  at any position  $x$  somewhere in the column for a steady state situation, with the result

$$0 = \phi_V c|_x - \phi_V c|_{x+dx} - k \pi D (c - c_i) dx \quad (4.81)$$

This species balance leads to the differential equation

$$\frac{\pi}{4} D^2 v \frac{dc}{dx} = -k \pi D c \quad (4.82)$$

with the boundary condition  $c(0) = c_0$ . The mass transfer coefficient  $k$  is to be found via the Sherwood number and with the help of Equation (4.79), and  $v$  is a constant (does not depend on  $x$ ) – providing the two criteria as to the values of  $Re$  and  $Sc$  are met. The integration then straightforwardly results in

$$\frac{c}{c_0} = \exp \left( -\frac{4k}{vD} x \right) = \exp \left( -\frac{4ID}{vD^2} Sh x \right) \quad (4.83)$$

The second question relates to  $M$  which can be found either by integrating the 3<sup>rd</sup> term of the right-hand side of Equation (4.81) – which stands for the local mass transfer rate – from 0 to  $L$

$$M = \int_0^L k \pi D c(x) dx = \phi_V c_0 \left\{ 1 - \exp \left( -\frac{4kL}{vD} \right) \right\} \quad (4.84)$$

or from the expression  $\phi_V \{c_0 - c(L)\}$  which, due to balance (4.81), gives the same result. In both cases, result (4.83) is to be substituted for  $c(x)$  and  $c(L)$ . □

**Example 4.8. An evaporating sphere**

A sphere made from pure substance X (with  $\rho = 1950 \text{ kg/m}^3$ ) is hung from a thread in an air flow. The air flow being supplied does not contain species X, has a temperature of  $20^\circ\text{C}$ , a uniform velocity  $v$  of  $5 \text{ m/s}$  and a kinematic viscosity  $\nu$

of  $1.5 \cdot 10^{-5} \text{ m}^2/\text{s}$ . The diameter of the sphere at the start of the experiment is  $D_0 = 25 \text{ mm}$ . Temperature effects due to the evaporation may be ignored. The following applies to substance X: molar mass  $M = 120 \text{ g/mol}$ , vapour pressure in the prevailing conditions  $p^* = 0.01 \text{ bar}$ , and diffusion coefficient  $ID = 0.5 \cdot 10^{-5} \text{ m}^2/\text{s}$ .

Determine the point in time at which the diameter of the sphere is exactly 20 mm.

The mass balance for the evaporating sphere is

$$\rho \frac{dV}{dt} = \rho \frac{\pi}{2} D^2 \frac{dD}{dt} = -\pi D^2 k \left( M \frac{p^*}{RT} - 0 \right) \quad (4.85)$$

Additional information here is that the concentration of X in the air far away from the sphere is zero (and remains so). Also, the volume of the sphere  $\pi D^3/6$  is differentiated according to time.

Equation (4.85) is the differential equation that describes the change of the diameter of the sphere as a function of time. Before integrating this equation, it is first necessary to find the relationship between  $k$  and  $D$ . This relationship generally follows from Equation (4.80) but, with a view to the integration of Equation (4.85), this has an awkward form. From Equation (4.80), it follows that Sh has a minimal value of 80 during the evaporation. With pinpoint accuracy, the relationship between  $k$  and  $D$  is simplified to

$$k = \frac{Sh ID}{D} = 0.66 ID \left( \frac{v}{v} \right)^{1/2} \left( \frac{v}{ID} \right)^{1/3} D^{-1/2} \quad (4.86)$$

Entering this into Equation (4.85) leads to

$$D^{1/2} \frac{dD}{dt} = -C \quad \text{where} \quad C = 1.32 \frac{M}{\rho} \frac{p^*}{RT} ID^{2/3} v^{-1/6} v^{1/2} \quad (4.87)$$

Thanks to boundary condition  $D(0) = D_0$ , the solution to this differential equation is

$$\frac{2}{3}(D^{3/2} - D_0^{3/2}) = -C t \quad (4.88)$$

Substituting the numerical data shows that  $D = 20 \text{ mm}$  at  $t = 5.5 \cdot 10^3 \text{ s}$ , which is around 1.5 hours.  $\square$

### Chilton and Colburn

The above analogy between convective heat and mass transport implies that  $k$  can be determined from knowledge of  $h$  (and vice versa). In particular, for Re values that are not too small, it is generally possible to write the following

$$\text{Nu} = C \text{Re}^m \text{Pr}^n \quad (4.89)$$

and

$$\text{Sh} = C \text{Re}^m \text{Sc}^n \quad (4.90)$$

In each of the cases given above,  $n$  is equal to  $1/3$  – related to the ratio of the respective boundary layer thicknesses (see the discussion after Figure 3.24). Chilton and Colburn used this in order to introduce two new non-dimensional transfer numbers one for heat transfer ( $J_H$ ) and one for mass transfer ( $J_D$ ).

$$J_H = \frac{\text{Nu}}{\text{Re} \text{Pr}^{1/3}} = \frac{h}{\rho c_p v} \left( \frac{v}{a} \right)^{2/3} \quad (4.91)$$

$$J_D = \frac{\text{Sh}}{\text{Re} \text{Sc}^{1/3}} = \frac{k}{v} \left( \frac{v}{ID} \right)^{2/3} \quad (4.92)$$

These numbers relate the velocity of the heat and mass transfer process respectively (perpendicular to the main flow) to the convective transport of the main flow (see also Figure 3.23). This makes these numbers a measure for the effectiveness of the transfer process. In this sense,  $J_H$  and  $J_D$  are comparable to the Reynolds number see Equation (2.49).

Combining the four above equations now reveals – where the Reynolds number is not too small – that both these new numbers for geometrically similar situations are equal to each other and dependent only on the Reynolds number.

$$J_H = J_D = C \text{Re}^{m-1} \quad (4.93)$$

The discovery that  $J_H$  and  $J_D$  are equal to each other can be rewritten as a link between transfer coefficients  $k$  and  $h$  with the help of the definitions of  $J_H$  and  $J_D$ . Owing to the Definitions (4.91) and (4.92) the convective velocity drops out of the relation between  $k$  and  $h$ .

$$k = \frac{h}{\rho c_p} \left( \frac{ID}{a} \right)^{2/3} = \frac{h}{\rho c_p} \text{Le}^{-2/3} \quad (4.94)$$

The Lewis number (Le) appears in Equation (4.94) for the definition, see Equation (2.38). It therefore seems that  $k$  can be determined by measuring  $h$  and by looking for a number of mass constants. In practice, this is highly beneficial, as only relatively simple temperature measurements have to be carried out for  $h$ , while

determining  $k$  often requires very time-consuming and difficult mass transfer experiments, in many cases for different species. With the help of Equation (4.94), therefore, only knowledge of  $h$  and some mass constants are needed. The relationship does not contain the Reynolds number, and not explicitly the geometry either.

#### Example 4.9. Dissolving encrustation

Over time, a solid has become encrusted on the bottom of an ideally stirred tank (diameter  $D = 3 \text{ m}$ ). In order to remove this, a pure solvent is allowed to flow through the tank. The encrusted matter slowly dissolves in this solvent. The flow rate of this solvent is  $\phi_V = 0.5 \cdot 10^{-3} \text{ m}^3/\text{s}$ .

Heat transfer measurements on the tank have been carried out which have shown that

- the heat transfer coefficient  $h$  on the bottom depends on the number of revolutions of the stirrer according to  $h \propto N^{2/3}$ ,
- for a certain level of revolutions,  $h = 3000 \text{ W/m}^2\text{K}$ , and
- the power  $P$  that is supplied to the stirrer varies by  $N^3$

Data

diffusion coefficient of the crust in the solvent	$ID = 10^{-9} \text{ m}^2/\text{s}$
density of solvent	$\rho = 1200 \text{ kg/m}^3$
specific heat of solvent	$c_p = 3000 \text{ J/kgK}$
thermal conductivity coefficient of solvent	$\lambda = 0.5 \text{ W/mK}$
solubility of the crust in the solvent	$c^* = 50 \text{ kg/m}^3$

The question is this: during this slow dissolution process, what is the constant dissolution velocity in the event that  $h = 3000 \text{ W/m}^2\text{K}$ , and how does this dissolution velocity change if twice as much power is supplied to the stirrer?

A dissolution process of the kind described means that mass has to be transferred from a thinly saturated layer just above the crust to the bulk of the stirred tank, in which as a result of this dissolution and flow of solvent contains a constant (in terms of time) concentration of dissolved mass. In this steady-state situation, the mass balance for the crust that is dissolved in the solvent ( $c$  = concentration in the bulk) is

$$0 = -\phi_V c + k \frac{\pi}{4} D^2 (c^* - c) \quad (4.95)$$

The second term on the right-hand side is the dissolution velocity that was asked for, but knowledge of the bulk concentration is required in order to be able to calculate this. To that end, it is necessary to solve Equation (4.95), and for that, a value for  $k$  is needed. Because the heat transfer experiment was carried out in the same conditions in the same geometry, it is possible to use Expression (4.94) to

work out that  $k = 3.1 \cdot 10^{-5} \text{ m/s}$ . From this, it follows that the concentration in the bulk is equal to  $c = 15.2 \text{ kg/m}^3$ . This means that the following applies to the dissolution velocity:

$$\phi_m = k \frac{\pi}{4} D^2 (c^* - c) = 7.6 \cdot 10^{-3} \text{ kg/s} \quad (4.96)$$

When doubling the level of power supplied, the following applies

$$P_n = 2P \rightarrow N_n = 2^{1/3}N \rightarrow$$

$$h_n = 2^{2/3}h \rightarrow k_n = 2^{2/3}k = 3.6 \cdot 10^{-5} \text{ m/s} \quad (4.97)$$

and therefore

$$c_n = 16.9 \text{ kg/m}^3 \rightarrow \phi_{m,n} = 8.5 \cdot 10^{-3} \text{ kg/s} \quad (4.98)$$

□

#### 4.5.3 Mass transfer in the case of free convection

How heat is transported if free convection is involved was discussed in § 3.5.3. This mechanism is also possible with mass transfer. The analogy here is, if anything, even greater than is the case with forced convection. After all, it does not matter whether the difference in density that is needed for free convection comes from expansion as a result of a change of temperature or is caused by dissolving salt, for example, leading to a local increase in density. An example in which mass transport through free convection is involved concerns a vertical wall that consists of salt and which is in contact with pure water. The water at a large distance from the slice is pure, and has a density of  $\rho_\infty$ . The layer of water immediately adjacent to the salt slice has a higher density as salt has dissolved into it. Free convection will now therefore occur of its own accord.

The effect of free convection on the mass transfer is accounted for by a Grashof number, exactly as in the case of heat transfer. The Grashof number  $Gr$  that is used in describing free convection has previously been written, not without reason, in Equation (3.157), in terms of the difference in density that occurs

$$Gr = \frac{x^3 g \Delta \rho}{v^2 \langle \rho \rangle} \quad (4.99)$$

In the relationships involving the Sherwood number and the Grashof number, the Schmidt number must of course appear where, in the case of heat transfer, the Prandtl number figured in the relationships involving the Nusselt number and the Grashof number. Mass transfer coefficient  $k$ , in the case of free convection, can therefore be obtained from

$$Sh = f(Gr Sc) \quad (4.100)$$

The same relations apply to mass transfer resulting from free convection as they do to heat transfer resulting from free convection (where the geometry is equal) providing that the following are translated  $\text{Pr} \rightarrow \text{Sc}$  and  $\text{Nu} \rightarrow \text{Sh}$

### Summary

Mass transfer with forced and free convection is entirely analogous to heat transport with forced and free convection. Translations only have to be made as follows

$$\text{Nu} \leftrightarrow \text{Sh}$$

$$\text{Pr} \leftrightarrow \text{Sc}$$

Chilton and Colburn have used this in order to link  $k$  and  $h$  to each other exclusively via mass constants, where the values of the Reynolds number are sufficiently large

## 4.6 Mass transfer across a phase interface

### 4.6.1 Introduction on dealing with two phases

In such processes as evaporating or dissolving *pure* substances, it is sufficient to consider the transport in only one phase. The other phase (the evaporating droplet, the dissolving particle) then only produces the boundary condition for the concentration field. In the Examples 2.2 and 4.8, the (temperature-dependent) *equilibrium vapour pressure*  $p^*$  is used, and the (temperature dependent) *solubility*  $c^*$  in the Examples 4.2, 4.3 and 4.9

Actually, this is the second important difference between heat transport and mass transport that was already mentioned in § 4.1 (in addition to unilateral diffusion). If two substances are in thermal equilibrium, they have the same temperature. However, if two substances containing a dissolved species A are in equilibrium with each other, then in general the concentrations  $c_A$  in both substances will be different. In § 4.6.2 it will be explained that the chemical potentials of species A in the two phases will be equal rather than the concentrations of A.

Something similar to this was dealt with in Example 4.2 with the solubility of helium in glass; there, the concept of *solubility* was introduced for the first time to instantaneously produce and steadily maintain the equilibrium concentration  $c^*$  in the glass at the interface with the gas. This  $c^*$  is different from but depends on the density (in the case of a pure gas) or concentration (in the case of gas mixture) in the adjacent gas phase.

Many relevant processes do not deal with pure substances indeed, but with mixtures or solutions. In many gas-liquid cases and for equilibrium conditions only it is then possible to use *Henry's law*

$$p_A = H_A \cdot y_A \quad (4.101)$$

in which the *Henry coefficient*  $H_A$  denotes the proportionality coefficient between the mole fraction  $y_A$  of dissolved gas A in a liquid and the partial pressure  $p_A$  of the gas above the liquid<sup>18</sup>. Henry's law may best be used for dilute solutions.

### Example 4.10. Mass transfer to a rain drop

A rigid, spherical rain drop 5 mm in diameter  $D$  is falling at its terminal velocity  $v$  through a layer of air (thickness  $z_0 = 250$  m) that contains a high ammonia concentration which is expressed in terms of a (constant) partial vapour pressure  $p_0$ . The ammonia concentration in the rain drop right before it enters the air/ammonia blanket is zero. The diffusion coefficient  $D$  of ammonia in water amounts to  $1.49 \cdot 10^{-9} \text{ m}^2/\text{s}$  (at the prevailing temperature of  $20^\circ\text{C}$ ) and the value of the Henry coefficient of ammonia is  $2.8 \cdot 10^5 \text{ Pa}$ .

The rain drop retains its spherical shape<sup>19</sup> all the time and remains rigid (no internal flows), the air with the ammonia behaves as an ideal gas, and evaporation of water from the drop and the related heat effect may be ignored.

The eventual question is about the ratio of the average ammonia concentration in the rain drop at the moment it leaves the air/ammonia blanket, to the ammonia concentration  $c_0$  in the air.

The mass transfer of the ammonia from the air into the rain drop is a transient process: the amount of ammonia in the rain drop may increase in time as long as the rain drop is in contact with the air/ammonia mixture (and saturation conditions have not been attained). It should further be realized that the mass transport comprises two steps: the external transport of ammonia from the bulk of the air towards the phase interface and the internal transport from the phase interface into the interior of the drop.

The external mass transport is of the convective type, owing to the terminal velocity of the drop through the air/ammonia mixture, while the internal mass transport in the water (where the molecules are much closer together than in the gas phase) is due to diffusion, individual ammonia molecules finding their way in between the water molecules. Although it therefore seems reasonable to submit that the internal, diffusive mass transport is rate limiting - the internal resistance

<sup>18</sup> See also Janssen, L P B M and M M C G Warmoeskerken, Transport Phenomena Data Companion, VSSD, Delft, 2006, p 137

<sup>19</sup> Actually, a rain drop of 5mm diameter will not be spherical. We use that here for simplicity.

to mass transport may be the largest – this supposition should be verified quantitatively

At the phase interface, equilibrium is attained instantaneously, exactly as in Example 3.5, but this does not imply that at either side of the phase interface the concentrations are equal rather, Henry's law applies here. In such a two-phase mass transfer process, this law does not apply to the average variables in the bulk of the phases involved as long as equilibrium has not been attained yet.

Obviously, the internal mass transport resistance is both molecular and transient. Then the question is relevant whether either penetration theory at short times (§ 4.2.5) applies or the unsteady-state long-term diffusion solution (§ 4.2.6). To answer this question, the contact time is needed the time interval  $\tau$  during which the rain drop is in contact with the air/ammonia mixture. This contact time can be calculated from the terminal velocity of the drop which in its turn follows from a force balance over the drop see § 2.3.3. The same terminal velocity is also needed to calculate the external mass transfer coefficient with the help of the relevant Sh-relation from § 4.5.2

From a force balance, the terminal velocity is found  $v = 11.7 \text{ m/s}$ , the contact time then follows  $\tau = z_0/v = 21.4 \text{ s}$ . This terminal velocity leads to  $\text{Re} = 3900$ , and Equation (4.80), along with  $\text{Sc} = 0.64$ , then results in  $\text{Sh} = 37.5$  and  $k_e = 0.21 \text{ m/s}$ .

After 21.4 s, the penetration depth – see e.g., Equation (4.40) – is just 0.32 mm, pretty much smaller than the drop diameter. This makes this case an obvious example of short-time penetration theory, this value of 0.32 mm illustrates how slow diffusion in the liquid phase is and – in other words – how large the internal resistance to mass transport is! Although at  $t = 0$  the internal mass transfer coefficient  $k_i$  is infinitely large according to Equation (4.36), this  $k_i$  decreases sharply to a value of  $4 \cdot 10^{-6} \text{ m/s}$  at  $t = 21.4 \text{ s}$  according to the same equation and very fast becomes very much smaller than  $k_e$ . Further on in this § 4.6, we will see that in the case of mass transfer across a phase interface the answer to the question in which phase the resistance to mass transport is largest, does not depend on just the ratio  $k_e/k_i$ . However, in this case, the internal resistance to mass transport is rate limiting indeed.

The external resistance to mass transport may therefore be ignored, as a result, the ammonia concentration at the air side of the phase interface is taken equal to the bulk concentration in the air, while the ammonia concentration  $c_g$  at the water side of the phase interface is calculated by using Henry's law:  $c_g = 0.0034 p_0$ . Finally, the average ammonia concentration  $\langle c_i \rangle$  in the rain drop is found with the help of similar expressions as the Equations (4.37) and (4.42):  $\langle c_i \rangle = 119 c_0$ . The

latter result – a much higher average concentration inside the drop than outside – illustrates once more that in the case of mass transfer from one phase to another the concentration difference is NOT the driving force for mass transport. □

In the case of such multi-component processes as distillation, extraction, absorption and stripping in particular, the concentrations in both phases vary both in time and in space. In many of those cases, transport limitations in both phases, at either side of the interface, have to be considered explicitly.

### 4.6.2 The partition coefficient

By way of example, a layer of benzene has been added to a layer of water in Figure 4.7a. If this system is in equilibrium, then the temperature in the water and in the benzene will be the same  $T^W = T^B$ . Of course, the temperature  $T_i$  of the interface between the two phases is at the same value (see Figure 4.7b). The driving force for heat transport is therefore zero  $\Delta T = T^W - T^B = 0$ .

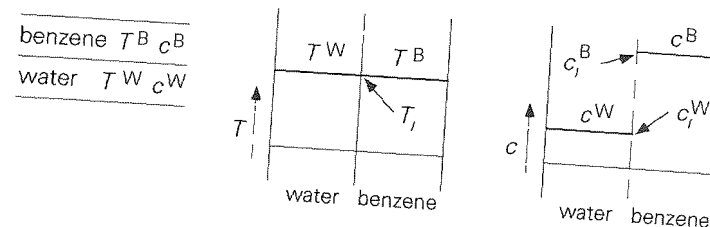


Figure 4.7

Figure 4.7c shows the equilibrium situation for a layer of benzene on a layer of water when acetic acid has been dissolved in both. In the *equilibrium* situation shown, the concentration is uniform in every layer (otherwise transport would occur, and then we would not speak of an equilibrium!). In general, it is now not the case that  $c^B$  and  $c^W$  are equal. This is the result of differences in the relationship between the chemical potential (which accounts for the interactions between the molecules of the dissolved species and the solvent) and the concentration there is only equilibrium if a dissolved substance in both solvents experiences the same chemical potential, and this is generally the case with different concentrations.

Nonetheless, the equilibrium situation requires that the driving force for mass transport is equal to zero. Clearly, the driving force is not  $\Delta c = c^B - c^W$ , as even with equilibrium this is not equal to zero. This can be solved by introducing the *partition coefficient*  $m$  defined such that the driving force, at *equilibrium*, is zero:

$$0 = c^B - m c^W \Leftrightarrow m = \left[ \frac{c^B}{c^W} \right]_{\text{equilibrium}} \quad (4.102)$$

The partition coefficient  $m$  is a property of the three substances that are at play here (in this case, benzene, water and acetic acid). In the case of the system acetic acid – benzene – water, the value of  $m$  is greater than unity (see Figure 4.7c).

#### Example 4.11. Aerating water

A small quantity of water at 20°C is saturated with oxygen. This is done by putting the water into contact with a large quantity of air at 20°C and with a pressure of 1 bar. The mass fraction of oxygen in the air is about 20%. After a long time, the water is saturated and the O<sub>2</sub> concentration  $c_w$  in the water amounts to 8 mg/l. The water is now brought into contact with air of the same composition and temperature, but at a pressure of 0.5 bar. In the equilibrium situation, what will be the O<sub>2</sub> concentration in the water?

In order to be able to answer the question, it is first necessary to calculate the partition coefficient  $m$ . For this, the O<sub>2</sub> concentration in the 1-bar air has to be established. The density of air can be calculated with the ideal gas law, from the air composition and with the molar masses of N<sub>2</sub> and O<sub>2</sub>:  $\rho = 1.2 \text{ kg/m}^3$ . The oxygen concentration in air is therefore  $c_{\text{air}} = 0.2 \cdot 1.2 = 0.24 \text{ kg/m}^3$ . This value is much higher than the saturation concentration in water:  $c_w = 0.008 \text{ kg/m}^3$ . With the partition coefficient at equilibrium defined as  $m = c_{\text{air}}/c_w$ , the value for  $m$  is found to be  $0.24/0.008 = 30$ .

The concentration of oxygen in the air at 0.5 bar is  $c_{\text{air}} = 0.12 \text{ kg/m}^3$  and so the new concentration in the water at equilibrium (after a long time) will be  $c_w = 4 \text{ mg/l}$ . Starting from water with 8 mg/l oxygen dissolved, oxygen is transported from the water to the air at the lower pressure – although the oxygen concentration in the air is higher than that in the water – until the oxygen concentration in the water will have fallen to 4 mg/l.

□

#### 4.6.3 Mass transfer across a phase interface

If there is no equilibrium between the two layers in terms of the chemical potential, mass transfer will occur across the phase interface. An example of such a non-equilibrium situation is shown in Figure 4.8, in this example for the acetic acid-in-water/benzene system:  $c_b^W < c_b^B$  but also  $mc_b^W > c_b^B$ . The driving force for the acetic acid transport from the bulk (denoted by subscript  $b$ ) of the water to the bulk of the benzene is then  $\Delta c = mc_b^W - c_b^B$ , because the definition of Equation (4.102) is not complied with, in relation to the bulk of both phases. At the interface, however, the equilibrium does instantaneously adapt:

$$c_i^B = mc_i^W \quad (4.103)$$

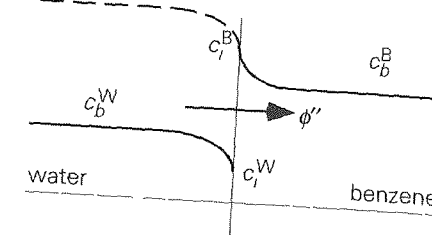


Figure 4.8

This implies that no equilibrium any longer prevails in the bulk of either of the two liquids, and that in the bulk of either phase a transport is created towards and away from the interface, respectively. As can be seen from the profiles in Figure 4.8, the acetic acid moves from the bulk of the water to the benzene-water interface, across the interface, and then from the benzene-water interface into the bulk of the benzene. Essentially, this transport is analogous to the heat transport in Figure 3.10.

The acetic acid flux will be affected by the mass transfer coefficients in both phases  $k_B$  and  $k_W$ . Analogous to Example 3.5, the fluxes in the two layers separately run as

$$\phi''_B = k_B (c_i^B - c_b^B) \quad (4.104)$$

$$\phi''_W = k_W (c_b^W - c_i^W) \quad (4.105)$$

As a matter of fact – an interface cannot host mass – both fluxes are equal, and therefore the subscript with the flux will be omitted from now on.

With the help of Equation (4.103) an expression can be found for  $c_i^W$ :

$$c_i^W = \frac{k_W c_b^W + k_B c_b^B}{k_W + m k_B} \quad (4.106)$$

Apart from  $m$  in the denominator, Equation (4.106) strongly resembles Equation (3.85). Combining Equations (4.105) and (4.106) results in

$$\phi'' = \left[ \frac{1}{k_B} + \frac{m}{k_W} \right]^{-1} (m c_b^W - c_b^B) \quad (4.107)$$

entirely analogously to Equation (3.62) for heat transfer across an interface. It can be seen that the partition coefficient  $m$  appears not just in the driving force, but also in the overall mass transfer coefficient  $K$ :

$$\frac{1}{K} = \frac{1}{k_B} + \frac{m}{k_W} \quad (4.108)$$

which expresses – on the analogy of Equation (3 59) and Ohm's law – that the total resistance to mass transport consists of two partial resistances

The (4 107) - (4 108) system can also be written differently (although it is of equal validity)

$$\phi'' = \left[ \frac{1}{m k_B} + \frac{1}{k_W} \right]^{-1} (c_b^W - \frac{1}{m} c_b^B) \quad (4 109)$$

$$\frac{1}{K^*} = \frac{1}{m k_B} + \frac{1}{k_W} \quad (4 110)$$

Exactly as with heat transport, it is common practice to ignore the smallest of the two partial resistances to mass transport if the ratio of the two exceeds (or is below) a certain value. It follows from the above derivation that in determining in which of the two phases the resistance to mass transport exists, it is not only  $k_W$  and  $k_B$  that should be considered, but that also the partition coefficient  $m$  should be involved.

$$\frac{\text{weerstand in benzeen}}{\text{weerstand in water}} = \frac{1/(m k_B)}{1/k_W} \quad (4 111)$$

Again, this ratio of partial mass transport resistances is denoted as a *Biot-number*

#### Example 4.12. $H_2S$ stripper

In a reactor (see Figure 4 9),  $H_2S$  is produced in oil. In order to remove this dissolved  $H_2S$  from the oil (or to 'strip' it), hydrogen is passed through the oil continuously (at a flow rate  $\phi_V$ ). The  $H_2S$  is transferred to the gas, which it allows to flow out of the reactor. The increase in the gas flow rate that results may be disregarded. The reactor is stirred intensively, so that gas phase and liquid phase can be regarded as ideally mixed. The volume of the gas phase in the reactor is  $V_g$ , and the volume of the liquid phase is  $V_l$ .

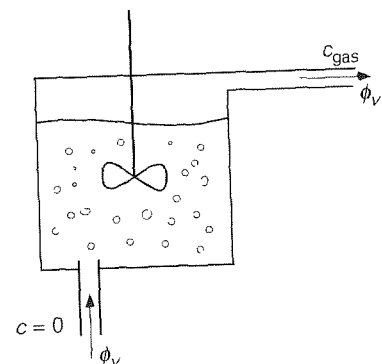


Figure 4 9

From a certain point in time ( $t = 0$ ), no more  $H_2S$  is produced in the reactor. The concentration of  $H_2S$  in the oil at  $t = 0$  is denoted by  $c_{l0}$ . Because of the intensive stirring, the gas stream is broken up into very small bubbles, with a large phase interface  $A$  available for mass exchange, as a result, it may be assumed that the liquid phase and the gas phase are practically in equilibrium and that  $c_l = m c_g$ . Finally, assume that  $A$  is constant during this process.

The question now is to determine the concentration of  $H_2S$  in the oil as a function of time.

Firstly, two mass balances will have to be drawn up for the  $H_2S$ : one for the oil phase and one for the gas phase. For the driving force for the mass transfer to the gas phase, the following is chosen  $\Delta c = c_l - m c_g$ . This means that the overall mass transfer coefficient  $K$  is based on the liquid phase. The two balances are now as follows:

$$V_l \frac{dc_l}{dt} = -KA(c_l - m c_g) \quad (4 112)$$

$$V_g \frac{dc_g}{dt} = -\phi_V c_g + KA(c_l - m c_g) \quad (4 113)$$

In Equation (4 113), the incoming gas was assumed not to contain any  $H_2S$ .

In a process like this, the resistance to mass transfer is often in the liquid phase, then  $K \approx k_l$ . In such cases, one often talks about the quantity  $k_l a$  with the specific interfacial area  $a$  defined as  $A/V_l$ .

There is now a problem with Equations (4 112) and (4 113). It has been stated that the liquid phase and the gas phase are virtually in equilibrium. This would mean that the driving force  $\Delta c = c_l - m c_g$  is zero and that there is therefore no  $H_2S$  transfer from the oil to the gas. However, this is not a true representation of the facts. What is actually happening is that the driving force has become almost zero precisely because the product of  $KA$  is very large (because of the intensive stirring). The transfer from oil to gas is therefore the product of '∞' and '0'. This problem is elegantly circumvented by adding up both equations: the transfer from oil to gas then disappears.

$$V_l \frac{dc_l}{dt} + V_g \frac{dc_g}{dt} = -\phi_V c_g \quad (4 114)$$

From this,  $c_g$  can be eliminated given the fact that virtual equilibrium between the two phases predominates in the reactor:  $c_g = c_l/m$ . This produces

$$\frac{dc_1}{dt} = - \frac{\phi_v}{m V_l + V_g} c_l \quad (4.115)$$

and with the boundary condition at  $t = 0 \rightarrow c_1 = c_{10}$  it then follows that

$$c_1(t) = c_{10} \exp\left(-\frac{\phi_v}{m V_l + V_g} t\right) \quad (4.116)$$

□

#### 4.6.4 Penetration theory at a phase interface

The derivation in § 4.6.3 is also applicable to non-steady state situations. Here, too, the fluxes that go to and from the interface are taken as starting points. Of course, these two are equal at all times, as an interface cannot absorb mass.

In the early stage of a process of contacting two layers of immiscible liquids with some species being susceptible to exchange by just diffusion, penetration theory applies – just like with unsteady-state heat conduction (§ 3.3). In either phase, the mass transfer coefficient  $k$  then is given by

$$k = \sqrt{\frac{ID}{\pi t}} \quad (4.117)$$

completely analogous to the model description presented in § 3.3.2 and § 3.3.3.

Expression (4.117) then can be substituted into the expression for the mass flux  $\phi_m''$  to render Equations like (4.104) and (4.105). Of course, penetration theory and its related expressions are valid as long as the penetration depth  $\sqrt{\pi IDt}$  is sufficiently smaller than the thickness of the layer into which diffusion takes place – i.e., as long as the driving force for diffusion is constant and still equal to the value  $|c_{b0} - c_i|$  at the time  $t = 0$  when the layers were brought into contact. [For longer times, long-term relations may be required analogous to those treated in § 3.3.5.]

##### Example 4.13. Acetic acid-benzene-water

A layer of benzene (thickness 1 cm) is laid carefully (without creating any flow) on a layer of pure water (also 1 cm thick). Acetic acid has been dissolved in the benzene with a concentration of  $10^{-2}$  mol/l. The partition coefficient  $m$ , defined as the ratio between the acetic acid concentrations in benzene and water at equilibrium, is 10. The diffusion coefficients of acetic acid in benzene and in water are  $0.5 \cdot 10^{-9}$  m<sup>2</sup>/s and  $1.5 \cdot 10^{-9}$  m<sup>2</sup>/s respectively.

There are a number of questions that need to be answered about the situation in these two layers, ten minutes after the layers come into contact with each other:

a) Determine the penetration depths in both layers

b) Calculate the interface concentrations

c) How great are the concentration gradients on both sides of the interface?

Indices B and W again denote benzene and water respectively, while  $b$  and  $i$  serve to represent a value in the bulk and at the interface, respectively.

Penetration depth of acetic acid in water after 10 minutes  $\sqrt{\pi ID_W t} = 1.7$  mm

Penetration depth of acetic acid in benzene after 10 minutes  $\sqrt{\pi ID_B t} = 0.97$  mm

Both penetration depths are clearly smaller than the thickness of the layers, so application of the penetration theory is allowed. This means that the fluxes on both sides of the interface are known, moreover, they are equal to each other, as all the acetic acid that comes out of the benzene goes into the water. In formula form

$$\phi_m'' = \sqrt{\frac{ID_B}{\pi t}} (c_b^B - c_i^B) = \sqrt{\frac{ID_W}{\pi t}} (c_i^W - c_b^W) \quad (4.118)$$

Because both fluxes must be equal at any point in time, a link between the four concentrations at stake follows from Equation (4.118). In addition, the interface concentrations are presented as *m*, i.e.,  $c_i^B = 10 c_i^W$ . With data,  $c_b^B = 10^{-2}$  mol/l and  $c_b^W = 0$ , it now follows that

$$c_i^B = 0.85, \quad c_b^B = 8.5 \text{ mmol/l}, \quad c_i^W = 0.085 \text{ and } c_b^W = 0.85 \text{ mmol/l}$$

The gradients at the interface now follow from the concentrations and the penetration depths

$$\left. \frac{dc^W}{dx} \right|_i = - \frac{c_i^W - c_b^W}{\sqrt{\pi ID_W t}} = - 0.5 \text{ mol l}^{-1} \text{ m}^{-1} \quad (4.119)$$

$$\left. \frac{dc^B}{dx} \right|_i = - \frac{c_b^B - c_i^B}{\sqrt{\pi ID_B t}} = - 1.55 \text{ mol l}^{-1} \text{ m}^{-1} \quad (4.120)$$

Comparing this example with Example 3.5 (bitumen on oak) shows that these expressions are essentially identical. The only difference is the role of the partition coefficient,  $m$ . If this were now to be introduced artificially for heat transport (with  $m=1$  at equilibrium), then both expressions would be completely identical. □

### Summary

For mass transfer across a phase interface, there is an important difference with heat transport: in equilibrium, the concentrations of species X in two phases A and B that are in contact with each other, generally are *not* equal. They are related by the so-called partition coefficient  $m$ , which is a property of the three substances involved – A, B and X.

This has consequences for the driving force for the mass exchange between the two phases: this is  $\Delta c = c^A - m \cdot c^B$ , where  $m$  is defined by requiring that  $\Delta c = 0$  for the equilibrium situation in this relation. This also means that the expression for the overall mass transfer coefficient includes  $m$ , as well as  $k^A$  and  $k^B$ . For the flux  $\phi_m''$  of X, the following applies

$$\phi_m'' = \left[ \frac{1}{k^A} + \frac{m}{k^B} \right]^{-1} (c^A - mc^B)$$

where  $\left[ \frac{1}{k^A} + \frac{m}{k^B} \right]^{-1}$  stands for the total mass transfer coefficient  $K$

### 4.7 Simultaneous transport of heat and mass: the wet bulb temperature

In this Section, we will finally analyse what happens when flow is forced to run along a damp surface. It is to be expected that the liquid will evaporate in such a situation: a question of mass transport. Given the heat that is required for evaporation, however, this evaporation results in the surface cooling down, which therefore leads to a heat flow from the surroundings to the damp body. We will look at this process with the help of the following example.

Consider a spherical liquid droplet in a gas flow, which is not saturated with the vapour of the liquid. At first, the temperature of the liquid is the same as that of the gas. Because of the evaporation of the liquid, the droplet cools off and a steady-state situation is eventually reached (see Figure 4.10). Assume in the analysis that the total quantity of liquid that evaporates is so slight that the diameter of the sphere remains constant.

So much heat has to be supplied from the air in this quasi steady-state situation that it actually compensates for the heat of evaporation associated with the mass flow rate

$$\phi_q = \phi_m \Delta h_v \quad (4.121)$$

where  $\Delta h_v$  represents the *enthalpy of evaporation* of the liquid

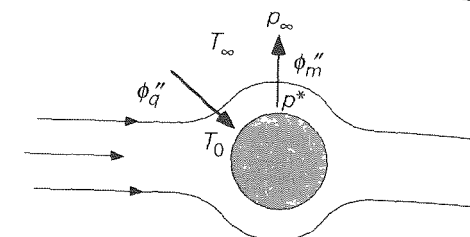


Figure 4.10

The mass flow rate depends on the driving force  $\Delta c$  in the gas phase and the mass transfer coefficient  $k$  in the gas phase. For the heat flow, this depends on  $\Delta T$  and  $h$ , entirely analogously

$$\phi_m = \pi D^2 k \frac{M}{RT} (p^* - p_\infty) \quad (4.122)$$

$$\phi_q = \pi D^2 h (T_\infty - T_0) \quad (4.123)$$

In these two equations,  $M$  stands for the molar mass of the liquid,  $p^*$  for the vapour pressure of the substance at temperature  $T_0$ ,  $T_\infty$  for the temperature of the incoming gas,  $p_\infty$  for the vapour pressure of the incoming gas (which of course has to be less than  $p^*$ , otherwise no evaporation could occur), and  $T_0$  for the *wet-bulb temperature* which is the temperature that the droplet assumes in the equilibrium situation, for  $T$  in Equation (4.122), the usual choice is the mean of  $T_\infty$  and  $T_0$ .

Substituting Equations (4.122) and (4.123) in Equation (4.121) gives

$$\frac{p_\infty - p^*}{T_\infty - T_0} = - \frac{RT}{M \Delta h_v} \frac{h}{k} \quad (4.124)$$

For the two unknowns  $T_0$  and  $p^*$ , one needs two equations. Equation (4.104) and an expression for the saturation pressure  $p^*(T)$ . For a graphical solution technique, the *humidity chart* of Figure 4.11 is used (for air-water at 1 bar). Because of the minus sign on the right-hand side of Equation (4.124), the straight lines in Figure 4.11 (shown with the term ‘adiabatic saturation line’) all have a negative angle of inclination.

If  $Re$  is not too small, then the following applies to  $h/k$ , thanks to Chilton to Colburn

$$\frac{h}{k} = \rho c_p \text{Le}^{2/3} \quad (4.125)$$

where  $\text{Le}$  stands for the *Lewis number* see also Equation (2.38). This means that the following applies, where  $Re$  is not too small

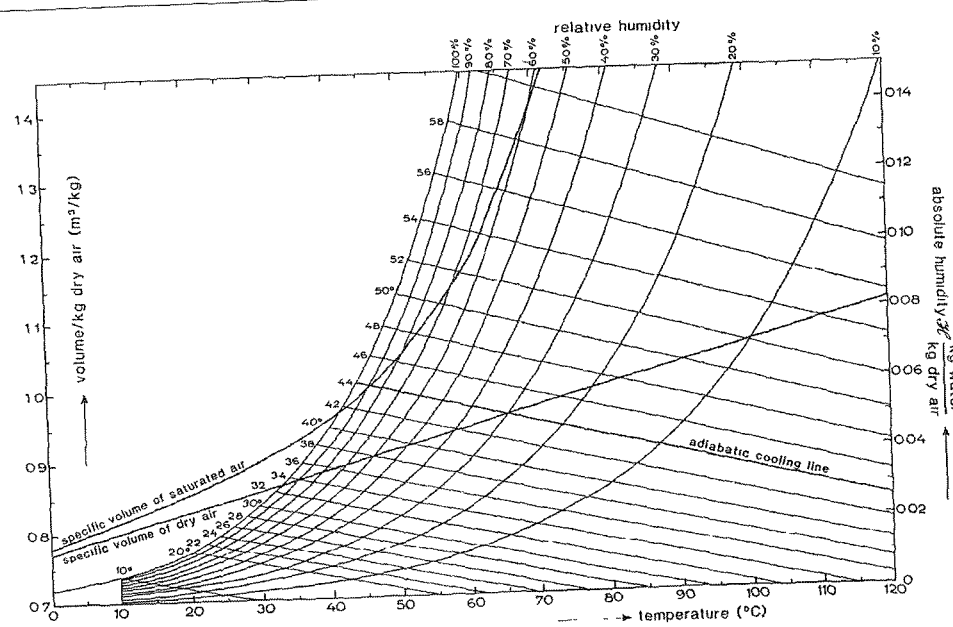


Figure 4.11

$$\frac{p_\infty - p^*}{T_\infty - T_0} = - \frac{RT\rho c_p}{M \Delta h_v} \text{Le}^{2/3} \quad (4.126)$$

Equation (4.126) is actually an equation for  $T_0$ , because the *equilibrium vapour pressure*  $p^*$  is a function of the temperature of the liquid, so for  $p^*$  the value at the *vapour pressure line* at  $T_0$  has to be taken. Notice that in Equation (4.126) neither the Reynolds number nor the diameter of the sphere occurs! For conditions of exclusively molecular transport around the sphere (shown by  $\text{Nu} = 2$  and  $\text{Sh} = 2$ ), Relation (4.126) applies as well.

The principle of the wet-bulb temperature is used among other things to help determine the humidity of a gas flow. Many drying and humidity related fields often involve – rather than vapour pressures – the use of the *absolute humidity* which is defined as the mass (in kg) of vapour in a gas per kg of dry gas. Other terms also feature, such as *relative humidity* – the pressure of the vapour in a gas mixture divided by the saturation pressure of vapour at the same temperature – and *dew point* – the temperature at which condensation of vapour begins when humid gas is cooled down. In other words, the temperature at which humid gas is saturated with vapour.

Some examples in which the humidity chart is used, are given below.

#### Example 4.14. Determining the dew point

What are the absolute humidity and the relative humidity of air at 70 °C with a wet-bulb temperature of 55 °C? What is the dew point?

The intersection of the adiabatic saturation line of this air with the saturation line is at 55 °C. We will now move along this adiabatic saturation line to the right to 70 °C and see that the absolute humidity is 0.105 kg water/kg dry air. We also see that the relative humidity is 39%.

Cooling the air increases the relative humidity, the absolute humidity does not change in the process. In the humidity chart we can see that air with an absolute humidity of 0.105 kg water/kg dry air is saturated at 53.7 °C. This is the dew point we were looking for.

#### Example 4.15. Condensing through cooling

The same air is cooled to 30 °C.

How much vapour will condense for every m<sup>3</sup> of saturated air at 30 °C?

The humidity chart tells us that saturated air at 30 °C contains 0.027 kg water/kg dry air. Therefore,  $0.105 - 0.027 = 0.078$  kg water/kg dry air has condensed. We also see from the humidity chart that the saturated volume for air at 30 °C is 0.88 m<sup>3</sup>/kg dry air. The quantity of condensed vapour is therefore

$$\frac{0.078}{0.88} = 0.089 \text{ kg water/m}^3 \text{ saturated air at } 30^\circ\text{C}$$

Incidentally, this principle of simultaneous transport of mass and heat is not restricted to liquid-gas systems. When *dissolving* crystals, for example, in a liquid, this combined effect of mass and heat transfer occurs as well.

#### Summary

One of the best illustrations of the analogy between heat and mass transfer is found with the wet bulb, where heat transport supplies the heat of evaporation that is needed for the evaporation process (the mass transport). In some circumstances, the wet-bulb temperature is independent of flow conditions and sphere dimensions. The wet bulb also illustrates that in some cases mass transport is limited by heat transfer. In any case, heat transport plays a role in processes that involve a phase transition.

# 5 Fluid mechanics

## 5.1 Introduction

Chapter 1 saw the introduction of balances, which proved to be very useful in that and subsequent chapters when solving all kinds of transport problems. The form of these balances is always the same

$$\frac{d}{dt} = \text{in} - \text{out} + \text{production} \quad (5.1)$$

At the start of this Chapter on fluid mechanics, it seems a good idea to demonstrate again, using balances, how flow is obtained through the supply of momentum (unit Ns) and how a flow obeys and is described by mass, momentum and energy balances

### Example 5.1. A wastewater pump

A basin contains water, in which a highly corrosive substance is dissolved. The water has to be pumped into tanks via a transport pipeline. However, the pump that is available may not come into contact with the corrosive substance, so a separate structure is created, as shown in Figure 5.1

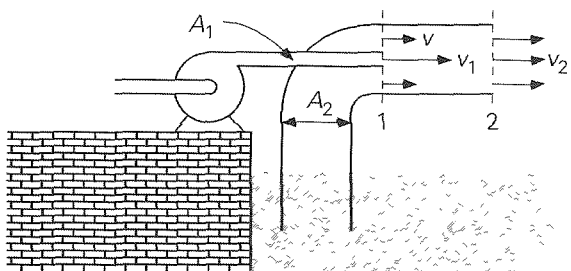


Figure 5.1

A smaller pipe with cross-sectional area  $A_1 = 20 \text{ cm}^2$  is connected to the discharge side of the pump and is then inserted into the pipeline with cross-sectional area  $A_2 = 180 \text{ cm}^2$  on the exterior of a bend. The pump pushes clean water at a uniform velocity of  $v_1 = 10 \text{ m/s}$  into the pipeline. Part of the momentum of this water is transferred to the contaminated water in the pipeline. This way, water is sucked out of the basin and pumped to the tanks. At some distance (at point 2 in the diagram) downstream of the mixing point (point 1), the velocity at  $A_2$  is again

uniform and equal to  $v_2 = 2 \text{ m/s}$ . This situation can be considered as steady state over time. Also, for the sake of simplicity, friction on the walls of the pipes may be disregarded, and it can be assumed that the density of the clean and contaminated water is equal (that is,  $10^3 \text{ kg/m}^3$ ).

First to follow is the velocity  $v$  of the contaminated water at point 1, thanks to a mass balance for the entire volume between 1 and 2, from the given velocities  $v_1$  and  $v_2$ :

$$0 = \rho A_1 v_1 + \rho (A_2 - A_1) v - \rho A_2 v_2 \quad (5.2)$$

Entering the values given shows that velocity  $v$  is equal to 1 m/s and that the flow rate of the contaminated water is 16 l/s.

Every force operating in the direction of flow has to be included in a balance for the momentum in the direction of flow. Given that friction on the walls can be disregarded, friction forces along the walls of the pipe are not relevant. And because gravity does not work in the direction of flow, the only force to remain is pressure forces at the entrance and exit planes at points 1 and 2. There is a uniform pressure  $p_1$  in the whole of plane 1 after all, there is no radial flow there. This means that the momentum balance for the same control volume between planes 1 and 2 is

$$0 = \rho A_1 v_1 v_1 + \rho (A_2 - A_1) v v - \rho A_2 v_2 v_2 + A_2 p_1 - A_2 p_2 \quad (5.3)$$

Eliminating  $v$  from Equation (5.3) with the help of Equation (5.2) produces, for the pressure drop from 1 to 2

$$p_1 - p_2 = -\rho \frac{A_1}{A_2 - A_1} (v_1 - v_2)^2 < 0 \quad (5.4)$$

There is therefore no pressure drop, but an increase  $p_2 = p_1 + 8 \cdot 10^3 \text{ Pa}$ ! The fact that at point 1 there is underpressure compared with at point 2 is due to the transfer of momentum from the discharge pipe of the pump. This input of momentum is now the driving force behind the flow it sucks as it were the contaminated water from the basin. Where the velocities between clean and contaminated water are levelled out and the sucking action is over, pressure  $p_2$  is higher precisely because of the input of momentum through plane 1, which is not yet expressed in (static) pressure  $p_1$ . From Bernoulli's law, we know that kinetic energy can be converted into 'pressure' energy and that deceleration can lead to an increase in pressure.

The transfer of momentum to the contaminated water is, it should be mentioned, accompanied by dissipation of mechanical energy. This follows directly from the mechanical energy balance

$$0 = \rho A_1 v_1 \left( \frac{1}{2} v_1^2 + \frac{p_1}{\rho} \right) + \rho (A_2 - A_1) v \left( \frac{1}{2} v^2 + \frac{p_1}{\rho} \right) + \\ - \rho A_2 v_2 \left( \frac{1}{2} v_2^2 + \frac{p_2}{\rho} \right) - \phi_m e_{fr} \quad (5.5)$$

Eliminating  $v$  with the help of the mass balance (5.3), eliminating  $p_1 - p_2$  with the help of the momentum balance (5.4), and dividing by the mass flow rate produces, for the dissipation

$$e_{fr} = \frac{A_1 v_1}{A_2 v_2} \frac{1}{2} v_1^2 + \frac{A_2 v_2 - A_1 v_1}{A_2 v_2} \frac{1}{2} \left( \frac{A_2 v_2 - A_1 v_1}{A_2 - A_1} \right)^2 + \\ - \frac{1}{2} v_2^2 - \frac{A_1}{A_2 - A_1} (v_1 - v_2)^2 \\ = 18 \text{ J/kg} \quad (5.6)$$

Of course, this mechanical energy is lost in the heating up of the water. The increase in temperature can be determined using the thermal energy balance. Assume here that the water at point 1 is at uniform temperature  $T_1$ . The internal energy concentration  $u$  of the contaminated water at point 1 is now therefore equal to that of the clean water (the same  $T$  and  $c_p$ ). The thermal energy balance for the control volume is

$$0 = \rho A_1 v_1 u_1 + \rho (A_2 - A_1) v u_1 - \rho A_2 v_2 u_2 + \phi_m e_{fr} \quad (5.7)$$

and with the help of mass balance (5.2) can be easily simplified to

$$u_2 - u_1 = e_{fr} \rightarrow T_2 - T_1 = \frac{e_{fr}}{c_p} = 4.3 \cdot 10^{-3} \text{ K} \quad (5.8)$$

□ It was possible to make statements about the flow in this example because information was known about the velocities  $v_1$  and  $v_2$  (and therefore about the driving force and resulting overall flow rate). In spite of the different balances, this information led us to values for the contaminated water flow rate, difference in pressure and increase in temperature. This is in fact a specific example, just as in Example 1.20 where the flow rate and the difference in pressure between two positions in a flow were given. In practice, this much information will not be available, especially at a design stage.

Usually just one fact is known and the remainder are needed for a given difference in pressure (or, generally, a driving force), how great will the flow rate be, or what magnitude of the difference in pressure is required in order to bring about a particular flow rate. In these cases, it will be necessary to know more about the

associated energy dissipation This will concern the  $e_{fr}$  term in the mechanical energy balance introduced in Chapter 1

The emphasis in the first part of this chapter lies on *engineering fluid mechanics* how energy dissipation can be calculated with the help of empirical friction or pressure drop coefficients First, a number of different flow meters will be looked at (in § 5.2), before the focus shifts onto the link between flow rate through and pressure drop over transport pipelines (§ 5.3 and § 5.4) and packed beds (§ 5.5) Balances play an important role here as well

Laminar flows are covered in the second part of this chapter The technique that is used in describing these flows entails drawing up force balances for typical volume elements somewhere in the flow field (micro balances) In the case of laminar flows, the transport of momentum perpendicular to the direction of flow (usually expressed in terms of shear stresses see § 2.1.4) is solely maintained by the molecules, for this reason, a distinction has to be made between fluids that obey *Newton's law* concerning the link between shear stress and velocity gradient (that is, concerning *molecular momentum transport*, the so-called *Newtonian liquids*) and fluids that do not do so (the so-called *non-Newtonian liquids*) This will be dealt with separately in § 5.6 and § 5.7 respectively At the end of the chapter (in § 5.8), the Navier-Stokes equations will be introduced, which describe any flow in a multi-dimensional domain, including time-dependent, and compressible or incompressible ones

## 5.2 Flow meters

Various instruments were discussed in § 1.3.3 with which the flow velocities of liquids or gases can be determined, namely the pitot tube and the Venturi tube Three more *flow rate meters* will be introduced in this Section the weir, the orifice meter, and the rotameter The weir requires a somewhat more detailed examination based on the Bernoulli equation than the pitot tube and the Venturi tube, while energy dissipation should certainly not be disregarded as far as the orifice meter and rotameter are concerned

### 5.2.1 Weir

Figure 5.2 shows a *weir* in a stretch of water (a ditch, a canal, or a stream) The weir, which is effectively a wall in the water and thereby forms an obstruction to the flow, extends across the full width of the water Let us assume for now that the crest of the weir is sharp and horizontal The water level upstream of the weir is higher than the crest, while that downstream is lower If the upstream water level is sufficiently higher than the crest, and providing that the supply of water is sufficiently great, a layer of water will pass over the sharp crest (because of the inertia of the water) and

plunge into the water downstream This sheet of water, or *nappe*, which stretches across the full width of the stretch of water, passes over the crest without any friction at all (so  $e_{fr} = 0$ ) and moves freely through the air so that the pressure throughout the sheet of water just after the weir is atmospheric Figure 5.2a gives a side view, and shows that the water level starts to fall as it approaches the weir (because the water depth of the stretch of water, water that is lower than the crest of the weir will also flow over it All told, then, the water velocities above the sharp edge of the weir are not purely horizontal

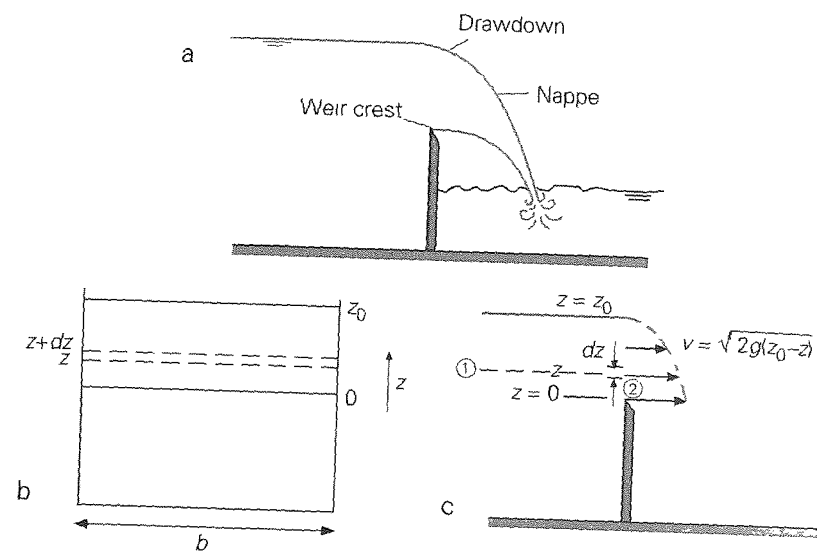


Figure 5.2

In a steady-state situation, the flow rate over the weir depends on the upstream water level,  $z_0$  (measured from the crest of the weir) This means that the flow rate can be regulated by moving the wall vertically upwards or downwards The question here is how the flow rate depends quantitatively on  $z_0$

To answer this question, we should realise that the flow rate in the stretch of water is equal to the product of velocity times cross-sectional area, both in the vertical plane 1 and the vertical plane 2 (see Figure 5.2c) In plane 1 nothing is known about the local velocity profile or the averaged velocity, while in plane 2 the flow rate depends on  $z_0$  Figure 5.2b shows how the flow rate in plane 2 is made up of contributions from thin, horizontal strips of height  $dz$ , the average velocity in each strip being (potentially) a function of  $z$  How the water exactly flows off the crest, depends on the local energy housekeeping as described in terms of the mechanical energy balance between the points 1 and 2, with point 1 sufficiently far upstream of the weir and with point 2 exactly above it (see Figure 5.2c)

To this end, it is useful and usual to simplify the situation somewhat see Figures 5.2b and 5.2c. The fall of the water level, or drawdown, upstream of the weir is ignored, the velocity of the water above the crest of the weir is assumed to be horizontal, and the pressure is assumed to be atmospheric ( $p = p_0$ ) already above the horizontal, and the pressure is assumed to be atmospheric ( $p = p_0$ ) already above the sharp crest (and not just in the nappe). Further,  $\rho$  is constant,  $\phi_w = 0$ ,  $\phi_q = 0$  and  $e_{fr} = 0$ . This means that the Bernoulli equation – Equation (1.126) – can be used here.

$$\frac{1}{2}v_1^2 + gz_1 + \frac{p_1}{\rho} = \frac{1}{2}v_2^2 + gz_2 + \frac{p_2}{\rho} \quad (5.9)$$

For points 1 and 2 at the same height  $z$  (above the crest of the weir) the following applies

$$\text{point 1 } z_1 = z, v_1 = v(z), p_1 = p_0 + \rho g (z_0 - z)$$

$$\text{point 2 } z_2 = z, v_2 \gg v_1, p_2 = p_0$$

It should be pointed out that this latter assumption is only justified if  $z_0$  is markedly smaller than the depth of the stream upstream of the weir (at point 1). It is evident that the unknown variable here is  $v_2(z)$ . Entering this into Equation (5.9) gives

$$v_2 = \sqrt{2g(z_0 - z)} \quad (5.10)$$

Actually,  $v_2$  depends on  $z$ . Equation (5.10) expresses that the velocity at height  $z$  depends on the thickness  $z_0 - z$  of the liquid layer above height  $z$  that in a way ‘pushes’ the liquid at height  $z$  over the weir. Equation (5.10) further implies that at height  $z_0$  (i.e. on the free water surface) the water velocity is zero. This result relates to the above simplification  $v_2 \gg v_1$  that leads to  $v_1(z) = 0$ . Close to the water surface ( $z = z_0$ ), this simplification is rather dubious.

Equation (5.10) can now be used to calculate the contribution made by a thin strip between  $z$  and  $z + dz$  (see Figure 5.2b) to the flow rate over the weir

$$d\phi_v = v_2(z) b dz = b \sqrt{2g(z_0 - z)} dz \quad (5.11)$$

The overall flow rate follows from integrating Equation (5.11)

$$\begin{aligned} \phi_v &= b \sqrt{2g} \int_0^{z_0} \sqrt{z_0 - z} dz = \\ &= b \sqrt{2g} z_0^{3/2} \int_0^1 \sqrt{1-t} dt = \frac{2}{3} b \sqrt{2g z_0^3} \end{aligned} \quad (5.12)$$

A new and important aspect of the above analysis is the use of the Bernoulli equation for calculating the velocity locally, that is, at height  $z$  – in line with the physics of the situation.

In fact, the situation at a weir is not essentially different to that of Example 1.21, except that in Example 1.21 the variation of the velocity over the height of the gap could be disregarded, because the size of the hole was considered very small in comparison with the liquid height  $H$  in the container.

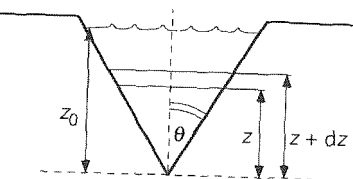


Figure 5.3

There are all kinds of other types of weir or overflow, such as those in the form of a triangle (see Figure 5.3). The analysis used in this case is entirely in parallel with that of a completely horizontal weir, with the only difference being in determining the flow rate. After all, the width  $b$  of the strip is also a function of  $z$ :  $b = 2z \tan \theta$ . The flow rate can now be calculated from

$$\phi_v = 2 \tan \theta \sqrt{2g} \int_0^{z_0} z \sqrt{z_0 - z} dz = \frac{8}{15} \tan \theta \sqrt{2g} z_0^{5/2} \quad (5.13)$$

Expressions (5.12) and (5.13) overestimate the actual flow rates. This is caused primarily by the simplifications that were made for Figure 5.2b. In fact, the lowering of the water level in the run towards the weir means that the size of the area that is available to flow is smaller. In addition, the velocity above the crest is not horizontal throughout. These effects are corrected with the help of a discharge coefficient  $C_d$ , with  $C_d < 1$ , to be entered into the equation for the flow rate, this means, for example, that Equation (5.12) changes to

$$\phi_v = \frac{2}{3} C_d b \sqrt{2g z_0^3} \quad (5.14)$$

This method is entirely comparable to that in Example 1.21 for the outflow through a small hole see Equation (1.169). There, too, the area through which the flow passes, is, as a result of contraction, smaller than the through-flow area available from a geometric perspective, and consequently the flow rate is also smaller. In effect,  $C_d$  stands for the ratio of the actual area through which the flow passes to the size of the surface available for flow but not utilized by the fluid.

If the water does not ‘shoot’ over the crest, but simply runs slowly over it, or if the weir does not have a sharp edge, then energy dissipation will play a role, and the flow rates such as those shown in Equations (5.12) – (5.14) will have to be corrected accordingly as well. The above derivative is not entirely correct either in the event

that the water level downstream of the weir is not particularly low, so that there is no real 'free fall' of water passing over the weir

Weirs are also used with trays in distillation towers (in oil refineries, for example) for separating (or fractionating) multicomponent mixtures according to their boiling point. A distillation tower contains a large number of trays, two of which are shown in Figure 5.4. Each tray is kept at a certain temperature, with the tray at the bottom of the tower being the hottest, and the tray at the top, the least hot. The aim with each tray is to maintain a balance with regard to the composition of vapour and liquid, for which rising vapour and falling liquid flows have to be brought into close contact. This is achieved by bubbling vapour through a layer of liquid on each tray. The height of the liquid on each tray, and therefore the duration of the contact between the vapour and the liquid, depends very much on the weir height.

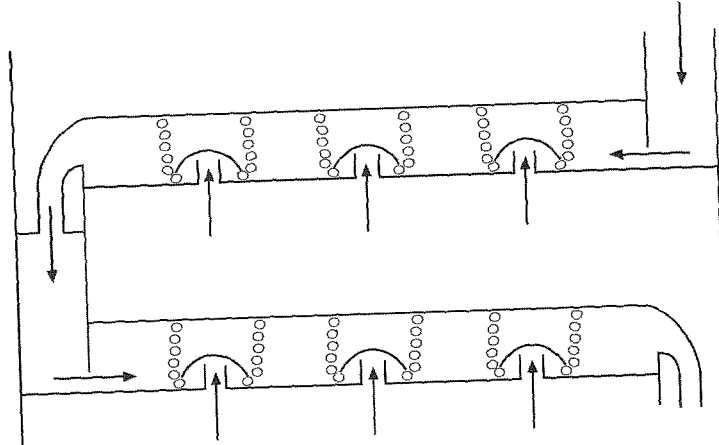


Figure 5.4

### 5.2.2 Orifice meter

The *Venturi tube* was discussed in § 1.3.4 – this is used for measuring the flow rate through a pipe. A Venturi tube includes both a gradual narrowing of the diameter and a very gradual widening that prevents energy dissipation. This narrowing can also be made very 'sudden', in which case *energy dissipation* can no longer be disregarded! This is the case with the *orifice meter*.

This involves placing a disk in the pipe with a small hole, or orifice, in it (see Figure 5.5). As can be seen in the diagram, eddies occur primarily to the rear of the disk, which cause a considerable dissipation of mechanical energy. Contraction of the flow also occurs here as it passes the discharge opening. An analysis using Bernoulli now therefore has to be 'corrected' to allow for dissipation and contraction with the help of a *discharge coefficient*  $C$  that depends on the points at which pressures  $p_1$  and  $p_2$  are measured. The discharge coefficient is also a function of  $Re$  and of the

ratio of the pipe diameter and the orifice diameter. For example, for an orifice meter with a sharp-edged hole, the following applies  $C = 0.62$  providing that  $Re > 10^4$

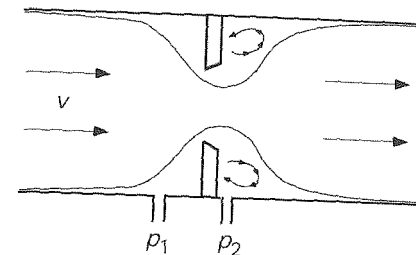


Figure 5.5

A significant disadvantage of using orifice meters is dissipation after the orifice meter, the pressure does not return to the value that was present upstream, because mechanical energy has been destroyed. This means that a considerable pressure drop can occur over the orifice meter. In summary, the flow rate (for liquids) as a function of the pressure drop measured is as follows

$$\phi_m = C \left( Re, \frac{D_2}{D_1} \right) \sqrt{\frac{A_2}{1 - \left( \frac{A_2^2}{A_1^2} \right)}} \sqrt{2\rho(p_1 - p_2)} \quad (5.15)$$

where  $D_1, A_1$  and  $D_2, A_2$  are the diameter and the cross-sectional area of the pipe and the orifice opening respectively

### 5.2.3 Rotameter

The *rotameter* is a smart variant of the orifice meter. Again, the principle is based on a change to the diameter in the pipe and measuring pressure difference that results from this. Instead of a fixed disk in the pipe, however, a float is fitted (see Figure 5.6). The rotameter should always be fitted exactly vertically. The reason for this is simple: the upward flow exerts a force on the float, which in a steady-state situation makes equilibrium with gravity and with the *buoyancy* of the float, which allows it to float.

If the tube of the rotameter were to have a constant diameter, there would be just one flow rate at which the float would be in equilibrium. This is impractical for a flow rate meter. For this reason, the rotameter has a variable diameter: the tube gets wider and wider towards the top. This means that with a certain flow rate, the float will remain floating at a particular height. It is precisely this property that makes the rotameter such a useful measuring instrument: the position of the float is a measure for the force of the upward flow on the float and therefore for the flow rate. By making the tube transparent, it is possible to see the position of the float and therefore determine the flow rate.

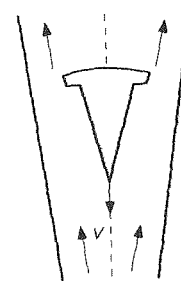


Figure 5.6

In principle, the force of the flow on the float (float volume  $V_o$ ,  $A_o$  the area of the largest cross-section of the float,  $\rho_o$  the density of the float material) can be modelled according to the recipe in § 2.3. In § 2.3, it was assumed that the object around which the flow was moving was in an ‘infinite’ medium, so that there were no influences from the sides. With the rotameter, the tube wall is very nearby. This is why the rotameter is modelled differently: analogous to the expression for the orifice meter. The pressure drop over the float as a result of the flow is replaced by the net gravity that affects the float, thanks to a force balance on the float. For the flow rate, this produces

$$\phi_m = C \left( A_{tube}(z) - A_o \right) \cdot \sqrt{2\rho_f(\rho_v - \rho_f)g \frac{V_o}{A_o}} \quad (5.16)$$

where  $\rho_f$  is the density of the liquid and  $A_{tube}(z)$  the cross-sectional area of the vertical tube at height  $z$ . If  $Re$  (related to the annular gap between float and tube wall) is sufficiently large, then discharge coefficient  $C$  is constant.

Equation (5.16) expresses how the flow rate depends on the vertical position  $z$  in the tube that is taken by the float in response to the forces exerted on it. A calibration graph is usually used instead of Equation (5.16) for the relation between position  $z$  of the float and the flow rate. Note that every type of float (shape, material) requires a different calibration graph. A rotameter is generally made in such a way that  $A_{tube}$  increases linearly by height  $z$  so that the calibration graph of the rotameter is virtually linear.

### Summary

Three flow meters have been analysed in this Section: the weir, the orifice meter, and the rotameter. All three analyses have taken the Bernoulli equation as their starting point. A correction had to be made to the results of the analyses due to contraction of the liquid flow and because of energy dissipation. In principle, this so-called discharge coefficient depends on the geometries and the Reynolds number.

In the case of the weir, dissipation plays a secondary role. With the orifice meter and rotameter, however, there is a considerable degree of dissipation and therefore a striking pressure drop with the orifice meter or float respectively.

## 5.3 Pressure drop along a straight pipeline

In § 1.3, we looked at a horizontal straight round tube, through which water flowed as a result of a difference in pressure over the tube imposed by a pump. With the help of an energy balance, it was derived that the pressure energy (= mechanical energy) in the pipe was converted to internal energy (= thermal energy). This process is known as dissipation of mechanical energy. The underlying mechanism is friction. In this example, both pressure drop and flow rate were given. The link between pressure drop and flow rate will be discussed in more detail below so that one can be calculated if the other is known.

### 5.3.1 The concept of the friction factor

To this end, consider a straight horizontal pipe (length  $L$ , diameter  $D$ ) through which water is flowing at a given mean velocity  $\langle v \rangle$  – see Figure 5.7

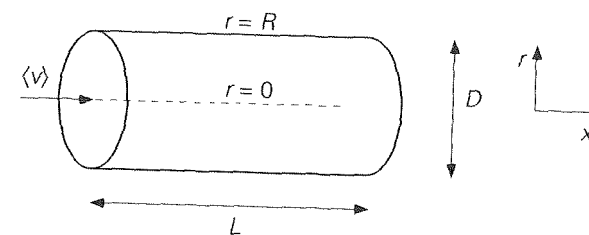


Figure 5.7

How large is the pressure drop that is needed in order to allow the water to flow through the pipe at mean velocity  $\langle v \rangle$ ?

This pressure drop is needed in order to overcome the *friction* at and resulting from the pipe walls. Friction is the result of shear stress between individual liquid layers or between a liquid layer and a wall. The term shear stress was introduced in § 2.1.4 as an alternative description to molecular momentum transport. The *shear stress* is a force per unit of surface area exerted by one layer of liquid on another (adjacent) layer or wall. This force is parallel to the direction of flow.

In order to be able to calculate the pressure drop in the pipe, it is therefore necessary to know what the shear stress at the wall is. The shear stress exerted by the wall on the liquid can in principle be calculated from the following:

$$\tau_{w \rightarrow f} = -\tau_{f \rightarrow w} = -\left\{ -\mu \left[ \frac{dv_x}{dr} \Big|_{r=R} \right] \right\} = \mu \left[ \frac{dv_x}{dr} \Big|_{r=R} \right] \quad (5.17)$$

To calculate the shear stress at the wall, it would therefore be necessary to know the velocity profile in the pipe, so that the derivative from that could be used to determine the velocity at the wall. In general, this is a difficult task, if not an impossible one. This is why the technique of the dimensional analysis will again be used in order to find out what the shear stress depends on.

The shear stress is a function of the mean liquid velocity  $\langle v \rangle$  in the pipe, the diameter  $D$  of the pipe, the viscosity  $\mu$ , and the density  $\rho$  of the liquid

$$\tau_{w \rightarrow f} = f(\langle v \rangle, D, \mu, \rho) \quad (5.18)$$

Carrying out the dimensional analysis produces

$$\frac{\tau_{w \rightarrow f}}{\rho \langle v \rangle^2} = k \left( \frac{\mu}{\rho \langle v \rangle D} \right)^a = k \cdot Re^{-a} \quad (5.19)$$

The shear stress exerted by a wall on a liquid flow can be modelled in the same way as the force exerted by a flow on an immersed body (see § 2.3):

$$\tau_{w \rightarrow f} = -f \frac{1}{2} \rho \langle v \rangle^2 \quad \text{with } f = f(Re) \quad (5.20)$$

The factor  $f$  is known as the *friction factor*. The minus sign in Equation (5.20) expresses the opposing character of the force exerted by the wall on the liquid.

With a view to determining the pressure drop over a pipe length  $L$  for a steady-state flow through a straight horizontal pipe from Figure 5.8, a momentum balance can be drawn up. The control volume is formed by the pipe wall and the two planes 1 and 2, separated by distance  $L$ .

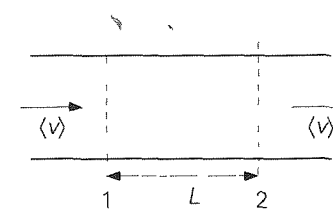


Figure 5.8

As long as the cross-sectional areas  $A_1$  and  $A_2$  of the tube at positions 1 and 2 are equal ( $=A$ ), the  $x$  momentum flow 'in' and the  $x$  momentum flow 'out' will cancel each other out. This means the  $x$  momentum balance is reduced to a force balance:

$$0 = p_1 A - p_2 A + \tau_{w \rightarrow f} SL \quad (5.21)$$

For a cylindrical tube,  $A = \pi D^2/4$ . The symbol  $S$  stands for the *wetted perimeter* (wetted by the 'liquid') of the tube, for an entirely filled cylindrical tube this is  $\pi D$ . Equation (5.21) is written in as general terms as possible, which means it also applies, for example, to an open ditch through which water is flowing. The term 'wetted perimeter' fully covers the cause of the pressure drop friction on the wall.

The pressure drop can be determined easily from Equation (5.21)

$$p_1 - p_2 = -\tau_{w \rightarrow f} \frac{SL}{A} \quad (5.22)$$

For the pressure drop resulting from energy dissipation due to wall friction (shear stress at the wall), combining Equations (5.20) and (5.22) produces

$$p_1 - p_2 = f \cdot \frac{SL}{A} \frac{1}{2} \rho \langle v \rangle^2 \quad (5.23)$$

For a cylindrical tube (with diameter  $D$ ) completely filled with liquid, it holds

$$\frac{SL}{A} = \frac{\pi D L}{\frac{\pi}{4} D^2} = 4 \frac{L}{D} \quad (5.24)$$

Entering this into Equation (5.23) produces what is known as the *Fanning pressure drop equation* that for flow through cylindrical tubes reproduces the wall friction

$$p_1 - p_2 = \Delta p = 4f \frac{L}{D} \frac{1}{2} \rho \langle v \rangle^2 \quad (5.25)$$

where the coefficient  $4f$  is denoted as the *Fanning friction factor*<sup>20</sup> being a function of the Reynolds number  $4f = 4f(Re)$ .

For non-cylindrical shaped tubes, an equation that is entirely analogous to Equation (5.25) is used. Diameter  $D$  is replaced to that end by the so-called *hydraulic diameter*  $D_h$ , which is defined as

$$D_h \equiv \frac{4A}{S} \quad (5.26)$$

Remember that  $A$  is the surface through which the flow passes. This is not necessarily the same as the cross-sectional area of the pipe. Moreover,  $S$  is the perimeter on which the shear stress is exerted (what is referred to as the *wetted perimeter*) and this in turn is not necessarily the same as the perimeter of the pipe.

<sup>20</sup> In the world of engineering, also the *Moody friction factor*  $f$  is widely used, being defined by Equation (5.25) without the '4' – implying that the numerical values of the Moody  $f$  are equal to Fanning's  $4f$  values. This textbook uses the Fanning friction factor just because of the ease of the hydraulic diameter.

**Example 5.2. Flow in an open channel**

Water flows through a rectangular channel (height of walls is  $H$ , width is  $w$ ) The height of the water level in the channel is  $h < H$

What is the hydraulic diameter of this system (see Figure 5 9)?

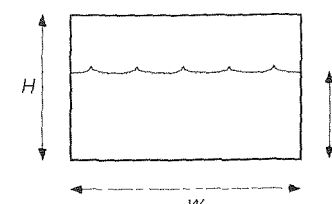


Figure 5 9

The cross-sectional area  $A$  through which the water flows is given by  $w h$  – not by  $w H$ . Similarly, for the wetted perimeter,  $S = 2h + w$  and not  $2H + 2w$  after all, there is no wall exerting shear stress on the surface of the water (the effect of the air is negligible compared with the effect of a channel wall!) The use of  $H$  instead of  $h$  for the wetted perimeter is also erroneous the height of the channel wall is not relevant here. For the hydraulic diameter, all this produces

$$D_h = \frac{4A}{S} = \frac{4wh}{2h+w} \quad (5.27)$$

□

**5.3.2 The use of the friction factor**

As already mentioned, the Fanning friction factor is a function of the Reynolds number (in relation to the tube diameter) In Figure 5 10,  $4f$  is plotted as a function of  $Re$  for tubes with a circular cross-section More or less analogously to how the resistance coefficient  $C_D$  for an object immersed in a flow depends on the Reynolds number related to the particle (see Figure 2 16), here too there are two separate regimes, namely that of *laminar* and of *turbulent pipe flow*

For the *laminar* regime, the following can be derived (see § 5 6 4)

$$4f = 64/Re \text{ providing that } Re < 2000 \quad (5.28)$$

while in the turbulent regime, the empirical formula of Blasius applies

$$4f = 0.316 Re^{-1/4} \text{ providing that } 4000 < Re < 10^5 \quad (5.29)$$

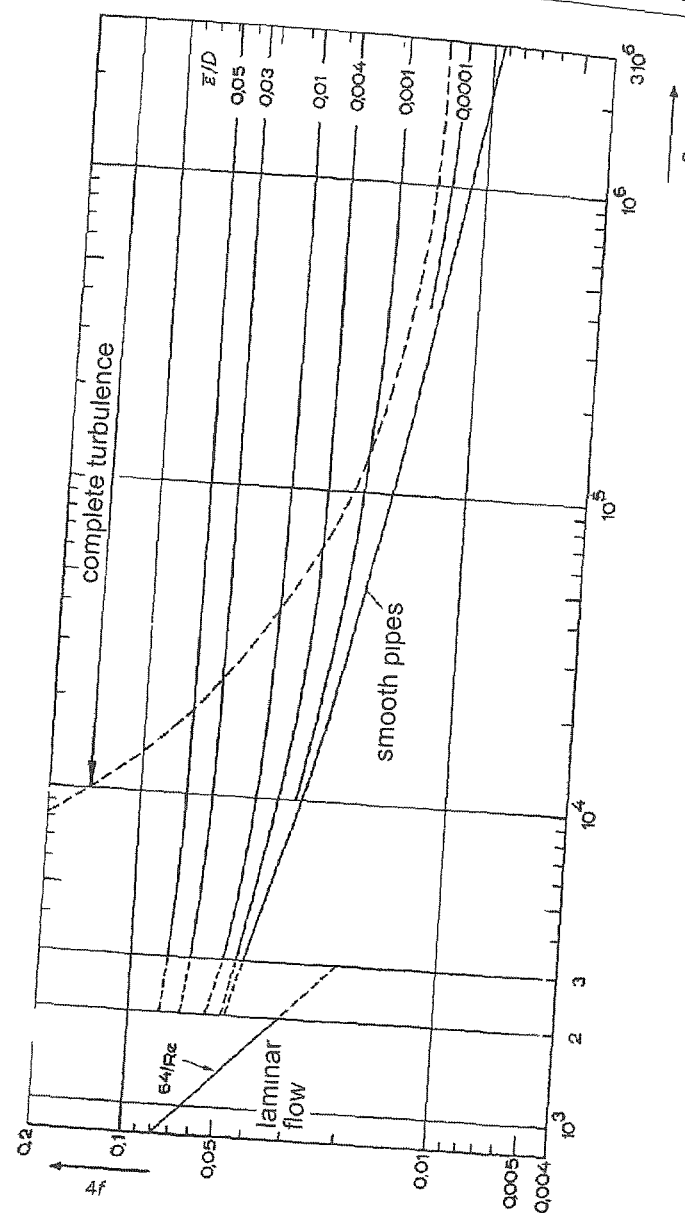


Figure 5 10

Remember that with  $C_D$ , the range in which  $C_D \propto 1/Re$  is limited to  $Re < 1$ , while the laminar regime with tubular flow extends to  $Re \approx 2000$ ! This once more illustrates that the critical value of the Reynolds number for the transition laminar – turbulent depends on the geometry

In Figure 5 10, several lines have been drawn for  $4f$  These show that the resistance that a fluid encounters in a tube also depends on the *wall roughness* This is logical

(see Figure 5.11), given that an extra eddy will occur behind any protrusion in the wall. Of course, this creates more dissipation of usable mechanical energy and therefore leads to more resistance. Or, in terms of shear stress, the extra eddy means that momentum will be transferred from the liquid to the wall more effectively. And shear stress is an alternative interpretation of molecular momentum transport.

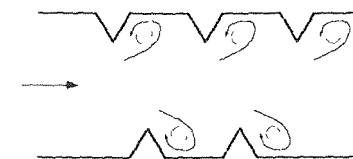


Figure 5.11

The roughness of the wall is usually described by the (non-dimensional) *relative roughness*  $\bar{\epsilon}/D$ , where  $\bar{\epsilon}$  is the absolute roughness, the mean height of the 'protrusions' on the wall. As shown in the  $4f$  versus  $Re$  plot,  $4f$  becomes constant if  $\bar{\epsilon}/D$  or  $Re$  are sufficiently great. The larger the relative roughness, the more  $4f$  will be constant as the value of  $Re$  gets smaller. This can be understood by using the image of the eddies transporting momentum. With a high level of relative wall roughness, the protrusions stick out relatively far, and the eddies effectively carry momentum from the bulk of the flow to the wall.

There now follow some examples for calculating pressure drops in straight pipelines.

#### Example 5.3. Pressure drop along a horizontal oil pipeline

A viscous oil ( $\mu = 70 \cdot 10^{-3} \text{ Ns/m}^2$ ,  $\rho = 900 \text{ kg/m}^3$ ) flows through a straight, horizontal, cylindrical tube (length 10 m, diameter 10 cm, smooth wall) in a steady state at a flow rate of  $7.85 \cdot 10^{-4} \text{ m}^3/\text{s}$ .

How great is the pressure drop  $\Delta p$  along this pipeline?

Equation (5.25) can be used directly for this calculation. From the flow rate, it follows that  $\langle v \rangle = 0.1 \text{ m/s}$ , from which it follows that  $Re = 129$ . The flow is therefore laminar and thanks to Equation (5.28), it follows that  $4f = 0.5$ . Entering this into Equation (5.25) now produces  $\Delta p = 225 \text{ Pa}$ .

#### Example 5.4. Velocity in a horizontal water pipeline

Water flows through a long, horizontal, straight pipe (length 1 km, diameter 10 cm, relative roughness 0.001). Again, the situation is steady. The pressure drop along the pipe is 2 bar.

What is the velocity of the water in the pipe?

Now, the velocity has to be solved with the help of Equation (5.25).

$$\langle v \rangle = \sqrt{\frac{D}{L} \frac{2\Delta p}{\rho} \frac{1}{4f}} \quad (5.30)$$

This produces the same problem as when determining the uniform velocity of a body falling or rising through a fluid. Velocity  $\langle v \rangle$  can only be calculated if  $4f$  is known, while  $4f$  itself is a function of  $\langle v \rangle$ . Here, too, an iterative solving procedure offers a way out: choose a velocity, say, of  $\langle v \rangle = 2 \text{ m/s}$ , this gives  $Re = 2 \cdot 10^5$ , looking this up on the  $4f$  versus  $Re$  plot gives (reading it from the relative roughness line = 0.001!)  $4f = 0.02$ , entering this value into Equation (5.30) produces a new  $\langle v \rangle$  namely, 1.4 m/s. This then means  $Re = 1.4 \cdot 10^5 \rightarrow 4f = 0.02$  and that's it! In general, this calculation procedure will have to be repeated several times before  $\langle v \rangle$  becomes constant.

Incidentally, a problem of the kind illustrated in Example 5.4 can also be solved in another way. To do this, Equation (5.25) is rewritten as follows:

$$\frac{\rho D^3}{4\mu^2} \frac{\Delta p}{L} = \frac{1}{2} f \left( \frac{\rho \langle v \rangle D}{\mu} \right)^2 = \frac{1}{2} f Re^2 \quad (5.31)$$

The left-hand side of this equation generally consists solely of variables that are given, this is also the case in Example 5.4. This implies the value of  $\frac{1}{2} f Re^2$  is known.  $Re$  can then be directly read from a  $Re$  versus  $\frac{1}{2} f Re^2$  graph (see Figure 5.12), which has been constructed from Figure 5.10, from which  $\langle v \rangle$  then follows.

In the above Example 5.4, this method produces

$$\frac{1}{2} f Re^2 = \frac{\rho D^3}{4\mu^2} \frac{\Delta p}{L} = 5 \cdot 10^7 \quad (5.32)$$

Looking up  $Re$  in Figure 5.12 produces  $Re = 1.2 \cdot 10^5$  and therefore  $\langle v \rangle = 1.2 \text{ m/s}$ . This value is slightly different from the first result. Both solutions can be made more similar to each other by using more accurate plots and by taking the readings more meticulously.

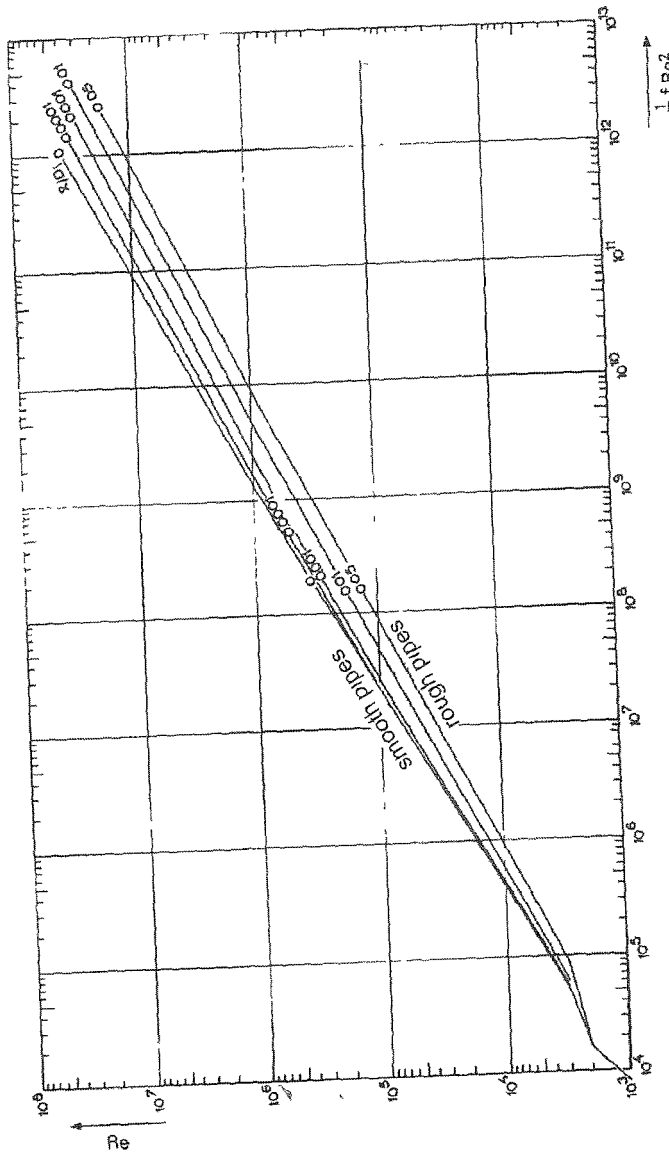


Figure 5.12

**Example 5.5.** Velocity in a horizontal milk pipeline

Milk ( $\rho = 10^3 \text{ kg/m}^3$ ,  $\mu = 2.1 \cdot 10^{-3} \text{ Ns/m}^2$ ) flows under steady-state conditions through a long, horizontal, straight pipeline (diameter 4 cm, length 20 m, smooth wall) as a result of a pressure drop of 2 kPa. What is the mean velocity in the pipeline?

This task can be solved using one of the two methods described above. However, there is a third way using the Blasius equation as given in Equation (5.29), providing that the requirement is met that the Reynolds number falls in the

specified Re range. But of course, this can only be verified retrospectively. Entering this expression into Equation (5.25) produces, for the pressure drop resulting from friction

$$\Delta p = 0.316 \text{ Re}^{-1/4} \frac{L}{D} \frac{1}{2} \rho \langle v \rangle^2 = \\ = 0.158 L D^{-5/4} \mu^{1/4} \rho^{3/4} \langle v \rangle^{7/4} \quad (5.33)$$

Entering this information gives  $\langle v \rangle = 0.5 \text{ m/s}$ . For the Reynolds number, this produces  $Re = 9500$ , Blasius may indeed be used, therefore. Remember that the Blasius equation is only valid for pipes with smooth walls.  $\square$

The above examples all relate to cylindrical pipelines. In general, the relationship between the pressure drop and the velocity in the pipeline is modelled with the hydraulic diameter. For pipelines or flow channels with any given diameter (but constant throughout the entire length of the pipeline), the very same  $4f(Re)$  can now be used *providing that the flow is turbulent*. The Reynolds number must then be determined with the help of the hydraulic diameter, of course. This agreement does not apply for the laminar flow area.

**Example 5.6.** Water transport through a rectangular pipe

Water flows in steady state through a horizontal, rectangular pipe (height 3 cm, width 5 cm, length 100 m, smooth walls). The water velocity is 1 m/s. What is the pressure drop along the channel?

It is first necessary to calculate the hydraulic diameter

$$D_h = \frac{4A}{S} = \frac{4bh}{2h+2b} = 3.75 \text{ cm} \quad (5.34)$$

From which it follows for the Reynolds number

$$Re_h = \frac{\rho \langle v \rangle D_h}{\mu} = 375 \cdot 10^4 \quad (5.35)$$

With the help of Figure 5.10 it again follows that  $4f = 0.02$ , and entering this value into Equation (5.25) produces

$$\Delta p = 4f \frac{1}{2} \rho \langle v \rangle^2 = 27 \cdot 10^4 \text{ Pa} = 0.27 \text{ bar} \quad (5.36) \quad \square$$

### 5.3.3 The analogy with heat and mass transfer

For the case of turbulent flow, the *film theory* for heat transfer was discussed in § 3.5.2, and reference was also made in § 4.5.2 to the film theory in the case of mass transfer. The subject of the *hydraulic film thickness*  $\delta_h$  was raised as well. The film theory involves laminar momentum transport, for which Newton's viscosity law, Equation (2.4), applies. Outside the film, the flow is turbulent and the velocity profile is therefore very flat thanks to the momentum transport by the eddies in the turbulent field of flow. In the film theory, the following applies to the momentum transport (*friction!*) from the bulk to the wall:

$$\tau_{f \rightarrow w} = f \cdot \frac{1}{2} \rho \langle v \rangle^2 = \mu \frac{\langle v \rangle}{\delta_h} \quad (5.37)$$

entirely analogously to the heat flux, Expression (3.144), according to the film theory approach for turbulent flow. Equation (5.37) states that the *friction drag* lies entirely in the film.

It has already been demonstrated, in § 3.5.2, that film thicknesses  $\delta_q$  and  $\delta_h$  depend on the degree of turbulence in the flow.  $\delta_q$  and  $\delta_h$  decrease as the Reynolds number increases. This means that heat transfer under turbulent conditions and hence the associated Nusselt number depend on the degree of turbulence and hence on  $\delta_h$  as well. The following realignment is in accordance with this reasoning:

$$Nu = \frac{hD}{\lambda} = \frac{D}{\delta_q} = \frac{D}{\delta_h} \frac{\delta_h}{\delta_q} = f \frac{\rho \langle v \rangle D}{2 \mu} \frac{\delta_h}{\delta_q} \quad (5.38)$$

where Equation (5.37) is used.

By also using the expression  $\delta_h/\delta_q \propto Pr^{1/3}$  (discussed previously in relation to Figure 3.24 in § 3.5.2), the following results

$$Nu \propto \frac{1}{2} f Re Pr^{1/3} \quad (5.39)$$

or

$$\frac{1}{2} f \propto \frac{Nu}{Re Pr^{1/3}} \quad (5.40)$$

The result obtained is very similar to Equations (4.91) and (4.92). Taking Expressions (4.93) and (5.29) into account as well, the *Chilton-Colburn analogy* can be extended to

$$J_H = J_D = \frac{1}{2} f = C Re^{-m-1} \quad (5.41)$$

The extended analogy of Expression (5.41) only applies when the *friction factor* stands solely for *wall friction*, in accordance with the derivation *Form drag*, which can be a significant part of the flow resistance of objects around which flow is passing (§ 2.3), is *not* associated with analogous heat or mass transfer effects.

### Summary

This Section has looked at the link between flow rate through and frictional pressure drop in a pipeline. Pressure drop, energy dissipation, wall friction and shear stress have been discussed in terms of their mutual relationships. The Fanning pressure drop equation has been derived

$$p_1 - p_2 = 4f \frac{L}{D} \cdot \frac{1}{2} \rho \langle v \rangle^2$$

with a plot for  $4f$  as a function of Reynolds and with two expressions for the friction factor  $4f$  for a cylindrical pipe: one for the laminar regime ( $4f = 64/Re$ ) and the Blasius equation for the turbulent regime.

The terms *hydraulic diameter* and *relative wall roughness* have also been introduced for use with turbulent pipe flows. Various solving strategies have been discussed for calculating the flow rate through a pipe when the pressure drop is known; one of these strategies is iterative, exactly the same as when calculating a uniform particle velocity from a force balance.

Also, the Chilton-Colburn analogy has been extended to include the friction factor, providing the flow resistance is only determined by the wall friction.

## 5.4 Pressure drop in pipeline systems

In § 5.3, we discussed how dissipation and the related frictional pressure drop for a straight pipeline are modelled with the help of the Fanning pressure drop equation. Because dissipation stands for the destruction of mechanical energy, it is obvious that the Fanning equation should be linked to the mechanical energy balance as introduced in Chapter 1 for steady-state conditions.

For a fluid of constant density flowing through a straight pipeline, this follows from Equation (1.125)

$$0 = \phi_m \left( \frac{1}{2} v_1^2 + \frac{p_1}{\rho} + g z_1 - \frac{1}{2} v_2^2 - \frac{p_2}{\rho} - g z_2 \right) + \phi_w - \phi_m e_f \quad (5.42)$$

For a horizontal, straight pipeline of constant cross-sectional area and in the absence of a pump, combining Equations (5.25) and (5.42) expresses the quantity of energy that is dissipated per unit of mass

$$e_{fr} = 4f \frac{L}{D_h} \frac{1}{2} \langle v \rangle^2 \quad (5.43)$$

in which the use of the hydraulic diameter  $D_h$  – see Equation (5.26) – renders the equation also valid for non-cylindrical conduits. With regard to the Fanning equation, combining Equations (5.42) and (5.43) has the advantage that there is space for pressure changes other than those caused by wall friction. Equation (5.43) expresses explicitly what the effect of *dissipation* is on the mechanical energy housekeeping in a pipeline.

Consider two identical tubes with the same diameter, one of which is placed horizontally, and the other vertically. An identical flow rate passes through both. The friction dissipation in both pipes is a direct consequence of friction on the wall. This friction depends only on the shear stress on the wall, and that in turn is determined by the velocity profile just next to the wall. In the horizontal pipe there is a pressure drop that just compensates the frictional force. In the vertical pipe (in which the liquid is flowing from bottom to top), the pressure drop has to make up for both frictional force and gravity. However, the wall friction depends only on the velocity gradient on the wall and not on the orientation of the pipe. For this reason, the same expression for the dissipation can be used. Notice that the mechanical energy balance now states exactly that in the vertical pipe the pressure energy has to compensate the potential energy ('gravity') and the dissipation ('frictional energy losses').

Of course, there are many pipelines that are not straight and do not have a constant diameter. As a rule, a system of pipes consists of all kinds of bends, valves or flaps, and narrow or wide sections (these are generally referred to as *appendages*, or *fittings*). All these types of 'obstacle' or impediment to the flow give rise to extra dissipation. In many cases, extra eddies occur in which mechanical energy is dissipated. For *turbulent* flow, all these appendages (fittings) can be easily modelled using an expression for the energy dissipation per unit of mass that is entirely analogous to Equation (5.43).

$$e_L = K_L \frac{1}{2} \langle v \rangle^2 \quad (5.44)$$

The convention is that here for  $\langle v \rangle$  the average velocity of the flow downstream of the relevant appendage is used.  $K_L$  is the *loss coefficient* of the appendage (fitting) and is constant, that is, not dependent on  $Re$ , providing that the flow is sufficiently turbulent. The loss coefficients can be found in tables (see, for example, Janssen & Warmoeskerken<sup>21</sup>). A small number of loss coefficients are given below.

<sup>21</sup> Janssen, L P B M and M M C G Warmoeskerken, Transport Phenomena Data Companion, Delft VSSD, Delft, 2006, p. 82–83

fitting	$K_L$
gate valve, open	0.2
gate valve, 1/2 closed	≈ 6
gate valve, 3/4 closed	≈ 24
90° bend, sharp angle	1.3
90° bend, long	0.5
entrance loss pipe, sharp	0.5
entrance loss pipe, rounded	0.05
exit loss pipe	1

With a view to the use of the mechanical energy balance for pressure drop calculations for pipeline systems with fittings, it can be stated in summary that, providing that the flow is turbulent, the *specific energy dissipation*  $e_{diss}$  (in J/kg) is generally modelled as the sum of  $e_{fr}$  and  $e_L$ :

$$e_{diss} = \sum_i \left( 4f \frac{L}{D_h} \frac{1}{2} \langle v \rangle^2 \right)_i + \sum_j \left( K_L \frac{1}{2} \langle v \rangle^2 \right)_j \quad (5.45)$$

The first part of the right-hand term of this equation represents the sum of the friction losses in all straight pipe sections, while the second part covers the dissipation in all the appendages. Note that changes in the diameter in the system are correctly accounted for: for each fitting the downstream velocity  $\langle v \rangle$  has to be used.

#### Example 5.7. Pumping upwards

A watery liquid has to be pumped from a very large container (A) to another very large container (B), which is situated at a higher level. For this, a pump is added to the pipeline system illustrated in Figure 5.13. Both containers are open at the top. The pipeline is 50 m long and has a diameter of 5 cm. The walls of the pipeline are smooth. There are two sharp right-angled bends and an open gate valve in the pipeline. The entrance to the pipeline (at container A) is sharp. The height of the liquid in container A is 3 m, and in container B it is 13 m (measured from the ground).

Calculations are needed for the following:

- the power that the pump has to supply in order to pump 2 l/s of water,
- the value of the greatest pressure that is present in the system.

Both questions can be solved with the help of the mechanical energy balance. First of all, this balance is applied to the system between points 1 and 3 (see Figure 5.13). Point 1 is located on the surface of the water in container A, where the following applies:

$$P_1 = P_0, \text{ where } P_0 \text{ is the ambient pressure, } v_1 \approx 0, z_1 = \text{given}$$

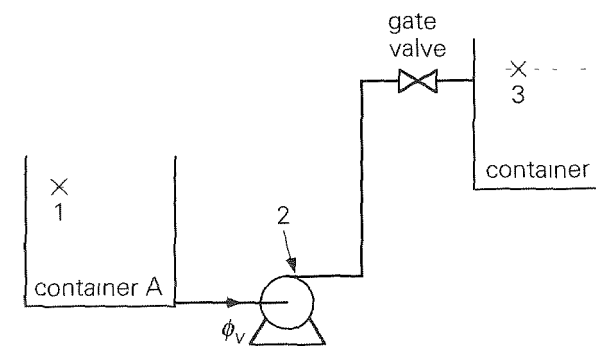


Figure 5.13

Point 3 is also chosen on the surface of the water in container B, so.

$$p_3 = p_0, v_3 \approx 0, z_3 = \text{given}$$

The loss coefficients  $K_L$  of the various fittings have to be looked up (with a view to the dissipation in the system)

two sharp right-angled bends	$\rightarrow 2 \times 1.3$
open valve	$\rightarrow 0.2$
sharp entrance	$\rightarrow 0.5$
exit	$\rightarrow 1$

The (average) velocity in the pipeline simply follows from the flow rate  $v = 1.0 \text{ m/s}$ . From this it follows that the Reynolds number for the flow is  $5 \cdot 10^4$ . The diameter of the pipeline is constant and so we can account for the total dissipation resulting from the wall friction and the fittings in one go – by using Equation (5.45). Looking up  $4f$  when  $\text{Re} = 5 \cdot 10^4$  produces  $4f = 0.02$ . All this gives

$$\begin{aligned} e_{\text{diss}} &= 4f \frac{L}{D} \frac{1}{2} v^2 + (2 \cdot 1.3 + 0.2 + 0.5 + 1) \frac{1}{2} v^2 \\ &= 12.15 \text{ J/kg} \end{aligned} \quad (5.46)$$

Further, we replace in Equation (5.42) the specific energy dissipation  $e_f$  by  $e_{\text{diss}}$ . For the pump capacity, it then follows that

$$\phi_w = \phi_m \{ g(z_3 - z_1) + e_{\text{diss}} \} = 220 \text{ W} \quad (5.47)$$

The highest pressure occurs just behind the pump, of course (!). This pressure can be calculated by drawing up a mechanical energy balance between points 1 and 2 (see Figure 5.13). The following applies to point 2

$$p_2 = ?, v = 1 \text{ m/s}, z_2 \approx 0$$

This means the mechanical energy balance between points 1 and 2 becomes

$$\frac{p_2 - p_1}{\rho} = g(z_1 - z_2) - \frac{1}{2} v^2 - e_{\text{diss}} + \frac{\phi_w}{\phi_m} \quad (5.48)$$

The dissipation per unit of mass  $e_{\text{diss}}$  now only relates to the inflow into the pipeline, i.e.  $e_{\text{diss}} = e_L = 0.5 \frac{1}{2} v^2$ , providing that the length of the pipe from container A to the pump is small enough to be ignored. With this,  $p_2 = 2.4 \text{ bar}$  is found  $\square$

### Example 5.8. A basin running empty

Processed water flows through a cylindrical conduit (length 20 m, diameter 10 cm, wall roughness 1 mm) from a large open basin, situated high up, into an open channel. The water level in the basin is 4 m above that in the channel. The pipeline contains 2 sharp  $60^\circ$  bends (with  $K_L = 1.86$ ) and a gate valve for controlling the water flow rate. The loss coefficients for the pipe entrance and exit are 0.2 and 1.0.

The question is to calculate the water flow rate when the gate valve is half closed. The solution to this problem is again found through a mechanical energy balance, between point 1 on the water surface in the basin and point 2 on the water surface in the channel (see Figure 5.14) – again two points on a water surface, because here statements can be made on quite some variables

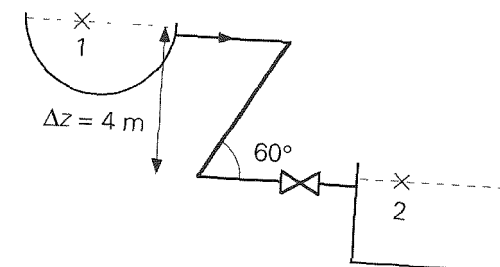


Figure 5.14

For point 1  $p_1 = p_0, v_1 \approx 0, z_1 = z_2 + \Delta z$ , and for point 2  $p_2 = p_0, v_2 \approx 0$ . Entering this into the mechanical energy balances produces

$$0 = -g \Delta z - e_{\text{diss}} \quad (5.49)$$

The total energy dissipation in the pipeline system at an (average) velocity  $v$  is given by

$$e_{\text{diss}} = \left( 4f \frac{L}{D} + K_{L,\text{tot}} \right) \frac{1}{2} v^2 \quad (5.50)$$

where  $K_{L,\text{tot}} = 2 \times 1.86 + 0.2 + 1.0 + 6 = 10.9$  takes care of the effects of all the fittings

Substituting Equation (5 50) in Equation (5 49) gives

$$v = \sqrt{\frac{2g \Delta z}{4f \frac{L}{D} + K_{L,\text{tot}}}} \quad (5 51)$$

From this, it is possible to obtain  $v$  with an iterative procedure, because  $4f$  is a function of  $v$  (which can be seen in Figure 5 10 with a relative roughness of 0.01). As an opening estimate, let  $v = 1$  m/s, say. This gives  $\text{Re} = 10^5$  and  $4f = 0.035$ . Using this value of  $4f$  in Equation (5 51) for calculating a better value for  $v$  gives  $v = 2.1$  m/s and from this it follows that  $\text{Re} = 2.1 \cdot 10^5$  and  $4f = 0.035$ . This means the iteration process need not be taken any further. The flow rate can now be easily calculated  $\phi_m = 16.5$  kg/s.  $\square$

Notice that in both examples, the flow in the pipeline is turbulent, so that the loss coefficients are indeed constant.

### Summary

The pressure drop in a pipeline system is not determined solely by friction. For that reason, it makes sense to use the mechanical energy balance, providing that expressions are available for the energy dissipation. For dissipation resulting from wall friction in a straight pipe, the following applies:

$$e_{fr} = 4f \cdot \frac{L}{D} \cdot \frac{1}{2} \langle v \rangle^2$$

If the Reynolds number of the flow is sufficiently large, the dissipation resulting from an appendage (or fitting) is modelled using a constant loss coefficient

$$e_L = K_L \cdot \frac{1}{2} \langle v \rangle^2$$

where the downstream velocity should be selected for  $\langle v \rangle$ . In general, the total dissipation  $e_{\text{diss}}$  is the sum of the wall friction  $e_{fr}$  in all straight pipe sections and of the energy dissipation  $e_L$  in all fittings.

## 5.5 Pressure drop across a packed bed

Pipeline systems are not the only systems in which pressure drop and dissipation are important. In fact, pressure drop and dissipation are important quantities in any flow system. In this Section, we will therefore look at another flow system, one that is found extensively in the process industry: the *packed bed*. This consists of a container filled with particles resting on each other. Liquid flows through the open

space located between the particles. The question now is how the dissipation and pressure drop in this system depends on the velocity at which the flow passes.

Before tackling this problem, it is useful first to look at how the dissipation is modelled if the flow does not go through the 'inside' of a pipeline, but actually alongside the 'outside' of a body. Consider the simplest case of a spherical particle that is motionless in a flowing medium with a uniform approach velocity of  $v$ . The force exerted by the flow on the particle is (see § 2.3)

$$F_D = C_D \cdot A_\perp \cdot \frac{1}{2} \rho v^2 \quad (5 52)$$

The dissipation around this particle can now be calculated analogously to the reasoning in § 5.4. There, the dissipation can be determined by using the mechanical energy balance. For a horizontal straight pipeline with a constant diameter, the following applies, based on Equation (5 42)

$$0 = \phi_m \frac{p_1 - p_2}{\rho} - \phi_m e_{\text{diss}} \quad (5 53)$$

However, this equation can be written differently by relating the difference in pressure  $p_1 - p_2$  to the shear stress on the wall via a force balance, see Equation (5 21). If the overall frictional force exerted by the wall on the liquid via the shear stresses is referred to as  $F_{fr}$ , this difference in pressure can be rewritten as

$$\phi_m \frac{p_1 - p_2}{\rho} = \rho A v \frac{p_1 - p_2}{\rho} = A (p_1 - p_2) v = F_{\text{diss}} v \quad (5 54)$$

Thus, for the dissipation around a single submerged free particle around which flow is passing, the following applies

$$\phi_m e_{\text{diss}} = F_D v \quad (5 55)$$

and from this it then follows

$$\phi_m e_{\text{diss}} = C_D A_\perp \frac{1}{2} \rho v^2 v = C_D A_\perp \frac{1}{2} \rho v^3 \quad (5 56)$$

In a uniform packed bed of more or less spherical, non-porous particles, the flow around the particles is of course not the same as with a free particle. However, it is to be expected that the frictional force on an individual particle in the bed can be modelled on the same lines as in the case of the free particle. The overall energy dissipation in a bed of  $N$  particles then follows by multiplying the dissipation resulting from the friction along one particle in the bed by the number of particles in column  $N$ .

For the flow around a particle in the bed, the local flow velocity has to be taken that is to say, the velocity  $\langle v \rangle$  in the channels between the particles as they rest against and on top of each other. However, this is not a very good velocity to include in the calculation, because although the overall volumetric flow rate that goes through the packed bed is known,  $\langle v \rangle$  is not. Nonetheless, this can be easily resolved.

The particles together occupy a volume,  $V_d$ , in the total volume,  $V_0$ , of the bed. Then, the volume fraction of the free space – known as the *bed porosity*  $\varepsilon$  – can be defined as  $\varepsilon = (1 - V_d/V_0)$ . The cross-sectional area of the empty container is  $A_0$  and so  $\varepsilon A_0$  is the cross-sectional area in the packed bed that is available for the flow. Further,  $v_0$  is the velocity that the liquid would have if it flowed through the empty container at the same flow rate – referred to as the *superficial velocity*.

The link between the volumetric flow rate and the flow velocity  $\langle v \rangle$  is therefore

$$\phi_v = A_0 v_0 = \varepsilon A_0 \langle v \rangle \rightarrow \langle v \rangle = \frac{v_0}{\varepsilon} \quad (5.57)$$

The volume occupied by the particles is  $(1 - \varepsilon) A_0 L$  (where  $L$  is the height of the bed), this means the number of particles (with diameter  $d$ ) in the bed is

$$N = \frac{(1 - \varepsilon) A_0 L}{\frac{\pi}{6} d^3} \quad (5.58)$$

Eventually, we arrive at the energy dissipation in the packed bed

$$\phi_m e_{\text{diss}} = \frac{(1 - \varepsilon) A_0 L}{\frac{\pi}{6} d^3} C_D \frac{\pi}{4} d^2 \frac{1}{2} \rho \left( \frac{v_0}{\varepsilon} \right)^3 \quad (5.59)$$

Finally, eliminating  $\phi_m = \rho A_0 v_0$  produces

$$e_{\text{diss}} = \frac{3}{2} C_D \frac{(1 - \varepsilon)}{\varepsilon^3} \frac{L}{d} \frac{1}{2} v_0^2 \quad (5.60)$$

We are now left with the matter of determining  $C_D$  for the flow around the particles in a packed bed. It is to be expected that  $C_D$  will be a function of the Reynolds number. However, this is not the only question. What does this function look like? And, which Reynolds number describes the flow through the bed? The typical velocity is  $\langle v \rangle$ , but the typical length is not simply the diameter of the particles.

A better dimension would appear to be the hydraulic diameter of the gaps between the particles. This can be estimated on the basis of the bed porosity  $\varepsilon$  and the size of the particles,  $d$ . This relates to  $4A/S$ , where  $A$  represents the cross-sectional area of the gap that is available for the flow, and  $S$  the wetted perimeter. The gaps are of course not neat straight channels, which is why it is better to use a *hydraulic*

*diameter* that is defined on the basis of the volume of a gap and the overall surface area of the gap

$$D_h = \frac{4 \times \text{volume of gap}}{\text{surface area of gap wall}} \quad (5.61)$$

Next, both the numerator and the denominator in this expression are related to the bed volume. For the numerator, this produces  $\varepsilon$ , while the denominator acquires the wall surface area of all the gaps per unit of volume, which is referred to as the specific surface area  $a$  ( $\text{m}^2/\text{m}^3$ ). This can be determined by multiplying the surface area  $\pi d^2$  of a single particle by the number of particles in the bed  $N$  and finally dividing it by the total bed volume.

With the help of Equation (5.58) for  $N$ , we get the following for the specific surface area

$$a = \frac{6(1-\varepsilon)A_0 L}{\pi d^3} \pi d^2 \frac{1}{A_0 L} = \frac{6(1-\varepsilon)}{d} \quad (5.62)$$

The Reynolds number is now

$$\text{Re}_h = \frac{\rho \langle v \rangle D_h}{\mu} = \frac{\rho \frac{v_0}{\varepsilon} \frac{4\varepsilon}{6(1-\varepsilon)/d}}{\mu} = \frac{2 \rho v_0 d}{3(1-\varepsilon)\mu} \quad (5.63)$$

The implicit result of this is that the Reynolds number for a packed bed includes the superficial velocity as a typical velocity and the diameter of the particles as the typical length scale, and that the porosity occurs here.

If  $\text{Re}_h$  is sufficiently large it is found that  $C_D$  becomes constant, analogous to the flow around a single sphere, however, the value is different, namely 2.3 (instead of 0.43). This result holds where  $\text{Re}_h > 2000$ . Where  $\text{Re}_h < 1$ , it is seen that  $C_D$  is inversely proportional to  $\text{Re}_h$ , entirely in accordance with a single sphere around which a flow is passing, however, here too the proportionality constant is different ( $C_D = 150/\text{Re}_h$  (for a single sphere the constant is 24)). The change to  $C_D$  for a packed bed as a function of  $\text{Re}_h$  is shown in Figure 5.15.

Ergun has drawn up an empirical equation for  $C_D$ , which gives a good description for the entire  $\text{Re}_h$  range in Figure 5.15. He simply added up the laminar and turbulent expressions

$$C_D = 2.3 + \frac{150}{\text{Re}_h} \quad (5.64)$$

Entering this *Ergun relation* into Equation (5.60) for the specific energy dissipation produces

$$\frac{p_1 - p_2}{\rho} = e_{diss} = \frac{1-\varepsilon}{\varepsilon^3} \left\{ 170 \frac{\mu}{\rho v_0 d} (1-\varepsilon) + 1.75 \right\} \frac{L}{d} v_0^2 \quad (5.65)$$

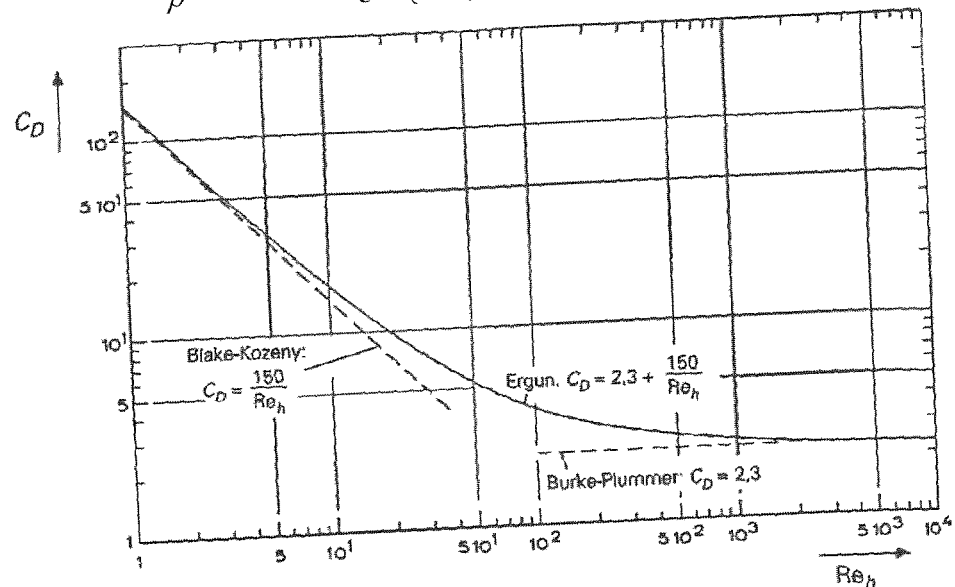


Figure 5.15

#### Example 5.9. Pressure drop over a packed bed

A flow of water with a flow rate of 0.3 l/s has to have  $\text{Ca}^{2+}$  ions removed from it. This takes place in a cylindrical packed bed made up of spherical ion-exchanging particles (diameter  $d = 2 \text{ mm}$ ). The porosity of the packed bed  $\varepsilon$  is 0.4. The length of the column is 2 m, and the diameter  $D$  of the column is 0.25 m. The water flows through the column from the bottom to the top. How large is the pressure drop over the column?

The answer follows from the mechanical energy balance for the whole packed bed. It is then clear that the pressure drop consists of two contributions: the pressure drop resulting from gravity (the hydrostatic pressure drop) and the pressure drop resulting from friction. This second contribution follows from determining  $e_{fr}$  according to Equation (5.65). For this,  $v_0$  first has to be determined from the flow rate

$$v_0 = \frac{\phi_V}{\frac{\pi}{4} D^2} = 6.1 \cdot 10^{-3} \text{ m/s} \quad (5.66)$$

This means the specific dissipation is

$$e_{diss} = \frac{1-\varepsilon}{\varepsilon^3} \left( 170 \frac{\mu}{\rho v_0 d} (1-\varepsilon) + 1.75 \right) \frac{L}{d} v_0^2 = 3.52 \text{ J/kg}$$

and the pressure drop is

$$\begin{aligned} \Delta p &= \rho g L + \rho e_{diss} \\ &= 1.96 \cdot 10^4 + 3.52 \cdot 10^3 = 2.31 \cdot 10^4 \text{ Pa} \approx 0.23 \text{ bar} \end{aligned} \quad (5.67)$$

#### Summary

In this Section, we have derived how pressure drop across and energy dissipation in a packed bed depend on the superficial velocity through the bed. To this end, the bed is regarded as a collection of particles that encounter forces from the liquid flowing around them. Terms like porosity, specific surface area and hydraulic diameter of the gaps between the particles have been introduced. The drag coefficient  $C_D$  of a particle in such a bed depends on a Reynolds number defined with the superficial velocity  $v_0$ , the diameter of the particles and the porosity. All of this leads to the Ergun relation

$$\Delta p = \frac{1-\varepsilon}{\varepsilon^3} \left( 170 \frac{\mu}{\rho v_0 d} (1-\varepsilon) + 1.75 \right) \frac{L}{d} \rho v_0^2$$

for the frictional pressure drop across a packed bed.

## 5.6 Laminar flow of Newtonian fluids

In Chapters 3 and 4, we discussed extensively how temperature and concentration profiles could be determined for molecular transport in a few simple geometries. The starting point was always an energy or mass balance for a thin slice of the material (for example, between  $x$  and  $x + dx$ ). The flows 'in' and 'out' were always modelled using Fourier's or Fick's law (or Stefan's law). A similar analysis is also possible for determining the velocity profile in a fluid flowing in the laminar regime.

The treatment of laminar flow will remain restricted to steady-state one-dimensional flows in geometrically simple situations. Finally, this Section will only look at fluids that comply with *Newton's viscosity law* (see Equation (2.4)).

### 5.6.1 Laminar flow in Cartesian coordinates – due to a moving wall

The first situation concerns a flat geometry: a liquid (a lubricating oil, for instance) between two very large horizontal plates, parallel to each other. The distance between the plates is  $D$ . The lower plate is motionless, and the upper one is moving

horizontally in the direction of  $x$  at a constant velocity,  $v_0$ . The velocity is low enough – actually the Reynolds number is low enough – for the liquid to be able to flow in ‘layers’ parallel to both plates. This means that the flow is *laminar* and that solely the individual molecules provide for the transport of  $x$  momentum in the direction of  $y$ . This steady-state situation is illustrated in Figure 5.16.

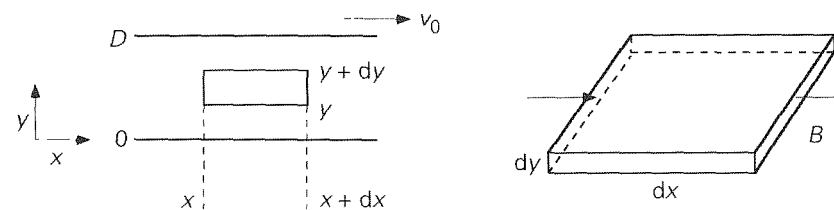


Figure 5.16

In order to determine the velocity profile, an  $x$  momentum balance for a thin slice with thickness  $dy$  (between  $y$  and  $y + dy$ ), with length  $dx$  (between  $x$  and  $x + dx$ ) and width  $B$  (perpendicular to the surface of the drawing) has to be drawn up.

However, in the case of these parallel plates and in the steady-state conditions stated, as much convective momentum flows into the control volume (the thin slice) through the left-hand plane (at  $x = x$ ) as convective momentum flows out through the right-hand plane (at  $x = x + dx$ ). Further, because the flow is laminar and one-dimensional, no convective momentum transport is crossing the other surfaces of the control volume. If in addition, in view of the discussion in § 2.1.4, the molecular (or diffusive) momentum transport is described in terms of shear stresses, then the momentum balance is reduced to a *force balance*. This force balance then contains information about the shear stress profile.

For the situation in Figure 5.16, it is only the force balance in the direction of  $x$  that is important. Only two forces are exerted on the control volume in the direction of  $x$  – a shear stress on the lower plane and a shear stress on the upper plane. The force on the lower plane is  $B dx \tau_{yx}|_y$ . This expression represents the force that the layer flowing just underneath the control volume exerts on the layer just above it in the control volume. Remember that the shear stress is defined precisely in this way so that the layer with the smallest coordinate exerts  $+\tau_{yx}$  on the layer with the greater coordinate (see § 2.1.4 again). This means that on the top side of the control volume, the force  $B dx [-\tau_{yx}|_{y+dy}]$  is exerted on the control volume by the fluid flowing over the control volume. The force balance is now therefore

$$0 = B dx \tau_{yx}|_y + B dx [-\tau_{yx}|_{y+dy}] \quad (5.68)$$

5 Fluid mechanics 287

This balance can be simply reduced to the differential equation that must be satisfied by the shear stress

$$\frac{d}{dy} \tau_{yx} = 0 \quad (5.69)$$

The solution to this equation is

$$\tau_{yx} = \text{constant}$$

It is useful to realise that so far no account has been taken of whether the liquid complies with Newton’s law

$$\tau_{yx} = -\mu \frac{dv_x}{dy} \quad (5.70)$$

The *shear stress profile* that has been established for this situation is clearly independent of the properties of the liquid. This finding has general validity (the shear stress profile is only dependent on the force balance (or rather the momentum balance) and not on the type of liquid).

With a view to determining the *velocity profile*, however, it is necessary to use a link between shear stress and velocity gradient. Suppose now that the liquid between the slices is Newtonian. This means that inserting Expression (5.70) into Equation (5.70) leads to

$$-\mu \frac{d}{dy} v_x = \text{const} \rightarrow \frac{d}{dy} v_x = C_1 \quad (5.72)$$

Solving Equation (5.72) gives

$$v_x(y) = C_1 y + C_2 \quad (5.73)$$

Both integration constants can be found with the help of the two given boundary conditions  $y = 0 \rightarrow v_x = 0$  and  $y = D \rightarrow v_x = v_0$ . This produces the velocity profile

$$v_x(y) = v_0 \frac{y}{D} \quad (5.74)$$

This finding is equivalent to Equation (3.5) for heat conduction through a slab and to Equation (4.11) for diffusion through a medium between two plates. Substituting Equation (5.74) in Newton’s viscosity law gives a constant value for the shear stress

$$\tau_{yx} = -\mu \frac{v_0}{D} \quad (5.75)$$

Just as the fluxes  $\phi_q''$  and  $\phi_m''$  are also constants according to Equations (3.6) and (4.12) respectively

Both the shear stress profile and the velocity profile have been drawn in Figure 5.17. It can clearly be seen here that the shear stress is negative every 'underlying' layer exerts a force in the negative  $x$  direction on the layer lying 'above' it, and so resists the flow resulting from the moving upper plate.

Finally, the above derivation clearly shows that in steady-state laminar flows there is no role for the fluid's density – the flow is dominated by viscosity. This applies to all flows in § 5.6 – and supports remarks made in Chapter 2 with respect to incorporating or leaving out density and viscosity in dimensional analyses of flows and convective heat and mass transfer.

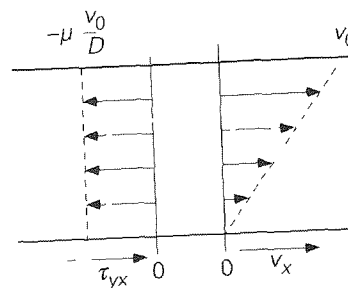


Figure 5.17

### 5.6.2 Laminar flow in Cartesian coordinates – due to a pressure gradient

The second situation again is a flat geometry and therefore Figure 5.16 still is a useful sketch, the difference however being that now the force driving the flow in the positive  $x$ -direction is not a moving plate or wall – as both plates do not move now – but an imposed pressure gradient  $[-\frac{dp}{dx}]$ . Here, the minus sign is introduced to

arrive at a positive driving 'force' in the positive  $x$ -direction, because as a matter of fact  $dp/dx$  is negative for a flow in the positive  $x$ -direction which is currently the case. Rather than  $[-dp/dx]$  also  $\Delta p/L$  could have been written, where  $\Delta p$  stands for the positive pressure difference over the distance  $L$  between two positions upstream and downstream that drives the flow. The unit of the pressure gradient is Pa/m, which can better be interpreted as Ns/m<sup>3</sup> to express that a pressure gradient is a means to supply momentum (in Ns) to a unit of volume per unit of time. Where we now consider a one-dimensional flow between parallel plates, the pressure gradient is constant in the  $x$ -direction and may be denoted by a constant, given  $\Gamma$  for convenience' sake.

Also in this situation the momentum balance reduces to a force balance, now with four forces acting in the  $x$ -direction on the slice of volume  $Bdxdy$ . Two of these

forces are the same as in the preceding case  $Bdx \tau_{yx}|_y$  and  $Bdx [-\tau_{yx}|_{y+dy}]$ , which act along the bottom and top surface of the slice, respectively, the other two forces are the result of the pressure field and act normal to the two ends of the slice:  $Bdy p|_x$  and  $Bdy [-p|_{x+dx}]$  where the minus sign in the latter force expresses that the force exerted from outside on the slice at position  $x + dx$  is in the negative direction. The force balance for the steady state says that the sum of the forces makes zero:

$$0 = Bdx \tau_{yx}|_y + Bdx [-\tau_{yx}|_{y+dy}] + Bdy p|_x + Bdy [-p|_{x+dx}] \quad (5.76)$$

Dividing all terms by  $Bdxdy$  and combining similar terms leads to the following differential equation

$$\frac{d\tau_{yx}}{dy} = -\frac{dp}{dx} = \Gamma \quad (5.77)$$

with the solution

$$\tau_{yx} = \Gamma y + C_1 \quad (5.78)$$

Again, the question whether the fluid is a Newtonian or a non-Newtonian liquid has not been considered so far. For any flow between two flat, stationary plates owing to a pressure gradient, the shear stress profile is therefore a linear function of the transverse coordinate  $y$  – irrespective of the properties of the fluid. Completely in agreement with the definition of the shear stress ('underlying' upon 'overhead' see again § 2.1.4), the lower stationary plate at  $y = 0$  slows the fluid down by exerting a force in the negative  $x$ -direction while the fluid flow exerts a force in the positive  $x$ -direction on the upper plate at  $y = D$ .

The integration constant,  $C_1$ , can be found with the help of the fact of life that in the case of two stationary plates the velocity halfway the two plates, in the plane of symmetry, is maximum. This implies that the derivative of the  $x$ -velocity versus  $y$  at that position is zero – and in its turn, at least for a Newtonian liquid, this results in the condition  $y = \frac{1}{2}D \rightarrow \tau_{yx} = 0$ . This turns Equation (5.78) into

$$\tau_{yx} = \Gamma \left( y - \frac{1}{2}D \right) = \Gamma D \left( \frac{y}{D} - \frac{1}{2} \right) \quad (5.79)$$

For a Newtonian liquid, Equation (5.79) leads to

$$v_x = -\frac{\Gamma}{\mu} \left( \frac{1}{2} y^2 - \frac{1}{2} D y \right) + C_2 \quad (580)$$

This second integration constant,  $C_2$ , can be determined with the help of a boundary condition for the velocity, due to the symmetry, at either  $y = 0$  or  $y = D$ , as  $v_x = 0$  at both positions. As a result:  $C_2 = 0$ . The eventual velocity profile is then given by

$$v_x = \frac{\Gamma}{2\mu} y (D-y) \quad (581)$$

This equation shows that for a viscous or laminar flow the velocity profile does not depend on the fluid's density – confirming the remark in Chapter 2 that density may and should be ignored when carrying out a dimensional analysis for (horizontal) viscous flows.

Rather than by determining  $C_1$  with the help of  $\tau_{yx} = 0$  at  $y = \frac{1}{2}D$ , the same result would have been obtained – still for a Newtonian liquid – by deriving an expression for the velocity profile by substituting Expression (571) into Equation (578), the result then contains both  $C_1$  and  $C_2$  which can be found by the two above boundary conditions for the velocity at  $y = 0$  and  $y = D$ . Using both boundary conditions implicitly implies that the plane  $y = \frac{1}{2}D$  is a symmetry plane for the velocity profile where the velocity is maximum and the shear stress equals zero.

Note that for the shear stress profile the plane  $y = \frac{1}{2}D$  is not a plane of symmetry! From the molecular interpretation of the shear stress  $\tau_{yx}$  as a flux of  $x$ -momentum in the  $y$ -direction (see § 2.1.4) we still can conclude that in this case  $\tau_{yx} = 0$  at  $y = \frac{1}{2}D$ . We again use here a symmetry argument seen from  $y = \frac{1}{2}D$  the flow looks the same whether we look upwards towards  $y = D$  or downwards towards  $y = 0$ . As a result, the transport of  $x$ -momentum in the  $y$ -direction at  $y = \frac{1}{2}D$  must be zero.

#### Example 5.10. Slot coating II<sup>22</sup>

We now return to the flow geometry discussed earlier in Example 2.7. Figure 5.18 again shows the cross-sectional view through the die of a specific coating machine. The very viscous Newtonian liquid is supplied via the vertical channel and is then entrained by the lower plate or belt (web) that moves to the right with velocity  $U$ . The result is that this plate or belt gets a coating of thickness  $\delta_\infty$  which is smaller than the gap height  $\delta$ .

Restricting the analysis to the  $x$ - $y$  plane suffices. Consider a steady-state situation in which the pressure  $P_1$  obviously is higher than the ambient pressure  $P_0$ , as a result of which the liquid also extends over a fixed, steady-state distance  $L_2$  in the ‘wrong’ direction. Velocities in the  $y$ -direction (among other things, in the area

<sup>22</sup> This problem has been derived from a problem in W H Deen, *Analysis of Transport Phenomena*, Oxford University Press, 2011

where the vertical flow is converted into flows in the  $x$ -direction) may be ignored. The situation may therefore be conceived as a steady-state laminar flow of a very viscous Newtonian liquid between two flat plates the lower one of which moves and the upper, stationary one consists of two parts

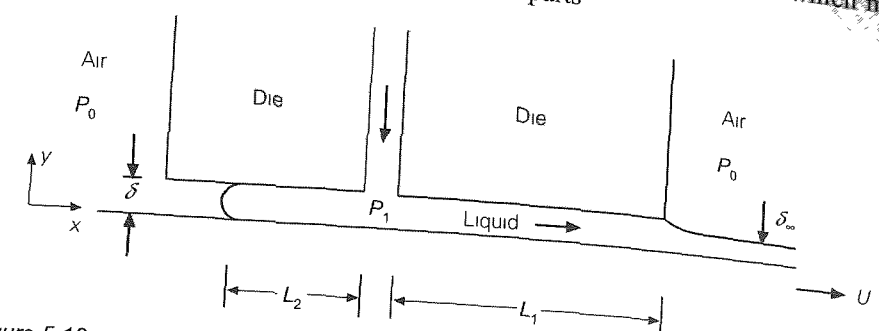


Figure 5.18

The following sub-questions should be answered

- Derive expressions for the shear stress profile and the velocity profile in domain  $L_1$  (sufficiently far from the vertical supply channel to allow for the presumption that the flow there is in the  $x$ -direction only). Make a sketch of the two profiles.
- Derive expressions for the shear stress profile and the velocity profile in domain  $L_2$  (sufficiently far from the vertical supply channel and from the convex end at  $x = L_2$  to allow again for the presumption that the flow is in the  $x$ -direction only). Make also a sketch of these two profiles.
- Derive an expression for the flow rate (per unit of depth) to the right and – in close connection – for the coating thickness  $\delta_\infty$  outside the die (sufficiently far from the tip of the die).
- Derive an expression for  $L_2$  with the help of the observation that the flow to the left is zero. Compare your answer with the outcome of Example 2.7.

Starting point for answering the above questions is in Equation (5.77). Substituting Newton's viscosity law, Equation (5.71), into Equation (5.77) results in

$$\mu \frac{d^2 v_x}{dy^2} = \frac{dP}{dx} = -\Gamma \quad (5.82)$$

with the solution

$$v_x = -\frac{\Gamma}{2\mu} y^2 + \frac{C_1}{\mu} y + C_2 \quad (5.83)$$

The boundary conditions for both domains  $L_1$  and  $L_2$  are

$$y=0 \quad v_x = U \quad (584)$$

$$y=\delta \quad v_x = 0$$

and result - together with Equation (583) - in the following expressions for shear stress and velocity profiles

$$\tau_{yx} = -\frac{\mu U}{\delta} + \Gamma \left( y - \frac{1}{2} \delta \right) \quad (585)$$

$$v_x = U \left( 1 - \frac{y}{\delta} \right) + \frac{\Gamma}{2\mu} y(\delta-y) \quad (586)$$

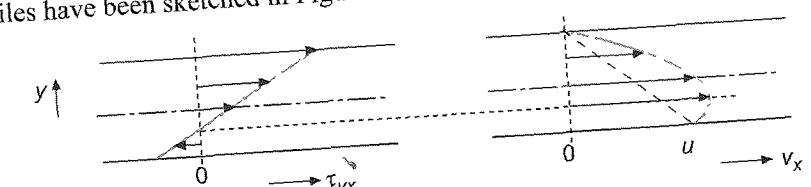
The difference between the two domains  $L_1$  and  $L_2$  is that in domain  $L_1$

$$\Gamma = -\frac{dp}{dx} = \frac{P_1 - P_0}{L_1} > 0 \quad (587)$$

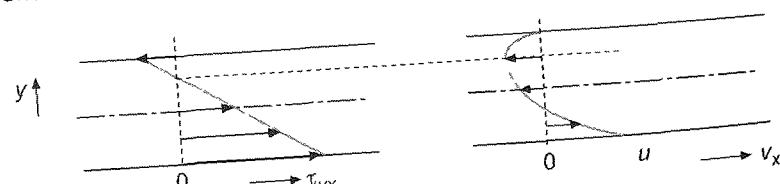
while in domain  $L_2$

$$\Gamma = -\frac{dp}{dx} = \frac{P_0 - P_1}{L_2} < 0 \quad (588)$$

This implies that in domain  $L_1$  the velocity profile is made up of two contributions both acting in the same positive  $x$ -direction: a drag term due to the moving wall plus a second term due to the pressure difference  $P_1 - P_0$ , while in domain  $L_2$  the pressure term is negative and counteracts the drag term. The respective velocity profiles have been sketched in Figure 5.19



a Shear stress profile and velocity profile in domain  $L_1$



b Shear stress profile and velocity profile in domain  $L_2$

Figure 5.19

The flow rate (per unit of depth) in domain  $L_1$  to the right, asked in sub-question c, is found by integrating the velocity profile

$$\begin{aligned} \phi'_v &= \int_0^\delta v_x(y) dy = \int_0^\delta \left[ U \left( 1 - \frac{y}{\delta} \right) + \frac{\Gamma}{2\mu} y(\delta-y) \right] dy = \\ &= \frac{1}{2} U \delta + \frac{P_1 - P_0}{12\mu L_1} \delta^3 \end{aligned} \quad (589)$$

Outside the gap, all liquid is moving at speed  $U$  as the boundary condition of zero velocity at the upper surface of the liquid layer does no longer apply there - resulting in a new expression for the flow rate per unit of depth

$$\phi'_v = U \delta_\infty \quad (590)$$

Owing to an overall mass balance, these two flow rates are equal, resulting in an expression for the eventual coating thickness  $\delta_\infty$

$$\frac{\delta_\infty}{\delta} = \frac{1}{2} + \frac{1}{12} \Gamma^* \quad (591)$$

in which the non-dimensional pressure gradient  $\Gamma^*$  denotes the ratio of pressure force to drag force

$$\Gamma^* = \frac{(P_1 - P_0) \delta^2}{\mu U L_1} \quad (592)$$

The distance  $L_2$  - the topic of sub-question d - can be found from the observation that in the steady-state considered there is no net flow to the right or to the left in domain  $L_2$ : the lower layers of the liquid are dragged to the right by the moving web, while the upper layers are pushed to the left by the pertinent pressure difference. These two effects just balance and determine the steady-state length  $L_2$ . By imposing the condition

$$\phi'_v = \int_0^\delta v_x(y) dy = 0 \quad (593)$$

and by substituting the Equations (586) and (588) into Equation (593), an expression for  $L_2$  is obtained

$$L_2 = \frac{(P_1 - P_0) \delta^2}{6\mu U} \quad (5.94)$$

which shows that e.g.,  $L_2$  decreases when  $U$  is increased. This result is in perfect agreement with the result of the dimensional analysis of Example 2.7

□

### 5.6.3 Laminar flow in Cartesian coordinates – due to gravity

In this example, it concerns a laminar flow of a Newtonian liquid between two very large vertical plates. The distance between the two plates (of width  $B$ ) is referred to now as  $2D$  (for reasons that will later become apparent). The flow here occurs only under the influence of gravity (there is no difference in pressure driving the flow). This steady-state situation is shown in Figure 5.20. Different to the earlier situations, the flow is now in the (negative)  $y$ -direction!

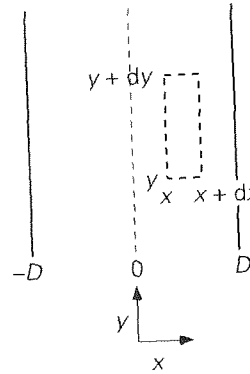


Figure 5.20

Here, too, the shear stress profile is determined first. And again, the  $y$  momentum balance for the control volume  $Bdxdy$  reduces to the force balance  $\sum F_y = 0$

$$0 = Bdx \tau_{xy} \Big|_y + Bdx \left[ -\tau_{xy} \Big|_{x+dx} \right] - Bdx dy \rho g \quad (5.95)$$

in which – in comparison with Equation (5.76) – the role of the two pressure terms is taken over by gravity. Gravity acts on the mass of the slice.  $F = Mg$  (in  $\text{kg m/s}^2$  or in  $\text{kg N/kg}$ ) and again supplies momentum (in  $\text{Ns}$ ) per unit of time and mass. From Equation (5.95) the following differential equation for the shear stress is obtained.

$$\frac{d\tau_{xy}}{dx} = -\rho g \quad (5.96)$$

with the solution being

$$\tau_{xy}(x) = -\rho g x + C_1 \quad (5.97)$$

The velocity profile then follows by using the fact that the liquid is Newtonian:

$$\tau_{xy} = -\mu \frac{d}{dx} v_y \rightarrow \frac{d}{dx} v_y = \frac{\rho g}{\mu} x - \frac{C_1}{\mu} \quad (5.98)$$

and by integrating Equation (5.98)

$$v_y = \frac{\rho g}{\mu} \frac{1}{2} x^2 - \frac{C_1}{\mu} x + C_2 \quad (5.99)$$

The two integration constants can be determined with the help of the two obvious boundary conditions for the velocity, that is  $x = \pm D \rightarrow v_y = 0$ . This gives  $C_1 = 0$  and  $2C_2 = -\rho g D^2 / \mu$ , and therefore

$$v_y(x) = -\frac{\rho g}{2\mu} (D^2 - x^2) \quad (5.100)$$

The velocity profile therefore has the form of a parabola. The liquid flows down of course – note the minus sign! The maximum velocity is found at  $x = 0$ . Figure 5.21 shows the shear stress and velocity profiles.

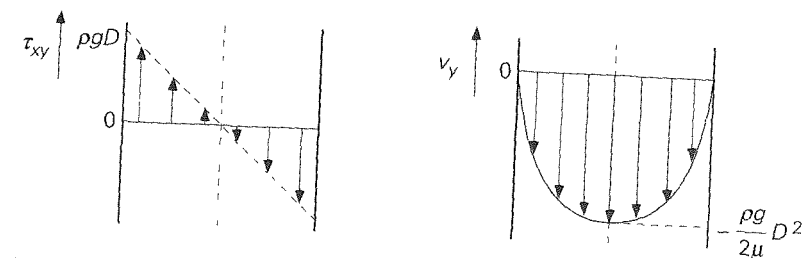


Figure 5.21

The integration constant  $C_1$  can be more directly determined in this case by using at an earlier stage the symmetry that is present in the problem. This symmetry is hidden above, in the two velocity-related boundary conditions: both plates are motionless walls with the same effect on the flow (just like in § 5.6.2). This symmetry also means that transport of  $y$  momentum through plane  $x = 0$  is not possible at all, because then the two ‘halves’ of the flow would be or become different. This means that both ‘halves’ exert no force (shear stress) on each other  $x = 0 \rightarrow \tau_{xy} = 0$ . It is precisely for this reason that in such a symmetrical situation the  $x = 0$  axis is selected halfway between the two plates.

Also, it is precisely because of the link between shear stress and velocity gradient that the velocity at  $x = 0$  is also at its maximum. The symmetry condition therefore makes it possible to directly conclude here too that with Equation (5.97),  $C_1 = 0$ , so that without having to go the roundabout route via the velocity profile it follows directly that

$$\tau_{xy}(x) = -\rho g x \quad (5.101)$$

#### Example 5.11. Film condensation II

With the help of the above theory, it is possible to further elaborate Equation (3.193) from Example 3.16 concerning film condensation. To do this, it is necessary to find out how  $\phi_v$  changes in the flow direction  $x$  (now selected as

downwards) This flow rate depends on both the thickness of the layer and the velocity profile in the layer. The dependence can be found by determining the velocity profile for a certain thickness  $\delta$  and the resulting liquid flow rate associated with that  $\delta$ .

In the situation in Figure 3.32, then, consider a thin slice of thickness  $dy$  at some distance from the wall (this is actually half of the aforementioned case of flow between two thin vertical slices). From a force balance for this slice it follows that, analogous to Equation (5.97), but thanks to the other choice of coordinate

$$\tau_{yx} = -\rho g y + C_1 \quad (5.102)$$

With boundary condition  $y = \delta \rightarrow \tau_{yx} = 0$  (because the maximum velocity is at the surface of the film and virtually no momentum is transferred to, or shear stress exerted on, the air compare a similar assumption concerning the interface of liquid and air in Example 3.10) it follows that

$$\tau_{vx} = \rho g (\delta - y) \quad (5.103)$$

For a Newtonian liquid, substituting Newton's law, integration and the use of the boundary condition  $y = 0 \rightarrow v = 0$  leads to

$$v = \frac{\rho g}{\mu} \left( \frac{1}{2} y^2 - y \delta \right) \quad (5.104)$$

Integrating this velocity profile for thickness  $\delta$  in the following expression for the flow rate across width  $b$ :

$$\phi_v = \frac{\rho g \delta^3 b}{3 \mu} \quad (5.105)$$

Differentiating versus  $\delta$  and substituting the result in Equation (3.193) gives

$$\Delta h_v \rho^2 g \delta^3 d\delta = \mu \lambda (T_w - T_w) dx \quad (5.106)$$

Integration between the limits  $x = 0 \rightarrow \delta = 0$  and  $x = L \rightarrow \delta = \delta_L$  leads to

$$\delta_L = \left( \frac{4 \mu \lambda (T_w - T_w) L}{\rho^2 g \Delta h_v} \right)^{1/4} \quad (5.107)$$

An expression for the heat transfer coefficient  $\langle h \rangle$  averaged over the height  $L$  follows from a heat balance for the whole film between  $x = 0$  and  $x = L$

$$\langle h \rangle (T_w - T_w) bL = \phi_v|_{x=L} \rho \Delta h_v \quad (5.108)$$

Combining Equations (5.105), (5.107) and (5.108) produces Equation (3.194).

### 5.6.4 Laminar flow in cylindrical coordinates – due to a pressure gradient

Finally, we will discuss an example of a flow involving a cylindrical geometry: steady-state laminar flow of a Newtonian liquid through a very long horizontal straight cylinder under the influence of a pressure gradient. A force balance can be drawn up for a cylindrical case within the liquid of thickness  $dr$  (between  $r$  and  $r + dr$ ) and length  $dx$  (see Figure 5.22).

A force  $p|_x 2\pi r dr$  is being exerted in the positive  $x$  direction on the left-hand end of the cylindrical case (at  $x=x$ ). Similarly, a force in the negative  $x$  direction, that is,  $-p|_{x+dx} 2\pi r dr$ , works on the right-hand end from outside (at  $x = x+dx$ ). Shear stress  $\tau_{rx}|_r$  is being exerted on the inside of the cylindrical case on surface  $2\pi r dx$ , while the stress  $-\tau_{rx}|_{r+dr}$  works on the outside on surface  $2\pi(r+dr)dx$ . This produces the following force balance

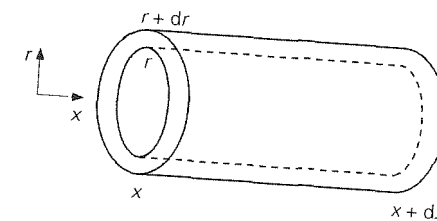


Figure 5.22

$$0 = p|_x 2\pi r dr + (-p|_{x+dx} 2\pi r dr) + \tau_{rx}|_r 2\pi r dx + [\tau_{rx}|_{r+dr} 2\pi(r+dr)dx] \quad (5.109)$$

This equation can also be written as

$$0 = p|_x 2\pi r dr - p|_{x+dx} 2\pi r dr + 2\pi(r\tau_{rx})|_r dx - 2\pi(r\tau_{rx})|_{r+dr} dx \quad (5.110)$$

where in the third and fourth term of the right-hand side the product of radius and shear stress is given in brackets because the perimeter (or surface area) and shear stress both depend on  $r$  (see also e.g. § 3.1.3). Equation (5.110) can be easily re-written (divide all terms by  $2\pi r dr dx$ ) to the differential equation for the shear stress

$$\frac{1}{r} \frac{d}{dr}(r\tau_{rx}) = -\frac{dp}{dx} = \Gamma \quad (5.111)$$

Now the pressure gradient is a given and constant, so – with for  $[-dp/dx]$  again the notation  $\Gamma$  (see § 5.6.2) – the equation can be solved fairly easily

$$\begin{aligned} \frac{d}{dr}(r\tau_{rx}) &= \Gamma r \rightarrow r\tau_{rx} = \frac{1}{2}\Gamma r^2 + C_1 \\ \rightarrow \tau_{rx} &= \frac{1}{2}\Gamma r + \frac{C_1}{r} \end{aligned} \quad (5.112)$$

Again, on the basis of symmetry considerations, it is the case that the shear stress on the axis of the cylinder must equal zero  $r = 0 \rightarrow \tau_{rx} = 0$ . This means that the integration constant  $C_1$  is zero. The shear stress profile is then

$$\tau_{rx}(r) = \frac{1}{2}\Gamma r \quad (5.113)$$

Remember that  $\Gamma > 0$ , there is always a pressure drop involved, because the friction on the wall and internally between the layers of liquid has to be overcome. Equation (5.113) shows that, in accordance with the definition of shear stress,  $\tau_{rx} \geq 0$ .

The velocity profile now follows by including the fact that the liquid is Newtonian, as a result

$$\frac{d}{dr}v_x = -\frac{\Gamma}{2\mu} r \quad (5.114)$$

The solution to this is

$$v_x = -\frac{\Gamma}{4\mu} r^2 + C_2 \quad (5.115)$$

Integration constant  $C_2$  can be determined using the boundary condition  $r = R \rightarrow v_x = 0$ . This gives

$$v_x(r) = \frac{\Gamma}{4\mu} (R^2 - r^2) = \frac{R^2 \Gamma}{4\mu} \left(1 - \frac{r^2}{R^2}\right) \quad (5.116)$$

Again, this is a parabola with the maximum velocity on the axis of the cylinder ( $r = 0$ ). The shear stress profile – Equation (5.113) – and the velocity profile – Equation (5.116) – are shown in Figure 5.23. Note that the centre-line  $r = 0$  is an axis of symmetry!

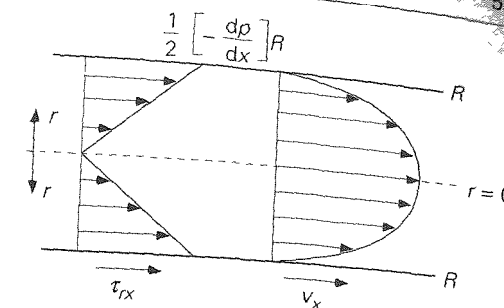


Figure 5.23

The mean liquid velocity is

$$\langle v \rangle = \frac{\int_0^R v_x(r) 2\pi r dr}{\int_0^R 2\pi r dr} = \frac{R^2 \Gamma}{8\mu} = \frac{R^2}{8\mu} \left(-\frac{dp}{dx}\right) \quad (5.117)$$

This is precisely half the maximum velocity in the cylindrical tube  $v_{max} = 2 \langle v \rangle$ . Equation (5.117) can also be written in another form, namely as an equation between the pressure drop  $\Delta p$  over a tube length  $L$  and the mean velocity

$$\Delta p = \frac{8\mu L}{R^2} \langle v \rangle = \frac{32\mu L}{D^2} \langle v \rangle = \frac{64\mu}{\rho \langle v \rangle D} \frac{L}{D} \frac{1}{2} \rho \langle v \rangle^2 \quad (5.118)$$

The latter term of this equation is deliberately written in a form that was also used for modelling energy dissipation ( $e_f$ ). This is easy to understand

$$\frac{\Delta p}{\rho} = e_f = \frac{64\mu}{\rho \langle v \rangle D} \frac{L}{D} \frac{1}{2} \langle v \rangle^2 \quad (5.119)$$

This therefore proves that in the case of laminar flow through a horizontal cylindrical tube, the Fanning friction factor  $4f$  is equal to  $64/\text{Re}$  indeed see Expression (5.28).

Finally, the flow rate that flows under influence of a pressure drop  $\Delta p$  through a pipeline with a circular cross-section and of length  $L$  follows from Equation (5.116) through integration

$$\phi_v = \int_0^R v_x(r) 2\pi r dr = \frac{\pi R^4}{8\mu} \frac{\Delta p}{L} \quad (5.120)$$

This equation is called the Hagen-Poiseuille law, the associated laminar flow is referred to as just Poiseuille flow.

The calculation of the velocity profile in tubes with a non-circular cross-section is a good deal more complicated. For a tube with a square-shaped cross-section with edge  $a$ , an equation applies that is very similar to Equation (5.120), but with a factor  $a^4/28.6$  instead of  $\pi R^4/8$ . Notice that the flow rate always remains proportional to the typical dimension to the power of four.

### Summary

For steady-state laminar flow, the velocity profile (= the radial momentum-concentration distribution) is easy to calculate if the geometry is sufficiently simple. This is analogous to the situation regarding molecular transport of heat or mass. To do this, it is necessary to draw up a momentum balance which, for simple geometries, is reduced to a force balance. The shear stress profile can be determined using this force balance.

This profile is *independent* of the type of liquid. It is only when determining the velocity profile that the link between shear stress and velocity gradient is important: does the fluid obey Newton's law or not? In many cases, the integration constants that appear during the integration process of force balance into velocity profile can be determined most safely from the boundary conditions related to the velocity.

For the steady-state laminar flow of a Newtonian liquid through a cylindrical tube, it has been derived that the shear stress is zero at the axis and increases in a radial direction, that the velocity profile is parabolic, and that the Hagen-Poiseuille law applies to the flow rate:

$$\phi_v = \frac{\pi R^4}{8\mu} \frac{\Delta p}{L}$$

but shear stress and velocity profiles have also been derived for other geometries.

## 5.7 Laminar flow of non-Newtonian liquids

In the previous Section, we looked only at fluids that obeyed Newton's viscosity law – see Equation (2.4) in § 2.1.2 – the standards of example of which are air and water. However, there are very many liquids that comply only slightly with the law, or indeed not at all. Some examples of liquids that display *non-Newtonian behaviour* are

- polymers
- toothpaste
- rubbers
- blood
- paint
- peanut butter
- wet cement
- margarine

Non-Newtonian behaviour is more the rule than the exception. This is because Newton's law applies only to spherical molecules which, apart from collisions, can move among each other relatively unimpeded. The molecules of most substances are not spherical, but instead consist of either longer or branched chains of atoms or groups of atoms, moreover, the molecules influence each other in terms of their movements, often through charge distributions within the molecules (polar groups). To pretend that the molecules behave like marbles is a long way removed from the truth.

Under the influence of shear forces that are imposed upon them, the molecules may rearrange themselves and/or intermolecular bonds between polar groups or branches may be broken to a greater or lesser degree. Only then perhaps does Newton's viscosity law apply.

Non-Newtonian liquids can be divided into different categories, each of which has their own rule for the link between the shear stress and the velocity gradient. The term for this link is the *rheology* of the liquid. We will discuss a number of commonly occurring categories in this Section.

### 5.7.1 Power Law liquids

A large number of liquids obey the *Ostwald - De Waele model* for the link between shear stress and velocity gradient

$$\tau_{xy} = -K \left| \frac{dV_y}{dx} \right|^{n-1} \frac{dV_y}{dx} \quad (5.121)$$

Equation (5.121) is also known as the *Power Law*, any liquid that obeys this law is referred to as a power law liquid. The constant  $K$  is called the *consistency* and  $n$  the *flow index*. Index  $n$  is non-dimensional, while  $K$  does of course have a dimension, which is dependent on the value of  $n$ . The vertical bars in this Power Law denote that the absolute value (or modulus) of the derivative between the bars should be taken here.

Note that Newtonian liquids form a special case of a power law liquid, namely when  $n=1$ . There is another distinction in this category of non-Newtonian liquids: power law liquids with an index  $n < 1$  are called *pseudoplastic*. An example of this is a 4 weight percent pulp in water for which  $n = 0.575$  and  $K = 20.0 \text{ Ns}^{0.575} \text{ m}^{-2}$  are found. If  $n > 1$ , we refer to a *dilatant* liquid, an example of which is wet cement.

Often, an *apparent viscosity* coefficient or *effective viscosity* coefficient  $\mu_e$  is used which is defined as

$$\mu_e = K \left| \frac{dV_y}{dx} \right|^{n-1} = K \gamma^{n-1} \quad (5.122)$$

This *apparent viscosity* coefficient  $\mu_e$  depends not only on the physical property  $K$ , but also on the (local) velocity gradient or *shear rate*  $\gamma$ , and expresses that  $\gamma$  leads to rearrangement of supramolecular structures and/or to (partial) breaking of bonds between polar groups or branches of the (polymer) molecules and in this way affects the flow properties of the liquid. Notice that it is only the magnitude (denoted by the modulus bars), not the sign of the velocity gradient that influences the intermolecular interaction. With this definition of an apparent viscosity, Expression (5.121) is converted into an equation which again resembles Newton's viscosity law but now with a flow dependent viscosity coefficient.

The solution to laminar, steady-state flow problems runs entirely analogously to that of Newtonian liquids, but  $\mu_e$  can have a different value anywhere in the flow domain, depending on the magnitude of the local velocity gradient. This effect should be factored in. This will be demonstrated by means of an example.

#### Example 5.12. A power law liquid between two vertical plates

Consider the laminar steady-state flow of a power law liquid between two very large vertical plates (see Figure 5.24). The flow is solely influenced by gravity, no pressure difference is imposed. The question is to derive an expression for the velocity profile.

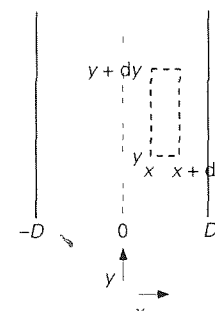


Figure 5.24

From the force balance  $\sum F_y = 0$  comes

$$0 = B dx \tau_{xy} \Big|_x + B dx \left( -\tau_{xy} \Big|_{x+dx} \right) - B dx dy \rho g \quad (5.123)$$

Of course, this equation again produces the shear stress profile of Equation (5.101)

$$\tau_{xy}(x) = -\rho g x \quad (5.124)$$

where, as before, use has been made of the symmetry plane at  $x = 0$  midway between the plates. Remember that the rheology of the liquid has no influence on the shear stress at all. In order now to determine the velocity profile, the fact that the liquid in question is a power law liquid should be taken into account:

$$\tau_{xy} = -K \left| \frac{dV_y}{dx} \right|^{n-1} \frac{dV_y}{dx} \quad (5.125)$$

First, the two vertical bars in Equation (5.125) need to be disposed of, for which we need the velocity gradient sign. Consider the domain  $0 \leq x \leq D$  and remember that – because of the symmetry in this problem – the velocity profile in the domain  $-D \leq x \leq 0$  can be obtained later through reflection of the ( $x = 0$ ) line. In the domain  $0 \leq x \leq D$ , velocity  $V_y$  becomes less negative as  $x$  increases, in other words, the derivative  $dV_y/dx > 0$ . On that case, the modulus lines can be dropped.

[In the other case – that is with  $dV_y/dx < 0$  –  $\left| \frac{dV_y}{dx} \right|$  should be replaced by  $\left( -\frac{dV_y}{dx} \right)$  to the effect that  $\left| \frac{dV_y}{dx} \right|^{\frac{1}{n}}$  becomes  $\left( -\frac{dV_y}{dx} \right)^{\frac{1}{n}}$ ]

Combining Equations (5.124) and (5.125) then produces for the domain  $0 \leq x \leq D$

$$-K \left( \frac{dV_y}{dx} \right)^n = -\rho g x \rightarrow \frac{dV_y}{dx} = \left( \frac{\rho g}{K} \right)^{\frac{1}{n}} x^{\frac{1}{n}} \quad (5.126)$$

Integration gives

$$V_y(x) = \left( \frac{\rho g}{K} \right)^{\frac{1}{n}} \frac{n}{n+1} x^{\frac{n+1}{n}} + C_2 \quad (5.127)$$

The integration constant,  $C_2$ , can be determined with the help of the boundary condition  $x = D \rightarrow V_y = 0$ . This means the velocity profile in the domain  $0 \leq x \leq D$  ultimately becomes

$$V_y(x) = -\frac{n}{n+1} \left( \frac{\rho g}{K} \right)^{\frac{1}{n}} \left( D^{\frac{n+1}{n}} - x^{\frac{n+1}{n}} \right) \quad (5.128)$$

Notice that for  $n = 1$ , the solution for Newtonian liquids, like the one determined in § 5.6.3, appears again. Figure 5.25 shows the velocity profiles for two cases  $n = \frac{1}{3}$  and  $n = 3$ .

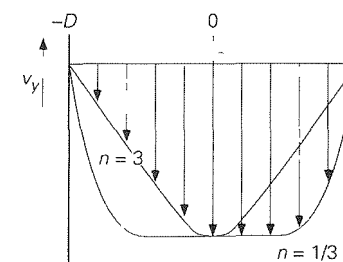


Figure 5.25

There are two other interesting limit cases.

- i)  $n \rightarrow \infty$   $v_y = -\left(\frac{\rho g}{K}\right)^{1/n} (D-x) \rightarrow -(D-x)$  see Figure 5.26
- ii)  $n \rightarrow 0$  the profile  $v_y$  approaches that of ideal plug flow, the latter assertion has been made visible in Figure 5.27 by drawing cases  $n = 1/10, 1/100, 1/1000$

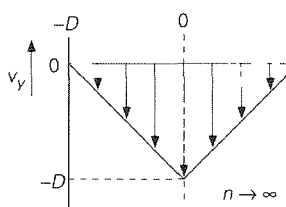


Figure 5.26

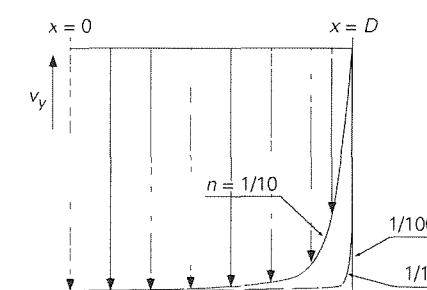


Figure 5.27

### 5.7.2 Bingham liquids

There are also materials which only start to flow once the shear stress exerted on them exceeds a certain value. Examples of these are clay and toothpaste. The behaviour of toothpaste in particular is well known if the tube (with the cap removed) is held upside down, nothing happens. It is only by squeezing (which actually means increasing the pressure in the tube) that the liquid flows out. Liquids that demonstrate this kind of behaviour are known as *Bingham liquids*. The link between the shear stress and the velocity gradient in the case of a Bingham liquid is:

□

$$|\tau_{xy}| - \tau_0 = \mu \left| \frac{dv_y}{dx} \right| \quad \text{for } |\tau_{xy}| \geq \tau_0$$

$$\frac{dv_y}{dx} = 0 \quad \text{for } |\tau_{xy}| < \tau_0 \quad (5.129)$$

The quantity  $\tau_0$  is called the *yield stress* and is a physical property of the compound involved. It is only when the tension being exerted exceeds a critical value – this yield stress – that a liquid may develop and exhibit velocity gradients because the intermolecular network then gives way. We will illustrate the use of a yield stress of this kind with an example.

**Example 5.13.** A Bingham liquid between two vertical plates

Consider again the situation in which a liquid is flowing downwards between two vertical and motionless plates under the influence of gravity. The Bingham liquid in this example has a yield stress that is numerically equal to  $\rho g D/2$  (Note: increasing or decreasing the distance  $D$  between the plates does not change the yield stress, here, it concerns just the value of the stress yield of the liquid considered.)

Now, the question is about the velocity profile

It follows still from a force balance for a typical volume element that

$$\tau_{xy} = -\rho g x \quad (5.130)$$

– cf Equations (5.101) and (5.124). In order to solve the velocity profile, the rheology of the liquid has to be specified. Because of the symmetry, only the domain  $0 \leq x \leq D$  has to be analysed. Here, the following applies

$$|\tau_{xy}| = \rho g x \quad (5.131)$$

It is then necessary – due to Equation (5.129) – to make a distinction between the domains where  $|\tau_{xy}| \geq \tau_0$  and where  $|\tau_{xy}| < \tau_0$ . Consider first the domain where  $|\tau_{xy}| \geq \tau_0$ . Here,

$$|\tau_{xy}| \geq \tau_0 \rightarrow \rho g x \geq \frac{1}{2} \rho g D \rightarrow x \geq \frac{1}{2} D \quad (5.132)$$

Because of  $dv_y/dx \geq 0$  for  $x \geq 0$ , it follows from Equations (5.129) – (5.132)

$$\rho g x - \tau_0 = \mu \frac{dv_y}{dx} \quad (5.133)$$

From this, it follows for the velocity gradient

$$\frac{dv_y}{dx} = \frac{\rho g}{\mu} x - \frac{\tau_0}{\mu} = \frac{\rho g}{\mu} \left( x - \frac{1}{2} D \right) \quad (5.134)$$

where the given expression for  $\tau_0$  has also been entered. The solution to this differential equation, thanks to the boundary condition  $x = D \rightarrow v_y = 0$ , is

$$v_y(x) = \frac{\rho g}{2\mu} (x^2 - Dx) \quad (5.135)$$

Then, the profile for the range  $0 \leq x < D/2$  has to be worked out. Here, given Expressions (5.129), the following applies  $|\tau_{xy}| < \tau_0$ , and therefore

$$\frac{dv_y}{dx} = 0 \rightarrow v_y = \text{constant} = v_y(\frac{1}{2}D) = -\frac{\rho g}{8\mu} D^2 \quad (5.136)$$

In this latter equation, a boundary condition has been used whereby the value of the velocity must be taken as  $x = D/2$ , as follows from the first part of the solution.

In Figure 5.28, the velocity profile of the Bingham liquid is shown after it has been reflected in relation to the symmetry axis. In the range  $-D/2 < x < D/2$ , it is not the case that  $v_y = 0$ , but  $v_y = \text{constant} \neq 0$ ! In this range, genuine plug flow occurs.

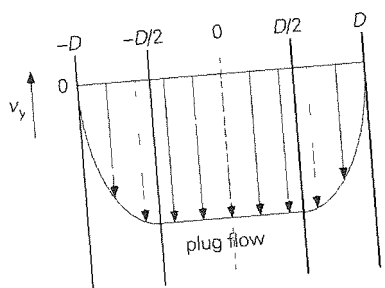


Figure 5.28

What would the solution to the velocity profile have been if the yield stress value had been greater than  $\rho g D$ ?

In that case,  $|\tau_{xy}| < \tau_0$  would have applied through-out the liquid and therefore everywhere the velocity  $v_y = \text{constant}$ . Applying the boundary condition  $x = D \rightarrow v_y = 0$  then means that the following applies to the whole liquid layer  $v_y = 0$ !

### 5.7.3 Casson liquids

The rheology of Casson liquids is described by

$$\begin{aligned} |\tau_{xy}|^{1/2} - \tau_C^{1/2} &= \mu_C^{1/2} \left| \frac{dv_y}{dx} \right|^{1/2} && \text{if } |\tau_{xy}| \geq \tau_C, \\ \frac{dv_y}{dx} &= 0 && \text{if } |\tau_{xy}| < \tau_C \end{aligned} \quad (5.137)$$

in which  $\tau_C$  again is a yield stress. Examples of liquids that fall into this category are yoghurt and blood.

### 5.7.4 Visco-elastic liquids

Depending on the circumstances (imposed stresses), some liquids also have *elastic properties*, the behaviour of liquids of this kind are often satisfactorily described by

$$\tau_{xy} + \lambda \frac{d\tau_{xy}}{dt} = -\mu \frac{dv_y}{dx} \quad (5.138)$$

where  $\lambda$  is the time constant that describes the elastic behaviour.

The remarkable thing about this is that the liquid behaves in part like a 'normal' viscous liquid in a steady-state condition. Equation (5.138) is reduced to the Newtonian equation. However, if the shear stress varies in time, the substance will display elastic properties. This behaviour too can be traced back to the formation of networks between strongly branched and rolled up molecules and the reaction of these networks to imposed stresses.

A very good illustration of this *visco-elastic* behaviour can be demonstrated through shark fin soup. If a spoon is used to stir the soup in the same direction for a longer period of time, a steady-state situation will arise. If the spoon is then removed from the liquid, then it will continue to rotate for a short time and come to a standstill as a result of viscosity. Now, however, the situation is no longer steady and the other properties of the liquid become clearly visible. The soup does not slowly come to a standstill, but actually abruptly reverses the direction of flow! It is as if the liquid (actually the polymer molecules in the soup) were stretched like an elastic band and, now that the spoon has been taken out, that the band wishes to resume its state of balance. This is a simple but effective test for finding out whether shark fin soup is in fact 'genuine' ( $\lambda \approx 1$  s).

At the end of this Section on non-Newtonian liquids, Figure 5.29 shows, by way of summary, the link between the shear stress and the velocity gradient for a number of types of liquid – Newtonian as well as non-Newtonian.

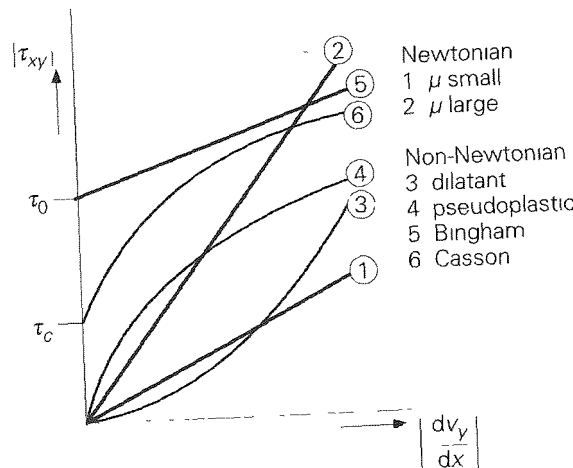


Figure 5.29

### Summary

The link between the velocity gradient and the shear stress is not shown for all liquids by Newton's law. On the contrary, most liquids that are used in industry and indeed in everyday life do not fall into this category. There are many different categories of liquid, each with their own link between shear stress and velocity gradient (see Figure 5.29). The field that is involved with this is an entirely separate part of fluid mechanics and is called *rheology*. The link between the shear stress and the velocity gradient is also referred to as the rheology of the liquid.

Remember that the shear stress profile does not depend on the rheology of the liquid, but the velocity profile does. Velocity profiles have been derived for power law liquids and Bingham liquids. Casson liquids and visco-elastic liquids have also been introduced. Sometimes, the flow starts to resemble plug flow.

## 5.8 The general equations of motion

### 5.8.1 Fluid mechanics and transport phenomena

In Chapters 1 and 2 of this book we discussed the techniques of drawing up balances and dimensional analysis. Additionally, all kinds of concepts (such as mechanical energy, residence time distribution, and shear stress), non-dimensional numbers, and several phenomenological laws have been introduced. We then looked at heat and mass transport in Chapters 3 and 4, focusing first on molecular transport before dealing with the use of transfer coefficients for convective transport. With the description, development, application and upscaling of process equipment, chemical engineers have come a long way on the basis of the aforementioned approach, which

has been substantiated by extensive empirical information. The analogy between heat and mass transfer was apposite and extremely helpful.

Fluid mechanics, which is actually momentum transport or momentum transfer, can also be considered analogously to heat and mass transfer. This was done in § 2.1 and § 5.6 for laminar flow (molecular transport) and in § 5.3.3 for friction drag (momentum transfer at solid walls) under turbulent flow conditions. Nonetheless, the sequence of the topics covered in this chapter on fluid mechanics has been largely different to that in Chapters 3 and 4. Chapter 5 starts with the phenomenological approach to friction and with pressure drop calculations, with molecular transport coming only thereafter. There are four reasons for this inverted sequence:

First, for many chemical engineers, pressure drop calculations across pipeline systems and packed beds are highly relevant, with the mechanical energy balance playing a major role. This balance falls slightly outside the classic analogy of momentum, heat and mass transfer, note that the friction factor (§ 5.3.1) and the loss coefficient of a fitting (§ 5.4) are defined in a very different way to the heat and mass transfer coefficients (in § 3.5 and § 4.5 respectively), although the analogy for the friction factor is restored again in § 5.3.3. With engineering practice in mind, the Chapter therefore began with engineering fluid mechanics for pressure drops that concurs with the coverage of mechanical energy balances and Bernoulli's law (in § 1.3.3 and Examples 1.20 and 1.21) and that of drag force (in § 2.3).

Second, apart from the analogy with heat and mass transport, there is – seen from the industrial engineering practice – no good reason for Chapter 5 to start with molecular momentum transport. The simplest version of molecular momentum transport is one-dimensional laminar flow.<sup>23</sup> This is not particularly relevant for pressure drop calculations in most of engineering fluid mechanics, while on the contrary molecular heat transport for example is important with regard to the description of convective heat transport (because of the term ‘resistance to heat transport’, the Nusselt number, and the overall heat transfer coefficient). This makes it possible to postpone the coverage of molecular momentum transport.

Third, reference was already made in Chapters 3 and 4 to the fact that a more precise alternative is available for the phenomenological approach to convective heat and mass transfer. In § 3.4 and § 4.4, after all, the generally valid micro balances that lead to the transport equations for time-dependent three-dimensional heat and mass transport were presented on the basis of the *cubic volume element method*. It was pointed out here that solving this transport equation requires an equally detailed knowledge of the (time-dependent three-dimensional) velocity field.

<sup>23</sup> One-dimensional laminar flows occur in microfluidics (micro-reactors, lab on a chip) in polymer technology (extrusion, coating processes), in the life sciences, and in the food industry. In the three latter fields, non-Newtonian liquid properties often play a dominant role.

The so-called Navier-Stokes equations of motion, which describe the flow (the momentum housekeeping) in a three-dimensional domain, will be looked at now, this links up to the coverage of the one-dimensional flows in § 5.6 and § 5.7. The coverage of the Navier-Stokes equations once again highlights the analogy between heat, mass, and momentum transport in all its glory—the transport equations for momentum ( $3x$ ), heat, and mass are also completely identical, mathematically.

Finally, whereas the Navier-Stokes equations used to be something of an oddity and the be-all and end-all of theory for many classically educated chemical engineers, they now serve as the starting point for modern chemical engineering, which uses numerical techniques in order to gain an inside picture of local transport and transfer phenomena in process equipment. This makes it much easier to understand and manage all kinds of effects of geometry and scale on the yield and selectivity of chemical reactions, for example, on the intensity and effectiveness of heat and mass transfer, and on separation processes (through variations in flow patterns, residence time distributions, contact times, etc.). The chapter ends with this highly promising future prospect.

### 5.8.2 The continuity equation

Before deriving the aforementioned Navier-Stokes equations for three-dimensional momentum transport in a flow domain, we will first use the *cubic volume element method* in order to derive an equation on the basis of an overall mass balance for a small cube, with which every flow field must comply. Once again, we will use only a Cartesian coordinate system, for the sake of simplicity (see Figure 5.30, which is identical to Figure 3.22). The control volume  $dxdydz$  is located at a random position somewhere in the field of flow, which is three-dimensional and time-dependent. This means that the three velocity species and the density  $\rho$  are all a function of both time and the  $x$ ,  $y$ , and  $z$  coordinates.

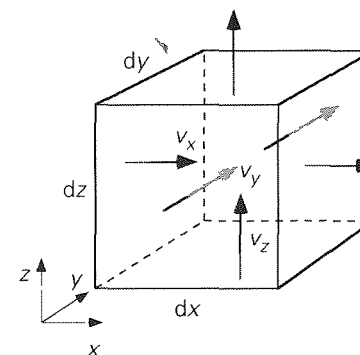


Figure 5.30

The micro balance for the total mass for the cube in Figure 5.30 contains, in addition to the accumulation term,

$$\frac{\partial}{\partial t} \rho dxdydz \quad (5.139)$$

only the convective transport terms through each of the six planes. As a result of convective transport, therefore,

$$[\rho v_x]_{x,y,z} dydz \quad (5.140)$$

of mass enters through the left-hand plane, while

$$[\rho v_x]_{x+dx,y,z} dydz \quad (5.141)$$

of mass leaves again through the right-hand plane. This produces a net contribution of convective mass transport in the direction of  $x$  of

$$[\rho v_x]_{x,y,z} dydz - [\rho v_x]_{x+dx,y,z} dydz = - \frac{\partial}{\partial x} (\rho v_x) dxdydz \quad (5.142)$$

In an identical manner, the convective mass flows through the rear and front planes produce, net

$$[\rho v_y]_{x,y,z} dx dz - [\rho v_y]_{x,y+dy,z} dx dz = - \frac{\partial}{\partial y} (\rho v_y) dxdydz \quad (5.143)$$

and through the top and bottom planes

$$[\rho v_z]_{x,y,z} dx dy - [\rho v_z]_{x,y,z+dz} dx dy = - \frac{\partial}{\partial z} (\rho v_z) dxdydz \quad (5.144)$$

Merging Equations (5.139), (5.142), (5.143), and (5.144), and dividing this by the fixed magnitude  $dxdydz$  of the cube produces what is known as the *continuity equation*

$$\frac{\partial \rho}{\partial t} = - \frac{\partial \rho v_x}{\partial x} - \frac{\partial \rho v_y}{\partial y} - \frac{\partial \rho v_z}{\partial z} \quad (5.145)$$

This continuity equation is a direct result of the *law of conservation of mass*. This is still the case if the density is constant, and Equation (5.145) therefore changes to

$$0 = \frac{\partial v_x}{\partial x} + \frac{\partial v_y}{\partial y} + \frac{\partial v_z}{\partial z} \quad (5.146)$$

What enters through the left-hand plane, for example, and does not exit through the right-hand plane must, where density is constant, exit through one or more of the

other planes This is the case at all times! Notice that the density (the mass) no longer features in Equation (5.146)

### Summary

The continuity equation has been derived with the help of the cubic volume element method, with which every velocity field must comply at all times the direct consequence of the law of conservation of mass

### 5.8.3 The Navier-Stokes equations

For the derivation of the general micro balances for momentum transport, or the Navier-Stokes equations, it is advisable to again use the term *momentum concentration* that was introduced in § 14 the velocity component  $v_x$  (in m/s) in the direction of  $x$  is actually a concentration of  $x$  momentum (in Ns/kg) This is also why  $\rho v_x$  represents the momentum concentration on the basis of volume (in Ns/m<sup>3</sup>)

The actual velocity distributions, or the field of velocity, in a flow domain come about because momentum is redistributed across the domain by convective and molecular momentum flows, while forces are exerted on the mass and on the boundaries of the domain Once again, the *cubic volume element method* is used in order to identify this momentum housekeeping

Because of the vector character of momentum and of forces, a separate momentum balance for the cube in Figure 5.30 should be drawn up for every direction Below, only the derivative for the  $x$  momentum balance is presented First, there is an inventory of the individual contributions to this micro balance

#### Accumulation

The unsteady-state term is

$$\frac{\partial}{\partial t} \rho v_x dxdydz \quad (5.147)$$

#### Convective transport

A volume flow rate of  $v_x(x,y,z,t) dydz$  enters the left-hand plane of the cube, while the  $x$  momentum concentration in this flow is  $\rho v_x(x,y,z,t)$  In general, the local velocity vector does not happen to be perpendicular to the left-hand plane This vector is decomposed into its components in the selected axis system, the  $x$  component of the velocity is the only one to bring mass into the cube through this left-hand plane, and this mass carries (among other things)  $x$  momentum with it Convectively, therefore,

$$[v_x \rho v_x]_{x,y,z} dydz \quad (5.148)$$

of  $x$  momentum enters the cube through the left-hand plane

$$[v_x \rho v_x]_{x+dx,y,z} dydz \quad (5.149)$$

exits the cube through the right-hand plane, where both  $v_x$  and  $\rho v_x$  have different values on the right to those they have on the left These flows make a net contribution in the direction of  $x$  of

$$[v_x \rho v_x]_{x,y,z} dydz - [v_x \rho v_x]_{x+dx,y,z} dydz = - \frac{\partial}{\partial x} (v_x \rho v_x) dxdydz$$

to the accumulation of  $x$  momentum in the cube Similarly, the  $y$  component of the velocity at the front plane of the cube brings in mass that carries (among other things)  $x$  momentum with it

$$[v_y \rho v_x]_{x,y,z} dxdz \quad (5.151)$$

Together with a similar term at the rear plane of the cube, the net contribution of the convective transport in the direction of  $y$  to the accumulation of the  $x$  momentum is obtained as follows

$$[v_y \rho v_x]_{x,y,z} dxdz - [v_y \rho v_x]_{x,y+dy,z} dxdz = - \frac{\partial}{\partial y} (v_y \rho v_x) dxdydz \quad (5.152)$$

Analogously, the net contribution by the top and bottom planes is

$$[v_z \rho v_x]_{x,y,z} dxdy - [v_z \rho v_x]_{x,y,z+dz} dxdy = - \frac{\partial}{\partial z} (v_z \rho v_x) dxdydz \quad (5.153)$$

#### Molecular transport

Providing that Newton's law applies, the molecular  $x$ -momentum flow through the front side can be written as follows

$$-\mu \left[ \frac{\partial v_x}{\partial y} \right]_{x,y,z} dxdz \quad (5.154)$$

and through the rear plane

$$-\mu \left[ \frac{\partial v_x}{\partial y} \right]_{x,y+dy,z} dxdz \quad (5.155)$$

So therefore a net contribution by the molecular transport of  $x$ -momentum in the direction of  $y$  to the accumulation results that is given by

$$-\mu \left[ \frac{\partial v_x}{\partial y} \right]_{x,y,z} dx dz - \left\{ -\mu \left[ \frac{\partial v_x}{\partial y} \right]_{x,y+dy,z} \right\} dx dz = \frac{\partial}{\partial y} \left[ \mu \frac{\partial v_x}{\partial y} \right] dx dy dz \quad (5.156)$$

The left and right-hand planes make a net contribution to the accumulation given by

$$\frac{\partial}{\partial x} \left[ \mu \frac{\partial v_x}{\partial x} \right] dx dy dz \quad (5.157)$$

It should be pointed out here that this concerns *molecular* transport of *x*-momentum to each of the two planes associated with the local values of the velocity gradient  $\partial v_x / \partial x$ . This gradient expresses whether, on average, molecules in the direction of *x* accelerate or decelerate, while  $\mu \partial v_x / \partial x$  is a measure for the local net transfer of *x* momentum by collisions of *individual* molecules, *given this average acceleration or deceleration*. This net transfer is different on the left and right, and it is from that that contribution of Expression (5.157) results.

Molecular transport of *x* momentum in the direction of *z* at the top and bottom planes results in the following net contribution

$$\frac{\partial}{\partial z} \left[ \mu \frac{\partial v_x}{\partial z} \right] dx dy dz \quad (5.158)$$

In the above derivations of the molecular transport terms, it has been assumed that, on each plane of a cube, either only a shear stress or only a normal stress prevails to each of which Newton's law applies. This representation – that was chosen because of the classical analogy between heat, mass and momentum transport (see § 3.4 and § 4.4) – is in fact erroneous, takes no account of the simultaneous occurrence and mutual relationship between shear and normal stresses in every transforming fluid element, and is at odds with a number of laws of physics. The eventual result, Equation (5.139), is correct, however. For the correct derivation, in physics terms, which uses a linear connection between stresses in a fluid and transformation velocities of fluid elements, readers should refer to Munson<sup>24</sup>.

#### Production

Production of *x* momentum is made by the *x*-components of all the forces that are exerted on the cube. As far as the pressure is concerned, in the direction of *x* it is exerted only on the left- and right-hand planes of the cube. The net result is

$$p|_x dy dz + \{-p|_{x+dx} dy dz\} = -\frac{\partial p}{\partial x} dx dy dz \quad (5.159)$$

A physically correct interpretation of this net contribution to the total *x*-momentum balance is that  $[-\partial p / \partial x]$  is a source term expressing that per unit of volume and per unit of time a certain amount of *x*-momentum (in Ns) is supplied to the volume element. Finally, the *x*-component  $g_x$  (in Ns/kg) of gravity also affects the mass in the cube

$$g_x \rho dx dy dz \quad (5.160)$$

This means that gravity is a typical example of a *body force* (in N/kg) where pressure (in N/m<sup>2</sup>) is exerted on a plane

#### The equations of motion

Merging Expressions (5.147), (5.150), (5.152), (5.153) and (5.156) through (5.160), dividing by  $dx dy dz$ , and considering the case of constant  $\mu$  provides the *x* momentum balance

$$\begin{aligned} \frac{\partial \rho v_x}{\partial t} = & -\frac{\partial}{\partial x} (\nu_x \rho v_x) - \frac{\partial}{\partial y} (\nu_y \rho v_x) - \frac{\partial}{\partial z} (\nu_z \rho v_x) + \\ & + \mu \left\{ \frac{\partial^2 v_x}{\partial x^2} + \frac{\partial^2 v_x}{\partial y^2} + \frac{\partial^2 v_x}{\partial z^2} \right\} - \frac{\partial p}{\partial x} + \rho g_x \end{aligned} \quad (5.161)$$

This equation is completely comparable and analogous to the Equations (3.135) and (4.72).

The *x*-momentum balance can also be derived in terms of shear stresses, which means it is valid for non-Newtonian fluids as well. This derivation contains no molecular transport terms of the kind of Expression (5.154), but the shear stresses on the six planes should be included under the heading *Production*. Consider the fluid flow in the direction of *x* along the front plane of the cube in Figure 5.30, because of the local shear stress as a result of the local velocity gradient  $\partial v_x / \partial y$ , this fluid exerts a force

$$\tau_{yx}|_{x,y,z} dx dz \quad (5.162)$$

on the fluid in the cube. There is a similar force in the direction of *x* on the rear plane as a result of the fluid that flows on the outside the cube there

$$-\tau_{yx}|_{x,y+dy,z} dx dz \quad (5.163)$$

Together, these forces produce a net force in the direction of *x*

$$-\frac{\partial \tau_{yx}}{\partial y} dx dy dz \quad (5.164)$$

<sup>24</sup> Munson, B R, D F Young & T H Okunishi, *Fundamentals of Fluid Mechanics*, Wiley, 1994, § 6.1

on the cube. Similar forces are exerted in the direction of  $x$  on the other four planes, giving the following net contributions

$$-\frac{\partial \tau_{xx}}{\partial x} dx dy dz \quad (5.165)$$

due to spatial variations in the normal stress  $\tau_{xx}$ , and

$$-\frac{\partial \tau_{zx}}{\partial z} dx dy dz \quad (5.166)$$

These latter two contributions to the  $x$ -momentum balance relate to the local velocity gradients  $\partial v_x / \partial x$  and  $\partial v_x / \partial z$ .

Merging Expressions (5.147), (5.150), (5.152), (5.153), (5.159), and (5.160) with (5.164) through (5.166) and dividing by  $dx dy dz$  produces

$$\begin{aligned} \frac{\partial \rho v_x}{\partial t} = & -\frac{\partial}{\partial x}(v_x \rho v_x) - \frac{\partial}{\partial y}(v_y \rho v_x) - \frac{\partial}{\partial z}(v_z \rho v_x) + \\ & -\frac{\partial \tau_{xx}}{\partial x} - \frac{\partial \tau_{yx}}{\partial y} - \frac{\partial \tau_{zx}}{\partial z} - \frac{\partial p}{\partial x} + \rho g_x \end{aligned} \quad (5.167)$$

The  $x$ -momentum balance is often presented in another form, for which the left-hand side of Equations (5.161) and (5.167) are written as

$$\rho \frac{\partial v_x}{\partial t} + v_x \frac{\partial \rho}{\partial t} \quad (5.168)$$

This means also that, e.g., the second convective term on the right-hand side of the Equations (5.161) and (5.167) is elaborated to

$$\rho v_y \frac{\partial v_x}{\partial y} + v_x \frac{\partial \rho v_y}{\partial y} \quad (5.169)$$

By doing the same thing with the two remaining convective terms, six terms are created on the right-hand side of the Equations (5.161) and (5.167). Thanks to the continuity equation, three of these cancel against the second term of Equation (5.168). This means that Equation (5.161) can be written as follows

$$\begin{aligned} \rho \frac{\partial v_x}{\partial t} + \rho v_x \frac{\partial v_x}{\partial x} + \rho v_y \frac{\partial v_x}{\partial y} + \rho v_z \frac{\partial v_x}{\partial z} = \\ = \mu \left\{ \frac{\partial^2 v_x}{\partial x^2} + \frac{\partial^2 v_x}{\partial y^2} + \frac{\partial^2 v_x}{\partial z^2} \right\} - \frac{\partial p}{\partial x} + \rho g_x \end{aligned} \quad (5.170)$$

where  $\mu$  has again been assumed to be constant.

Similar equations can be derived for the two remaining velocity components.

$$\begin{aligned} \rho \frac{\partial v_y}{\partial t} + \rho v_x \frac{\partial v_y}{\partial x} + \rho v_y \frac{\partial v_y}{\partial y} + \rho v_z \frac{\partial v_y}{\partial z} = \\ = \mu \left\{ \frac{\partial^2 v_y}{\partial x^2} + \frac{\partial^2 v_y}{\partial y^2} + \frac{\partial^2 v_y}{\partial z^2} \right\} - \frac{\partial p}{\partial y} + \rho g_y \end{aligned} \quad (5.171)$$

$$\rho \frac{\partial v_z}{\partial t} + \rho v_x \frac{\partial v_z}{\partial x} + \rho v_y \frac{\partial v_z}{\partial y} + \rho v_z \frac{\partial v_z}{\partial z} = \quad (5.172)$$

The Equations (5.170) – (5.172) are denoted as the equations of motion, govern and describe – along with the continuity equation, see Equation (5.145) – the flow of any Newtonian fluid (of constant  $\mu$ ), and are the cornerstone of the field of fluid mechanics. The equations of motion are named after Navier (1785–1836) and Stokes (1819–1903), and are therefore also denoted as the Navier-Stokes equations.

In vector notation, the set reads very compactly as follows

$$\rho \frac{\partial \mathbf{v}}{\partial t} + \rho \mathbf{v} \nabla \mathbf{v} = \mu \nabla^2 \mathbf{v} - \nabla p + \rho \mathbf{g} \quad (5.173)$$

In terms of shear stresses – going forward from Equation (5.167) – the following is true

$$\rho \frac{\partial \mathbf{v}}{\partial t} + \rho \mathbf{v} \nabla \mathbf{v} = -\nabla \cdot \boldsymbol{\tau} - \nabla p + \rho \mathbf{g} \quad (5.174)$$

For flows where viscous effects can be disregarded, the Euler equation applies

$$\rho \frac{\partial \mathbf{v}}{\partial t} + \rho \mathbf{v} \nabla \mathbf{v} = -\nabla p + \rho \mathbf{g} \quad (5.175)$$

For viscous (laminar) flows in which just the inertial terms may be ignored, and for steady-state conditions, Equation (5.173) simplifies to

$$0 = \mu \nabla^2 \mathbf{v} - \nabla p + \rho \mathbf{g} \quad (5.176)$$

It falls beyond the scope of this book to show the form of these systems of equations for cylinder or sphere coordinates. Readers are referred to Bird *et al.*<sup>25</sup> or the Data Companion<sup>26</sup>.

The set of Equations (5.173), (5.174) and (5.175) apply in a very general sense to time-dependent three-dimensional flows. An equation for a simpler type of flow, of the kind dealt with in § 5.6 for example, can easily be extracted from a general

<sup>25</sup> Bird, R B, W E Stewart & E N Lightfoot, Transport Phenomena, Wiley, 2nd Ed, 2002

<sup>26</sup> Janssen, L P B M & M M C G Warmoeskerken, Transport Phenomena Data Companion, Delft, VSSD, Delft, 2006

system. For the time-independent, one-dimensional, vertical, incompressible flow of a layer of uniform thickness, for example, Equation (5.96) can be obtained from Equation (5.174) by using the following assumptions

$$v_x = 0, v_z = 0, \frac{\partial v_y}{\partial y} = 0, \frac{\partial}{\partial t} = 0, g_x = g_z = 0, g_y = g$$

plus all pressure gradients being zero and all shear stresses being zero except  $\tau_{xy}$ . Similarly, Equation (5.82) can be obtained from Equation (5.176) in the absence of gravity.

In a way similar to that of the redefinition of Equation (5.161) to the end-result of Equation (5.170), that is, with the help of the continuity equation – see Equation (5.145) – also the earlier Equation (3.135) governing heat transport can be rewritten as

$$\rho \frac{\partial c_p T}{\partial t} + \rho v_x \frac{\partial c_p T}{\partial x} + \rho v_y \frac{\partial c_p T}{\partial y} + \rho v_z \frac{\partial c_p T}{\partial z} = \lambda \left\{ \frac{\partial^2 T}{\partial x^2} + \frac{\partial^2 T}{\partial y^2} + \frac{\partial^2 T}{\partial z^2} \right\} + q \quad (5.177)$$

In exactly the same way, Equation (4.72) can be rearranged

$$\frac{\partial c}{\partial t} + v_x \frac{\partial c}{\partial x} + v_y \frac{\partial c}{\partial y} + v_z \frac{\partial c}{\partial z} = D \left\{ \frac{\partial^2 c}{\partial x^2} + \frac{\partial^2 c}{\partial y^2} + \frac{\partial^2 c}{\partial z^2} \right\} + r \quad (5.178)$$

It should be pointed out that in Equation (5.177) the unit of combination  $c_p T$  is J/kg and can therefore be regarded as an *energy concentration*, as explained previously. Finally, Equation (5.177) for constant  $c_p$  changes to

$$\frac{\partial T}{\partial t} + v_x \frac{\partial T}{\partial x} + v_y \frac{\partial T}{\partial y} + v_z \frac{\partial T}{\partial z} = a \left\{ \frac{\partial^2 T}{\partial x^2} + \frac{\partial^2 T}{\partial y^2} + \frac{\partial^2 T}{\partial z^2} \right\} + \frac{q}{\rho c_p} \quad (5.179)$$

Find out yourself how Equation (3.72), for example, can be obtained from Equation (5.179).

Equations (5.170) through (5.172), (5.177), and (5.178) perfectly illustrate in their form the analogy between momentum, heat, and mass transport. Together with Equation (5.145) – the continuity equation – a system of six partial differential equations is available from which, in principle, with sufficient boundary and initial conditions, the spatial distributions of the three velocity components, pressure, temperature, and component concentration can be calculated as a function of time.

This system of six differential equations is strongly linked internally and, thanks to the convective terms, is also strongly non-linear.

### Summary

With the help of the *cubic volume element method*, it has been demonstrated how the Navier-Stokes equations can be derived for the  $x$  momentum. For each plane of a cube, both convective and molecular transport terms have to be formulated, and all relevant forces have to be taken into consideration. The molecular transport terms can also be represented as shear stresses. The continuity equation can be used for rewriting the momentum balances, and the same thing applies to the heat and component transport equations.

The classic analogy between momentum, heat, and mass transport is apparent from the similarity between the various transport equations. Finally, it is possible to obtain the specific equations for specific simple cases from the general transport equations by omitting non-relevant terms.

### 5.8.4 Computational Fluid Dynamics

Systems like the Equations (5.170) through (5.172), (5.177), (5.178) and (5.145) form the basis for what is nowadays known as Computational Fluid Dynamics (CFD). Modern chemical engineering exploits CFD in order to achieve better descriptions and designs of process equipment, for example, on the basis of information about *local* variables (velocities, pressure, temperature, concentrations). The state of computer technology means that the phenomenological approach to transport phenomena can be replaced to an increasing degree by CFD simulations. In one sense, though, there is nothing new – it is still all about the concepts, the laws, and the technique of drawing up balances, as covered in Chapters 1 and 2.

The systems of transport equations that have been mentioned are all derived using a small cube (Figure 5.30). The dimensions of the cube have not been specified, but they should preferably be small in comparison with the dimensions of the flow domain (the equipment) in order to arrive at local values for the variable. The absolute lower limit for the dimensions of the cube is the free path length of the molecules. If the dimensions approach this, then continuum terms like mean velocity and convective transport lose their significance. As long as this is not the case, the velocities, the temperature and the concentrations that are allocated in the *cubic volume element method* to a cube can be regarded as point properties at the centre of the cube.

For CFD calculations based on the *finite volume method*, the flow domain is divided up into a very large number of small volume elements (small cubes in a Cartesian coordinate system). In practice, the number of ‘cells’ is limited at the lower end by

the desired degree of detail (resolution), especially where steep gradients can be expected, and at the upper end by capacity, memory and speed of the computer

Mass, momentum, heat and/or species mass balances are drawn up for each of the volume elements. That is equivalent to solving the system (5.145), (5.170) through (5.172), (5.177) and (5.178), for example, at the discrete (grid) points – or nodes – of a grid – or lattice – that spans the whole flow domain, the variables only have values at the grid points which are in the heart of every cell. All terms with derivatives in the (micro) balances for the cells are discretised with the help of the variables in the adjacent lattice points, a large number of so-called differential schemes are available for this. This helps the partial differential equations to change into algebraic equations and to link the values of any variable to those at adjacent points. This procedure has been illustrated in § 3.1.5 for the simple case of two-dimensional heat conduction in a Cartesian coordinate system.

Every cell produces as many algebraic equations as there are balances set up for that cell. For the whole flow domain with its many cells, this actually means a very large number of algebraic equations that have to be solved simultaneously, or iteratively. There is a wide choice of methods for solving this. The iterations are continued until all the micro balances in the domain have been complied with throughout, to a predetermined level of accuracy.

It should be repeated here that most flows (both in process equipment and in nature) are *turbulent*. The lattice on which the flow should be calculated should be fine enough in order for the smallest eddies to be visible. The state of computer technology has not yet advanced to the stage that it is possible to allow this for higher Reynolds numbers (The smallest eddies become smaller as the Reynolds number increases). Moreover, most technologists are not interested in the instantaneous velocity field, including all its eddies. Generally, knowledge of mean quantities and their variations about the flow domain is more than sufficient.

This means that calculations are made using a coarser grid and that the *momentum transport* caused by the *eddies* is modelled as a separate contribution to the momentum housekeeping on a scale between convective transport by the (mean) flow and molecular transport. During their existence, all the eddies – individually and collectively – transport momentum, among other things (via convection). (See also § 3.5.2.) This turbulent momentum transport can, in a large number of cases, be modelled sufficiently successfully in terms of two core concepts from turbulence mechanics:

- the concentration of *turbulent kinetic energy*, denoted by  $k$  and with unit  $\text{m}^2/\text{s}^2$ , or  $\text{J/kg}$  a measure for magnitude and strength of all current velocity fluctuations as a result of the whole spectrum of turbulent eddies, and

- the rate  $\varepsilon$  at which  $k$  is dissipated into heat caused by viscosity inside the smallest eddies (the so-called *Kolmogorov eddies*), this means that  $\varepsilon$  has the unit  $\text{m}^2/\text{s}^3$  or  $\text{W/kg}$ . The image that goes with  $\varepsilon$  is that of the number of smallest eddies in which the *energy dissipation* takes place.

Both  $k$  and  $\varepsilon$  can clearly be regarded as concentrations, also, both variables appear to be able to vary considerably across a flow domain. In relation to local and transient momentum transport by eddies, it is therefore usually a good idea to calculate  $k$  and  $\varepsilon$  as well. Transport equations can be derived for both variables, which actually stand for micro balances for  $k$  and  $\varepsilon$  and, as far as their form is concerned (number and type of terms), display a strong similarity with the Navier-Stokes equations. However, it should be pointed out that  $k$  and  $\varepsilon$  are *not conserved quantities* (see the discussion in § 1.3.3). All of this means that the number of transport equations that have to be solved in this approach is greater still than for laminar flows.

If classical chemical engineering, which uses phenomenological concepts like mass and heat transfer coefficients, is compared to modern, CFD-based chemical engineering, then it is noticeable that

- both rely strongly on the drawing up of balances,
- both use the same concepts and laws,
- the phenomenological approach leads very quickly to a fairly accurate result and in the past has led to major successes,
- CFD produces much more detailed information and therefore promises much for the future,
- that further training in fluid mechanics (including turbulence) and numerical analysis is desirable for CFD.

It should be pointed out that, with the current state of CFD technology, experimental verification of simulation results is still very much required, especially in the case of turbulent flows. Partly for this reason, the phenomenological approach to transport phenomena and CFD simulations will, for the time being, continue to exist side-by-side as valuable and complementary techniques.

### Summary

The principle of Computational Fluid Dynamics (CFD), based on the general transport equations (micro balances) for momentum, heat and mass, has been set out. The procedure for finding solutions as laid down in the finite-volume method has been described in brief. For turbulent flows, two new variables – the turbulent kinetic energy  $k$  and the rate  $\varepsilon$  at which  $k$  is dissipated – has been introduced and their use explained. They help in the modelling of momentum transport through the eddies of the turbulent velocity field. Finally, it was stated that simulations created with the help of CFD are a welcome and highly promising extension to the toolbox of chemical engineers.

## List of Symbols

Only those symbols are reported here that are used throughout the textbook

		units
$a$	absorption coefficient	—
$a$	specific area	$\text{m}^2/\text{m}^3$
$a$	thermal diffusivity	$\text{m}^2/\text{s}$
$A$	area	$\text{m}^2$
$b$	width	$\text{m}$
$c$	concentration	$\text{kg}/\text{m}^3$ or $\text{kmol}/\text{m}^3$
$c^*$	saturation concentration, or solubility	$\text{kg}/\text{m}^3$ or $\text{kmol}/\text{m}^3$
$c_p$	specific heat at constant pressure	$\text{J}/\text{kgK}$
$c_v$	specific heat at constant volume	$\text{J}/\text{kgK}$
$C_d$	discharge coefficient	—
$C_D$	drag coefficient	—
$C(\theta)$	$C$ -function	—
$d$	diameter	$\text{m}$
$D$	diameter	$\text{m}$
$D_h$	hydraulic diameter	$\text{m}$
$ID$	diffusion coefficient	$\text{m}^2/\text{s}$
$e$	energy per unit of mass	$\text{J}/\text{kg}$
$e_{\text{diss}}$	specific total energy dissipation	$\text{J}/\text{kg}$
$e_f$	specific energy dissipation in pipes (friction)	$\text{J}/\text{kg}$
$e_L$	specific energy dissipation in fittings	$\text{J}/\text{kg}$
$e$	emission coefficient	—
$E$	energy	$\text{J}$
$E_q$	heat extraction coefficient	—
$E(\theta)$	$E$ -function	—
$f$	friction factor	—
$f_D$	Stefan's correction factor	—
$F_D$	drag force	$\text{N}$
$F$	force	$\text{N}$
$F(\theta)$	$F$ -function	—
$g$	gravitational acceleration	$\text{m}/\text{s}^2$
$h$	height	$\text{m}$
$h$	heat transfer coefficient	$\text{J}/\text{sm}^2\text{K}$

$h$	enthalpy per unit of mass	J/kg of J/kmol	$t$	transmission coefficient
$\Delta h_v$	heat of evaporation	J/kg	$T$	temperature
$H$	enthalpy	J	$u$	internal, or thermal, energy per unit of mass
$H$	Henry coefficient	Pa	$U$	overall heat transfer coefficient
$\mathcal{H}$	absolute humidity	kg/kg	$v$	velocity
$JD$	mass transfer number	—	$v_r$	relative velocity
$JH$	heat transfer number	—	$v_o$	superficial velocity
$k$	mass transfer coefficient	m/s	$V$	volume
$k$	concentration of turbulent kinetic energy	J/kg	$w$	impeller blade height
$k$	constant	—	$W$	width
$k_B$	Boltzmann constant	J/K	$W$	work
$k_r$	reaction rate constant	(varying)	$x$	length dimension
$K$	overall mass transfer coefficient	m/s	$x, y$	mass fraction
$K$	consistency (power law liquid)	(varying)	$z$	spatial coordinates
$K_L$	loss coefficient	—	$\beta$	vertical coordinate
$l$	length	m	$\delta$	thermal expansion coefficient
$L$	length (scale)	m	$\Delta$	film, gap, or coating thickness
$m$	mass of a molecule	kg	$\varepsilon$	difference, or interval
$m$	partition coefficient	—	$\varepsilon$	rate of dissipation of turbulent kinetic energy
$M$	(total) mass	kg/mol	$\varepsilon$	porosity
$M$	molar mass	—	$\gamma$	wall roughness
$n$	number	—	$\theta$	specific weight ( $= \rho g$ )
$n$	flow index (power law)	—	$\theta$	non-dimensional time
$N$	number of tanks in series	s <sup>-1</sup>	$\phi$	angle
$N$	number of impeller revolutions per unit of time	mol <sup>-1</sup>	$\phi'$	flow rate
$N_{\text{avo}}$	number of Avogadro	N/m <sup>2</sup>	$\phi''$	flow rate per unit of width
$p$	pressure	N/m <sup>2</sup>	$\phi_w$	flux ( $=$ flow rate per unit of area)
$p^*$	equilibrium vapour pressure	J/s	$\lambda$	work
$P$	power	s <sup>-1</sup>	$\lambda$	thermal conductivity coefficient
$P$	production	Ns	$\lambda$	time constant for visco-elastic fluids
$P$	power	J/m <sup>3</sup> s	$\mu$	wave length
$q$	rate of specific heat production	m	$\nu$	dynamic viscosity coefficient
$r$	radial coordinate	kmol/m <sup>3</sup> s	$\rho$	kinematic viscosity coefficient
$r$	chemical reaction rate	—	$\sigma$	density
$r$	reflection coefficient	m	$\sigma$	diameter of a molecule
$R$	radius	J/molK	$\sigma$	interfacial, or surface, tension
$R$	gas constant	m	$\sigma$	Stefan-Boltzmann constant
$s$	distance	m	$\tau$	residence time
$S$	(wetted) perimeter	s	$\tau_0$	yield stress
$t$	time		$\tau_{xy}$	shear stress

*subscripts*

<i>a</i>	ambient
<i>A</i>	component A
<i>buoy</i>	buoyancy
<i>B</i>	component B
<i>c</i>	value in centre
<i>e</i>	energy
<i>fr</i>	friction
<i>g</i>	gravity
<i>h</i>	hydraulic
<i>I</i>	interface
<i>l</i>	liquid
<i>L</i>	position L
<i>m</i>	measured
<i>m</i>	mass
<i>mol</i>	mol
<i>p</i>	momentum
<i>p</i>	particle
<i>q</i>	heat
<i>r</i>	relative
<i>s</i>	slip
<i>tot</i>	total
<i>u</i>	internal energy
<i>v</i>	vapour
<i>V</i>	volume
<i>w</i>	wall
<i>x,y,z</i>	<i>x,y,z</i> -direction
<i>X</i>	component X
<i>0</i>	start, entrance
<i>0</i>	wet bulb
<i>1, 2</i>	at position 1, 2
$\perp$	normal to direction of flow or motion
$\langle \rangle$	refers to spatial averaging
$\bar{}$	refers to averaging over time
<i>B<sub>1</sub></i>	Biot number
<i>Br</i>	Brinkman number
<i>Fo</i>	Fourier number
<i>Gr</i>	Grashof number

<i>Gz</i>	Graetz number
<i>Le</i>	Lewis number
<i>Nu</i>	Nusselt number
<i>Pe</i>	Péclet number
<i>Po</i>	Power number
<i>Pr</i>	Prandtl number
<i>Re</i>	Reynolds number
<i>Sc</i>	Schmidt number
<i>Sh</i>	Sherwood number
<i>Vi</i>	Viscosity number

# List of Examples

Example 1.1 Population	4
Example 1.2 A chemical reactor under steady conditions	9
Example 1.3 Coconut oil in an ideally stirred tank	11
Example 1.4 A plug flow reactor with recirculation	16
Example 1.5 F and C-functions for an ideally stirred tank	25
Example 1.6 F and C-function for two ideally stirred tanks in series	25
Example 1.7 F-function in the case of a plug flow	27
Example 1.8 F and C-functions for N ideally stirred tanks in series	29
Example 1.9 The bouncing ball	35
Example 1.10 Transport of water through a tube	39
Example 1.11 Compression of a gas	40
Example 1.12 The kettle	42
Example 1.13 The refrigerator	45
Example 1.14 Flue gases through a chimney	53
Example 1.15 The conveyor belt	57
Example 1.16 Filling a container	58
Example 1.17 A hanging droplet	60
Example 1.18 Flow through a bend	61
Example 1.19 The fire hose	64
Example 1.20 Flow round an immersed obstacle	65
Example 1.21 Outflow from a vessel through a hole	66
	79
Example 2.1 Heat conduction in a copper rod	80
Example 2.2 Evaporation of naphthalene from a tube	91
Example 2.3 Purging	101
Example 2.4 Purging II	102
Example 2.5 Pulling a wire	104
Example 2.6 A stirred tank	108
Example 2.7 Slot coating	118
Example 2.8 A hailstone	119
Example 2.9 An air bubble in glue	123
	131
Example 3.1 Heat production in a bar	139
Example 3.2 Radioactive sphere I	146
Example 3.3 Radioactive sphere II	147
Example 3.4 A copper slab	150
Example 3.5 Bitumen on oak	157
Example 3.6 A copper slab II	
Example 3.7 A glass sphere	

Example 3.8 The glass sphere II	158
Example 3.9 The glass sphere III	159
Example 3.10 A drum cooler	160
Example 3.11 The glass sphere IV	162
Example 3.12 Heating up water flowing through a tube	178
Example 3.13 Cooling of falling grains	180
Example 3.14 Heat transport between two horizontal plates	185
Example 3.15 A steam condenser	195
Example 3.16 Film condensation	195
Example 3.17 The temperature of the earth	200
Example 3.18 Radiant heat losses from an oven	203
Example 3.19 A thermometer in a cold room	206
Example 3.20 Solar radiation onto a flat roof	207
	214
Example 4.1 Transport of oxygen in human tissue	215
Example 4.2 Gas diffusion through a solid wall	217
Example 4.3 A spherical fungus flake	222
Example 4.4 A contaminated landfill I	224
Example 4.5 A contaminated landfill II	228
Example 4.6 Nickel carbonyl	234
Example 4.7 A wetted-wall column	235
Example 4.8 An evaporating sphere	238
Example 4.9 Dissolving incrustation	241
Example 4.10 Mass transfer to a rain drop	244
Example 4.11 Aerating water	246
Example 4.12 H <sub>2</sub> S stripper	248
Example 4.13 Acetic acid-benzene-water	252
Example 4.14 Determining the dew point	253
Example 4.15 Condensing through cooling	255
	268
Example 5.1 A wastewater pump	270
Example 5.2 Flow in an open channel	270
Example 5.3 Pressure drop along a horizontal oil pipeline	272
Example 5.4 Velocity in a horizontal water pipeline	272
Example 5.5 Velocity in a horizontal milk pipeline	273
Example 5.6 Water transport through a rectangular pipe	273
Example 5.7 Pumping upwards	277
Example 5.8 A basin running empty	279
Example 5.9 Pressure drop over a packed bed	284
Example 5.10 Slot coating II	290
Example 5.11 Film condensation II	295
Example 5.12 A power law liquid between two vertical plates	302
Example 5.13 A Bingham liquid between two vertical plates	305

# Index

absolute humidity, 252, 253  
 absorption, 243  
 absorption coefficient, 199, 200  
 absorptivity, 200, 202  
 adhesion, 61  
 adiabatic saturation line, 251, 253  
 albedo, 200  
 apparent viscosity coefficient, 301, 302  
 appendages, 276  
 average free path length, 84 – 86, 319  
 balances, 2  
 balance equation, 4, 5, 8, 10, 12, 15, 36, 38, 50, 68, 135, 201, 214  
 balance method, 4, 5, 42, 134  
 barycentric, 210  
 batch reactor, 13, 18  
 bed porosity, 282  
 Benard cells, 184  
 bend, 61 – 63, 276 – 279  
 Bernoulli equation, 49 – 55, 65, 67, 94, 111, 256 – 264, 309  
 Bingham plastics, 304  
 Biot number, 139  
 black radiator, 198  
 Blasius, formula of, 268  
 body force, 57, 294, 315  
 Boltzmann, 85, 86, 198, 324  
 boundary layer, 61, 112, 115, 117, 171, 179, 183, 184, 233, 237  
 boundary layer thickness, 233, 237  
 Brinkman number, 173  
 Buckingham -  $\Pi$  theorem, 100  
 buoyancy, 60, 117, 118, 120, 173, 263  
 C-function, 21 – 31  
 chemical enthalpy, 34  
 chemical potential, 243  
 chemical reaction, first-order, 13  
 Chilton and Colburn, 237  
 Chilton-Colburn analogy, 274  
 coating, 108, 109, 290 – 293, 309  
 cohesion, 61  
 concurrent flow, 190, 193  
 conduction, 75 – 80, 86, 121, 197  
 conservation law, 4, 6, 36, 47, 311  
 consistency, 301  
 continuity equation, 311, 316

Continuous Stirred Tank Reactor, 10, 18  
 contraction, 64, 67, 68  
 control volume, 2, 4 – 7, 10, 11, 14, 15, 18, 32, 36 – 39, 41 – 48, 55 – 60, 64, 73, 79, 80, 87, 89, 117, 197, 231, 257, 286, 294, 310  
 convection, 108, 173, 183, 197, 233, 239  
 convection, forced, 173, 183  
 convection, free, 173, 181, 239  
 convective transport, 47, 73, 79, 82, 89, 90, 91, 92, 94, 174, 209, 212, 230, 231, 232, 233, 237  
 coolant, 45, 190  
 countercurrently, 193  
 creeping flow, 113, 116  
 cubic volume element method, 168, 231, 309, 312, 319  
 dew point, 252  
 diffusion coefficient, 78, 81, 83 – 87, 98, 99, 209  
 dilatant liquid, 301  
 dimensional analysis, 89, 96 – 114, 143, 171, 172, 181, 233, 266, 288  
 dimensions, 4, 95 – 100, 110  
 discharge coefficient, 67, 261  
 discretisation scheme, 187, 188  
 dissipation, 35, 40, 47 – 55, 95, 111, 113, 256 – 258, 261, 265 – 277, 281  
 drag coefficient, 113 – 120, 281  
 drag force 109 – 120  
 drift flux, 225, 226  
 drift transport, 226  
 driving force, 2, 77, 81, 125, 130, 136, 137, 150, 169, 171, 172, 178, 195, 205, 213, 221, 243, 251  
 drum cooler, 160  
 dynamic pressure, 51, 52, 55, 94, 111  
 dynamic viscosity, 78, 79, 83, 87, 172, 287  
 eddies, 53, 66, 95, 111, 115, 177, 183, 262, 274, 320  
 effective viscosity coefficient, 301  
 E-function, 19, 20, 27  
 emission coefficient, 198  
 energy concentration, 32, 34, 35, 36, 37, 78, 209, 257, 318  
 energy dissipation, 35, 42, 52, 55, 62 – 66, 111, 258, 261, 267, 276, 281, 321  
 energy flow, 36 – 38, 56, 75, 78  
 energy production, 38, 48

enthalpy, 32, 34, 39, 43, 44, 46 – 49  
 enthalpy of evaporation, 44, 250  
 equilibrium interface concentration, 240  
 equilibrium vapour pressure, 81, 240, 252  
 Ergun relation, 283, 284  
 error function, 144, 220  
 exothermic chemical reaction, 38  
 expansion coefficient, 33, 172, 185  
 expansion valve, 45, 46  
 extraction, 243  
 F-function, 22 – 31  
 Fanning friction factor, 267  
 Fanning pressure drop, 267, 275  
 Fick's law, 77 – 82, 209, 225  
 film contactor, 234  
 film theory, 176, 228, 234, 274  
 flow index, 301  
 flow rate, 3  
 flux, 77, 78, 81 – 85, 88, 90, 94, 95, 121, 125, 145, 154, 177, 198, 205, 212, 225, 248, 274, 287, 290  
 force balance, 57, 60, 61, 88, 89, 117, 119, 264, 281, 286, 294  
 forced convection mass transfer, 233  
 form drag, 111, 112, 113, 275  
 Fourier number, 146, 155, 173, 175, 176, 221  
 Fourier's law, 77, 121, 209  
 free convection, 172, 239  
 free-convection mass transfer, 239  
 friction, 35, 47, 48, 57, 65 – 67, 88, 89, 94 – 96, 111 – 113, 274 – 278, 280, 281, 298  
 friction drag, 111 – 113, 274  
 frictional force, 57, 88, 89, 102  
 gate valve, 277, 279  
 Graetz number, 173, 175, 188  
 Grashof number, 173, 181  
 grid points, 320  
 Hagen-Poiseuille law, 299  
 heat exchangers, 189  
 heat extraction coefficient, 193  
 heat transfer coefficient, 137  
 heat transfer coefficients during convection, 233  
 heat transport in case of free convection, 181  
 Henry's Law, 241  
 hydraulic film thickness, 176, 274  
 hydrostatic pressure, 51, 55, 226, 284  
 ideal tubular reactor, 13, 16, 17, 18, 28  
 ideally stirred tank, 10, 13, 16, 18, 24, 25, 28 – 31  
 inertia, 67, 94, 95, 106, 107, 110, 115, 258  
 infrared, 199, 200, 201  
 interaction force, 110, 113  
 internal energy, 32 – 35, 40, 43, 47 – 49, 166, 257, 265  
 irreversible, 48, 49  
 Kármán vortex street, 115  
 kinematic viscosity, 79, 83  
 kinetic energy, 32 – 38, 46, 48, 51 – 55, 64, 73 – 75, 95, 111, 256, 320  
 kinetic gas theory, 83, 86  
 Kirchhoff's Law, 199  
 laminar, 7575 – 78, 87, 89, 93 – 96, 106 – 111, 117  
 laminar pipe flow, 174  
 lattice, 320  
 Lewis number, 90, 237, 251  
 lift, 110  
 logarithmic mean temperature difference, 193, 194  
 long-term heating, 152, 153, 223  
 loss coefficient, 276 – 280  
 macro balance, 2, 6, 18  
 mass balance, 6, 7, 9, 10, 11, 12, 13, 14, 15, 17, 18, 21, 23, 24, 25, 29, 32, 36, 39, 41, 42, 43, 46, 53, 58, 59, 62, 64, 66, 81, 87, 92, 112  
 mass flow rate, 37  
 mass fraction, 10  
 mass transfer coefficient, 218  
 mechanical energy, 35, 40, 47 – 50, 53 – 55, 64 – 66, 95, 257, 265, 275  
 micro balance, 15, 18, 92, 93, 165, 231, 309, 312, 320  
 molecular diffusion, 74  
 molecular momentum transport, 77, 86, 87, 88, 89, 258, 270, 309  
 molecular transport, 73, 76, 77, 82, 83, 87, 89, 90, 91, 93, 94, 209  
 momentum, 50, 55 – 67, 73, 75 – 79, 82, 83, 86 – 90, 93 – 95, 102, 112, 117, 176, 233, 266, 270, 274, 286, 309, 312, 320  
 momentum concentration, 55, 61, 76, 94, 169, 312  
 momentum flux, 88, 94, 95  
 Moody friction factor, 267  
 mutual diffusion, 212  
 Navier-Stokes equations 312  
 Newton's Law of Cooling, 137, 153, 171, 193, 205, 218, 233  
 Newton's viscosity law, 77, 87, 109, 274, 285, 300  
 Newtonian liquids, 78  
 non-dimensional numbers, 73, 90, 93, 96, 99 – 101, 107 – 109  
 non-Newtonian behaviour, 300  
 non-Newtonian liquids, 300  
 numerical diffusion, 187  
 Nusselt number, 138, 150, 155, 173, 175, 177, 179, 188, 239, 274  
 Ohm's law, 125, 137, 139, 213, 246  
 opaque, 199, 200, 202  
 Ostwald-De Waele model, 301  
 overall energy balance, 47, 49, 50, 54  
 overall heat transfer coefficient, 138  
 overall mass balance, 9  
 overall mass transfer coefficient, 219, 233, 245

- packed bed, 280  
partition coefficient, 243  
Peclet number, 90, 93  
penetration depth, 145, 220  
penetration theory, 141, 145, 175, 219, 220, 249  
phase transition, 34, 39, 44, 45, 47, 190, 194  
pipe flow, 174, 176, 234, 268, 297  
Pitot tube, 52, 55  
plug flow, 13, 16, 24, 27, 92, 304  
Poiseuille flow, 299  
potential energy, 32, 34, 35, 44–46, 53  
Power Law, 301  
Power number, 106, 107  
Prandtl number, 90, 173  
pressure energy, 32, 34, 35, 40, 51, 53, 55, 64, 94, 111, 256, 265  
pressure head, 51, 55  
pressure, dynamic, 55, 94, 111  
pressure, hydrostatic, 55, 284  
pressure, static, 55, 111, 256  
pseudoplastic, 301
- reaction rate constant, 13  
recirculation ratio, 17  
reflection coefficient, 199, 200  
relative humidity, 252  
residence time, 18, 19, 20, 23, 24, 27, 31  
residence time distribution, 19, 20, 24, 27  
resistance, 2, 65, 109, 125, 137–141, 145, 152, 161, 176, 191, 197, 213, 235, 246, 269, 309  
reversible, 48, 49  
Reynolds number, 68, 93, 94, 95, 96, 103, 105, 106, 107, 111, 113, 116, 120, 173, 177, 183, 186, 188, 233, 237, 240, 252, 278, 280  
rheology, 301
- shear stress, 57, 88, 89, 94, 109, 112, 113  
Sherwood number, 219, 221, 228, 233, 239  
Sieder&Tate-correction, 181  
solubility, 216, 238, 240  
species balance, 6  
stagnation point, 51, 111  
stagnation pressure, 51, 52, 55, 111, 113, 116  
stagnation pressure, 111  
static head, 55  
static pressure, 51, 52, 55, 111
- steady-state heat conduction, 121  
steady-state mutual diffusion, 212  
steady-state temperature distribution, 132  
Stefan's correction factor, 227  
Stefan's law, 227  
Stefan-Boltzmann Law, 197  
Stefan-Boltzmann, constant, 197  
stripping, 243  
surface tension, 60, 61
- tanks in series, 28, 29  
temperature contours, 135  
thermal diffusivity, 78, 83  
thermal diffusivity coefficient, 142  
thermal energy, 3, 32, 35, 47–50, 54, 78, 82  
thermal energy balance, 3, 47, 48, 49, 50, 54, 257  
thermal film thickness, 177  
transmission coefficient, 199, 200, 201, 325  
transparent, 199, 202, 263  
tubular reactor, 13, 15, 16, 18  
turbulent, 50, 68, 93, 95–96, 106, 107, 111, 115, 117, 171, 174, 283  
turbulent pipe flow, 176–234
- unilateral diffusion, 227  
unsteady-state heat conduction, 141  
unsteady-state mutual diffusion, 219  
unsteady-state penetration theory, 163  
upwind, 187
- vapour pressure line, 252  
velocity head, 51, 55  
Venturi tube, 52, 55  
viscosity group, 173–181  
visibility factor, 203, 204, 205  
volumetric flow rate, 8
- wet-bulb temperature, 251  
wetted-wall column, 234
- Wien's displacement law, 199, 200  
Winkelman experiment, 225  
work, 10, 34, 37–39, 43, 46–50, 55, 57, 61–65, 69